

Université de Montréal

**La structure de Jordan des matrices de transfert
des modèles de boucles et la relation avec les hamiltoniens XXZ**

par
Alexi Morin-Duchesne

Département de Physique
Faculté des arts et des sciences

Thèse présentée à la Faculté des études supérieures et postdoctorales
en vue de l'obtention du grade de Philosophiæ Doctor (Ph. D.)
en Physique

Août, 2012

© Alexi Morin-Duchesne, 2012.

Université de Montréal
Faculté des études supérieures et postdoctorales

Cette thèse intitulée :

**La structure de Jordan des matrices de transfert
des modèles de boucles et la relation avec les hamiltoniens XXZ**

présentée par
Alexi Morin-Duchesne

a été évaluée par un jury composé des personnes suivantes :

Richard MacKenzie	président-rapporteur
Yvan Saint-Aubin	directeur de recherche
Veronique Hussin	membre du jury
Philippe Ruelle	examineur externe
Michel Boyer	représentant du doyen

Thèse acceptée le 24 août 2012

RÉSUMÉ

Les modèles sur réseau comme ceux de la percolation, d'Ising et de Potts servent à décrire les transitions de phase en deux dimensions. La recherche de leur solution analytique passe par le calcul de la fonction de partition et la diagonalisation de matrices de transfert. Au point critique, ces modèles statistiques bidimensionnels sont invariants sous les transformations conformes et la construction de théories des champs conformes rationnelles, limites continues des modèles statistiques, permet un calcul de la fonction de partition au point critique. Plusieurs chercheurs pensent cependant que le paradigme des théories des champs conformes rationnelles peut être élargi pour inclure les modèles statistiques avec des matrices de transfert non diagonalisables. Ces modèles seraient alors décrits, dans la limite d'échelle, par des théories des champs logarithmiques et les représentations de l'algèbre de Virasoro intervenant dans la description des observables physiques seraient indécomposables.

La matrice de transfert de boucles $D_N(\lambda, u)$, un élément de l'algèbre de Temperley-Lieb, se manifeste dans les théories physiques à l'aide des représentations de connectivités ρ (*link modules*). L'espace vectoriel sur lequel agit cette représentation se décompose en secteurs étiquetés par un paramètre physique, le nombre d de défauts. L'action de cette représentation ne peut que diminuer ce nombre ou le laisser constant. La thèse est consacrée à l'identification de la structure de Jordan de $D_N(\lambda, u)$ dans ces représentations. Le paramètre $\beta = 2 \cos \lambda = -(q + q^{-1})$ fixe la théorie : $\beta = 1$ pour la percolation et $\sqrt{2}$ pour le modèle d'Ising, par exemple.

Sur la géométrie du ruban, nous montrons que $D_N(\lambda, u)$ possède les mêmes blocs de Jordan que F_N , son plus haut coefficient de Fourier. Nous étudions la non diagonalisabilité de F_N à l'aide des divergences de certaines composantes de ses vecteurs propres, qui apparaissent aux valeurs critiques de λ . Nous prouvons dans $\rho(D_N(\lambda, u))$ l'existence de cellules de Jordan intersectorielles, de rang 2 et couplant des secteurs d, d' lorsque certaines contraintes sur λ, d, d' et N sont satisfaites.

Pour le modèle de polymères denses critique ($\beta = 0$) sur le ruban, les valeurs propres de $\rho(D_N(\lambda, u))$ étaient connues, mais les dégénérescences conjecturées. En construisant un isomorphisme entre les modules de connectivités et un sous-espace

des modules de spins du modèle XXZ en $q = i$, nous prouvons cette conjecture. Nous montrons aussi que la restriction de l'hamiltonien de boucles à un secteur donné est diagonalisable et trouvons la forme de Jordan exacte de l'hamiltonien XX, non triviale pour N pair seulement.

Enfin nous étudions la structure de Jordan de la matrice de transfert $T_N(\lambda, \nu)$ pour des conditions aux frontières périodiques. La matrice $T_N(\lambda, \nu)$ a des blocs de Jordan intrasectoriels et intersectoriels lorsque $\lambda = \pi a/b$, et $a, b \in \mathbb{Z}^\times$. L'approche par F_N admet une généralisation qui permet de diagnostiquer des cellules intersectorielles dont le rang excède 2 dans certains cas et peut croître indéfiniment avec N. Pour les blocs de Jordan intrasectoriels, nous montrons que les représentations de connectivités sur le cylindre et celles du modèle XXZ sont isomorphes sauf pour certaines valeurs précises de q et du paramètre de torsion ν . En utilisant le comportement de la transformation \tilde{i}_N^d dans un voisinage des valeurs critiques (q_c, ν_c) , nous construisons explicitement des vecteurs généralisés de Jordan de rang 2 et discutons l'existence de blocs de Jordan intrasectoriels de plus haut rang.

Mots clés : transitions de phase, modèle d'Ising, modèle de Potts, modèle de Fortuin-Kasteleyn, matrice de transfert, hamiltoniens XXZ, théorie des champs logarithmique, structure de Jordan.

ABSTRACT

Lattice models such as percolation, the Ising model and the Potts model are useful for the description of phase transitions in two dimensions. Finding analytical solutions is done by calculating the partition function, which in turn requires finding eigenvalues of transfer matrices. At the critical point, the two dimensional statistical models are invariant under conformal transformations and the construction of rational conformal field theories, as the continuum limit of these lattice models, allows one to compute the partition function at the critical point. Many researchers think however that the paradigm of rational conformal field theories can be extended to include models with non diagonalizable transfer matrices. These models would then be described, in the scaling limit, by logarithmic conformal field theories and the representations of the Virasoro algebra coming into play would be indecomposable.

We recall the construction of the double-row transfer matrix $D_N(\lambda, u)$ of the Fortuin-Kasteleyn model, seen as an element of the Temperley-Lieb algebra. This transfer matrix comes into play in physical theories through its representation in link modules (or standard modules). The vector space on which this representation acts decomposes into sectors labelled by a physical parameter d , the number of defects, which remains constant or decreases in the link representations. This thesis is devoted to the identification of the Jordan structure of $D_N(\lambda, u)$ in the link representations. The parameter $\beta = 2 \cos \lambda = -(q + q^{-1})$ fixes the theory : for instance $\beta = 1$ for percolation and $\sqrt{2}$ for the Ising model.

On the geometry of the strip with open boundary conditions, we show that $D_N(\lambda, u)$ has the same Jordan blocks as its highest Fourier coefficient, F_N . We study the non-diagonalizability of F_N through the divergences of some of the eigenstates of $\rho(F_N)$ that appear at the critical values of λ . The Jordan cells we find in $\rho(D_N(\lambda, u))$ have rank 2 and couple sectors d and d' when specific constraints on λ , d , d' and N are satisfied.

For the model of critical dense polymers ($\beta = 0$) on the strip, the eigenvalues of $\rho(D_N(\lambda, u))$ were known, but their degeneracies only conjectured. By constructing an isomorphism between the link modules on the strip and a subspace of spin

modules of the XXZ model at $q = i$, we prove this conjecture. We also show that the restriction of the Hamiltonian to any sector d is diagonalizable, and that the XX Hamiltonian has rank 2 Jordan cells when N is even.

Finally, we study the Jordan structure of the transfer matrix $T_N(\lambda, \nu)$ for periodic boundary conditions. When $\lambda = \pi\alpha/b$ and $\alpha, b \in \mathbb{Z}^\times$, the matrix $T_N(\lambda, \nu)$ has Jordan blocks between sectors, but also within sectors. The approach using F_N admits a generalization to the present case and allows us to probe the Jordan cells that tie different sectors. The rank of these cells exceeds 2 in some cases and can grow indefinitely with N . For the Jordan blocks within a sector, we show that the link modules on the cylinder and the XXZ spin modules are isomorphic except for specific curves in the (q, ν) plane. By using the behavior of the transformation \tilde{i}_N^d in a neighborhood of the critical values (q_c, ν_c) , we explicitly build Jordan partners of rank 2 and discuss the existence of Jordan cells with higher rank.

Keywords : phase transitions, Ising model, Potts model, Fortuin-Kasteleyn model, transfer matrix method, XXZ Hamiltonian, logarithmic conformal field theory, Jordan structure.

TABLE DES MATIÈRES

RÉSUMÉ	iii
ABSTRACT	v
TABLE DES MATIÈRES	vii
LISTE DES FIGURES	xi
LISTE DES NOTATIONS ET DES SYMBOLES	xiv
REMERCIEMENTS	xv
1 INTRODUCTION	1
1.1 Trois exemples de transitions de phase	2
1.1.1 L'ébullition de l'eau	2
1.1.2 Le problème de la percolation	3
1.1.3 La transition de phase ferromagnétique	6
1.2 Les modèles statistiques	9
1.2.1 Le modèle d'Ising	9
1.2.2 Les observables physiques intéressantes	10
1.2.3 La matrice de transfert du modèle d'Ising en une dimension	12
1.2.4 Le modèle d'Ising en deux dimensions	15
1.2.5 Le modèle de Potts	19
1.2.6 Le modèle de Fortuin-Kasteleyn	20
1.3 La théorie des champs conforme	23
1.3.1 Les transformations conformes en deux dimensions	23
1.3.2 Les hypothèses d'invariance conforme et d'universalité des modèles statistiques	25
1.3.3 L'algèbre de Virasoro et ses représentations irréductibles	28
1.4 La matrice de transfert du modèle de boucles	33
1.4.1 L'algèbre de Temperley-Lieb	34

1.4.2	La matrice double-ligne $D_N(\lambda, u)$	36
1.4.3	Des identités utiles	37
1.4.4	Les symétries de la matrices de transfert	38
1.4.5	Des quantités plus faciles à étudier : \mathcal{H} et F_N	40
1.4.6	La représentation ρ et les premiers blocs de Jordan	42
1.5	Les hamiltoniens non diagonalisables et leur structure de Jordan . . .	46
1.5.1	La forme canonique de Jordan des matrices non diagonalisables	46
1.5.2	Un exemple : l'hamiltonien XXZ sur le ruban	48
1.5.3	Les théories des champs logarithmiques	51
1.5.4	Des méthodes pour identifier des structures de Jordan	54
1.6	Organisation de la thèse	57
2	LA STRUCTURE DE JORDAN DES MODÈLES DE BOUCLES	
	SUR LE RUBAN	59
	Objectifs et méthodologie	59
2.1	Introduction	62
2.2	Transfer matrices of Q-Potts and loop models	65
2.2.1	The Temperley-Lieb algebra as an algebra of connectivities . .	65
2.2.2	The link representation of $TL_N(\beta)$	67
2.2.3	Traces in the link representation	68
2.2.4	Q-Potts models with cylindrical boundary conditions	73
2.2.5	Q-Potts models with fixed, free and mixed boundary conditions	79
2.3	A central element of $TL_N(\beta)$	83
2.3.1	The last Fourier coefficient of $D_N(\lambda, u)$	84
2.3.2	The Wenzl-Jones Projector	89
2.3.3	Eigenvectors of $\rho(F_N(\lambda))$ for non-critical λ s	94
2.4	The Jordan structure of $\rho(D_N(\lambda, u))$	96
2.4.1	Jordan blocks and families of linear transformations	96
2.4.2	The singularities of P^d	100
2.4.3	Jordan blocks of $\rho(F_N(\lambda))$	101
2.4.4	Jordan blocks of $\rho(D_N(\lambda, u))$	107
2.5	Conclusion	109
2.A	The main lemmas	111
2.A.1	Labeling link states and matrix elements	111
2.A.2	$P_{\{m^m\}}^r$ and its singularities	113

2.A.3	$P_{\{n_1, n_2, \dots, n_k\}}^r$ with non trivial bubble patterns	117
2.A.4	Singular points of $P_{\{n_1, n_2, \dots, n_k\}}^r$	122
2.B	Matrix elements of $\rho(F_N(\lambda))$	131
3	LES RÈGLES DE SÉLECTION DU MODÈLE DE POLYMÈRES DENSES	
	CRITIQUE SUR LE RUBAN	137
	Objectifs et méthodologie	137
3.1	Introduction	139
3.2	Critical dense polymers and selection rules	141
3.2.1	The algebra $\mathbb{T}_N(\beta)$ and the double-row matrix	141
3.2.2	Two-column configurations	144
3.2.3	Conjectured degeneracies and selection rules	146
3.2.4	N odd	148
3.2.5	N even	150
3.3	The XXZ Hamiltonian	151
3.3.1	Free fermions	152
3.3.2	N odd	154
3.3.3	N even	156
3.4	The algebra $U_q(\mathfrak{sl}_2)$	158
3.4.1	S^\pm and $S^{\pm(2)}$ for free fermions	159
3.4.2	N odd	161
3.4.3	N even	162
3.5	The relation between H and \mathcal{H}_N	163
3.5.1	The homomorphism	163
3.5.2	The injectivity of i_N^d	166
3.5.3	The relation between $U_q(\mathfrak{sl}_2)$ and $i_N^d(V_N^d)$	168
3.6	The reduction of state space and the degeneracies	169
3.6.1	N odd	171
3.6.2	N even	172
3.7	Conclusion	174
3.A	The computation of $K'_{N/2}$, β_1 and β_2 (for N even)	174
3.B	Independence of states not in $i_N^d(V_N^d)$	175
4	LA STRUCTURE DE JORDAN DES MODÈLES DE BOUCLES	
	AVEC CONDITIONS PÉRIODIQUES	179
	Objectifs et méthodologie	179

4.1	Introduction	183
4.2	Periodic Temperley-Lieb algebras and loop models	186
4.2.1	Periodic Temperley-Lieb algebras	186
4.2.2	The loop transfer matrix $T_N(\lambda, \nu)$	188
4.2.3	Link states and representations of $\mathcal{E}TLP_N(\beta, \alpha)$	189
4.3	The loop transfer matrix and the Hamiltonians H_{XXZ}	192
4.3.1	An extended family of XXZ models	192
4.3.2	The map \tilde{i}_N^d between link and spin states	194
4.3.3	The factorization of the Gram matrix in terms of the map \tilde{i}_N^d	197
4.4	Jordan blocks between sectors	201
4.5	The intertwiner \tilde{i}_N^d and its critical curves	209
4.5.1	The Gram determinant on the strip	211
4.5.2	The relation between the open and the periodic cases	215
4.5.3	The factor $K_{d,r}$	220
4.5.4	The determinant of the Gram matrix	223
4.5.5	The determinant of $I_N^d(u, \nu)$	225
4.6	Jordan blocks within sectors	229
4.6.1	Basic observations and identities	229
4.6.2	An extended family of representations of $U_q(\mathfrak{sl}_2)$	231
4.6.3	The left nullspace of \tilde{i}_N^d	235
4.6.4	A construction of Jordan generalized eigenvectors : a simple example	238
4.7	Concluding remarks	244
5	CONCLUSION	247
	BIBLIOGRAPHIE	249

LISTE DES FIGURES

1.1	Le diagramme de phase de l'eau	2
1.2	Une configuration de percolation par lien en (a) et par site en (b) sur un réseau carré. La configuration en (a) permet une traversée horizontale et celle en (b) une traversée verticale.	4
1.3	La probabilité de traversée π_h de percolation par site sur un réseau de côté N en fonction de p , pour $N = 2, 4, 8, 16, 32, 64$ et 128 . Les courbes pour $N \geq 8$ proviennent de simulations numériques. Lorsque $N \rightarrow \infty$, la fonction $\pi_h(p)$ tend vers une fonction de Heaviside et sa dérivée en $p = p_c \simeq 0,59274598 \pm 0,00000004$ se comporte en $N^{3/4}$. La figure est tirée de [2].	5
1.4	Trois graphes illustrant la transition de phase ferromagnétique. En (a), le diagramme de phase d'un aimant ferromagnétique dans le plan B, T . En (b), la magnétisation spontanée en fonction de la température. En (c), la variation de la magnétisation en fonction du champ magnétique. Les figures sont des reproductions de figures dans [8].	7
1.5	Un anneau de spins d'Ising	13
1.6	En (a), un réseau carré de spins d'Ising, avec $N = 4$ et $M = 3$. Les liens K sont représentés par les traits pleins en rouge et les liens L par les traits discontinus en bleu. En (b), trois rangées successives de spins, représentant l'action de V, W et \mathcal{T}_N	16
1.7	Le diagramme de la transition de phase du modèle d'Ising en deux dimensions dans le plan K, L	17
1.8	Trois configurations obtenues à l'aide de simulations utilisant un algorithme de Swendsen-Wang pour le modèle d'Ising sur un réseau carré de 300×300 sites, avec les conditions aux limites périodiques dans les deux directions (sur le tore), pour (a) $T < T_c$, (b) $T = T_c$ et (c) $T > T_c$	19
1.9	Un graphe de Fortuin-Kasteleyn avec $\#(\mathcal{G}) = 12$, $N_{aK} = 10$ et $N_{aL} = 9$	21
1.10	Une transformation du plan complexe qui conserve les angles localement : $f(z) = \ln(z)$	24

- 1.11 La transformation conforme f envoie le domaine fermé de gauche vers le disque unité de droite. Les points A' , B' , C' et D' sont les images de A , B , C et D sous f 27
- 1.12 Un module de Verma $V_{c,h}$ est engendré par un vecteur $|v\rangle$ au niveau h . Lorsqu'on y applique les opérateurs L_i , $i > 0$, celui-ci engendre des descendants aux niveaux $h + 1$, $h + 2$, etc. Le nombre de descendants (indépendants via les équations (1.3.5) qui définissent **Vir**) au niveau $h + n$ est $p(n)$, le nombre de partitions de l'entier n , et est fidèlement représenté par le nombre de points noirs au niveau $h + n$. Une représentation graphique d'un module de Verma est donnée à gauche et, à droite, nous donnons les opérateurs qui engendrent les premiers descendants lorsqu'appliqués à $|v\rangle$. Certains descendants peuvent être singuliers et engendrer des sous-modules dont il faut faire le quotient pour obtenir une représentation irréductible. Ceux-ci apparaissent aux niveaux $h + 3$ et $h + 4$ sur le diagramme. Les sous-modules peuvent avoir un patron d'imbrication non-trivial, et c'est le cas pour le modèle d'Ising. 31
- 1.13 Les tables de Kac pour le modèle d'Ising ($c = \frac{1}{2}$) en (a) et de 3-Potts ($c = \frac{4}{5}$) en (b). Dans les cases blanches, les valeurs $h_{r,s}$ qui correspondent aux représentations irréductibles et unitaires. 32
- 1.14 Une illustration d'un *staggered module*. 52
- 2.1 A $N \times (2M)$ grid with $N = 4$ and $M = 3$ with a spin lattice at 45° : (a) with all vertices and bonds drawn, (b) a graph \mathcal{G} and (c) the corresponding loop configuration. 74
- 2.2 The states of spins marked by white or gray circles in (a) are specified by boundary conditions. To obtain fixed boundary conditions, the spins are tied to a spurious spin in the desired state like in (b) and the interaction between the new spin and those at the boundary is sent to infinity. Again K bonds are represented by dashed lines, J bonds by dotted lines and L bonds by alternating dots and dashes. 81
- 2.3 The pattern of Jordan blocks of $\rho(D_N(\lambda, u))$ for $\lambda = \pi/2$ (critical polymers), $\lambda = \pi/4$ (Ising) and $\lambda = \pi/6$ (3-Potts). 109

- 3.1 An admissible two-column configuration in $A_{4,6}^8$ with $L = (2, 3, 5, 8)$ and $R = (1, 2, 5, 6, 7, 8)$: blue sites are occupied and white sites unoccupied. To its right, the corresponding values of the ϵ_j s and μ_j s. . . . 145
- 3.2 A two-column admissible configuration in $\tilde{A}_{3,5}^8$ and, to the right, the corresponding Dyck path $\in DP_2^8$ and link state $\in V_8^2$ 146
- 3.3 A two-column admissible configuration in $A_{4,6}^8$ and its corresponding reduced configuration in $\tilde{A}_{1,3}^4$. It corresponds to the eigenvalue $-2 \cos \pi/17 - 2 \cos 4\pi/17 + 2 \cos 5\pi/17 - 2 \cos 7\pi/17$ of $\rho(\mathcal{H}_{N=17})$ and has degeneracy 3. 149
- 4.1 A depiction of the two bijections for a link state with $N = 12$, $d = 2$ and $r = 2$. The link state w has $\psi(w) = \{(2, 3), (6, 9), (7, 8), (11, 16), (12, 13)\}$, $\sum_{(i,j) \in \psi(w)} j - i = 11$, $H(\mathcal{B}^+(w)) = -2$ and $H(\mathcal{B}^-(w)) = -24$. 225
- 4.2 The domain containing all paths in the sum (4.5.19). 228
- 4.3 The Bratelli diagram for $q = e^{i\pi/2}$. Jordan cells in ω_d occur when pairs (N, d) are contained in a box. The construction of section 4.6.4 is for boxes with solid segments, while boxes with dashed lines are for Jordan blocks found by our exploration on a computer. The number of multiple dashed boxes indicates the number of Jordan partners in the largest Jordan cell of the given \tilde{V}_N^d . The first occurrence of rank 4 Jordan blocks within a sector appears for $(N, d) = (12, 0)$. Jordan cells between sectors d and d' in the representation ρ are indicated by solid segments connecting pairs (N, d) . For these, $\alpha = 2$ is assumed when N is even. 246

LISTE DES NOTATIONS ET DES SYMBOLES

c	La charge centrale
CFT	Une théorie des champs conforme
$D_N(\lambda, u)$	La matrice de transfert de boucles sur le ruban
$\mathcal{E}TLP_N(\alpha, \beta)$	L'algèbre de Temperley-Lieb périodique élargie
FK	Le modèle Fortuin et Kasteleyn
F_N	Le plus haut coefficient de Fourier de $D_N(\lambda, u)$ ou de $T_N(\lambda, \nu)$
$h_{r,s}$	Les plus hauts poids des représentations de Virasoro
LCFT	Une théorie des champs conforme logarithmique
ω_d	Les représentations de vecteurs de connectivités avec <i>twist</i> et d défauts
ρ	Les représentations de vecteurs de connectivités
$\mathbb{T}_N(\beta)$	L'algèbre de Temperley-Lieb sur le ruban
\mathcal{T}_N	La matrice de transfert de spins sur le ruban
$T_N(\lambda, \nu)$	La matrice de transfert de boucles sur le tore ou le cylindre
Vir	L'algèbre de Virasoro
Z	La fonction de partition

REMERCIEMENTS

J'aimerais tout d'abord remercier mon directeur de recherche, Yvan Saint-Aubin, dont l'enthousiasme, l'énergie, le travail méticuleux et la patience ont entraîné la transition de l'étudiant que j'étais jadis au chercheur que je suis aujourd'hui.

Un gros merci aussi à ma petite amie Jessica, dont les efforts pour évacuer les équations de mes pensées ont souvent été vains, mais dont le soutien a été présent (et indispensable) à tous les moments, bon an mal an.

Je voudrais aussi remercier mes parents, Danielle Morin et Georges Duchesne, de même que Huguette Morin, ma grand-mère, qui n'ont pas manqué de m'encourager tout au long des quatre dernières années ; mes frères et soeurs, Xavier, Magali, Adrien et Justine qui ont tout au long "acceptés" d'être taquinés, et avec lesquels je partage une relation hors du commun. Merci aussi à Michel, dont l'humour a su égayer ma vie, à Guillaume, avec lequel j'ai partagé des moments superbes sur et en dehors du terrain de soccer, à Louis, Éric, Joël, Arthur, Sabrina, Nadim, Bouboules. Une pensée également à toute la famille Nasica-Labouze. À vous tous, ainsi qu'à ceux que j'ai certainement oubliés, je lève mon verre. Mon succès est le vôtre !

Enfin, je ne saurais passer sous silence l'importance qu'ont eue les contributions financières généreuses du CRSNG, du FQRNT et de la FESP. Merci d'avoir cru en moi !

CHAPITRE 1: INTRODUCTION

Dans cette thèse, il sera question de l'importance d'hamiltoniens non hermitiens et parfois non diagonalisables pour certains problèmes en mécanique statistique et de méthodes pour diagnostiquer leur structure de Jordan. Ces hamiltoniens apparaissent dans l'étude de modèles statistiques simples visant à décrire le phénomène de transition de phase. Par *transition de phase*, on entend une modification macroscopique et subite des caractéristiques d'un système suite à une petite altération de certains de ses paramètres externes, par exemple la transition de liquide à gaz que subit l'eau lorsque la température passe de 99°C à 101°C . A priori, cette définition est vague. Elle peut inclure des phénomènes expliqués par la mécanique classique, par exemple le mouvement d'une masse sur un plan incliné (avec frottement) en fonction de l'angle d'inclinaison, ou le mouvement d'un système masse-ressort avec friction en fonction de la masse du bloc. Les transitions de phase sont plutôt des phénomènes en physique statistique, où les interactions entre de grandes quantités de particules font naître des comportements macroscopiques qui sont modifiés subitement par un changement infinitésimal des paramètres externes du système.

Dans la première partie de cette introduction, la section 1.1, une analyse de trois exemples de transitions de phase est présentée. Pour décrire ces transitions, il existe de nombreux modèles mathématiques, parmi lesquels un nombre très restreint possède la propriété d'avoir une solution analytique. À la section 1.2 seront introduits les modèles d'Ising, leur généralisation à plus de deux états (le modèle de Potts) et le modèle de Fortuin-Kasteleyn. La solution du modèle d'Ising en deux dimensions est connue, ce qui ne s'étend aux deux modèles de Potts et de Fortuin-Kasteleyn en général. À la section 1.3, nous verrons que les modèles statistiques semblent jouir d'une invariance sous les transformations conformes et que les hypothèses d'invariance conforme et d'universalité, de même que la construction de théories des champs conformes, permettent de faire des prédictions intéressantes sur ces modèles, même dans les cas où la solution exacte est inconnue. Les arguments utilisés dans la formulation originale des théories des champs conformes pour faire ces prédictions présupposent que les hamiltoniens et matrices de transfert sont diagonalisables, mais il existe des situations où cette hypothèse n'est pas satisfaite. C'est

le cas des matrices de transfert de boucles, dans les représentations de vecteurs de connectivités, qui peuvent être non diagonalisables. La matrice de transfert double-ligne $D_N(\lambda, u)$, de même que le formalisme de l'algèbre de Temperley-Lieb et de ses représentations de lien, sont introduits à la section 1.4. À la section 1.5, nous présentons les caractéristiques des matrices non diagonalisables et faisons un survol des méthodes qui seront utilisées pour diagnostiquer cette non diagonalisabilité. Nous soulignons au passage les modifications qui doivent être faites aux arguments de théories conformes lorsqu'une structure de Jordan est présente dans l'hamiltonien.

1.1 Trois exemples de transitions de phase

1.1.1 L'ébullition de l'eau

Le premier exemple que nous introduisons est bien connu : celui de l'ébullition de l'eau. Lorsqu'à pression ambiante, de l'eau sous forme liquide est chauffée jusqu'à atteindre 100°C , elle subit une transition de phase de premier ordre. L'énergie fournie, plutôt que de contribuer à une hausse de température, sert à altérer les liens entre les molécules d'eau. Il résulte de cette hausse minime de la température une chute abrupte de la densité : il y a passage de l'état liquide à l'état gazeux. Cette transition est caractérisée physiquement par un changement macroscopique du système : elle est marquée par un saut (une discontinuité) de la densité en fonction de la température. Par contraste, des transitions d'ordre supérieur, ou transitions continues, sont des transitions pour lesquelles le changement au système n'est pas aussi apparent à grande échelle et qui sont caractérisées par une discontinuité dans les dérivées des quantités macroscopiques comme la densité.

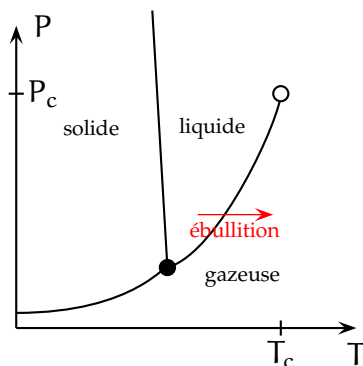


FIGURE 1.1 – Le diagramme de phase de l'eau

La transition décrite précédemment est illustrée dans le diagramme de la figure

1.1 par la flèche rouge, et elle survient précisément lorsque la température et la pression prennent leurs valeurs sur la courbe qui sépare la phase liquide et la phase gazeuse. Il existe toutefois un point (T_c, P_c) , dit *point critique*, où cette courbe se termine. Pour l'eau, ce point est à $P_c = 218 \text{ atm}$ et $T_c = 341^\circ\text{C}$; ce sont des conditions très éloignées des températures et pressions ambiantes. Autour de ce point, il est possible de passer d'une phase liquide à une phase gazeuse sans transition de premier ordre : il s'agit de modifier les paramètres T et P de manière à contourner le point critique. Par ce processus, le système passera par des états où les phases liquides et gazeuses coexistent. La densité varie continûment en fonction de la température et la transition de premier ordre est absente (pour plus de détails, voir [1]).

1.1.2 Le problème de la percolation

Un second exemple, de nature plus mathématique, est celui du modèle de percolation par lien et par site. Soit un réseau carré de $N \times N$ sites, comme à la figure 1.2 (a), où chaque site a quatre voisins (sauf ceux à la frontière). Pour la percolation par lien, nous supposons entre deux sites voisins un lien sur lequel est apposé un pont avec probabilité p (avec $0 \leq p \leq 1$), ou pas de pont avec probabilité $1 - p$. Chaque configuration a alors une probabilité $p^n(1 - p)^m$ où n est le nombre de ponts, $m = N_L - n$ est le nombre de liens sans pont et $N_L = 2N(N - 1)$ est le nombre total de liens. La question cruciale en percolation est de savoir s'il y a une traversée horizontale et, plus précisément, de calculer la probabilité $\pi_h(p)$ d'une telle traversée. Pour une configuration donnée, il y a une traversée horizontale s'il est possible d'aller d'un site sur la frontière de gauche à un site de la frontière de droite en permettant le passage d'un site à l'autre uniquement lorsque ceux-ci sont liés par un pont. Ainsi la configuration de la figure 1.2 (a) admet une traversée horizontale, mais pas de traversée verticale. La probabilité $\pi_h(p)$ sera alors la somme des probabilités de toutes les configurations qui admettent une traversée horizontale.

Le problème de percolation par site diffère de celui par lien en ce sens que ce sont les sites qui sont occupés (en noir) ou inoccupés (en blanc) plutôt que les liens. Le passage entre sites adjacents est possible s'ils sont tous deux occupés et l'observable intéressante demeure la probabilité de traversée horizontale. Dans l'exemple de la figure 1.2 (b), il y a une traversée verticale, mais pas de traversée horizontale.

Quoique les problèmes de percolation soient des modèles mathématiques rela-

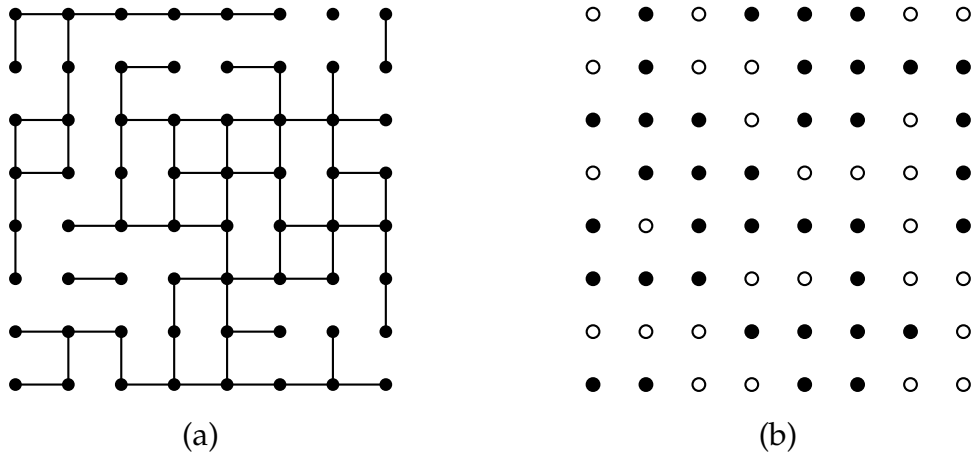


FIGURE 1.2 – Une configuration de percolation par lien en (a) et par site en (b) sur un réseau carré. La configuration en (a) permet une traversée horizontale et celle en (b) une traversée verticale.

tivement simples, ils s'appliquent à de nombreux phénomènes physiques. Parmi ceux-ci, on trouve la modélisation de la pénétration d'un gaz à travers un solide poreux. Les pores du solide sont répartis aléatoirement et le gaz peut traverser le solide lorsqu'il y a une traversée horizontale [2]. On utilise également le modèle de percolation pour modéliser la conductivité d'un matériau. Les sites du réseau représentent alors des régions hautement conductrices reliées à leurs voisines avec probabilité p . S'il y a une traversée, le matériau est conducteur, sinon il est isolant [1].

La fonction $\pi_h(p)$ a un comportement particulier lorsque $N \rightarrow \infty$: Kesten [3] a montré qu'il existe dans cette limite une probabilité $p_c \in (0, 1)$ telle que

$$\lim_{N \rightarrow \infty} \pi_h(p) = \begin{cases} 0 & \text{lorsque } p < p_c, \\ 1 & \text{lorsque } p > p_c, \end{cases}$$

et ce pour la percolation par site et par lien. La transition de phase s'opère à $p_c = \frac{1}{2}$ pour la percolation par lien [3] et à $p_c \simeq 0,59274598 \pm 0,00000004$ pour la percolation par site [4]. À part des valeurs différentes de p_c , les deux modèles sont assez similaires ; dans les deux cas, la probabilité de traversée $\pi_h(p)$ tend vers une fonction de Heaviside lorsque $N \rightarrow \infty$, ce qui est illustré à la figure 1.3 pour la percolation par site. Enfin le problème de percolation met en lumière plusieurs concepts qui seront utiles pour la suite :

- Les transitions de phase n'ont lieu que dans la *limite thermodynamique*, c'est-à-dire lorsque le nombre de particules N tend vers l'infini. Pour des valeurs

finies de N , les observables physiques sont des fonctions analytiques et différentiables, ce qui ne tient pas forcément lorsque $N \rightarrow \infty$.

- La pente de la fonction $\pi_h(p)$ en $p = p_c$ croît avec N . Si $\pi_h(p)$ tend vers une fonction de Heaviside en $p = p_c$, alors la pente $d\pi_h(p)/dp$ devient infinie en $p = p_c$ lorsque $N \rightarrow \infty$. Plus précisément, la fonction $d\pi_h(p)/dp|_{p=p_c}$ se comporte en $N^{1/\nu}$ lorsque N est suffisamment grand, où ν est un *exposant critique* : des simulations numériques et des arguments théoriques indiquent que $\nu = 4/3$ [5, 6, 2] pour la percolation par lien et par site. On dit de ν qu'il est universel, en ce sens qu'il demeure inchangé pour une grande classe de problèmes de percolation en deux dimensions. Par exemple, les courbes $\pi_h^{\text{tri}}(p)$ obtenues sur un réseau triangulaire possèdent également des dérivées dont le comportement est décrit (lorsque N est grand) par $N^{1/\nu}$ avec le même ν , même si la probabilité critique p_c^{tri} est différente de celle pour le réseau carré.
- Smirnov [7] a montré que le problème de percolation sur le réseau triangulaire est invariant conforme dans la limite thermodynamique, c'est-à-dire invariant sous toutes les transformations préservant les angles. Nous reviendrons sur les implications de cette invariance à la section 1.3.

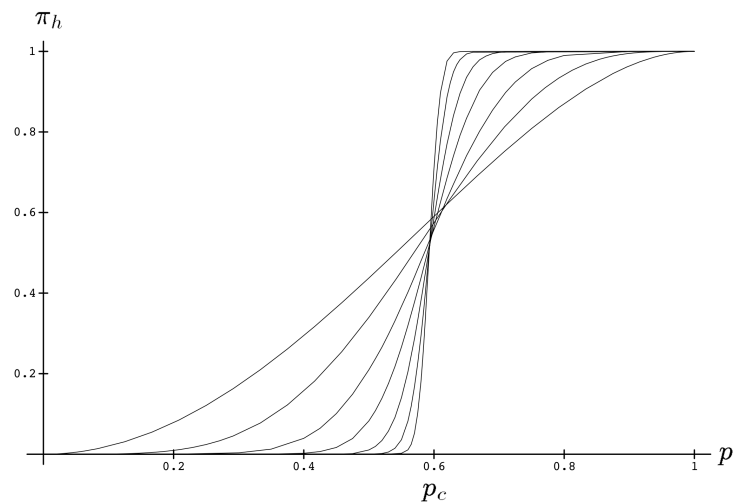


FIGURE 1.3 – La probabilité de traversée π_h de percolation par site sur un réseau de côté N en fonction de p , pour $N = 2, 4, 8, 16, 32, 64$ et 128 . Les courbes pour $N \geq 8$ proviennent de simulations numériques. Lorsque $N \rightarrow \infty$, la fonction $\pi_h(p)$ tend vers une fonction de Heaviside et sa dérivée en $p = p_c \simeq 0,59274598 \pm 0,00000004$ se comporte en $N^{3/4}$. La figure est tirée de [2].

1.1.3 La transition de phase ferromagnétique

Le troisième exemple, sans doute le plus important pour ce qui suit, est la transition de phase ferromagnétique. Prenons le cas d'une barre de fer plongée dans un champ magnétique pointant dans une direction \hat{z} . À basse température et à champ non nul, les spins sont dans une phase ordonnée et pointent dans la direction du champ magnétique. La magnétisation $M = M(T, B)$, dont une définition précise est explicitée à la section 1.2.2, vaut $+\hat{z}$: M donne la direction où les spins pointent en moyenne. Si, toujours à basse température, le champ magnétique est lentement réduit à 0, il y a une magnétisation résiduelle $M_0\hat{z}$ non nulle qui demeure : les spins ont une mémoire du champ magnétique disparu et une majorité d'entre eux pointent toujours dans sa direction. Par contre, dès qu'un champ magnétique $B < 0$ (pointant en $-\hat{z}$) est instauré, les spins changent d'orientation, s'alignant instantanément avec ce nouveau champ, et M change subitement de signe. La définition formelle de la magnétisation M_0 est

$$\lim_{B \rightarrow 0^+} M(T, B) = M_0(T)\hat{z}.$$

Puisque, à une température sous T_c ,

$$\lim_{B \rightarrow 0^+} M(T, B) \neq \lim_{B \rightarrow 0^-} M(T, B),$$

la magnétisation est une fonction discontinue en $B = 0$ et il y a transition de phase.

À haute température, il y a plutôt un régime désordonné. Partant d'un fort champ magnétique, il appert que, suite à une diminution à zéro du champ magnétique, les spins viennent à pointer graduellement dans des directions variées. En $B = 0$, la magnétisation résiduelle est nulle : les spins n'ont pas de mémoire et pointent dans des directions indépendantes du champ magnétique original.

En fait, la magnétisation résiduelle M_0 est une fonction décroissante de la température, et elle devient nulle de manière subite en une température $T = T_c$, la *température de Curie*, tel qu'il est illustré à la figure 1.4 (b). Le point $B = B_c = 0, T = T_c$ est le point critique et, à cause de ses particularités, il sera au coeur des calculs faits dans cette thèse. C'est d'ailleurs pour reproduire la transition de phase du ferromagnétisme que les modèles d'Ising et de Potts, introduits à la section 1.2, ont d'abord été étudiés. Nous mettons l'emphase ici sur trois caractéristiques importantes du point critique qui apparaissent dans la transition ferromagnétique.

En premier lieu, tout comme pour la percolation, le point critique est caractérisé par ses exposants critiques. Au point critique, une ou plusieurs quantités thermodynamiques peuvent ne pas être continues ou différentiables. Dans l'exemple présent,

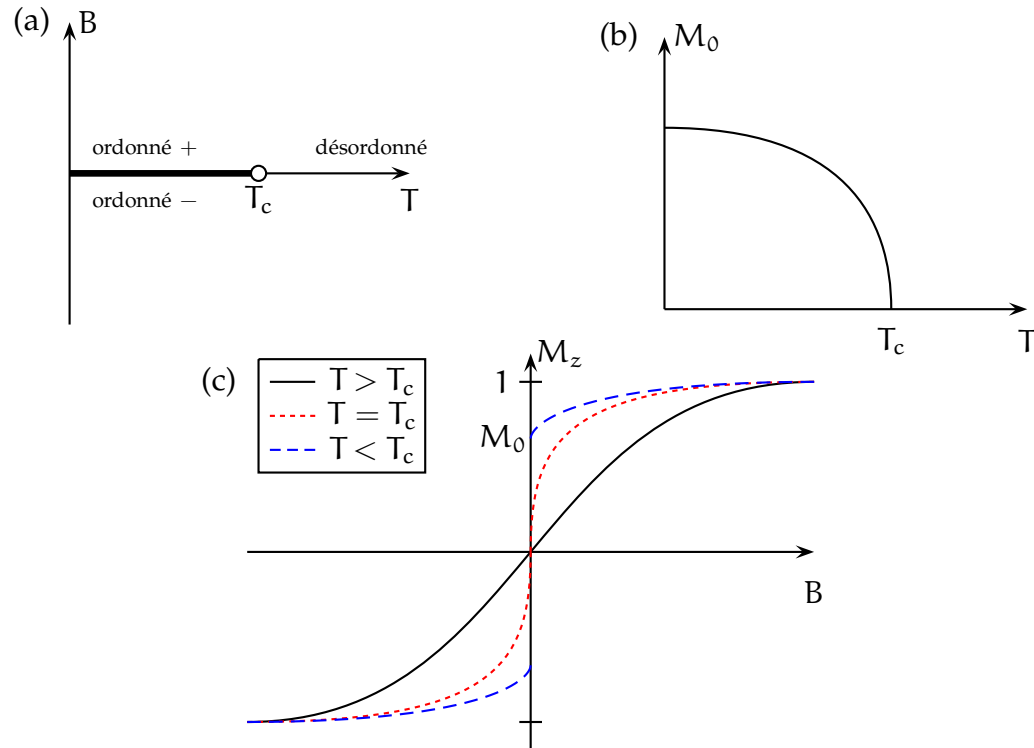


FIGURE 1.4 – Trois graphes illustrant la transition de phase ferromagnétique. En (a), le diagramme de phase d’un aimant ferromagnétique dans le plan B, T . En (b), la magnétisation spontanée en fonction de la température. En (c), la variation de la magnétisation en fonction du champ magnétique. Les figures sont des reproductions de figures dans [8].

la magnétisation résiduelle n’est pas différentiable au point critique en fonction de T et la magnétisation n’est pas continue en fonction de B , tel qu’illustré à la figure 1.4. Il est alors attendu que, dans le voisinage du point critique,

$$\begin{aligned} M(T_c, B) &\propto B^{1/\delta} \hat{z} & \text{lorsque } B \rightarrow 0, \\ M_0(T) &\propto (T - T_c)^\beta & \text{lorsque } T \rightarrow T_c^-, \end{aligned} \quad (1.1.1)$$

où β et δ sont deux exposants critiques qui caractérisent le comportement de la magnétisation près du point critique. Pour un système physique réel, ils peuvent être calculés expérimentalement alors que, pour un modèle mathématique donné, ils peuvent être calculés exactement dans certains cas et numériquement dans plusieurs autres.

Une deuxième caractéristique remarquable de la physique au point critique est le comportement de la corrélation entre deux spins placés en position x_i et x_j . La fonction de corrélation $G_{i,j}$ sera définie à la section 1.2.2 pour le modèle d’Ising :

comme son nom l'indique, cette observable nous informe de la corrélation entre des spins i et j qui ne sont pas forcément voisins. Lorsque le champ B est nul, on peut interpréter la fonction de corrélation comme la probabilité que les spins i et j pointent dans la même direction. À une température supérieure à T_c , la corrélation décroît de manière exponentielle lorsque $N \rightarrow \infty$:

$$G_{i,j} \propto \exp(-|x_i - x_j|/\xi), \quad (1.1.2)$$

où ξ est la longueur de corrélation. Elle dépend généralement de T et de B , mais aussi de l'orientation du vecteur unitaire liant les points i et j . Au point critique, ξ devient infinie : il se forme des plages macroscopiques de spins pointant dans la même direction, et la fonction de corrélation, au lieu de décroître exponentiellement, décroît plutôt comme une loi de puissance. En $T = T_c$,

$$G_{i,j} \propto |x_i - x_j|^{2-d-\eta}, \quad (1.1.3)$$

où d est le nombre de dimensions et η , l'exposant critique lié à la fonction de corrélation.

En dernier lieu, la physique au point critique est caractérisée par l'apparition de symétries supplémentaires. Les modèles que nous introduirons dans les prochaines sections auront souvent des symétries sous translation et sous certaines rotations qui seront évidentes et indépendantes des paramètres du modèle (par exemple de B et de T). Au point critique et dans la limite $N \rightarrow \infty$, le terme dominant de $G_{i,j}$ devient indépendant de la direction du vecteur liant i et j et ne dépend plus que de la distance $|x_i - x_j|$; c'est une invariance plus grande que celle qui est manifeste dans le réseau choisi. Il apparaît également une invariance d'échelle, qui se manifeste concrètement par

$$G_{\lambda i, \lambda j} = \lambda^{2-d-\eta} G_{i,j} \quad (1.1.4)$$

où λi est un abus de notation qui indique que nous avons pris le spin en position λx_i . Nous verrons à la section 1.3 que l'existence de ces symétries supplémentaires au point critique joue un rôle primordial, rendant possible le calcul de la fonction de partition d'une manière détournée.

1.2 Les modèles statistiques

1.2.1 Le modèle d'Ising

Pour tenter de reproduire mathématiquement la transition de phase ferromagnétique, Wilhelm Lenz proposa en 1925 un modèle statistique simple à son élève Ernst Ising, aujourd'hui connu sous le nom de *modèle d'Ising*. Il s'agit d'un modèle de spins sur réseau avec une interaction très simple. Le réseau est un ensemble de sites, vivant dans un espace de dimension d , avec des liens reliant certains de ces sites qui identifient lesquels sont des voisins immédiats. Sur chacun des sites, étiquetés par des nombres entiers i ou j , se trouve une particule de spin $\frac{1}{2}$ dont l'état est décrit par la variable $\sigma_i \in \{+1, -1\}$. Les spins interagissent uniquement avec leurs voisins immédiats. Deux particules voisines avec spins identiques contribuent $-J$ à l'énergie totale de la configuration, et deux spins voisins différents y contribuent J . Finalement, la définition générale du modèle d'Ising inclut aussi un champ magnétique B en chaque point i du réseau, avec contribution $-B\sigma_i$ à l'énergie de la configuration. Ainsi, l'énergie d'une configuration est

$$E(\sigma) = -J \sum_{\langle i,j \rangle} \sigma_i \sigma_j - B \sum_i \sigma_i \quad (1.2.1)$$

où la notation $\langle i, j \rangle$ indique que la somme est prise sur les paires de sites i et j voisins immédiats dans le réseau. Pour la suite, nous travaillerons surtout avec des réseaux carrés en deux dimensions, mais le choix du réseau est libre dans la définition qui précède.

Lorsque J est positif, des spins voisins parallèles mènent à une énergie moindre que des spins antiparallèles et le modèle est ferromagnétique. La configuration de moindre énergie est celle où tous les spins sont parallèles et de même signe que B . Lorsque $B = 0$, il y a deux configurations d'énergie minimale. À l'opposé, le modèle est antiferromagnétique lorsque J est négatif. L'existence d'une unique configuration de moindre énergie n'est pas assurée et peut alors dépendre de J et de B , mais aussi du réseau.

Il est essentiel de comprendre les simplifications et hypothèses qui sont faites. Les réseaux pour lesquels les calculs analytiques sont possibles sont bidimensionnels et idéaux, alors que dans un aimant réel, les particules ne sont pas immobiles et fixées dans un patron d'un réseau parfait. En plus, l'état de particules de spin $\frac{1}{2}$ peut prendre n'importe quelle valeur entre $-\frac{1}{2}$ et $\frac{1}{2}$. L'énergie d'interaction classique de

deux dipôles magnétiques avec moments dipolaires magnétiques \mathbf{m}_1 et \mathbf{m}_2 est (voir [9])

$$E = \frac{\mu_0}{4\pi r^3} (\mathbf{m}_1 \cdot \mathbf{m}_2 - 3(\mathbf{m}_1 \cdot \hat{\mathbf{r}})(\mathbf{m}_2 \cdot \hat{\mathbf{r}})), \quad (1.2.2)$$

où $\hat{\mathbf{r}}$ est le vecteur unitaire reliant les deux particules et r la distance entre celles-ci. Pour l'interaction quantique, on trouve dans le livre de Cohen-Tannoudhi [10] que l'interaction entre le spin d'un proton et celui d'un électron est obtenue en remplaçant $\mathbf{m}_i = \frac{q_i g_i}{2m_i} \mathbf{s}_i$ dans l'équation qui précède, où q_i , g_i , \mathbf{s}_i et m_i sont respectivement la charge, le facteur de Landé, le spin et la masse de la particule i . La situation est similaire pour le cas de deux électrons dont les spins interagissent. L'interaction d'Ising tente de reproduire le premier terme de (1.2.2). Quant au second terme, il est absent dans le modèle d'Ising, et on peut supposer alors que les deux orientations des spins \mathbf{s}_i sont contraintes à être perpendiculaires aux plans du réseau choisi. Aussi, l'énergie d'interaction entre dipôles a une dépendance en la position relative des dipôles de r^{-3} . Le modèle d'Ising offre donc une simplification supplémentaire, puisqu'elle ne considère l'interaction qu'entre voisins immédiats. Malgré sa simplicité au niveau microscopique, le modèle d'Ising cache de nombreuses subtilités mathématiques et, remarquablement, parvient à reproduire le phénomène macroscopique complexe qu'est la transition de phase. Cela est surprenant au vu de toutes les approximations qui sont faites.

Pour conclure cette introduction, le modèle d'Ising a aussi des applications diverses, autres que la modélisation du ferromagnétisme. Il peut être utilisé en biologie pour comprendre le comportement de l'ADN et de l'hémoglobine (voir [11]). Il peut aussi modéliser la transition de phase d'un liquide comme celle de la section 1.1.1. En chaque site, $\sigma_i = +1$ indique que le site est occupé par une molécule et $\sigma_i = -1$ indique que le site est vide. L'interaction d'Ising approxime le potentiel de Lennard-Jones très grossièrement. Lorsque de gros amas de spins identiques se forment, la phase est liquide ; lorsque ces spins sont répartis de manière désordonnée, c'est la phase gazeuse. Pour plus de détails, voir [8], section 1.9.

1.2.2 Les observables physiques intéressantes

À toute configuration d'un modèle statistique est associé un poids de Boltzmann $e^{-\beta E(\sigma)}$ à partir duquel on définit la probabilité d'une configuration :

$$P(\sigma) = \frac{e^{-\beta E(\sigma)}}{Z}, \quad \text{où} \quad Z = \sum_{\sigma} e^{-\beta E(\sigma)}$$

est la fonction de partition, avec $\beta = \frac{1}{kT}$, la constante de Boltzmann k et la température T . De cette définition de probabilité, on peut définir pour n'importe quelle observable $X(\sigma)$ sa valeur moyenne,

$$\langle X \rangle = \sum_{\sigma} P(\sigma) X(\sigma).$$

La fonction de partition, somme des poids de Boltzmann de toutes les configurations, est en fait le facteur de normalisation des probabilités. C'est une quantité que les physiciens passent un temps stupéfiant à calculer, et pour de bonnes raisons : à partir de diverses opérations sur Z , il est possible de calculer plusieurs quantités thermodynamiques d'intérêt. Parmi celles-ci, on compte l'énergie libre

$$F = -kT \ln Z,$$

l'énergie moyenne

$$\langle E \rangle = kT^2 \partial(\ln Z) / \partial T$$

et la chaleur spécifique

$$C = \langle E^2 \rangle - \langle E \rangle^2 = \partial \langle E \rangle / \partial T.$$

Pour les modèles de spins comme le modèle d'Ising, la magnétisation M et la susceptibilité magnétique χ , données par

$$M = \frac{1}{N} \langle \sum_i \sigma_i \rangle = \frac{kT}{N} \frac{\partial \ln Z}{\partial B},$$

$$\chi = \frac{1}{NkT} \left(\langle (\sum_i \sigma_i)^2 \rangle - \langle \sum_i \sigma_i \rangle^2 \right) = \frac{\partial M}{\partial B},$$

fournissent aussi des informations fondamentales sur les caractéristiques macroscopiques du système : la magnétisation M nous donne le spin moyen et la susceptibilité χ , ses variations. Enfin, une dernière observable utile est la fonction de corrélation à deux points, $G_{i,j} = \langle \sigma_i \sigma_j \rangle - \langle \sigma_i \rangle \langle \sigma_j \rangle$. Pour le modèle d'Ising en $B = 0$, $\langle \sigma_i \rangle$ sera toujours nul parce que le modèle est invariant sous l'inversion de tous les spins. Le terme $\langle \sigma_i \sigma_j \rangle$ qui reste a alors l'interprétation probabilistique donnée à la section 1.1.3. La fonction de corrélation offre une alternative pour calculer la susceptibilité, puisque $\chi = (NkT)^{-1} \sum_{i,j} G_{i,j}$, mais cette observable est surtout intéressante à cause de son comportement au point critique, tel qu'expliqué à la section 1.1.3.

Le concept de l'ordre d'une transition de phase a été mentionné à la section 1.1.1. Pour une transition de phase donnée, son ordre est le nombre de dérivées de la fonction de partition nécessaire pour obtenir une quantité thermodynamique discontinue ou divergente en fonction d'un des paramètres du modèle. Pour le modèle d'Ising en deux dimensions par exemple, une transition de phase de second ordre a lieu : la susceptibilité magnétique est la quantité qui est discontinue à une température T_c finie et non nulle.

1.2.3 La matrice de transfert du modèle d'Ising en une dimension

La méthode de la matrice de transfert est une technique extrêmement puissante dont l'objectif est le calcul analytique de la fonction de partition pour toute grandeur du réseau. Elle ramène le problème de calculer Z à celui de trouver les valeurs propres d'une matrice, la matrice de transfert. Pour la majorité des modèles statistiques sur des réseaux en deux dimensions, les valeurs propres de la matrice de transfert ne sont pas connues et lorsqu'elles le sont, leur calcul requiert souvent des prouesses techniques qui dépassent les visées de cette thèse. Ainsi, en deux dimensions, le calcul a été fait uniquement lorsque $B = 0$ et c'est déjà un tour de force, réussi pour la première fois par Onsager en 1944 [12]. En trois dimensions ou plus, on ne connaît pas d'expression pour les valeurs propres. Pour s'accoutumer à la technique de la matrice de transfert, il est utile de commencer par un exemple plus simple et le calcul de la fonction de partition du modèle d'Ising en une dimension, fait pour la première fois par Ising en 1925 dans sa thèse doctorale [13], nous procure cette opportunité. Il sera alors possible de calculer toutes les quantités thermodynamiques et les exposants critiques. La présentation de cette section suit assez fidèlement celle de Baxter [8].

La difficulté du calcul de la fonction de partition

$$Z = \sum_{\sigma} \exp\left(J \sum_{\langle i,j \rangle} \sigma_i \sigma_j + B \sum_i \sigma_i\right)$$

provient de la somme sur les plus proches voisins du réseau. Le facteur $\beta = \frac{1}{kT}$ a été enlevé pour alléger la notation, mais il faudra faire attention de le réinsérer dans la définition des constantes J et B lors de calculs requérant des dérivées par rapport à J , B ou T .

Soit une chaîne de N spins d'Ising, telle que présentée à la figure 1.5. Chaque spin a deux voisins. Commençons par le cas trivial où la chaîne ne comporte que

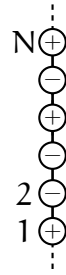


FIGURE 1.5 – Un anneau de spins d’Ising

deux spins et où le champ magnétique B est nul. Chaque spin peut être $+$ ou $-$, et la matrice suivante (dite *de transfert*)

$$\mathcal{T}(J) = \begin{matrix} + & - \\ - & + \end{matrix} \begin{pmatrix} e^J & e^{-J} \\ e^{-J} & e^J \end{pmatrix} \quad (1.2.3)$$

donne les quatre fonctions de partition pour les quatre choix de spins, et permet de calculer la fonction de partition pour $N = 2$ pour n’importe quel choix de conditions à la frontière. Si nous voulons permettre aux deux sites d’être *libres*, c’est-à-dire de pouvoir être $+$ ou $-$, alors $Z_{\text{libre}} = \langle v_f | \mathcal{T}(J) | v_i \rangle = 4 \cosh J$, avec $|v_i\rangle = |v_f\rangle = \begin{pmatrix} 1 \\ 1 \end{pmatrix}$ et $\langle v | = |v\rangle^T$. Avec $\mathcal{T}(J)$, nous pouvons aussi calculer $Z_{\text{pér}}$ pour la chaîne périodique avec un seul spin : dans ce cas, ce spin est son propre voisin. S’il est $+$, l’énergie est $+J$, et de même s’il est $-$, de sorte que $Z_{\text{pér}} = 2e^J$. Pour calculer cette fonction de partition avec la matrice de transfert $\mathcal{T}(J)$, il suffit de prendre la chaîne de deux spins et de supposer les deux spins identiques, c’est-à-dire prendre la trace de la matrice de transfert : $Z_{\text{pér}} = \text{tr } \mathcal{T}(J) = 2e^J$.

Pour le cas où la chaîne comporte trois spins, on peut cette fois écrire

$$\mathcal{T}_2(J) = \begin{matrix} + & - \\ - & + \end{matrix} \begin{pmatrix} e^{2J} + e^{-2J} & 2 \\ 2 & e^{2J} + e^{-2J} \end{pmatrix}, \quad (1.2.4)$$

où les entrées correspondent aux quatre différents choix de conditions aux frontières pour les spins 1 et 3, et où la somme sur les deux choix de spins possibles pour le site intermédiaire a été faite. Les arguments donnés précédemment nous permettent alors de calculer $Z_{\text{libre}} = 8 \cosh^2 J$ et, pour la chaîne périodique à deux spins, $Z_{\text{pér}} = \text{tr } \mathcal{T}_2(J) = 4 \cosh(2J)$.

L’utilité de ce formalisme provient du fait remarquable que $\mathcal{T}_2(J) = (\mathcal{T}(J))^2$. La multiplication $\mathcal{T}(J) \times \mathcal{T}(J)$ se charge de la somme sur le spin intermédiaire faite dans le calcul de (1.2.4). De manière générale, $\mathcal{T}_n(J) = (\mathcal{T}(J))^n$, et pour la chaîne

périodique à N spins, $Z_{\text{pér}} = \text{tr } \mathcal{T}(J)^N$. Parce que la matrice $\mathcal{T}(J)$ est symétrique, il est possible de l'écrire sous la forme

$$\mathcal{T}(J) = S \begin{pmatrix} \lambda_+ & 0 \\ 0 & \lambda_- \end{pmatrix} S^{-1},$$

où λ_+ et λ_- sont les valeurs propres de $\mathcal{T}(J)$. En utilisant la propriété de cyclicité des traces $\text{tr}(AB) = \text{tr}(BA)$, on trouve que

$$Z_{\text{pér}} = \text{tr } \mathcal{T}(J)^N = \text{tr} \begin{pmatrix} \lambda_+^N & 0 \\ 0 & \lambda_-^N \end{pmatrix} = \lambda_+^N + \lambda_-^N.$$

Inclure le champ magnétique B dans le calcul n'est guère plus compliqué, mais il faut prendre garde à ne pas compter deux fois sa contribution. La matrice de transfert à considérer est

$$\mathcal{T}(J, B) = \begin{pmatrix} e^{J+B} & e^{-J} \\ e^{-J} & e^{J-B} \end{pmatrix}$$

avec valeurs propres $\lambda_{\pm} = e^J \cosh B \pm \sqrt{e^{2J} \sinh^2 B + e^{-2J}}$. Puisque nous voulons diagnostiquer la présence ou l'absence d'une transition de phase, il est nécessaire de prendre la limite $N \rightarrow \infty$. Pour $T > 0$ ($J < \infty$), l'inégalité $\lambda_+ > \lambda_-$ est satisfaite quel que soit B , et l'énergie libre par spin et la magnétisation sont

$$f = \lim_{N \rightarrow \infty} \frac{-kT \ln Z}{N} = -kT \ln \lambda_+,$$

$$M = \frac{\partial \ln \lambda_+}{\partial B} = \frac{\sinh B}{\sqrt{\sinh^2 B + e^{-4J}}}.$$

En une dimension, la technique de la matrice de transfert permet aussi de calculer exactement les fonctions de corrélation en calculant

$$\langle \sigma_i \rangle = \frac{1}{Z} \text{tr} (\mathcal{T}^i \sigma_z \mathcal{T}^{N-i}) = \frac{1}{Z} \text{tr} (\sigma_z \mathcal{T}^N),$$

$$\langle \sigma_i \sigma_j \rangle = \frac{1}{Z} \text{tr} (\mathcal{T}^i \sigma_z \mathcal{T}^{j-i} \sigma_z \mathcal{T}^{N-j}) = \frac{1}{Z} \text{tr} (\sigma_z \mathcal{T}^{j-i} \sigma_z \mathcal{T}^{N+i-j}),$$

pour lesquelles les expressions figurent dans le livre de Baxter [8].

L'invariance sous translation se manifeste directement par la propriété de cyclicité de la trace. Le comportement de la fonction de corrélation lorsque $i - j \ll N$ et $N \rightarrow \infty$ est alors

$$G_{i,j} \xrightarrow{N \rightarrow \infty} A \left(\frac{\lambda_-}{\lambda_+} \right)^{j-i}$$

où A est une fonction analytique de J et de B , indépendante de i, j et N . La longueur de corrélation est donc $\xi = (\ln(\lambda_+/\lambda_-))^{-1}$ et, puisque pour $T > 0$, $\lambda_+ > \lambda_-$ et il n'y a

pas de transition de phase. Malgré cela, le point $T = 0, B = 0$ a les caractéristiques d'un point critique : $\lim_{T \rightarrow 0^+} \lambda_- / \lambda_+ = 1$ et la longueur de corrélation devient infinie. La fonction de corrélation est constante (et est donc invariante sous dilatation), la magnétisation vaut 1 et en comparant avec (1.1.1) et (1.1.3), on peut lire les exposants critiques, $\delta = \infty$ et $\eta = 1$. Puisque $T < 0$ n'a pas de sens physique, l'exposant critique β ne peut être calculé.

1.2.4 Le modèle d'Ising en deux dimensions

Le modèle d'Ising en deux dimensions avec lequel nous travaillerons est celui d'un réseau carré dessiné à une inclinaison de 45° , tel qu'illustré à la figure 1.6 (a). Dans ce réseau, il y a $2M$ rangées qui ont alternativement N et $N + 1$ spins. Pour les conditions aux limites du réseau, nous identifions les spins de la ligne $2M$ à ceux de la première ligne (condition périodique), mais considérons que les spins de la première et de la $(N + 1)$ -ème colonne sont distincts (condition libre) et ont uniquement deux voisins. Nous qualifierons la géométrie décrite par cette condition aux frontières de *ruban*, alors que *tore* et *rectangle* sont réservés respectivement pour les conditions périodique-périodique et libre-libre. Par rapport à la définition du modèle d'Ising donnée à la section 1.2.1, il y a deux différences. D'une part, le champ B est mis à 0. En effet, peu de résultats analytiques pour le modèle d'Ising en deux dimensions sont connus pour un champ non nul. D'autre part, une *anisotropie* est ajoutée : les sites situés dans des colonnes impaires sont liés à leurs voisins des colonnes paires par une constante d'interaction K par la droite, mais avec une constante L par la gauche. L'énergie d'une configuration de spins d'Ising est alors

$$E(\sigma) = -K \sum_{\langle i,j \rangle}^{(K)} \sigma_i \sigma_j - L \sum_{\langle i,j \rangle}^{(L)} \sigma_i \sigma_j. \quad (1.2.5)$$

Ainsi la somme $\sum_{\langle i,j \rangle}^{(K)}$ est une somme sur tous les liens rouges de la figure 1.6 et $\sum_{\langle i,j \rangle}^{(L)}$, une somme sur les liens bleus. Ce choix, de même que celui de prendre le réseau avec l'inclinaison de 45° , découle de considérations mathématiques plutôt que physiques : les matrices de transfert pour ces réseaux satisfont des symétries qui rendent le calcul des valeurs propres de la matrice de transfert plus facile.

Il est possible de définir une matrice de transfert, $\mathcal{T}_N = VW$, où les éléments des

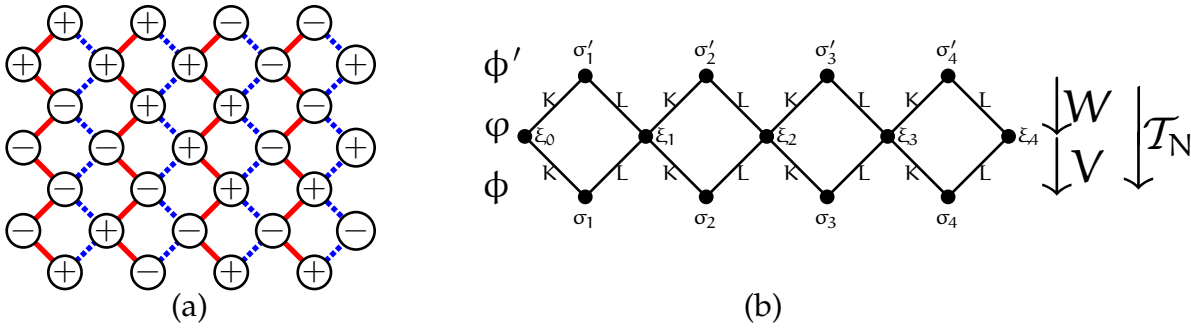


FIGURE 1.6 – En (a), un réseau carré de spins d’Ising, avec $N = 4$ et $M = 3$. Les liens K sont représentés par les traits pleins en rouge et les liens L par les traits discontinus en bleu. En (b), trois rangées successives de spins, représentant l’action de V , W et \mathcal{T}_N .

matrices V et W sont

$$\begin{aligned}
 V_{\phi, \varphi} &= \exp \left[K \sigma_1 \xi_0 + L \sigma_N \xi_N + \sum_{j=1}^{N-1} (L \sigma_j \xi_j + K \sigma_{j+1} \xi_j) \right], \\
 W_{\varphi, \phi'} &= \exp \left[K \xi_0 \sigma'_1 + L \xi_N \sigma'_N + \sum_{j=1}^{N-1} (L \xi_j \sigma'_j + K \xi_j \sigma'_{j+1}) \right].
 \end{aligned} \tag{1.2.6}$$

Les étiquettes $\phi = (\sigma_1, \dots, \sigma_N)$ et $\phi' = (\sigma'_1, \dots, \sigma'_N)$ des matrices V et W sont des configurations d’une rangée de N spins, alors que l’étiquette $\varphi = (\xi_1, \dots, \xi_{N+1})$ est une configuration d’une rangée de $N+1$ spins. L’action de V , W et \mathcal{T}_N est représentée à la figure 1.6 (b). Puisque le nombre de configurations possibles sur une rangée de N spins est de 2^N , \mathcal{T}_N est une matrice $2^N \times 2^N$. Cette matrice permet de calculer la fonction de partition pour le réseau de la figure 1.6 (b) pour n’importe quel choix de configuration ϕ et ϕ' . Le produit entre V et W , deux matrices rectangulaires de grandeurs respectives $2^N \times 2^{N+1}$ et $2^{N+1} \times 2^N$, se charge d’effectuer la somme sur les 2^{N+1} configurations de la ligne intermédiaire de $N+1$ spins.

Parce que $W = V^T$, \mathcal{T}_N est symétrique, comme dans le cas à une dimension. Pour calculer la fonction de partition pour un réseau avec conditions libres sur le rectangle avec M quelconque, l’idée est la même que pour la chaîne en une dimension :

$$Z_{\text{libre}} = \langle v | \mathcal{T}_N^M | v \rangle, \quad \text{avec} \quad |v\rangle = \begin{pmatrix} 1 \\ 1 \\ \vdots \\ 1 \end{pmatrix}.$$

De même, pour les conditions aux limites périodiques, la fonction de partition est

$$Z_{\text{pér}} = \text{tr } \mathcal{T}_N^M.$$

Le calcul de la fonction de partition revient à celui des valeurs propres d'une matrice, en l'occurrence une matrice de format $2^N \times 2^N$. C'est un problème plus compliqué que le cas unidimensionnel où la matrice était 2×2 .

Les premiers calculs des valeurs propres d'une matrice de transfert pour le modèle d'Ising en deux dimensions ont été faits par Onsager [12] et Kaufman [14]. Calcul prodigieux, il a été fait sur un réseau carré "normal" (sans l'inclinaison de 45°) sans contrainte sur K et L , a permis de calculer la fonction de partition et a montré que la chaleur spécifique a une divergence lorsque

$$\sinh(2K) \sinh(2L) = 1. \quad (1.2.7)$$

Puisque la chaleur spécifique s'obtient par une deuxième dérivée de la fonction de partition (et parce que les premières dérivées de Z ne sont pas divergentes), la transition est de deuxième ordre. Sur le réseau carré incliné, la transition de phase du modèle d'Ising s'effectue aussi lorsque l'équation (1.2.7) est satisfaite, et ce, indépendamment des conditions aux frontières [15]. L'argument y menant, plus simple que le calcul complet de la fonction de partition, est basé sur le fait que le réseau dual du réseau carré est également carré.

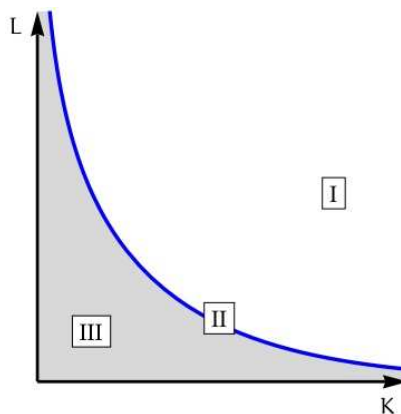


FIGURE 1.7 – Le diagramme de la transition de phase du modèle d'Ising en deux dimensions dans le plan K, L .

Le diagramme de phase est illustré à la figure 1.7. La droite $K = L$ est l'analogue de la droite $B = 0$ de la figure 1.4 (a) (mais $T = 0$ correspond à $K = L \rightarrow \infty$) : les

phases I, II et III sont, dans l'ordre, les phases ordonnée, critique et désordonnée. Celles-ci sont illustrées à la figure 1.8 par trois configurations obtenues à l'aide de simulations numériques avec $K = L$ à trois différentes températures. Le comportement est celui qui a été décrit à la section 1.1.3.

Pour la suite nous serons surtout intéressés à la phase II, courbe que nous paramétrisons par la variable d'anisotropie $u \in [0, \pi/4]$, définie par

$$\sinh(2K) = \cot(2u), \quad \sinh(2L) = \tan(2u).$$

Avec cette paramétrisation, un calcul fastidieux permet de trouver les valeurs propres de la matrice de transfert $\mathcal{T}_N(u)$ et de les écrire sous la forme simple suivante (voir [17], où la définition de la matrice de transfert diffère par une constante),

$$\Lambda = 2^{N+1} \prod_{k=1}^N \left(\csc \left(\frac{\pi(2k-1)}{2(2N+1)} \right) \csc(4u) + \mu_k \right). \quad (1.2.8)$$

Chacune des valeurs propres Λ est caractérisée par ses valeurs de $\mu_1, \dots, \mu_N \in \{+1, -1\}$. Elles sont au nombre de 2^N et sont réelles puisque \mathcal{T}_N est symétrique. La plus grande valeur propre, Λ_0 , est celle pour laquelle tous les signes μ_k sont $+1$. On peut alors calculer l'énergie libre par site,

$$\begin{aligned} f_s &= \lim_{N, M \rightarrow \infty} \frac{F}{(2N+1)M} = \lim_{N, M \rightarrow \infty} \frac{-kT \ln Z_{\text{pér}}}{(2N+1)M} = \lim_{N, M \rightarrow \infty} \frac{-kT \ln \Lambda_0^M}{(2N+1)M} \\ &= -\frac{kT}{2} \left(\ln 2 + \int_0^1 dx \ln (1 + \csc(4u) \csc(\pi x/2)) \right). \end{aligned} \quad (1.2.9)$$

Enfin, nous notons $\Lambda_{k_1, k_2, \dots, k_r}$ une valeur propre qui a $\mu_{k_1}, \mu_{k_2}, \dots, \mu_{k_r}$ tous égaux à -1 , et tous les autres μ , à $+1$. Lorsque $N \gg 1$, on trouve que

$$\frac{\Lambda_{k_1, k_2, \dots, k_r}}{\Lambda_0} \stackrel{N \gg 1}{\approx} \exp \left(\epsilon \sum_{i=1}^r (2k_i - 1) \right) \quad \text{où} \quad \epsilon = \frac{\pi \sin(4u)}{2N},$$

et que les valeurs propres sont égales au premier ordre en $\frac{1}{N}$. Avec ce développement, on peut montrer que la fonction de partition admet l'expression

$$Z_{\text{pér}} \stackrel{N \gg 1}{\approx} \Lambda_0^M \sum_{\text{valeurs propres } \Lambda} (\Lambda/\Lambda_0)^M = \Lambda_0^M \prod_{n \in 2\mathbb{N}-1} (1 + q^n)$$

où $q = \exp(\epsilon M)$. La fonction de partition a une forme finale très simple, et nous y reviendrons à la section 1.3. Par contre, cette expression vaut au point critique exclusivement. Elle ne permet pas le calcul des exposants critiques du modèles d'Ising, qui est néanmoins possible : les exposants β , δ et η introduits à la section 1.1.3 valent $\beta = 1/8$, $\delta = 15$ et $\eta = 1/4$ [18, 19, 20].

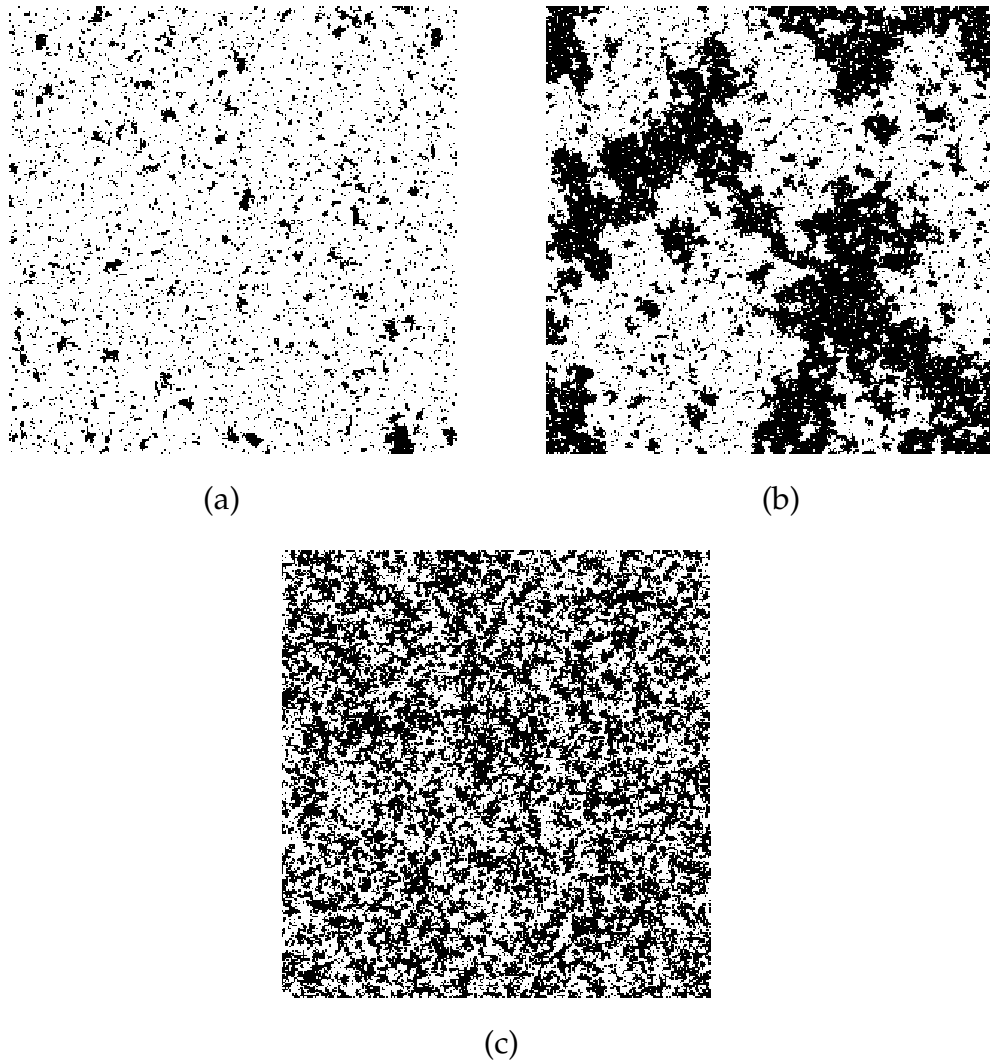


FIGURE 1.8 – Trois configurations obtenues à l’aide de simulations utilisant un algorithme de Swendsen-Wang pour le modèle d’Ising sur un réseau carré de 300×300 sites, avec les conditions aux limites périodiques dans les deux directions (sur le tore), pour (a) $T < T_c$, (b) $T = T_c$ et (c) $T > T_c$.

1.2.5 Le modèle de Potts

Le modèle de Q-Potts, introduit par R. B. Potts [21], est une généralisation du modèle d’Ising au cas où les spins σ_i peuvent prendre Q valeurs différentes (avec $Q \geq 2$). Nous travaillerons avec ce modèle sur le réseau de la figure 1.6. L’énergie d’une configuration est donnée par

$$E(\sigma) = -K' \sum_{\langle i,j \rangle}^{(K)} \delta_{\sigma_i, \sigma_j} - L' \sum_{\langle i,j \rangle}^{(L)} \delta_{\sigma_i, \sigma_j}. \quad (1.2.10)$$

Quand des spins voisins sont identiques, la contribution à $E(\sigma)$ est $-K'$ (ou $-L'$), mais elle est nulle lorsqu'ils sont différents. Les Q différentes valeurs que les spins σ_i peuvent prendre n'ont pas d'importance ; il importe uniquement qu'elles soient différentes et au nombre de Q . Lorsque $Q = 2$ et $\sigma_i \in \{+1, -1\}$, les équations (1.2.1) et (1.2.10) ne sont pas tout à fait identiques, mais puisque $\delta_{\sigma_i, \sigma_j} = (\sigma_i \sigma_j + 1)/2$, les énergies de deux configurations sont égales à une constante additive près si on impose $K' = 2K$ et $L' = 2L$.

L'argument de dualité qui permet de déterminer la courbe critique pour le modèle d'Ising fonctionne aussi pour le modèle de Potts. Il donne [22] :

$$v_K v_L = Q \quad (1.2.11)$$

avec $v_K = e^{K'} - 1$ et $v_L = e^{L'} - 1$. Cela est équivalent à (1.2.7) en $Q = 2$ avec la transformation susmentionnée. En se restreignant aux cas $2 \leq Q \leq 4$, la paramétrisation de la courbe critique que nous utilisons est

$$\frac{v_K}{\sqrt{Q}} = \frac{\sin(\lambda - u)}{\sin(u)}, \quad (1.2.12)$$

où les trois valeurs de λ correspondantes, $\lambda = \pi/4, \pi/6$ et 0 , sont toutes dans l'intervalle $\in [0, \pi/2]$ et sont telles que $Q = 4 \cos^2 \lambda$. Le paramètre $u \in [0, \lambda]$, qui paramétrise la courbe critique dans la figure 1.7, est le *paramètre d'anisotropie*. Ce choix de paramétrisation est justifié par la simplicité résultante de l'équation de Yang-Baxter, un outil très utile pour l'étude des matrices de transfert. En effet, l'équation de Yang-Baxter permet de montrer qu'au point critique, deux matrices de transfert évaluées à des anisotropies u et v différentes commutent, $[\mathcal{T}_N(u), \mathcal{T}_N(v)] = 0$. Nous montrerons à la section 1.4.4 comment l'équation de Yang-Baxter du modèle de boucles permet d'étendre ce résultat aux matrices de transfert de boucles $D_N(\lambda, u)$.

Le modèle de Potts admet également un traitement via une matrice de transfert comme celle de la section 1.2.4, sauf que \mathcal{T}_N est de dimension $Q^N \times Q^N$. Pour Q général, la forme des valeurs propres de \mathcal{T}_N n'est pas connue et notre connaissance des exposants critiques provient de simulations numériques.

1.2.6 Le modèle de Fortuin-Kasteleyn

Le modèle de Fortuin-Kasteleyn [23] est différent des modèles de spins d'Ising et de Q -Potts, puisqu'il s'agit d'un modèle de tuiles plutôt que de spins sur un réseau. À partir du réseau de la figure 1.6 (a), une boîte carrée est apposée à chaque endroit

où il y avait un lien joignant des spins voisins. Le résultat est un réseau de $2M \times 2N$ tuiles, comme à la figure 1.9. Une configuration de Fortuin-Kasteleyn est obtenue en faisant le choix $\begin{array}{|c|} \hline \diagdown \\ \hline \end{array}$ ou $\begin{array}{|c|} \hline \diagup \\ \hline \end{array}$ pour chacune des tuiles.

Les conditions aux frontières choisies sont de type ruban (ou *cylindre*) : le haut et le bas sont identifiées (condition périodique), mais pas la droite et la gauche, où des demi-cercles sont apposés pour compléter les courbes tracées par les tuiles (condition libre ou *ouverte*). Chaque configuration a alors un poids

$$P(\sigma) = \frac{\beta^{\#(\mathcal{G})} w_K^{N_{aK}} w_L^{N_{aL}}}{Z},$$

où $\#(\mathcal{G})$, N_{aK} , N_{aL} , w_K et w_L sont définies comme suit. Le nombre $\#(\mathcal{G})$ compte le nombre de courbes fermées dans le diagramme résultant. Attention, cela ne correspond pas toujours au nombre de composantes connexes, ces amas de points noirs réunis par le tracé des courbes. Par exemple dans la figure 1.9, il y a 12 courbes fermées, mais uniquement 10 composantes connexes. Une des composantes connexes entoure le cylindre et celle-ci est bornée par deux courbes qui enveloppent aussi le cylindre. L'autre courbe fermée en surplus naît de la présence d'un cycle fermé dans cette même composante connexe. Dans la figure 1.9, les endroits où les spins prennent place dans les modèles d'Ising et de Potts demeurent marqués d'un point noir. Si le choix de tuile est tel qu'il permet de joindre deux de ces points noirs, alors une arête $\cdots\cdots$ est ajoutée. Les nombres N_{aK} et N_{aL} comptent alors les nombres d'arêtes sur les liens de types K et L respectivement (voir la figure 1.6) et w_K et $w_L \in \mathbb{R}$, sont les poids de Boltzmann de chacune de ces arêtes.

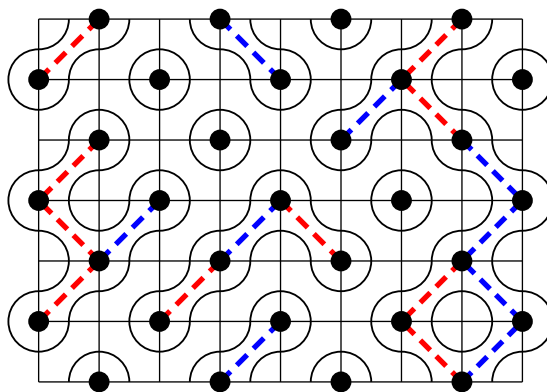


FIGURE 1.9 – Un graphe de Fortuin-Kasteleyn avec $\#(\mathcal{G}) = 12$, $N_{aK} = 10$ et $N_{aL} = 9$

Le modèle de Fortuin-Kasteleyn se démarque des modèles de spins par l'observable physique non locale qui entre dans sa définition : le nombre de boucles

fermées. En effet, puisqu'une courbe fermée peut s'étendre sur une grande région du réseau, le comptage des boucles ne peut être fait localement : il nécessite une connaissance de la totalité du réseau.

Le modèle de Fortuin-Kasteleyn a plusieurs attraits. Le premier est qu'il offre une avenue alternative pour le calcul de la fonction de partition du modèle de Potts au point critique : si $\beta = \sqrt{Q}$, $w_K = v_K/\beta$ et $w_L = v_L/\beta$, alors

$$Z_{\text{Potts}} = \beta^{N_s} Z_{\text{FK}}$$

où $N_s = M(2N + 1)$ est le nombre total de sites occupés par des spins. La preuve de cet énoncé sera le sujet de la section 2.2.4. Cette égalité vaut lorsque les conditions à la frontière du modèle de Fortuin-Kasteleyn et de Potts sont de type ruban. Il existe des conditions aux frontières pour le modèle de Fortuin-Kasteleyn qui généralisent ce dernier résultat aux réseaux de spins avec conditions toroïdales et rectangulaires. Notons aussi que nous prendrons souvent le paramètre β du modèle de Fortuin-Kasteleyn dans l'intervalle $[0, 2]$, en le paramétrisant par $\beta = 2 \cos \lambda$, $\lambda \in [0, \pi/2]$, en référence aux modèles de Potts.

Le second attrait du modèle de Fortuin-Kasteleyn provient du cas $\beta = 1$, où le modèle est équivalent à celui de la percolation par lien sur le réseau de la figure 1.6 (a). En effet, en posant $\beta = 1$ et en choisissant $w_K = w_L \equiv w$, on trouve que la probabilité d'une configuration est :

$$P(\sigma) = \frac{w^{N_a}}{Z} = \frac{1}{Z} (1 + w)^{N_L} \left(\frac{w}{1 + w} \right)^{N_a} \left(\frac{1}{1 + w} \right)^{N_L - N_a}$$

où $N_L = 4MN$ est le nombre total de liens possibles et $N_a = N_{aK} + N_{aL}$ le nombre total d'arêtes. Puisque $w/(1 + w) = 1 - 1/(1 + w)$, en choisissant $p = w/(1 + w)$ on trouve que

$$P(\sigma) = \frac{(1 + w)^{N_L}}{Z} P_{\text{perco}}(\sigma),$$

où $P_{\text{perco}}(\sigma)$ est la probabilité d'une configuration en percolation, avec les liens ouverts indiqués par les arêtes telles qu'apposées à la figure 1.9. Le modèle de percolation est, en quelque sorte, la limite $Q \rightarrow 1$ du modèle de Q-Potts. Dans cette limite, l'équation (1.2.11) donne $w^2 = Q = 1$ et la probabilité critique est $p_c = \frac{1}{2}$ tel qu'attendu.

Le modèle de Fortuin-Kasteleyn admet lui aussi une formulation en termes d'une matrice de transfert. Ces matrices de transfert, pour les modèles de boucles,

sont différentes des matrices de transfert de spins. Elles seront introduites aux sections 1.4.2 et 2.2.1 pour le ruban et à la section 4.2.2 pour le tore, et auront la particularité de n'être ni symétriques ni hermitiennes.

1.3 La théorie des champs conforme

Le calcul de la fonction de partition en deux dimensions, fait à la section 1.2.4, est unique au modèle d'Ising : pour les modèles de Potts et de Fortuin-Kasteleyn, les valeurs propres de la matrice de transfert demeurent inconnues. Or notre intérêt pour ces modèles réside réellement dans leurs propriétés dans la limite thermodynamique. Dans cette limite, de nombreux indicateurs nous poussent à croire que les modèles statistiques sont invariants sous les transformations conformes, et cela a même été démontré dans quelques cas précis. Les théories des champs conformes sont des théories des champs où une action S bâtie pour un champ ϕ est telle que la fonction de partition est invariante sous les transformations conformes. En poussant l'étude des théories conformes rationnelles, il est possible de faire des prédictions remarquables, notamment de calculer la fonction de partition au point critique. La construction de telles théories est non triviale, et prouver que les modèles statistiques convergent vers ces théories conformes l'est encore moins. On peut trouver un exposé détaillé sur cette construction dans le livre de Di Francesco, Mathieu et Sénéchal [24]. Nous exposerons plutôt un raccourci, tel que présenté dans [25], qui permet de reproduire l'expression de la fonction de partition du modèle d'Ising en utilisant des arguments de symétries, mais en évitant les délicates intégrales de chemin.

1.3.1 Les transformations conformes en deux dimensions

Les transformations dites *conformes* sont les transformations qui préservent les angles. Pour les décrire, les deux dimensions de \mathbb{R}^2 sont représentées par un seul paramètre complexe $z = x + iy$. En fonction de cette variable, les translations, rotations et dilatations sont respectivement les transformations $f(z) = z + a$, $f(z) = ze^{i\theta}$ et $f(z) = \lambda z$ avec $a \in \mathbb{C}$, $\theta \in \mathbb{R}$ et $\lambda \in \mathbb{R}^\times$. Ce sont trois transformations conformes globales, en ce sens qu'elles laissent les angles inchangés, envoient $\mathbb{C} \cup \{\infty\}$ vers $\mathbb{C} \cup \{\infty\}$ et sont inversibles. Les transformations conformes globales comprennent aussi $f(z) = 1/z$ de même que les compositions de plusieurs transformations conformes

globales. En toute généralité, elles s'écrivent sous la forme

$$f(z) = \frac{az + b}{cz + d}$$

avec la contrainte $ad - bc \neq 0$.

Il existe d'autres transformations conformes dites *locales*; ce sont celles qui conservent les angles dans des sous-domaines de la sphère de Riemann $\mathbb{C} \cup \{\infty\}$. Il est possible que les transformations locales ne soient pas bien définies partout et ne soient pas inversibles. Par exemple à la figure 1.10 est illustrée la transformation $f(z) = \ln z$, qui envoie le plan complexe vers un ruban infini de largeur 2π . Un problème survient dans le voisinage de la demi-droite $y = 0, x \geq 0$, région qui est envoyée vers deux régions éloignées dans le graphe de $f(z)$. Ainsi, alors que les trois droites radiales (en bleu) se croisent à l'origine avec des angles de $\pi/3$ dans la figure de gauche, elles ne se croisent pas dans celle de droite et sont plutôt représentées par six droites parallèles.

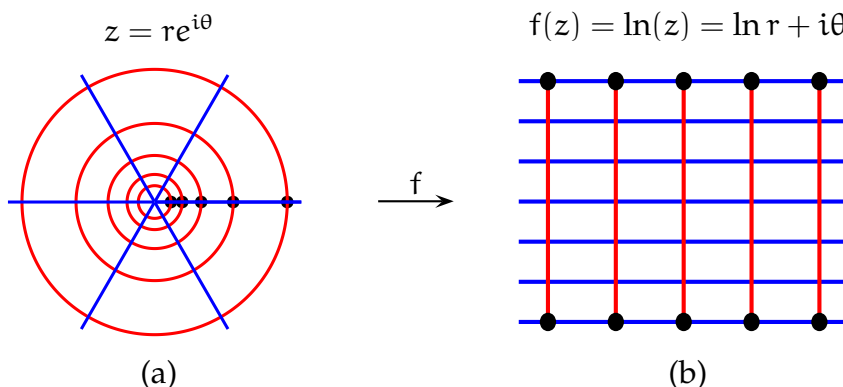


FIGURE 1.10 – Une transformation du plan complexe qui conserve les angles localement : $f(z) = \ln(z)$.

Une propriété remarquable des transformations conformes infinitésimales en deux dimensions est qu'elles forment une algèbre de Lie de dimension infinie. Pour être conforme, une transformation $f(z, \bar{z})$ doit être soit holomorphe ou antiholomorphe, c'est-à-dire s'écrire comme $f(z)$ ou comme $f(\bar{z})$. Il est utile d'étudier les transformations conformes avec leur écriture sous forme de série de Laurent,

$$f(z) = \sum_{k \in \mathbb{Z}} c_k z^k, \quad f(\bar{z}) = \sum_{k \in \mathbb{Z}} d_k \bar{z}^k, \quad (1.3.1)$$

où le nombre de c_k et d_k non nuls avec $k < 0$ est fini. Les transformations infinitésimales qui transforment z en $z + c_i z^i$ et \bar{z} en $\bar{z} + d_i \bar{z}^i$ sont générées par les opérateurs

$L_i = z^{i+1} \frac{d}{dz}$ et $\bar{L}_i = \bar{z}^{i+1} \frac{d}{d\bar{z}}$ qui satisfont les relations de commutation

$$[L_i, L_j] = (j - i)L_{i+j}, \quad [\bar{L}_i, \bar{L}_j] = (j - i)\bar{L}_{i+j}, \quad [L_i, \bar{L}_j] = 0. \quad (1.3.2)$$

Ce sont là deux copies de l'algèbre de *Witt*. On peut trouver une bonne introduction sur les transformations conformes dans [24].

1.3.2 Les hypothèses d'invariance conforme et d'universalité des modèles statistiques

L'objectif de cette section est de décrire deux hypothèses à propos des modèles statistiques, l'invariance conforme et l'universalité, qui ont des conséquences remarquables pour la compréhension des modèles statistiques à leurs points critiques.

Dans la définition des modèles statistiques introduits précédemment, plusieurs symétries sont manifestes. Par exemple pour un réseau carré, on peut s'attendre à une invariance du modèle sous les rotations de 90° . Lorsque des conditions périodiques sont imposées dans les deux directions, il est manifeste que le modèle est invariant sous les translations verticales et horizontales du système.

Lorsque $N \rightarrow \infty$, le groupe des transformation sous lesquelles les modèles sont invariants grandit. Certaines manifestations de ce groupe de symétrie élargi sont apparentes à la figure 1.8. Par exemple, pour des conditions aux frontières autres que périodiques, l'invariance sous rotation et translation se manifeste comme ceci : dans les régions du réseau assez éloignées des frontières pour ne ressentir aucun effet de bord, les observables physiques sont invariantes de l'emplacement de la région dans le réseau et de l'orientation de celui-ci. Autrement dit, un observateur futé auquel nous fournissons le zoom d'une région du réseau aurait bien du mal à identifier l'emplacement de la région agrandie dans le reste du réseau. Dans les trois configurations sélectionnées lors de la simulation, l'invariance sous une rotation par 90° semble être étendue à une invariance plus grande, sous des rotations quelconques. En $T = T_c$, cette invariance se traduit par une dépendance des fonctions de corrélations à deux points en $|\kappa_i - \kappa_j|$ uniquement. Par contre, regarder la figure 1.8 peut aussi être trompeur, puisque pour $T > T_c$, les fonctions de corrélations se comportent comme en (1.1.2), avec des longueurs de corrélations ξ qui peuvent dépendre de la direction étudiée dans le système et ne pas être invariantes sous n'importe quelle rotation [8].

En $T = T_c$, une symétrie supplémentaire fait son apparition : la dilatation. Dans la figure 1.8 (b), il y a coexistence de petites et de grosses plages de spins de même

signe. Si on prend un sous-domaine du réseau et que l'on effectue un agrandissement, on trouve que cette propriété est inchangée et que la configuration obtenue a un comportement fractal : elle a les mêmes caractéristiques que la configuration originale. Plus exactement, l'invariance sous dilatation se manifeste par un comportement en loi d'échelle de la fonction de corrélation (voir l'équation (1.1.4)).

L'invariance sous certaines transformations conformes globales des modèles statistiques bidimensionnels en leur point critique mène naturellement à la question suivante : ces modèles sont-ils invariants sous tout le groupe des transformations conformes ? Pour le modèle de percolation, l'hypothèse d'invariance conforme a d'abord été vérifiée numériquement [2], puis prouvée pour le réseau triangulaire [7]. Cette invariance se manifeste notamment comme ceci : soit un réseau carré sur lequel un modèle de percolation est défini. Nous dessinons sur ce réseau deux courbes fermées \mathcal{C}_1 et \mathcal{C}_2 , qui prennent des formes possiblement différentes. Supposons maintenant que sur \mathcal{C}_1 , nous identifions quatre points A , B , C et D et définissons $\pi(\overline{AB} \rightarrow \overline{CD})$ comme étant la probabilité de traversée en percolation entre l'intervalle de \mathcal{C}_1 compris entre A et B et celui entre C et D . Le théorème de l'application conforme de Riemann nous assure qu'il existe une transformation conforme $f(z)$ qui envoie \mathcal{C}_1 sur \mathcal{C}_2 et la région contenue dans \mathcal{C}_1 sur celle dans \mathcal{C}_2 . Les points A , B , C et D sont envoyés vers $A' = f(A)$, $B' = f(B)$, $C' = f(C)$ et $D' = f(D)$ (voir figure 1.11). Certains problèmes peuvent apparaître si les domaines ont des coins, c'est-à-dire si les courbes \mathcal{C}_1 et \mathcal{C}_2 ne sont pas dérivables en certains points (c'est le cas de la courbe \mathcal{C}_1 dans la figure 1.11). Le théorème de l'application de Riemann assure alors qu'il existe une fonction f qui est conforme à l'intérieur des domaines et continue à la frontière.

Si on réduit la maille du réseau carré jusqu'à atteindre 0 en laissant la taille de \mathcal{C}_1 et de \mathcal{C}_2 inchangées, alors l'hypothèse d'invariance conforme du modèle de percolation énonce alors qu'en $p = p_c$,

$$\pi(\overline{AB} \rightarrow \overline{CD}) = \pi(\overline{A'B'} \rightarrow \overline{C'D'}).$$

Qui plus est, lorsque la courbe \mathcal{C}_2 est le cercle de rayon unité, la probabilité de traversée $\pi(\overline{A'B'} \rightarrow \overline{C'D'})$ ne dépend que du rapport anharmonique

$$\eta = \frac{(A' - B')(C' - D')}{(A' - C')(B' - D')}$$

où A' , B' , C' et D' sont les points sur le cercle unité vers lesquels A , B , C et D sont

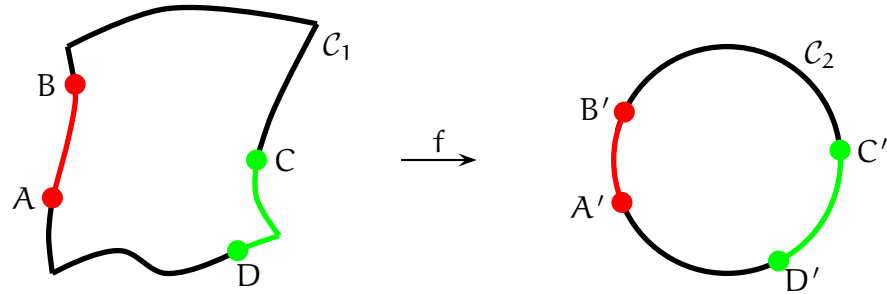


FIGURE 1.11 – La transformation conforme f envoie le domaine fermé de gauche vers le disque unité de droite. Les points A' , B' , C' et D' sont les images de A , B , C et D sous f .

envoyés. Cette probabilité est donnée par la formule de Cardy [26],

$$\pi(\overline{A'B'} \rightarrow \overline{C'D'}) = \frac{3\Gamma(\frac{2}{3})}{\Gamma(\frac{1}{3})^2} \eta^{\frac{1}{3}} {}_2F_1(\frac{1}{3}, \frac{2}{3}; \frac{4}{3}; \eta) \quad (1.3.3)$$

où ${}_2F_1$ est la fonction hypergéométrique. Avec l'invariance conforme, l'équation (1.3.3) permet le calcul des probabilités de traversée pour n'importe quel domaine compris à l'intérieur d'une courbe fermée \mathcal{C} , tant et aussi longtemps que la fonction f transformant \mathcal{C} en le cercle unité est connue.

Ceci nous amène naturellement à la deuxième hypothèse, l'universalité. Bien que les deux seuls cas avec preuve de l'invariance conforme en deux dimensions sont la percolation sur le réseau triangulaire [7] et le modèle d'Ising sur le réseau carré [27], il est généralement accepté que les modèles de percolation et d'Ising sur d'autres réseaux sont aussi invariants conformes, et de même pour les modèles de Potts à Q états et de Fortuin-Kasteleyn. Deux modèles sont dans la même classe d'universalité si ils ont à leur point critique des comportements similaires : ils ont les mêmes exposants critiques et toutes leurs fonctions de corrélation sont identiques. Plusieurs quantités macroscopiques auront un comportement qui sera indépendant du détail microscopique du réseau et même des conditions aux limites. De nombreux indicateurs nous poussent à croire que les modèles de percolation par site et par lien sur des réseaux carrés, triangulaires, hexagonaux, etc., sont dans la même classe d'universalité. Le modèle d'Ising en deux dimensions sur tous ces réseaux formeraient aussi une classe d'universalité, distincte de celle des modèles de percolation. Il n'existe par contre aucune preuve de l'hypothèse d'universalité des modèles statistiques.

Ces deux hypothèses, l'invariance conforme et l'universalité, ont d'autres conséquences remarquables, comme nous le verrons à la prochaine section.

1.3.3 L'algèbre de Virasoro et ses représentations irréductibles

Dans certains systèmes de mécanique quantique, il est possible d'utiliser la théorie de la représentation pour calculer le spectre d'hamiltoniens, notamment lorsqu'il s'agit de l'un des générateurs de l'algèbre sous laquelle le modèle est invariant. Par exemple, pour l'atome d'hydrogène, l'hamiltonien admet une séparation de variables entre une partie radiale et une partie azimutale qui s'avère être le générateur L^2 de l'algèbre $su(2)$. L'information sur la physique du système est alors contenue dans les valeurs propres de cet opérateur dans les représentations irréductibles et unitaires de $su(2)$. Pour les modèles statistiques, l'opérateur dont nous voulons connaître les valeurs propres est la matrice de transfert et il n'est pas évident, a priori, que son spectre peut être trouvé en étudiant le spectre d'un générateur L_i introduit à la section 1.3.1, mais c'est effectivement le cas. L'identification est la suivante :

$$\lim_{N \rightarrow \infty} \mathcal{T}_N(\mathbf{u}) \leftrightarrow z^{L_0}, \quad (1.3.4)$$

où z est une constante à déterminer. Un argument peu rigoureux qui mène à cette identification est le suivant : dans le plan complexe, par exemple celui de la figure 1.10 (a), l'opérateur L_0 est responsable des transformations infinitésimales de dilatation et de rotation, puisque $(1 + \epsilon L_0)z = (1 + \epsilon)z$ engendre une rotation si ϵ est imaginaire et une dilatation s'il est réel. Or les réseaux sur lesquels nous concentrons nos efforts pour les modèles de spins sont périodiques dans la direction verticale. La transformation $f(z) = \ln z$ envoie justement le plan complexe vers un ruban dont le haut et le bas sont identifiés. Qui plus est, l'action radiale et azimutale de L_0 devient, par f , une action de translation horizontale et verticale dans la figure 1.10 (b). Si on retourne à la définition de la matrice de transfert, on s'aperçoit que son action est très analogue à celle d'une telle translation : elle permet de passer d'une ligne de spins à la suivante (voir la figure 1.6 (b)).

L'identification entre la matrice de transfert et l'opérateur L_0 , obtenue par la construction des théories des champs conformes, doit être précisée. Pour un réseau comme celui de la figure 1.6, les valeurs propres de la matrice de transfert, dans la limite $N \rightarrow \infty$, ont la forme [17, 45]

$$\frac{1}{2} \ln(\Lambda_i(\mathbf{u})) = -2Nf_s - f_f - \frac{\pi}{2N} \sin\left(\frac{\pi \mathbf{u}}{\lambda}\right) \left(-\frac{c}{24} + \gamma_i\right)$$

où γ_i est une valeur propre de L_0 , f_s est l'énergie libre par spin, f_f l'énergie libre due aux spins à la frontière et c la charge centrale, un paramètre qui dépend du

modèle et sera défini plus loin. Les énergies libres f_s et f_f dépendent aussi du modèle ; par exemple l'énergie libre par spin du modèle d'Ising est donnée à l'équation (1.2.9). L'opérateur d'évolution L_0 donne donc beaucoup d'information sur la théorie physique et son spectre, c'est-à-dire l'ensemble de ses valeurs propres, est une première chose à calculer. Toute l'information sur les valeurs propres de L_0 et ses dégénérescences est contenue dans le *caractère* de L_0 ,

$$\chi(z) = \sum_i z^{\gamma_i},$$

où z est une constante $\in \mathbb{C}$ et la somme est sur toutes les valeurs propres γ_i de L_0 dans une représentation donnée.

La théorie de la représentation de l'algèbre de symétrie joue un rôle crucial dans ce calcul. L'algèbre de Witt, identifiée plus tôt, n'est pas la seule qui soit importante dans l'étude des phénomènes critiques. Puisque la limite thermodynamique des modèles sur réseau est souvent décrite par une théorie des champs quantiques, l'état du système physique est alors représenté par un rayon dans un espace d'Hilbert et la construction des représentations agissant sur l'espace d'Hilbert doit inclure cette liberté sur la phase du vecteur représentant le système. Ces représentations sont appelées *représentations projectives*. Une façon efficace de les étudier est d'étendre l'algèbre de symétries, ici l'algèbre de Witt, par un élément central C représentant l'action des générateurs le long des rayons. L'extension de l'algèbre de Witt par cet élément est appelée l'algèbre de Virasoro et c'est cette algèbre qui décrit de nombreuses familles de systèmes physiques en leur point critique. Le générateur supplémentaire C , la *charge centrale*, commute avec tous les générateurs L_i , mais apparaît dans les relations de commutation $[L_i, L_{-i}]$. Ce générateur est toujours représenté par un multiple de l'identité, $C = c \cdot \text{id}$. Les relations

$$[L_i, C] = 0, \quad [L_i, L_j] = (j - i)L_{i+j} + \frac{C}{12}(j^3 - j)\delta_{i,-j}, \quad (1.3.5)$$

définissent **Vir**, l'algèbre de Virasoro. Le modèle de percolation, d'Ising et de 3-Potts sont décrits par des charges centrales respectives de $c = 0$, $c = \frac{1}{2}$ et $c = \frac{4}{5}$ et, pour le modèle de Fortuin-Kasteleyn avec paramètre $\beta = 2 \cos \lambda$, par

$$c = 1 - \frac{6(\lambda/\pi)^2}{1 - \lambda/\pi}.$$

Puisqu'un système physique critique est caractérisé par une charge centrale c donnée, il est important de connaître les représentations de l'algèbre de Virasoro où

l'élément central C prend cette valeur. Dans les travaux originaux de Belavin, Polyakov et Zamolodchikov [16], certaines hypothèses sont d'origine physique : tout d'abord, l'existence d'un plus haut poids (lié au comportement à petite distance des fonctions de corrélation), et ensuite, l'unitarité (qui est naturelle en théorie des champs, mais moins naturelle en mécanique statistique). Enfin, une troisième hypothèse, l'irréductibilité des représentations, est habituelle en théorie des champs : cependant, nous montrerons dans la présente thèse que cette hypothèse n'est pas réalisée dans plusieurs systèmes physiques. La construction détaillée des représentations de plus haut poids, irréductibles et unitaires dépasse les visées de cette thèse. Nous nous contentons d'énumérer les étapes de cette construction et de donner les résultats pour le modèle d'Ising.

- Réaliser que \mathbf{Vir} se scinde en $\mathbf{Vir} = \mathbf{Vir}_- \oplus \mathbf{Vir}_0 \oplus \mathbf{Vir}_+$, où

$$\mathbf{Vir}_0 = \mathbb{C} L_0 \oplus \mathbb{C} C, \quad \mathbf{Vir}_+ = \bigoplus_{i=1}^{\infty} \mathbb{C} L_i, \quad \mathbf{Vir}_- = \bigoplus_{i=1}^{\infty} \mathbb{C} L_{-i},$$

et que chacun des \mathbf{Vir}_- , \mathbf{Vir}_+ et \mathbf{Vir}_0 est une sous-algèbre de \mathbf{Vir} .

- Supposer l'existence d'un vecteur $|v\rangle$ de plus haut poids h , propre de L_0 , c'est-à-dire que $L_0|v\rangle = h|v\rangle$ et $L_i|v\rangle = 0$ pour tout $i < 0$.
- Construire l'ensemble des vecteurs descendants de $|v\rangle$, $L_{k_1} L_{k_2} \dots L_{k_n} |v\rangle$ (pour $k_i > 0, \forall i$) et trouver une base de vecteurs indépendants engendrant cet espace vectoriel. En utilisant les relations (1.3.5), on peut montrer que chacun de ces vecteurs est propre de L_0 avec valeur propre $\lambda = h + \sum_{i=1}^n k_i$. L'opérateur L_0 est donc diagonal. On appelle *module de Verma* $V_{c,h}$ l'ensemble des vecteurs descendants d'un vecteur de plus haut poids, et un exemple d'un tel module est illustré à la figure 1.12.
- Il peut arriver, pour certaines valeurs précises de h et c , que certains états $|w\rangle$, combinaisons linéaires de vecteurs descendants de $|v\rangle$ au niveau h' (avec $h' - h \in \mathbb{N}$), soient tels que $L_i|w\rangle = 0$ pour tout $i < 0$. Le vecteur $|w\rangle$ engendre lui-même une représentation de \mathbf{Vir} de plus haut poids h' et est dit *singulier*. Les représentations irréductibles de l'algèbre \mathbf{Vir} sont obtenues en quotientant le module de Verma $V_{c,h}$ par les sous-modules générés par ses descendants singuliers. En introduisant une forme bilinéaire sur les vecteurs descendants (la *forme de Shapovalov*), il est possible d'identifier, pour une charge centrale c fixée, les niveaux h' de ces descendants singuliers : ces niveaux h' sont ceux pour lesquels le déterminant de la forme bilinéaire s'annule.
- Imposer l'unitarité, c'est-à-dire imposer qu'aucun descendant de $|v\rangle$ n'ait une norme nulle ou négative vis-à-vis la forme de Shapovalov.

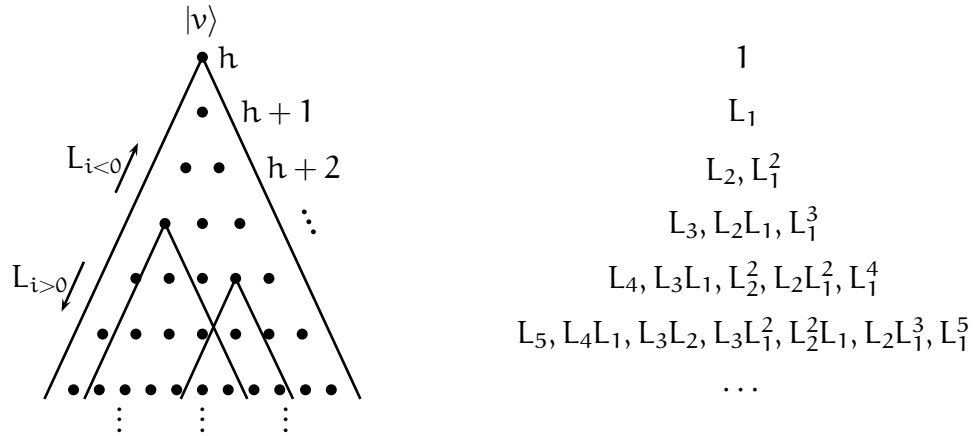


FIGURE 1.12 – Un module de Verma $V_{c,h}$ est engendré par un vecteur $|v\rangle$ au niveau h . Lorsqu'on y applique les opérateurs L_i , $i > 0$, celui-ci engendre des descendants aux niveaux $h+1$, $h+2$, etc. Le nombre de descendants (indépendants via les équations (1.3.5) qui définissent \mathbf{Vir}) au niveau $h+n$ est $p(n)$, le nombre de partitions de l'entier n , et est fidèlement représenté par le nombre de points noirs au niveau $h+n$. Une représentation graphique d'un module de Verma est donnée à gauche et, à droite, nous donnons les opérateurs qui engendrent les premiers descendants lorsqu'appliqués à $|v\rangle$. Certains descendants peuvent être singuliers et engendrer des sous-modules dont il faut faire le quotient pour obtenir une représentation irréductible. Ceux-ci apparaissent aux niveaux $h+3$ et $h+4$ sur sur le diagramme. Les sous-modules peuvent avoir un patron d'imbrication non-trivial, et c'est le cas pour le modèle d'Ising.

Dans l'algèbre $\mathfrak{su}(2)$ intervenant dans la description de l'atome d'hydrogène, il résulte des conditions d'irréductibilité et d'unitarité que les représentations sont de dimension finie et que les plus hauts poids h peuvent seulement être entiers ou demi-entiers. Pour l'algèbre \mathbf{Vir} , la situation est différente, notamment parce que les représentations sont, sauf exception, des matrices infinies. Les seules valeurs de $c < 1$ et de h pour lesquelles les représentations construites sont irréductibles et unitaires sont [28]

$$c = c(m) = 1 - \frac{6}{m(m+1)}, \quad h = h_{r,s} = \frac{((m+1)r - ms)^2 - 1}{4m(m+1)}, \quad (1.3.6)$$

avec $m \in \mathbb{N}$, $1 \leq r < m$ et $1 \leq s < m+1$. Pour une valeur de c fixée, on appelle la *table de Kac* le tableau des valeurs des plus hauts poids $h_{r,s}$ compatibles pour une charge centrale donnée $c(m)$. Aux valeurs $m = 2, 3$ et 5 sont associées les charges centrales respectives des modèles de percolation, d'Ising et de 3-Potts. Les tables de Kac de ces deux derniers modèles sont données sur fond blanc à la figure 1.13. Les théories des champs décrites par les valeurs données en (1.3.6) sont dites *rationnelles*. Cet épithète est réservé à une famille de théories des champs conformes

qui peuvent être décrites avec un nombre fini de champs primaires étiquetés par les plus hauts poids de la table de Kac. (Ces champs doivent être fermés sous l'opération "produit d'opérateurs". Voir [24].)

$\frac{5}{2}$	1	$\frac{1}{6}$	0
$\frac{21}{16}$	$\frac{5}{16}$	$-\frac{1}{48}$	$\frac{5}{16}$
$\frac{1}{2}$	0	$\frac{1}{6}$	1
$\frac{1}{16}$	$\frac{1}{16}$	$\frac{35}{48}$	$\frac{33}{16}$
0	$\frac{1}{2}$	$\frac{5}{3}$	$\frac{7}{2}$

(a)

7	$\frac{22}{5}$	$\frac{12}{5}$	1	$\frac{1}{5}$	0
$\frac{115}{24}$	$\frac{323}{120}$	$\frac{143}{120}$	$\frac{7}{24}$	$-\frac{1}{120}$	$\frac{7}{24}$
3	$\frac{7}{5}$	$\frac{2}{5}$	0	$\frac{1}{5}$	1
$\frac{13}{8}$	$\frac{21}{40}$	$\frac{1}{40}$	$\frac{1}{8}$	$\frac{33}{40}$	$\frac{17}{8}$
$\frac{2}{3}$	$\frac{1}{15}$	$\frac{1}{15}$	$\frac{2}{3}$	$\frac{28}{15}$	$\frac{11}{3}$
$\frac{1}{8}$	$\frac{1}{40}$	$\frac{21}{40}$	$\frac{13}{8}$	$\frac{133}{40}$	$\frac{45}{8}$
0	$\frac{2}{5}$	$\frac{7}{5}$	3	$\frac{26}{5}$	8

(b)

FIGURE 1.13 – Les tables de Kac pour le modèle d'Ising ($c = \frac{1}{2}$) en (a) et de 3-Potts ($c = \frac{4}{5}$) en (b). Dans les cases blanches, les valeurs $h_{r,s}$ qui correspondent aux représentations irréductibles et unitaires.

Pour le modèle d'Ising, en $c = \frac{1}{2}$, il n'existe que trois représentations irréductibles et unitaires, avec plus hauts poids $h = 0, \frac{1}{2}$ et $\frac{1}{16}$. Chacune est de dimension infinie, et un calcul permet de donner aux caractères de L_0 dans ces trois représentations les expressions suivantes [29] :

$$\begin{aligned} \chi_{h=0}(z) &= \frac{1}{2} \left(\prod_{n \in 2\mathbb{N}-1} (1 + z^{n/2}) + \prod_{n \in 2\mathbb{N}-1} (1 - z^{n/2}) \right), \\ \chi_{h=\frac{1}{2}}(z) &= \frac{1}{2} \left(\prod_{n \in 2\mathbb{N}-1} (1 + z^{n/2}) - \prod_{n \in 2\mathbb{N}-1} (1 - z^{n/2}) \right), \\ \chi_{h=\frac{1}{16}}(z) &= z^{\frac{1}{16}} \prod_{n=1}^{\infty} (1 + z^n). \end{aligned}$$

Un grand succès de ce calcul réside dans le fait que la fonction de partition périodique de la section 1.2.4 se réécrit comme

$$Z_{\text{pér}} = \Lambda_0^M \left(\chi_{h=0}(q^2) + \chi_{h=\frac{1}{2}}(q^2) \right) \quad (1.3.7)$$

où $q = \exp(-\frac{\pi \sin(4u)M}{2N})$. Le caractère de la représentation $h = 1/16$ n'intervient pas dans l'expression de $Z_{\text{pér}}$, mais joue un rôle lorsque le choix des conditions aux frontières à la gauche et à la droite du réseau d'Ising de la figure 1.6 est différent. En notant par (c_g, c_d) les contraintes sur ces spins à la gauche et à la droite, alors [17]

$$Z = \Lambda_0^M \times \begin{cases} \chi_0(q^2) & \text{avec conditions } (+, +), \\ \chi_{\frac{1}{2}}(q^2) & \text{avec conditions } (+, -), \\ \chi_{\frac{1}{16}}(q^2) & \text{avec conditions } (+, \text{libre}), \end{cases}$$

Le fait que la fonction de partition pour les diverses conditions aux frontières (c_g, c_d) s'écrive avec les caractères des trois mêmes représentations irréductibles de l'algèbre de Virasoro est un indicateur très convainquant de l'hypothèse d'invariance conforme pour le modèle d'Ising. Lorsque le domaine sur lequel le système physique est défini n'a pas de frontière, l'algèbre de symétrie est élargi au produit de deux copies de l'algèbre de Virasoro. Les caractères décrivant le spectre de L_0 sont alors des produits de deux caractères de représentations de l'algèbre de Virasoro. Par exemple, pour le cas de conditions droite-gauche périodiques (sur le tore), la définition de la matrice de transfert est un peu différente et, avec $q = \exp(-\frac{\pi i e^{-4iu}}{2N})$, la fonction de partition est obtenue par

$$Z = \Lambda_0^M \left(\chi_0(q^2)\chi_0(\bar{q}^2) + \chi_{\frac{1}{2}}(q^2)\chi_{\frac{1}{2}}(\bar{q}^2) + \chi_{\frac{1}{16}}(q^2)\chi_{\frac{1}{16}}(\bar{q}^2) \right).$$

L'analyse des systèmes sur de tels domaines est souvent plus ardue que celle sur une géométrie avec frontière comme celle du ruban. La complexité des résultats que nous trouvons au chapitre 4 relativement à ceux du chapitre 2 en est peut-être un exemple.

Pour les autres valeurs de la charge centrale, le calcul des caractères des représentations irréductibles est possible, mais les formes ne sont pas aussi simples et ne permettent pas de vérification aussi spectaculaire, puisque le spectre des matrices de transfert de spins n'est pas connu. Aussi les succès de la théorie des champs conforme s'étendent au-delà du calcul des fonctions de partition. Elles parviennent par exemple à décrire les fonctions de corrélations à n points et à faire certaines prédictions pour les exposants critiques d'observables géométriques (par exemple dans [30]).

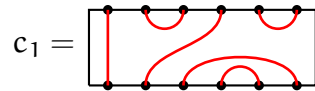
1.4 La matrice de transfert du modèle de boucles

Le calcul de la fonction de partition du modèle de Fortuin-Kasteleyn peut aussi être fait avec des matrices de transfert, dites de boucles. Nous étudierons les caractéristiques

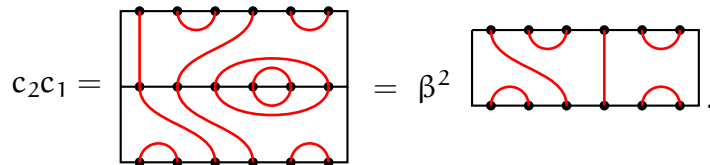
téristiques de ces matrices de transfert pour deux géométries : $D_N(\lambda, u)$ sur le ruban (conditions ouvertes) et $T_N(\lambda, v)$ sur le tore (conditions périodiques). Les deux objets sont des éléments d'une algèbre abstraite, l'algèbre de Temperley-Lieb, qui est adaptée au choix de la géométrie. Puisque les objets mathématiques sont plus simples sur le ruban, nous choisissons d'introduire ce cas dans le cadre de cette introduction. Cette section se veut donc une préparation au chapitre 2 : nous décrivons la construction de $D_N(\lambda, u)$ et certaines de ses propriétés qui suscitent notre intérêt, dont plusieurs sont tirées de [45].

1.4.1 L'algèbre de Temperley-Lieb

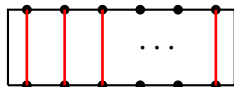
Avant de pouvoir introduire la matrice de transfert du modèle de boucles, il faut définir une algèbre abstraite, l'algèbre de Temperley-Lieb $TL_N(\beta)$, dont les éléments sont des *connectivités*. Soit un rectangle sur lequel on identifie N points sur chacun des segments inférieur et supérieur. Une connectivité c_1 est une connexion de deux des $2N$ points par des courbes ne s'intersectant pas et contraintes à demeurer à l'intérieur du rectangle. Par exemple, pour $N = 6$,



est une connectivité. Si deux connectivités c_1 et c_2 sont telles qu'il est possible de déformer continûment les courbes c_1 en celles de c_2 , alors c_1 et c_2 sont considérées égales. Avec cette définition, le nombre de connectivités est fini et égal à $\frac{1}{N+1} \binom{2N}{N}$. Le produit entre deux connectivités c_1 et c_2 , dépendant d'un paramètre complexe β , est défini de la manière suivante : pour calculer c_2c_1 , il faut apposer le diagramme de c_1 sur celui de c_2 et relier les N points du segment supérieur de c_2 à ceux du segment inférieur de c_1 . La connectivité résultante est obtenue en lisant, dans le diagramme résultant, la connexion entre les points du haut et ceux du bas. Il est possible que certaines courbes soient fermées à la frontière entre c_1 et c_2 , et pour chacune il faut ajouter à la connectivité résultante un poids β . Par exemple,



Pour ce produit, la connectivité



agit à titre d'identité : elle laisse inchangée toute connectivité qui la multiplie et sera notée id . L'algèbre de Temperley-Lieb $\mathcal{TL}_N(\beta)$ est alors l'espace vectoriel généré par les connectivités, muni du produit entre celles-ci. Autrement dit, $\mathcal{TL}_N(\beta)$ comprend non seulement les connectivités, mais aussi leurs combinaisons linéaires, et le produit est étendu linéairement lorsqu'appliqué à des combinaisons linéaires de connectivités.

Il est possible de donner une définition alternative de $\mathcal{TL}_N(\beta)$. Soit les $N - 1$ connectivités e_i suivantes :

$$e_i = \begin{array}{c} \text{---} \bullet \text{---} \bullet \text{---} \bullet \text{---} \bullet \text{---} \bullet \text{---} \\ | \quad | \quad | \quad | \quad | \quad | \quad | \\ \dots \\ | \quad | \quad | \quad | \quad | \quad | \quad | \\ \text{---} \bullet \text{---} \bullet \text{---} \bullet \text{---} \bullet \text{---} \bullet \text{---} \\ 1 \quad 2 \quad i \quad \dots \quad N \end{array} \quad i = 1, \dots, N - 1.$$

Avec la définition du produit entre connectivités, ces générateurs satisfont les relations

$$\begin{aligned} e_i^2 &= \beta e_i, \\ e_i e_j &= e_j e_i, \quad \text{pour } |i - j| > 1, \\ e_i e_{i \pm 1} e_i &= e_i \quad \text{lorsque } i, i \pm 1 \in \{1, 2, \dots, N - 1\}, \end{aligned} \tag{1.4.1}$$

par exemple,

$$\begin{aligned} e_i^2 &= \begin{array}{c} \text{---} \bullet \text{---} \bullet \text{---} \bullet \text{---} \bullet \text{---} \bullet \text{---} \\ | \quad | \quad | \quad | \quad | \quad | \quad | \\ \dots \\ | \quad | \quad | \quad | \quad | \quad | \quad | \\ \text{---} \bullet \text{---} \bullet \text{---} \bullet \text{---} \bullet \text{---} \bullet \text{---} \\ 1 \quad 2 \quad i \quad \dots \quad N \end{array} = \beta \begin{array}{c} \text{---} \bullet \text{---} \bullet \text{---} \bullet \text{---} \bullet \text{---} \bullet \text{---} \\ | \quad | \quad | \quad | \quad | \quad | \quad | \\ \dots \\ | \quad | \quad | \quad | \quad | \quad | \quad | \\ \text{---} \bullet \text{---} \bullet \text{---} \bullet \text{---} \bullet \text{---} \bullet \text{---} \\ 1 \quad 2 \quad i \quad \dots \quad N \end{array} = \beta e_i, \\ \\ e_i e_{i+1} e_i &= \begin{array}{c} \text{---} \bullet \text{---} \bullet \text{---} \bullet \text{---} \bullet \text{---} \bullet \text{---} \\ | \quad | \quad | \quad | \quad | \quad | \quad | \\ \dots \\ | \quad | \quad | \quad | \quad | \quad | \quad | \\ \text{---} \bullet \text{---} \bullet \text{---} \bullet \text{---} \bullet \text{---} \bullet \text{---} \\ 1 \quad 2 \quad i \quad \dots \quad N \end{array} = \begin{array}{c} \text{---} \bullet \text{---} \bullet \text{---} \bullet \text{---} \bullet \text{---} \bullet \text{---} \\ | \quad | \quad | \quad | \quad | \quad | \quad | \\ \dots \\ | \quad | \quad | \quad | \quad | \quad | \quad | \\ \text{---} \bullet \text{---} \bullet \text{---} \bullet \text{---} \bullet \text{---} \bullet \text{---} \\ 1 \quad 2 \quad i \quad \dots \quad N \end{array} = e_i. \end{aligned}$$

On peut aussi montrer que toute connectivité peut être écrite en termes d'un produit de e_i s. Par exemple, $c_1 = e_4 e_3 e_2 e_5$ et $c_2 = e_1 e_2 e_3 e_5 e_4$. Pour calculer $c_2 c_1$, il suffit d'apposer l'expression de c_2 en termes des e_i s devant celle de c_1 et de simplifier en utilisant les relations (1.4.1). Dans l'exemple précédent, on trouve, par ce processus, $c_2 c_1 = \beta^2 e_5 e_1 e_2$. L'algèbre de Temperley-Lieb est donc l'ensemble

des *mots* possibles (et de leurs combinaisons linéaires) avec les *lettres* (*générateurs*) $\text{id}, e_1, \dots, e_{N-1}$, et deux mots sont équivalents si, en utilisant (1.4.1), ils admettent la même écriture. Ainsi, l'algèbre de Temperley-Lieb est formellement définie par $\mathbb{T}_N(\beta) = \langle \text{id}, e_1, e_2, \dots, e_{N-1} \rangle / (\text{les relations (1.4.1)})$. Cette algèbre sera utilisée aux chapitres 2 et 3 pour les conditions limites du ruban, et sa généralisation au cas périodique sera présentée à la section 4.2.1.

1.4.2 La matrice double-ligne $D_N(\lambda, u)$

La matrice de transfert pour le modèle de boucles, dite *matrice double-ligne* et notée $D_N(\lambda, u)$, est un élément de l'algèbre de $\mathbb{T}_N(\beta)$. C'est une somme pondérée de connectivités, donnée par

$$D_N(\lambda, u) = \begin{array}{c} \overbrace{\hspace{10em}}^N \\ \begin{array}{|c|c|c|c|} \hline \cdot & \cdot & & \cdot \\ \hline \lambda-u & \lambda-u & \dots & \lambda-u \\ \hline u & u & & u \\ \hline \cdot & \cdot & & \cdot \\ \hline \end{array} \end{array} \quad (1.4.2)$$

où chaque tuile $\begin{array}{|c|} \hline u \\ \hline \end{array}$ est la combinaison linéaire

$$\begin{array}{|c|} \hline u \\ \hline \end{array} = \sin(\lambda - u) \begin{array}{|c|} \hline \text{red arcs} \\ \hline \end{array} + \sin u \begin{array}{|c|} \hline \text{red arcs} \\ \hline \end{array}. \quad (1.4.3)$$

Le paramètre λ , dit *paramètre spectral*, est pris dans l'intervalle $(0, \pi/2)$ et est relié au paramètre β par la relation $\beta = 2 \cos \lambda$. (La définition de $D_N(\lambda, u)$ pour $\lambda = \pi/2$ utilisée au chapitre 3 aura une normalisation différente.) Le paramètre $u \in [0, \lambda]$ est le paramètre d'anisotropie et nous montrerons à la section 2.2.4 qu'il est relié au paramètre d'anisotropie u défini pour les modèles de spins (voir l'équation 1.2.12). Puisque dans (1.4.2), il y a $2N$ tuiles, la matrice double-ligne $D_N(\lambda, u)$ est une somme de 2^{2N} termes. Par exemple, pour $N = 2$,

$$D_2(\lambda, u) = \begin{array}{c} \begin{array}{|c|c|} \hline \cdot & \cdot \\ \hline \text{red arcs} \\ \hline \end{array} + \begin{array}{|c|c|} \hline \cdot & \cdot \\ \hline \text{red arcs} \\ \hline \end{array} \\ \sin^2 u \sin^2(\lambda - u) \quad \sin u \sin^3(\lambda - u) \\ + \begin{array}{|c|c|} \hline \cdot & \cdot \\ \hline \text{red arcs} \\ \hline \end{array} + \begin{array}{|c|c|} \hline \cdot & \cdot \\ \hline \text{red arcs} \\ \hline \end{array} + \begin{array}{|c|c|} \hline \cdot & \cdot \\ \hline \text{red arcs} \\ \hline \end{array} \\ \beta \sin u \sin^3(\lambda - u) \quad \beta \sin^2 u \sin^2(\lambda - u) \quad \sin u \sin^3(\lambda - u) \end{array}$$

$$\begin{aligned}
& + \begin{array}{c} \text{Diagram 1} \\ \beta^2 \sin^2 u \sin^2(\lambda - u) \end{array} + \begin{array}{c} \text{Diagram 2} \\ \beta \sin^2 u \sin^2(\lambda - u) \end{array} + 9 \text{ autres termes} \\
& = \alpha_1 \begin{array}{c} \text{Diagram 3} \end{array} + \alpha_2 \begin{array}{c} \text{Diagram 4} \end{array}
\end{aligned} \tag{1.4.4}$$

où les poids des connectivités ont exceptionnellement été placés sous celles-ci. Notons aussi qu'un facteur β a été ajouté pour chaque boucle fermée. Chacun des seize diagrammes peut être déformé en la connectivité id ou en e_1 . La matrice double-ligne $D_2(\lambda, u)$ est donc une combinaison linéaire de ces deux générateurs, et les poids α_1 et α_2 , deux fonctions de u et de λ (et de $\beta = 2 \cos \lambda$), apparaissent à l'équation (2.2.1).

1.4.3 Des identités utiles

La matrice de transfert satisfait certaines relations de symétrie qui sont le sujet de la section 1.4.4. Dans cette section, nous développons quatre identités qui sont satisfaites par les tuiles \boxed{u} et seront utiles pour étudier ces symétries. La première, dite *relation de croisement*, prend la forme suivante :

$$\boxed{\lambda - u} = \sin u \begin{array}{c} \text{Diagram 5} \end{array} + \sin(\lambda - u) \begin{array}{c} \text{Diagram 6} \end{array} = \boxed{u} \tag{1.4.5}$$


où \boxed{u} signifie que, par rapport à l'équation (1.4.3), les deux tuiles ont subi une rotation de 90° .

Pour les trois autres identités de cette section, la méthode est la même : il faut identifier les *sorties*, c'est-à-dire les positions où les courbes quittent le diagramme (elles seront indiquées par un point noir \bullet), qui sont équivalentes de part et d'autre de l'équation. Il faut ensuite s'assurer que les poids de chacune des connexions reliant ces sorties sont identiques pour les deux membres de l'équation. La deuxième identité importante est la *relation d'inversion* :

$$\begin{array}{c} \text{Diagram 7} \\ u \quad -u \end{array} = \sin(\lambda - u) \sin(\lambda + u) \begin{array}{c} \text{Diagram 8} \end{array} \tag{1.4.6}$$

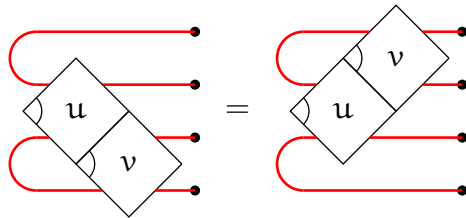
En faisant un développement du terme de gauche, on trouve quatre termes, soit

$$\begin{aligned} & \sin(\lambda - u) \sin(\lambda + u) \text{ [diagram 1]} + \sin(u) \sin(\lambda + u) \text{ [diagram 2]} \\ & + \sin(\lambda - u) \sin(-u) \text{ [diagram 3]} + \beta \sin(u) \sin(-u) \text{ [diagram 4]} . \end{aligned}$$

Puisque pour les trois derniers termes, la connexion entre les sorties est identique, on peut additionner leurs poids. En n'oubliant pas que $\beta = 2 \cos \lambda$, on peut montrer que la somme des poids est nulle, et la seule contribution, le premier terme, a effectivement la même connexion que . Ensuite, la troisième relation est l'équation de Yang-Baxter,

$$\begin{array}{c} \bullet \\ \bullet \\ \bullet \\ \bullet \end{array} \begin{array}{c} \text{v} \\ \text{u} \end{array} \begin{array}{c} \diagup \\ \diagdown \end{array} \begin{array}{c} \bullet \\ \bullet \\ \bullet \\ \bullet \end{array} = \begin{array}{c} \bullet \\ \bullet \\ \bullet \\ \bullet \end{array} \begin{array}{c} \text{v-u} \\ \text{v-u} \end{array} \begin{array}{c} \diagup \\ \diagdown \end{array} \begin{array}{c} \bullet \\ \bullet \\ \bullet \\ \bullet \end{array} , \tag{1.4.7}$$

où le fait que la tuile $v - u$ soit plus grande ne change pas sa signification (1.4.3). Chacun des deux membres de l'équation comporte huit termes et des simplifications trigonométriques montrent que le poids de chaque connexion des six sorties est égal de part et d'autre. Enfin une dernière relation,



porte le nom de *équation de Yang-Baxter à la frontière* et est vérifiée par la même méthode.

1.4.4 Les symétries de la matrices de transfert

La matrice de transfert $D_N(\lambda, u)$ possède plusieurs propriétés remarquables. Parmi celles-ci, on trouve les deux relations suivantes :

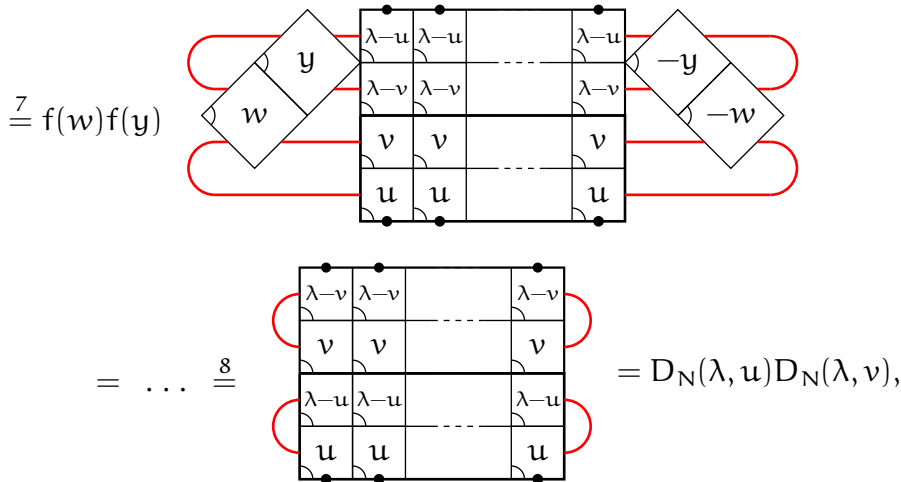
$$[D_N(\lambda, u), D_N(\lambda, v)] = 0, \tag{1.4.8}$$

$$D_N(\lambda, u) = D_N(\lambda, \lambda - u). \tag{1.4.9}$$

Les preuves de ces équations utilisent les identités de la section précédente. Nous nous contentons de prouver la première, qui est aussi la plus compliquée. Cette égalité est non triviale puisqu'elle implique que tous les coefficients des connectivités dans le développement de $D_N(\lambda, u)D_N(\lambda, v) - D_N(\lambda, v)D_N(\lambda, u)$ sont nuls. L'argument, entièrement graphique, est le suivant :

$$D_N(\lambda, v)D_N(\lambda, u) =$$

$$\stackrel{1}{=} \quad \stackrel{2}{=} f(w) \quad \stackrel{3}{=} f(w) \quad \stackrel{4}{=} f(w) \quad \stackrel{5}{=} f(w)f(y) \quad \stackrel{6}{=} f(w)f(y)$$



où $w = u + v - \lambda$, $y = u - v$ et $f(x) = \csc(\lambda + x) \csc(\lambda - x)$, qui n'est pas singulier sur le domaine de λ et de x .

Voici l'explication des étapes de la preuve : dans le diagramme correspondant au produit $D_N(\lambda, v)D_N(\lambda, u)$, deux lignes parallèles sont remplacées par une tuile \diamond (1). Ceci est possible puisque ni les connexions ni les poids ne sont altérés par cette opération. En utilisant la relation d'inversion, la tuile ajoutée est remplacée par deux tuiles d'anisotropie w et $-w$ (2). Le choix de $w = u + v - \lambda$ est judicieux, car il permet d'utiliser l'équation de Yang-Baxter, inversant ainsi les positions des tuiles u et $\lambda - v$ (3). Cette étape est répétée $N - 1$ autres fois, jusqu'à ce que la tuile \diamond ait fait une traversée complète du réseau de tuiles (4). Les étapes 1 et 2 sont ensuite répétées avec des tuiles d'anisotropie y et $-y$ (5). Le choix $y = u - v$ est à nouveau approprié, permettant l'utilisation de l'équation de Yang-Baxter N fois (6). Enfin, les tuiles aux extrémités gauche et droite sont transformées par l'utilisation de l'équation de Yang-Baxter à la frontière (7). À nouveau par l'équation de Yang-Baxter, les tuiles w et y font la traversée dans l'autre direction. En utilisant l'équation d'inversion à deux reprises, on arrive au résultat voulu (8).

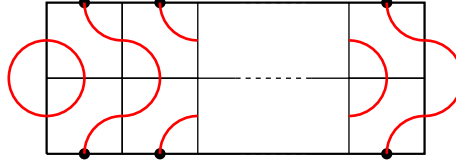
1.4.5 Des quantités plus faciles à étudier : \mathcal{H} et F_N

Étudier la matrice double-ligne $D_N(\lambda, u)$ directement s'avère difficile vu le grand nombre de termes qui entrent dans son développement et la longueur des expressions des coefficients, comme en fait foi l'exemple, pour $N = 2$, de l'équation (1.4.4). Pour remédier à ce problème, nous introduisons deux objets plus simples, l'hamiltonien \mathcal{H} et le plus haut coefficient de Fourier F_N , qui sont obtenus en faisant des développements en série de $D_N(\lambda, u)$ et partagent certaines de ses propriétés. L'ha-

miltonien est obtenu en prenant la série de Taylor de $D_N(\lambda, u)$ autour de $u = 0$. Au premier ordre en u ,

$$\boxed{u} = (\sin \lambda - u \cos \lambda) \begin{array}{|c|} \hline \text{---} \\ \hline \end{array} + u \begin{array}{|c|} \hline \text{---} \\ \hline \end{array} + \mathcal{O}(u^2). \quad (1.4.10)$$

Dans la série de Taylor de $D_N(\lambda, u)$, le terme d'ordre 0 en u est proportionnel à id : l'unique diagramme qui y contribue est donné par



et son poids est $\beta \sin^{2N} \lambda$. Le terme suivant est plus complexe et se divise en $2N$ contributions : pour une des $2N$ tuiles données, à partir de (1.4.10), il faut choisir le terme d'ordre 1 en u pour cette tuile et le terme d'ordre 0 pour toutes les autres. Le terme d'ordre 1 du développement de $D_N(\lambda, u)$ est obtenu en appliquant ce procédé à chacune des $2N$ tuiles et en prenant leur somme. La série résultante est

$$D_N(\lambda, u) = \beta \sin^{2N} \lambda \left(\text{id} + \frac{2u}{\sin \lambda} \left((\beta^{-1} - N \cos \lambda) \text{id} + \mathcal{H} \right) \right) + \mathcal{O}(u^2), \quad \text{où } \mathcal{H} = \sum_{i=1}^{N-1} e_i$$

est l'hamiltonien de boucles. Alors que $D_N(\lambda, u)$ est une somme compliquée de connectivités, l'hamiltonien \mathcal{H} est simplement la somme des générateurs e_i et est plus facile à étudier.

Une autre avenue possible est l'écriture de la matrice double-ligne sous la forme d'une série de Fourier en le paramètre d'anisotropie,

$$D_N(\lambda, v + \lambda/2) = \frac{1}{2} C_0 + \sum_{i=1}^N C_{2i}(\lambda) \cos(2iv),$$

où chaque coefficient de Fourier $C_{2i}(\lambda)$ est un élément de $\mathbb{T}_N(\beta)$. Plusieurs remarques doivent être faites. Tout d'abord, à cause de l'équation (1.4.9), la matrice de transfert $D_N(\lambda, v + \lambda/2)$ est paire en v , et sa série de Fourier en v ne contient que des cosinus. Parce que

$$\boxed{\pi+u} = - \boxed{u},$$

la matrice double-ligne, qui est composée d'un nombre pair de tuiles, satisfait $D_N(\lambda, u + \pi) = D_N(\lambda, u)$: puisque sa périodicité en u est de π , la série de Fourier en v ne contient que les termes $C_j \cos(jv)$ avec j pair. Ensuite, on remarque,

comme à l'équation (1.4.4), que tous les coefficients dans $D_N(\lambda, u)$ ont la forme $\beta^y \sin^x u \sin^{2N-x}(\lambda - u)$ avec $x \in [0, 2N]$ et $y \in \mathbb{N}$. La série de Fourier est donc finie, puisque tous les coefficients C_j avec $j > 2N$ sont nuls. Enfin, la relation de commutation (1.4.8) implique que $[C_i, C_j] = 0$, et de même $[C_i, D_N(\lambda, u)] = [C_i, \mathcal{H}] = 0$, pour tout i, j . Parce qu'ils commutent avec $D_N(\lambda, u)$, on dit que les coefficients de Fourier $C_{2i}(\lambda)$ sont des *quantités conservées*. La relation (1.4.8) qui est une conséquence de l'équation de Yang-Baxter et des autres identités de la section 1.4.3 montre donc que la dynamique représentée par la matrice de transfert $D_N(\lambda, u)$ possède de nombreuses quantités conservées, ce qui vaut à ces modèles le nom de *modèles complètement intégrables*.

Le plus haut coefficient $C_{2N}(\lambda)$ peut être obtenu en prenant la limite de $D_N(\lambda, u)$ vers $u \rightarrow -i\infty$ de manière appropriée (voir la section 2.3.1). Nous montrerons alors que $C_{2N}(\lambda) = 2^{-2N+1}F_N(\lambda)$, où

$$F_N(\lambda) = \begin{array}{c} \overbrace{\hspace{10em}}^N \\ \begin{array}{|c|c|c|c|c|} \hline \bullet & \bullet & \dots & \bullet & \bullet \\ \hline & & & & \\ \hline \bullet & \bullet & \dots & \bullet & \bullet \\ \hline \end{array} \end{array}$$

avec

$$\begin{array}{|c|} \hline \hline \hline \\ \hline \end{array} = ie^{i\lambda/2} \begin{array}{|c|} \hline \text{---} \\ \hline \end{array} - ie^{-i\lambda/2} \begin{array}{|c|} \hline \text{---} \\ \hline \end{array}$$

et $\begin{array}{|c|} \hline \hline \hline \\ \hline \end{array}$ est la rotation de $\begin{array}{|c|} \hline \hline \hline \\ \hline \end{array}$ par 90° . L'élément $F_N(\lambda)$ sera d'une grande utilité au chapitre 2 pour comprendre la structure de Jordan de $D_N(\lambda, u)$.

1.4.6 La représentation ρ et les premiers blocs de Jordan

Pour calculer les fonctions de partition des modèles statistiques, la forme de $D_N(\lambda, u)$ en tant qu'élément de l'algèbre abstraite $\mathcal{TL}_N(\beta)$ n'est pas utile. Dans cette section, nous décrivons la construction de la représentation des vecteurs de connectivité de $\mathcal{TL}_N(\beta)$ et donnons les premiers exemples de blocs de Jordan qui apparaissent dans ces représentations, qui seront étudiées au chapitre 2.

Soit N points alignés et équidistants sur un segment (imaginaire) horizontal. Un *vecteur de connectivité* (ou *link state*) est un ensemble de courbes, sans intersection et contraintes à demeurer au-dessus du segment imaginaire, qui connectent tout point à un autre des N points ou à un point à l'infini. Les points connectés à l'infini sont appelés des *défauts*. Il peut y avoir plus d'un défaut et le nombre de défauts,

souvent noté par la lettre d , a toujours la même parité que N . Pour un N donné, l'ensemble de tous les vecteurs de connectivités possibles est noté B_N , et le sous-ensemble des états à d défauts, B_N^d . Le nombre d'états dans B_N^d est donné par $|B_N^d| = \binom{N}{(N-d)/2} - \binom{N}{(N-d)/2-1}$. Ainsi, pour $N = 4$,

$$B_4^0 = \{ \text{diagramme 1}, \text{diagramme 2} \}, \quad B_4^2 = \{ \text{diagramme 3}, \text{diagramme 4}, \text{diagramme 5} \}, \quad B_4^4 = \{ \text{diagramme 6} \} \tag{1.4.11}$$

et $B_4 = B_4^0 \cup B_4^2 \cup B_4^4$. L'espace vectoriel engendré par les éléments de B_N est noté V_N , et le sous-espace engendré par ceux de B_N^d est V_N^d .

Pour bâtir une représentation à partir de V_N , il faut définir une action des éléments de Temperley-Lieb sur les vecteurs de connectivités. Soit c une connectivité de $TL_N(\beta)$ et $w \in B_N$. L'action de c sur w , notée cw , est obtenue en posant les N points du vecteur de connectivité w aux N points du segment supérieur de c . Le vecteur de connectivité résultant est obtenu en lisant les connexions des N points au bas de c , et il est multiplié par β^n , où n est le nombre de boucles fermées dans le diagramme de cw . Avec cette définition, toute connectivité dans $TL_N(\beta)$ est représentée par une matrice $\rho(c)$ carrée de grandeur $|B_N|$. Voici un exemple d'un produit cw et de la matrice $\rho(c)$:

$$\left(\text{diagramme} \right) = \beta \left(\text{diagramme} \right), \quad \rho \left(\text{diagramme} \right) = \begin{pmatrix} \beta & 1 & 1 & 0 & 0 & 0 \\ 0 & 0 & 0 & 0 & 0 & 0 \\ 0 & 0 & 0 & 1 & \beta & 1 \\ 0 & 0 & 0 & 0 & 0 & 0 \\ 0 & 0 & 0 & 0 & 0 & 0 \\ 0 & 0 & 0 & 0 & 0 & 0 \end{pmatrix}, \tag{1.4.12}$$

où l'ordre des états dans B_4 est celui de (1.4.11). Le β en rouge dans la matrice $\rho(c)$ est celui calculé dans l'exemple du produit cw à gauche.

Alors, la définition du produit cw est étendue linéairement aux combinaisons linéaires de vecteurs de connectivités dans V_N et de connectivités dans $TL_N(\beta)$. On peut alors montrer (voir le lemme 2.2.1) que ρ est une représentation de $TL_N(\beta)$, c'est-à-dire que pour deux éléments $c_1, c_2 \in TL_N(\beta)$ quelconques, $\rho(c_1)\rho(c_2) = \rho(c_1c_2)$.

Une remarque importante est que l'action des connectivités sur un élément de B_N^d ne peut jamais faire augmenter le nombre de défauts. À cet égard, le nombre d est une quantité qui ne peut que rester constante ou diminuer. À l'équation (1.4.12), nous avons mis dans la matrice $\rho(e_3e_2e_1)$ des traits pointillés qui indiquent le domaine et l'image des différents secteurs $d = 0$, $d = 2$ et $d = 4$. Parce que le nombre

de défauts ne peut jamais croître, les sous-matrices qui se situent sous la diagonale sont toujours composées de zéros uniquement. On dira alors que $\rho(c)$ est bloc-triangulaire supérieure. Les blocs sur la diagonale, notés $\rho(c)|_d$, engendrent aussi des représentations de $\mathbb{T}\mathbb{L}_N(\beta)$.

Dans les sections 2.2.3 à 2.2.5, la fonction de partition des modèles de Fortuin-Kasteleyn sera écrite en termes de $\rho(D_N(\lambda, u))$ de la même manière que celle des modèles de spins pouvait être calculée à partir de \mathcal{T}_N : en termes de ses valeurs propres ou certains éléments de matrice, selon les conditions aux limites.

Une matrice bloc-triangulaire supérieure a la propriété que ses valeurs propres sont celles de ses blocs sur la diagonale et n'est en général pas hermitienne. Si une telle matrice est non diagonalisable, la non diagonalisabilité peut survenir à l'intérieur d'un secteur ou entre des secteurs étiquetés par des valeurs d et d' différentes. Une introduction sur les blocs de Jordan et les structures de Jordan non triviales sera présentée à la section 1.5. Néanmoins, nous sommes déjà en mesure de donner deux exemples de matrices non diagonalisables. Tout d'abord, pour $N = 2$, $V_2 = \{\downarrow\downarrow, \curvearrowright\}$ et les générateurs id et e_1 sont représentés par les matrices $\rho(\text{id}) = \begin{pmatrix} 1 & 0 \\ 0 & 1 \end{pmatrix}$ et $\rho(e_1) = \begin{pmatrix} \beta & 1 \\ 0 & 0 \end{pmatrix}$. Vu la forme (1.4.4) de $D_2(\lambda, u)$, dans la représentation ρ elle prend la forme

$$\rho(D_2(\lambda, u)) = \begin{pmatrix} \beta a_2 + a_1 & a_2 \\ 0 & a_1 \end{pmatrix},$$

(a_1 et a_2 apparaissent à l'équation (2.2.1)) et il est évident que $\rho(D_2(\lambda, u))$ n'est pas symétrique. Pour $\beta = 0$ ($\lambda = \pi/2$), le modèle porte le nom de *modèle de polymères denses critique*. Alors, a_1 et a_2 se simplifient et

$$\rho(D_2(\pi/2, u)) = \begin{pmatrix} \sin 2u & \sin^2 2u \\ 0 & \sin 2u \end{pmatrix}.$$

Cette matrice a ses deux valeurs propres égales à $\sin 2u$ et, tant que $\sin 2u \neq 0$, elle est non diagonalisable : on ne peut trouver qu'un seul vecteur propre associé à la valeur propre $\sin 2u$: $\begin{pmatrix} 1 \\ 0 \end{pmatrix}$.

Comme second exemple, nous étudions \mathcal{H} pour $N = 4$:

$$\rho(\mathcal{H}) = \begin{pmatrix} 2\beta & 2 & 1 & 0 & 1 & 0 \\ 1 & \beta & 0 & 0 & 0 & 0 \\ 0 & 0 & \beta & 1 & 0 & 1 \\ 0 & 0 & 1 & \beta & 1 & 1 \\ 0 & 0 & 0 & 1 & \beta & 1 \\ 0 & 0 & 0 & 0 & 0 & 0 \end{pmatrix}.$$

Il est encore une fois indéniable que la matrice $\rho(\mathcal{H})$ n'est ni symétrique, ni hermitienne, ni normale. (Une matrice M est normale si $[M, M^\dagger] = 0$, condition suffisante pour assurer sa diagonalisabilité.) Pour $\beta = 0$, il est impossible de trouver une transformation $S\rho(\mathcal{H})S^{-1}$ qui transforme $\rho(\mathcal{H})$ en matrice diagonale. Il en va de même pour $\beta = \sqrt{2}$, valeur du paramètre correspondant au modèle d'Ising. Dans chaque cas, il existe plutôt une transformation qui envoie $\rho(\mathcal{H})$ sur $\rho'(\mathcal{H})$, avec

$$\rho'(\mathcal{H})_{\beta=0} = \left(\begin{array}{cc|ccc|c} -\sqrt{2} & 0 & 1 & 0 & 0 & 0 \\ 0 & \sqrt{2} & 0 & 1 & 0 & 0 \\ \hline 0 & 0 & -\sqrt{2} & 0 & 0 & 0 \\ 0 & 0 & 0 & \sqrt{2} & 0 & 0 \\ \hline 0 & 0 & 0 & 0 & 0 & 0 \\ 0 & 0 & 0 & 0 & 0 & 0 \end{array} \right),$$

$$\rho'(\mathcal{H})_{\beta=\sqrt{2}} = \left(\begin{array}{cc|ccc|c} \frac{3+\sqrt{5}}{\sqrt{2}} & 0 & 0 & 0 & 0 & 0 \\ 0 & \frac{3-\sqrt{5}}{\sqrt{2}} & 0 & 0 & 0 & 0 \\ \hline 0 & 0 & 2\sqrt{2} & 0 & 0 & 0 \\ 0 & 0 & 0 & \sqrt{2} & 0 & 0 \\ \hline 0 & 0 & 0 & 0 & 0 & 1 \\ 0 & 0 & 0 & 0 & 0 & 0 \end{array} \right).$$

Ces matrices sont presque diagonales ; en fait les valeurs sur la diagonale sont les valeurs propres, concept qui est bien défini même pour les matrices non diagonalisables (voir la section 1.5.1). Les 1 hors diagonaux qu'on ne parvient pas à enlever couplent des valeurs propres dégénérées et témoignent de l'impossibilité de trouver un nombre de vecteurs propres associés à cette valeur propre égal à sa dégénérescence. On dit des matrices qui ont ce comportement qu'elles ont des *blocs* (ou *cellules*) de Jordan. Notons aussi que le changement de base a été choisi pour que les valeurs propres d'un secteur d demeurent dans le bloc $\rho'(\mathcal{H})|_d$. Dans les deux exemples, les valeurs propres problématiques proviennent de secteurs d et d' différents ($d = 0$ et $d' = 2$ pour $\lambda = \pi/2$ et $d = 2$ et $d' = 4$ pour $\lambda = \pi/4$). Le but du chapitre 2 sera de déterminer dans quelles circonstances la non diagonalisabilité survient.

Pour l'exemple qui précède, nous notons que les matrices

$$\rho(F_4)_{\beta=0} = \left(\begin{array}{cc|cc|cc|c} 0 & 0 & 4 & 0 & 4 & 4 & 0 \\ 0 & 0 & 0 & 4 & 0 & 4 & 0 \\ \hline 0 & 0 & 0 & 0 & 0 & 0 & 0 \\ 0 & 0 & 0 & 0 & 0 & 0 & 0 \\ \hline 0 & 0 & 0 & 0 & 0 & 0 & 0 \\ 0 & 0 & 0 & 0 & 0 & 0 & 0 \end{array} \right),$$

$$\rho(F_4)_{\beta=\sqrt{2}} = \left(\begin{array}{cc|cc|cc} \sqrt{2} & 0 & 2 & 0 & 2 & 2-2\sqrt{2} \\ 0 & \sqrt{2} & 0 & 2 & 0 & 2 \\ \hline 0 & 0 & -\sqrt{2} & 0 & 0 & 4-2\sqrt{2} \\ 0 & 0 & 0 & -\sqrt{2} & 0 & 4-4\sqrt{2} \\ \hline 0 & 0 & 0 & 0 & -\sqrt{2} & 4-2\sqrt{2} \\ \hline 0 & 0 & 0 & 0 & 0 & -\sqrt{2} \end{array} \right),$$

dont l'expression provient des résultats de la section 2.B, sont également non diagonalisables. Pour chacune des deux valeurs de β , on peut montrer que les blocs de Jordan de $\rho(F_4)$ couplent les mêmes secteurs d et d' que les blocs de Jordan de \mathcal{H} . Nous montrerons que ceci s'étend aussi à $\rho(D_4(\lambda, u))$ pour toutes les valeurs de u , sauf peut-être un nombre fini d'entre elles. Le point $u = 0$, où $\rho(D_N)$ est un multiple de l'identité, fait partie des valeurs de u pour lesquelles les blocs de Jordan disparaissent.

1.5 Les hamiltoniens non diagonalisables et leur structure de Jordan

1.5.1 La forme canonique de Jordan des matrices non diagonalisables

L'étude de la mécanique quantique a habitué les physiciens à travailler avec des hamiltoniens hermitiens et donc diagonalisables, sous le prétexte que de tels hamiltoniens ont des valeurs propres réelles, ce qui est nécessaire pour que le modèle ait une interprétation physique. Des travaux récents ont montré que la contrainte d'hermiticité était trop forte et que certains hamiltoniens non hermitiens en mécanique quantique ont tout de même des valeurs propres réelles et des applications physiques véritables [31]. En plus, les hamiltoniens et matrices de transfert en mécanique statistique n'ont pas toujours des valeurs propres réelles. C'est le cas, par exemple, pour la matrice de transfert de spins avec conditions aux limites périodiques, qui a des valeurs propres complexes (voir [17]). Les matrices de transfert et hamiltoniens de boucles, introduits aux sections 1.4.2 et 4.2.2, sont aussi des exemples où l'hermiticité n'est pas nécessaire. Cette section se veut donc une brève introduction aux matrices non diagonalisables. Le lecteur intéressé pourra se référer à [32] et à [33] où sont présentées de bonnes introductions sur la forme de Jordan de matrices non diagonalisables.

Soit M une matrice complexe de grandeur $N \times N$ et $\lambda \in \mathbb{C}$. Le *polynôme caracté-*

ristique de M , noté $p_M(\lambda)$ et donné par

$$p_M(\lambda) = \det(M - \lambda \cdot \text{id}),$$

est de degré N en λ . Les valeurs propres de M sont les valeurs de λ qui satisfont $p_M(\lambda) = 0$. Elles peuvent être dégénérées et nous notons $\lambda_i, i = 1, \dots, n$, les valeurs propres distinctes de M et d_i leur dégénérescence respective. Alors $\sum_{i=1}^n d_i = N$ et on peut écrire

$$p_M(\lambda) = \prod_{i=1}^n (\lambda - \lambda_i)^{d_i}.$$

Pour une matrice M donnée, le polynôme *minimal* de M , $q_M(\lambda)$, est le polynôme de plus petit degré tel que $q_M(M) = 0$. Même si $p_M(M) = 0$, $p_M(\lambda)$ et $q_M(\lambda)$ ne sont pas toujours égaux. Nous avons plutôt que $q_M(\lambda)$ divise $p_M(\lambda)$, et donc

$$q_M(\lambda) = \prod_{i=1}^n (\lambda - \lambda_i)^{e_i}$$

avec $e_i \leq d_i$ pour tout i . En particulier, lorsque M est diagonalisable, $e_i = 1$ pour tous les i : pour chaque valeur propre λ_i , il est possible de trouver un nombre d_i de vecteurs *propres* v linéairement indépendants, satisfaisant $(M - \lambda_i \cdot \text{id})v = 0$. Il existe alors une matrice inversible S , de sorte que $D = SMS^{-1}$ est diagonale. Lorsque $e_i > 1$ pour un certain i , un tel changement de base n'est plus possible. Il existe plutôt une matrice S inversible telle que $J = SMS^{-1}$ prend la forme

$$J = \begin{pmatrix} J_1 & 0 & 0 & \dots & 0 \\ 0 & J_2 & 0 & \dots & 0 \\ 0 & 0 & J_3 & \dots & 0 \\ \vdots & \vdots & \vdots & \ddots & \vdots \\ 0 & 0 & 0 & \dots & J_m \end{pmatrix},$$

où chaque matrice $J_k, k = 1, \dots, m$, est de la forme

$$J_k = \begin{pmatrix} \lambda_k & 1 & 0 & \dots & 0 & 0 \\ 0 & \lambda_k & 1 & \dots & 0 & 0 \\ 0 & 0 & \lambda_k & \dots & 0 & 0 \\ \vdots & \vdots & \vdots & \ddots & \vdots & \vdots \\ 0 & 0 & 0 & \dots & \lambda_k & 1 \\ 0 & 0 & 0 & \dots & 0 & \lambda_k \end{pmatrix}$$

(et différents J_k peuvent être associés à la même valeur propre de M). Nous dirons alors que la matrice J est la matrice de Jordan associée à M et que J_k est une cellule

de Jordan associée à la valeur propre λ_k . Pour une matrice M donnée, la matrice de Jordan J est unique, modulo des permutations des blocs J_k . Pour une matrice M diagonalisable, chacun des J_k est de grandeur 1. Pour une matrice M non diagonalisable, la construction d'une base de vecteurs propres indépendants échoue et est remplacée par la construction de *vecteurs propres généralisés* (ou *vecteurs de Jordan*). À une cellule de Jordan J_k donnée de dimension s sont associés des vecteurs v_i , $i = 1, \dots, s$, qui satisfont $(M - \lambda_k \cdot \text{id})^i v_i = 0$, mais $(M - \lambda_k \cdot \text{id})^{i-1} v_i \neq 0$. Le nombre s est le *rang* (ou l'*ordre*) du vecteur propre généralisé, et on dira d'une matrice M qui a un vecteur généralisé de rang s qu'elle a une cellule de Jordan (ou un *bloc de Jordan*) de rang s .

Un premier exemple est de mise. Soit la matrice

$$M = \begin{pmatrix} 1 & 1 & 0 \\ 0 & 1 & b \\ 0 & 0 & a \end{pmatrix}.$$

Le polynôme caractéristique de M est $p_M(\lambda) = (\lambda - a)(\lambda - 1)^2$. Lorsque $a \neq 1$, $q_M(\lambda) = p_M(\lambda)$ et parce que $(\lambda - 1)$ est à la puissance 2 dans $q_M(\lambda)$, M n'est pas diagonalisable. En effet, à la valeur propre 1, on associe un seul vecteur propre $\begin{pmatrix} 1 \\ 0 \\ 0 \end{pmatrix}$ et un vecteur de Jordan $\begin{pmatrix} 0 \\ 1 \\ 0 \end{pmatrix}$. M a un bloc de Jordan de rang 2 et un de rang 1. Puisque pour la suite, nous nous intéressons aux matrices non diagonalisables, nous soulignerons rarement l'existence de blocs de Jordan de rang 1.

Le cas $a = 1$ se divise en deux sous-cas. Lorsque $b = 0$, $q_M(\lambda) = (\lambda - 1)^2$ et M possède à nouveau un bloc de Jordan de rang 2. Lorsque $b \neq 0$, $q_M = (\lambda - 1)^3$, et M a un bloc de Jordan de rang 3. Pour $b = 1$, M est déjà sous sa forme de Jordan.

1.5.2 Un exemple : l'hamiltonien XXZ sur le ruban

Le modèle XXZ sur le ruban est un exemple d'hamiltonien qui possède un spectre réel, mais une structure de Jordan parfois non triviale. Cet hamiltonien fera surface aux chapitres 3 et 4, où sera utilisé un lien qui relie la matrice de transfert pour le modèle de boucles en deux dimensions et cet hamiltonien, qui régit l'interaction d'un système de spins en une dimension. Cette introduction sur les matrices de Jordan représente l'occasion idéale pour une introduction pédagogique des hamiltoniens XXZ.

L'interaction XXZ pour une chaîne de N spins est une interaction entre plus

proches voisins plus complexe que l'interaction d'Ising. L'hamiltonien est [34]

$$H_{\text{XXZ}} = -\frac{1}{2} \left(\sum_{j=1}^{N-1} (\sigma_j^x \sigma_{j+1}^x + \sigma_j^y \sigma_{j+1}^y + \Delta \sigma_j^z \sigma_{j+1}^z) + B_1 \sigma_1^z + B_N \sigma_N^z \right). \quad (1.5.1)$$

Chaque matrice σ_j^a (pour $a \in \{x, y, z, +, -\}$) est une matrice carrée de grandeur 2^N donnée par

$$\sigma_j^a = \underbrace{\text{id}_2 \otimes \cdots \otimes \text{id}_2}_{j-1} \otimes \sigma^a \otimes \underbrace{\text{id}_2 \otimes \cdots \otimes \text{id}_2}_{N-j}$$

où

$$\sigma^x = \begin{pmatrix} 0 & 1 \\ 1 & 0 \end{pmatrix}, \quad \sigma^y = \begin{pmatrix} 0 & -i \\ i & 0 \end{pmatrix}, \quad \sigma^z = \begin{pmatrix} 1 & 0 \\ 0 & -1 \end{pmatrix}, \quad \sigma^+ = \begin{pmatrix} 0 & 1 \\ 0 & 0 \end{pmatrix}, \quad \sigma^- = \begin{pmatrix} 0 & 0 \\ 1 & 0 \end{pmatrix},$$

et le produit tensoriel entre des matrices A et B est

$$A \otimes B = \begin{pmatrix} a_{1,1}B & a_{1,2}B & \cdots & a_{1,n}B \\ a_{2,1}B & a_{2,2}B & \cdots & a_{2,n}B \\ \vdots & \vdots & \ddots & \vdots \\ a_{m,1}B & a_{m,2}B & \cdots & a_{m,n}B \end{pmatrix} \quad \text{lorsque} \quad A = \begin{pmatrix} a_{1,1} & a_{1,2} & \cdots & a_{1,n} \\ a_{2,1} & a_{2,2} & \cdots & a_{2,n} \\ \vdots & \vdots & \ddots & \vdots \\ a_{m,1} & a_{m,2} & \cdots & a_{m,n} \end{pmatrix}.$$

Lorsque A et C (et B et D) sont des matrices carrées de mêmes dimensions, l'équation $(A \otimes B)(C \otimes D) = (AC \otimes BD)$ est satisfaite et il en résulte que $[\sigma_i^a, \sigma_j^b] = 0$ lorsque $i \neq j$. L'espace vectoriel sur lequel ces opérateurs agissent est de dimension 2^N et est noté $(\mathbb{C}^2)^{\otimes N}$. La base d'états propres communs des matrices $\sigma_1^z, \dots, \sigma_N^z$ nous sera utile. Nous noterons les éléments de cette base par des états de N signes + ou -, dénotant les N valeurs propres des matrices $\sigma_1, \dots, \sigma_N$. Par exemple, l'ensemble

$$\{| + + + \rangle, | + + - \rangle, | + - + \rangle, | - + + \rangle, | + - - \rangle, | - + - \rangle, | - - + \rangle, | - - - \rangle\}$$

engendre $(\mathbb{C}^2)^{\otimes 3}$.

Dans l'hamiltonien (1.5.1), le j-ième terme de la somme est une interaction entre les spins j et j + 1 qui prend la forme

$$\underbrace{\text{id}_2 \otimes \cdots \otimes \text{id}_2}_{j-1} \otimes \begin{pmatrix} -\Delta/2 & 0 & 0 & 0 \\ 0 & \Delta/2 & -1 & 0 \\ 0 & -1 & \Delta/2 & 0 \\ 0 & 0 & 0 & -\Delta/2 \end{pmatrix} \otimes \underbrace{\text{id}_2 \otimes \cdots \otimes \text{id}_2}_{N-j-1}.$$

On note que le nombres de spins + et - sont conservés, propriété partagée aussi par les deux termes de frontières (dits magnétiques) : H_{XXZ} commute donc avec $S^z = \sum_{j=1}^N \sigma_j^z/2$. Pour des considérations futures, le sous-espace de $(\mathbb{C}^2)^{\otimes N}$ où la valeur de S^z vaut s sera noté $(\mathbb{C}^2)^{\otimes N}|_{S^z=s}$, et s peut valoir $\frac{N}{2}, \frac{N}{2} - 1, \dots, -\frac{N}{2}$.

Lorsque Δ , B_1 et B_N sont tous réels, H_{XXZ} est symétrique : ses valeurs propres sont réelles et il est diagonalisable. Lorsque

$$\Delta = (q + q^{-1})/2, \quad B_1 = -(q - q^{-1})/2 \quad \text{et} \quad B_N = (q - q^{-1})/2 \quad (1.5.2)$$

où q est un nombre complexe sur le cercle unitaire, il appert que les valeurs propres de H_{XXZ} sont également réelles (quoi qu'une preuve de ceci demeure un problème ouvert). Pour certaines valeurs précises de q , H_{XXZ} n'est pas diagonalisable. Par exemple pour $N = 3$, dans la base de $(\mathbb{C}^2)^{\otimes 3}$ fournie plus haut, H_{XXZ} prend la forme

$$H_{XXZ} = \Delta \text{id} + \begin{pmatrix} 0 & 0 & 0 & 0 & 0 & 0 & 0 & 0 \\ 0 & q & -1 & 0 & 0 & 0 & 0 & 0 \\ 0 & -1 & q + q^{-1} & -1 & 0 & 0 & 0 & 0 \\ 0 & 0 & -1 & q^{-1} & 0 & 0 & 0 & 0 \\ 0 & 0 & 0 & 0 & q & -1 & 0 & 0 \\ 0 & 0 & 0 & 0 & -1 & q + q^{-1} & -1 & 0 \\ 0 & 0 & 0 & 0 & 0 & -1 & q^{-1} & 0 \\ 0 & 0 & 0 & 0 & 0 & 0 & 0 & 0 \end{pmatrix}.$$

La matrice 3×3 correspondant à $(H_{XXZ} - \Delta \text{id})$ dans le sous-espace $S^z = \frac{1}{2}$ a les valeurs propres

$$0, \quad \frac{q^{3/2} - q^{-3/2}}{q^{1/2} - q^{-1/2}} \quad \text{et} \quad \frac{q^{3/2} + q^{-3/2}}{q^{1/2} + q^{-1/2}},$$

qui sont toutes réelles lorsque $|q| = 1$. Pour q générique, H_{XXZ} a trois valeurs propres distinctes et est diagonalisable, mais il existe des valeurs de q qui font exception à cette règle. Lorsque $q = e^{i\pi/3}$ par exemple, le vecteur

$$|v\rangle = e^{-2i\pi/3} |++-\rangle + e^{-i\pi/3} |+-+\rangle + |-++\rangle$$

est propre de H avec valeur propre Δ , alors que le vecteur

$$|w\rangle = -\sqrt{3}e^{-i\pi/6} |+-\rangle - |+ - +\rangle$$

satisfait $(H_{XXZ} - \Delta \text{id})|w\rangle = |v\rangle$: il y a un bloc de Jordan de rang 2.

Il existe de nombreuses variantes du modèle XXZ. L'hamiltonien avec les valeurs de Δ , B_1 et B_N données à l'équation (1.5.2) a été étudié pour la première fois dans [35] à cause de son lien avec l'algèbre $U_q(\mathfrak{sl}_2)$. C'est la variante qui sera utile au chapitre 3 pour $q = i$ et qu'on appelle communément *modèle XX* parce que les termes $\sigma_j^z \sigma_{j+1}^z$ sont absents. Celle présentée au chapitre 4 est pour une chaîne périodique, c'est-à-dire que la somme dans (1.5.1) se termine à $j = N$, les termes magnétiques sont absents et $\sigma_{N+1}^a \equiv \sigma_1^a$. Il comportera aussi des interactions supplémentaires $\sigma_j^x \sigma_{j+1}^y$ et $\sigma_{j+1}^x \sigma_j^y$, de même qu'une nouvelle variable, le paramètre de torsion ν (*twist parameter*).

1.5.3 Les théories des champs logarithmiques

Les représentations de l'algèbre de Virasoro intervenant dans les théories rationnelles (section 1.3.3) sont des représentations irréductibles et unitaires où l'opérateur L_0 est diagonalisable. Pour la description complète de certaines observables physiques, ces contraintes sont trop strictes et d'autres représentations peuvent être nécessaires [36, 37, 38]. Ainsi des théories conformes autres que les rationnelles doivent être introduites. Les matrices de transfert pour le modèle de boucles sur le ruban (sections 1.4.2 et 2.2.1) et sur le tore (section 4.2.2) ne sont pas symétriques, ce qui représente une différence importante avec les matrices de transfert de spin. Cela ne change pas l'identification faite à la section 1.3.3 entre l'action de la matrice de transfert et le générateur des dilatations L_0 . Quelles représentations de l'algèbre de Virasoro interviennent alors dans la description du spectre de ces matrices de transfert de boucles ? La réponse à cette question n'est pas simple. L'une des hypothèses faites dans la construction des représentations de la section 1.3.3, l'existence d'un état de plus haut poids $|v\rangle$ anéanti par tous les $L_i, i < 0$, et engendrant tous les autres états, assurait la diagonalisabilité de L_0 . Cette hypothèse ne peut être faite pour des représentations où L_0 n'est pas diagonalisable.

Pour bâtir des représentations où L_0 a des blocs de Jordan de rang 2 par exemple, il existe deux options [39] :

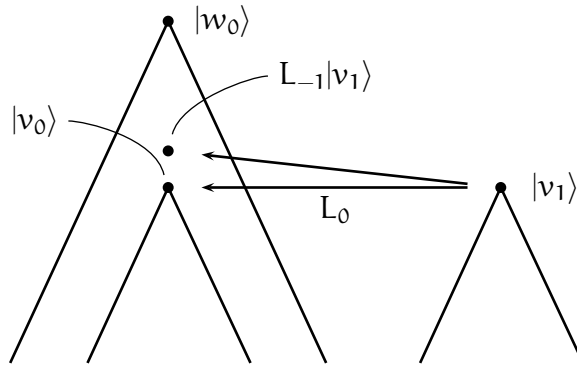
- les représentations de plus haut poids de Jordan : deux états $|v_0\rangle$ et $|v_1\rangle$ satisfont

$$L_0|v_0\rangle = h|v_0\rangle, \quad L_0|v_1\rangle = h|v_1\rangle + |v_0\rangle, \quad L_i|v_0\rangle = L_i|v_1\rangle = 0 \quad \text{pour } i < 0.$$

Les descendants de $|v_0\rangle$ et de $|v_1\rangle$ engendrent cette représentation.

- les *staggered modules* : les états $|v_0\rangle$ et $|v_1\rangle$ satisfont les mêmes relations que ci-haut, sauf que $L_i|v_1\rangle \neq 0$ au moins pour $i = -1$. De plus il existe un état $|w_0\rangle$ de plus haut poids de sorte que $|v_0\rangle$ et $L_{-1}|v_1\rangle$ figurent parmi les descendants de $|w_0\rangle$ (mais pas $|v_1\rangle$). Le *staggered module* est alors engendré par tous les descendants de $|w_0\rangle$ et $|v_1\rangle$. On peut trouver une classification partielle des *staggered modules* dans l'article de Ridout et Kytölä [40], et un diagramme d'un tel module est donné à la figure 1.14

Dans ces représentations de **Vir**, L_0 a des cellules de Jordan d'ordre 2, mais les constructions peuvent être généralisées aux cas où le rang des blocs de Jordan est plus élevé. Comme dans la section 1.3.3, la réussite de ces constructions est sujette

FIGURE 1.14 – Une illustration d'un *staggered module*.

à des contraintes pour les valeurs de la charge centrale, qui doit s'écrire comme

$$c(p, p') = 1 - 6 \frac{(p - p')^2}{pp'}, \quad p, p' \in \mathbb{Z} \quad \text{avec} \quad p > p'$$

et du plus haut poids, qui doit être dans l'ensemble

$$h_{r,s} = \frac{(p'r - ps)^2 - (p - p')^2}{4pp'}, \quad \text{pour} \quad r, s = 1, 2, \dots$$

Ces valeurs figurent dans la table de Kac étendue, qui s'étend à l'infini et dont une portion est donnée à la figure 1.13 pour $c = \frac{1}{2}$ et $c = \frac{4}{5}$. Les restrictions sur r et s semblent avoir disparu, mais en fait elles dépendent à la fois du type de représentation (*staggered* ou non) et du rang des blocs de Jordan. Par exemple, pour les représentations de plus haut poids de Jordan, la construction échoue toujours si le plus haut poids n'est pas dans l'ensemble $\{h_{r,p} : 1 \leq r < |p'|\} \cup \{h_{p',s} : 1 \leq s < |p|\}$ (voir [41]), que l'on retrouve en gris pâle dans à la figure 1.13.

Quel est l'impact du type de théorie des champs, rationnelle ou logarithmique, pour la description d'un modèle statistique particulier ? Dans la limite thermodynamique, le comportement des fonctions de corrélation des modèles statistiques sur réseau est étudié à travers le comportement de la fonction de corrélation du champ $\phi(z)$ dans la théorie des champs sous-jacente. Pour les théories des champs rationnelles, ce comportement est celui d'une loi de puissance en la position relative des champs. Par exemple, la fonction de corrélation à deux points est

$$\langle \phi(z)\phi(w) \rangle = \frac{A}{(z-w)^\mu},$$

où z et w sont dans le plan complexe et μ est l'exposant critique. Pour les théories rationnelles, ce comportement en loi de puissance décrit toujours les fonctions de

corrélation à plusieurs points lorsque les positions z et w des deux champs sont suffisamment proches. Or le qualificatif *logarithmique* des théories des champs logarithmiques provient d'une correction logarithmique à cette loi de puissance. Par exemple, lorsque L_0 a des blocs de Jordan d'ordre 2, les fonctions de corrélations de certains champs prennent la forme

$$\langle \phi(z)\phi(w) \rangle = \frac{A - B \log(z-w)}{(z-w)^\nu} \quad (1.5.3)$$

et lorsque les blocs de Jordan ont un rang supérieur à 2, les fonctions de corrélation à deux et trois champs prennent des formes d'une complexité accrue [42]. Dans les modèles d'Ising et de Potts, il a été montré que certaines observables avaient des dépendances logarithmiques [43]. Pour le modèle de percolation, Vasseur, Jacobsen et Saleur [44] ont récemment trouvé une observable physique qui, dans la limite d'échelle, a le comportement logarithmique de (1.5.3). Pour les autres valeurs de Q et λ , les observables qui auront la correction logarithmique sont pour l'instant inconnus.

Cela dit, la discussion qui précède ne permet pas de répondre à la question posée ci-haut, à savoir l'identification des représentations qui interviennent dans la description des modèles de boucles sur réseau. Pearce, Rasmussen et Zuber [45] ont introduit leurs matrices de transfert de boucles avec de nombreux choix de conditions aux frontières, et parmi celles-ci, celle présentée à la section 1.4.2 est la plus simple. Alors que les matrices de transfert de boucles sont introduites sur des réseaux finis, la nature des représentations de Virasoro qui entrent en jeu et donnent le spectre de $\rho(D_N(\lambda, u))$ est une information qui se trouve dans la limite $N \rightarrow \infty$. Néanmoins, en étudiant le spectre des matrices de transfert pour de petites valeurs de N , ces auteurs réussissent à identifier numériquement les plus hauts poids de chacune des représentations de L_0 reliées à chacune de leurs conditions aux frontières pour $D_N(\lambda, u)$, et ces poids entrent dans la table de Kac étendue. Leur exploration numérique leur permet aussi de trouver des cas où la matrice de transfert n'est pas diagonalisable.

La structure de Jordan de ces matrices demeurerait alors une question ouverte. Quand les matrices de transfert, non hermitiennes, sont-elles non diagonalisables? Quel est le rang des blocs de Jordan et dans quelles représentations apparaissent-ils? La structure de Jordan persiste-t-elle pour de larges valeurs de N ? Ce sont là des questions importantes, puisque la nature des représentations de Virasoro et le comportement des observables physiques en dépendront.

1.5.4 Des méthodes pour identifier des structures de Jordan

Dans les chapitres 2, 3 et 4, plusieurs approches sont utilisées pour sonder la présence ou l'absence de cellules de Jordan des matrices de transfert et des hamiltoniens. Dans cette section, nous fournissons une liste de cinq de ces méthodes.

(i) Supposons qu'une matrice $M(x)$, dont les entrées sont des fonctions d'une variable complexe x (dans les cas qui nous intéressent, les fonctions sont polynomiales ou trigonométriques), s'écrive comme

$$M(x) = A + B(x),$$

de sorte que la matrice A soit indépendante de x et satisfasse $[A, B(x)] = 0$ pour tout x . Si la matrice A a une structure de Jordan non triviale, alors $M(x)$ aura aussi une structure de Jordan non triviale pour toutes les valeurs de x sauf peut-être pour un nombre fini de valeurs isolées de x .

Ce résultat est démontré à la proposition 2.4.1. Il est ensuite utilisé à la section 2.4.4 et permet d'étudier la structure de Jordan de la matrice de transfert $D_N(\lambda, u)$ à travers celle de F_N , son plus haut coefficient de Fourier, et de même à la section 4.4 pour $T_N(\lambda, v)$.

(ii) Soit une matrice $M(x)$ qui dépend d'un paramètre libre x pour laquelle deux vecteurs propres $v_1(x)$ et $v_2(x)$, correspondant aux valeurs propres $\lambda_1(x)$ et $\lambda_2(x)$, sont connus. Soit aussi une valeur x_c de x qui est telle que $\lambda_1(x_c) = \lambda_2(x_c)$, la limite $\lim_{x \rightarrow x_c} v_1(x)$ existe et

$$\begin{aligned} \lambda_1(x) - \lambda_2(x) &\propto (x - x_c), \\ v_2(x) &= \frac{a_1}{x - x_c} + a_2 + \mathcal{O}(x - x_c), \end{aligned} \quad (1.5.4)$$

où a_1 et a_2 sont des vecteurs non nuls en $x = x_c$. Alors $M(x)$ a un bloc de Jordan non trivial lié à la valeur propre $\lambda \equiv \lambda_1(x_c) = \lambda_2(x_c)$. La preuve de ce résultat sera faite au lemme 2.4.7. Un exemple tiré des matrices $\rho(F_N)$ du chapitre 2 est

$$M(x) = \begin{pmatrix} 2 \cos x & 4 \sin^2 x \\ 0 & 2 \cos 3x \end{pmatrix}$$

avec valeurs propres et vecteurs propres

$$\begin{aligned} \lambda_1(x) &= 2 \cos x, & v_1(x) &= \begin{pmatrix} 1 \\ 0 \end{pmatrix}, \\ \lambda_2(x) &= 2 \cos 3x, & v_2(x) &= \begin{pmatrix} -1 \\ \frac{1}{2 \cos x} \end{pmatrix}. \end{aligned}$$

En $x_c = (n + \frac{1}{2})\pi, n \in \mathbb{Z}$, toutes les conditions (1.5.4) sont satisfaites et $M(x)$ n'est pas diagonalisable. En effet, en x_c , la matrice $M(x_c)$ est $\begin{pmatrix} 0 & 4 \\ 0 & 0 \end{pmatrix}$. Cette technique est utilisée aux sections 2.4.3 et 4.4 pour calculer la forme de Jordan des matrices $\rho(F_N)$ sur le ruban et le tore.

(iii) Au chapitre 3, il nous sera possible de trouver tous les vecteurs propres et les vecteurs de Jordan de l'hamiltonien XX par la transformation de Jordan-Wigner. Ainsi, nous verrons que l'hamiltonien XX pour N spins sur un ruban est une matrice $2^N \times 2^N$ qui admet l'expression

$$H = \sum_{k=0}^{N-1} \Lambda_k b_k a_k \quad \text{pour } N \text{ impair,}$$

$$H = b_0 a_1 + \sum_{k=0}^{N-1} \Lambda_k b_k a_k \quad \text{pour } N \text{ pair,}$$

où les Λ_k sont des nombres réels et les a_i et $b_i, i = 0, \dots, N-1$, sont des matrices $2^N \times 2^N$ qui satisfont aux relations d'anticommutation fermioniques

$$\{b_n, a_{n'}\} = \delta_{n,n'}, \quad \{b_n, b_{n'}\} = \{a_n, a_{n'}\} = 0. \quad (1.5.5)$$

À partir du vecteur $|0\rangle = |+\dots+\rangle$, on peut générer un ensemble de vecteurs indépendants $a_{k_1} a_{k_2} \dots a_{k_n} |0\rangle$, qui sont tous propres dans le cas N impair. Pour N pair, on peut utiliser les relations de commutation et montrer que $b_0 a_1$ est responsable de l'apparition de blocs de Jordan dans H : tous les états qui comportent le générateur a_0 mais pas le générateur a_1 sont des partenaires de Jordan. Tous les autres états sont propres.

(iv) Soit $\mathcal{H}(x)$ et $H(x)$ deux matrices dépendantes d'un paramètre x . Supposons aussi que $H(x)$ est hermitien et qu'il existe une troisième matrice $I(x)$ qui est telle que $I(x)\mathcal{H}(x) = H(x)I(x)$. Si $\det I(x) \neq 0$, alors $I(x)$ est inversible, $\mathcal{H}(x)$ et $H(x)$ sont des matrices similaires et puisque $H(x)$ est diagonalisable, $\mathcal{H}(x)$ l'est aussi. Par contre, lorsque la condition $\det I(x) \neq 0$ n'est pas satisfaite, $\mathcal{H}(x)$ n'est pas forcément diagonalisable. Dans l'exemple suivant tiré du chapitre 4, \mathcal{H} est un hamiltonien de boucles et H un hamiltonien XXZ :

$$\mathcal{H} = \begin{pmatrix} 2(u^2 + u^{-2}) & 2 & 2 & 0 & 2 & 2 \\ 1 & u^2 + u^{-2} & 0 & 0 & 0 & 0 \\ 0 & 0 & u^2 + u^{-2} & 1 & 0 & 0 \\ 0 & 2 & 2 & 2(u^2 + u^{-2}) & 2 & 2 \\ 0 & 0 & 0 & 1 & u^2 + u^{-2} & 0 \\ 1 & 0 & 0 & 0 & 0 & u^2 + u^{-2} \end{pmatrix}$$

$$H = \begin{pmatrix} 2(u^2 + u^{-2}) & 1 & 1 & 0 & 1 & 1 \\ 1 & u^2 + u^{-2} & 0 & 1 & 0 & 0 \\ 1 & 0 & u^2 + u^{-2} & 1 & 0 & 0 \\ 0 & 1 & 1 & 2(u^2 + u^{-2}) & 1 & 1 \\ 1 & 0 & 0 & 1 & u^2 + u^{-2} & 0 \\ 1 & 0 & 0 & 1 & 0 & u^2 + u^{-2} \end{pmatrix}.$$

La matrice de transformation I qui relie les matrices \mathcal{H} et H est donnée par

$$I = \begin{pmatrix} u^2 & 1 & 1 & u^{-2} & 1 & 1 \\ 0 & u^2 & 0 & 1 & 0 & u^{-2} \\ 1 & 0 & u^2 & 0 & u^{-2} & 0 \\ u^{-2} & 1 & 1 & u^2 & 1 & 1 \\ 1 & 0 & u^{-2} & 0 & u^2 & 0 \\ 0 & u^{-2} & 0 & 1 & 0 & u^2 \end{pmatrix}.$$

Lorsque $u = e^{i\gamma}$, $\gamma \in \mathbb{R}$, l'hamiltonian H est symétrique et diagonalisable, et il en va de même pour \mathcal{H} lorsque

$$\det I = (u^2 - u^{-2})^4 (u^4 - u^{-4}) \neq 0.$$

Lorsque $u = e^{i\pi/4}$, les vecteurs

$$v_1 = \begin{pmatrix} 0 \\ -1 \\ 1 \\ 0 \\ 1 \\ -1 \end{pmatrix} \quad \text{et} \quad v_2 = \begin{pmatrix} -1 \\ 0 \\ 0 \\ 1 \\ 0 \\ 0 \end{pmatrix}$$

forment une paire de Jordan associée à la valeur propre 0 de \mathcal{H} . À la section 4.6, nous présentons une construction explicite des états v_1 et v_2 en termes des vecteurs

$$w_1 = \begin{pmatrix} -i \\ -1 \\ 1 \\ i \\ 1 \\ -1 \end{pmatrix} \quad \text{et} \quad w_2 = \begin{pmatrix} i \\ -1 \\ 1 \\ -i \\ 1 \\ -1 \end{pmatrix},$$

propres de la matrice H en $u = e^{i\pi/4}$, aussi avec valeur propre 0. À la section 4.6, cette méthode sera utilisée pour calculer les vecteurs de cellules de Jordan d'une famille infinie d'hamiltoniens de boucles.

(v) Une dernière méthode utilisée pour prouver l'existence d'une structure de Jordan non triviale est le calcul explicite des éléments de matrices du polynôme minimal. Par exemple, la matrice

$$M = \begin{pmatrix} 1 & 2 & 3 & 4 \\ 0 & 1 & 2 & 3 \\ 0 & 0 & 1 & 2 \\ 0 & 0 & 0 & 1 \end{pmatrix}$$

a comme unique valeur propre $\lambda = 1$ dégénérée quatre fois, et puisque $M \neq \text{id}$, elle a une structure de Jordan non triviale. Nécessairement, $(M - I)^4 = 0$, et on peut vérifier que $(M - I)^3 \neq 0$ en calculant

$$(M - I)^3 \cdot \begin{pmatrix} 0 \\ 0 \\ 0 \\ 1 \end{pmatrix} = \begin{pmatrix} 8 \\ 0 \\ 0 \\ 0 \end{pmatrix},$$

c'est-à-dire que M a donc un bloc de Jordan de rang 4. Cette astuce sera utilisée à la section 4.4 pour diagnostiquer la présence de cellules de Jordan intersectorielles de F_N dans la représentation ρ .

1.6 Organisation de la thèse

L'objectif de cette thèse est de comprendre les structures de Jordan des matrices de transfert de boucles. Deux méthodes sont utilisées : l'étude de la structure de Jordan de F_N , plus haut coefficient de Fourier de la matrice de transfert, et un homomorphisme entre les représentations de boucles et celles des modèles XXZ. L'organisation de la suite de la thèse est la suivante.

Nous commençons, au chapitre 2, par étudier la matrice de transfert $D_N(\lambda, u)$ sur le ruban. Nous montrons comment $\rho(D_N(\lambda, u))$ permet de calculer les fonctions de partition des modèles de Potts et de Fortuin-Kasteleyn sur le ruban et le rectangle. L'étude de la structure de Jordan de la matrice $\rho(D_N(\lambda, u))$ est faite à travers celle de $\rho(F_N)$. Nous calculons certaines composantes des vecteurs propres de $\rho(F_N)$ pour λ générique, montrons que les blocs de Jordan surviennent aux valeurs de λ auxquelles ces composantes divergent et trouvons les conditions sur λ , N et d pour que les cellules de Jordan existent.

Au chapitre 3, nous travaillons avec le modèle de polymères denses critique ($\beta = 0$, et donc $\lambda = \pi/2$) sur le ruban, pour lequel les valeurs propres de $D_N(\pi/2, u)$

ont été calculées exactement et les dégénérescences conjecturées par Pearce et Rasmussen [46]. Nous introduisons la représentation de l'algèbre de Temperley-Lieb agissant sur les spins XXZ et montrons qu'il existe un isomorphisme i_N^d entre la représentation ρ restreinte au secteur à d défauts et le noyau $\ker S^+$ dans le sous-espace propre de S^z avec valeur propre $d/2$ des représentations XXZ. En comparant le spectre de l'hamiltonien dans ces deux représentations, nous démontrons la conjecture de Pearce et de Rasmussen. Nous trouvons par la même occasion que la matrice $\rho(\mathcal{H})$ restreinte à un secteur d est diagonalisable, mais que l'hamiltonien du modèle XXZ a des cellules de Jordan de rang 2 lorsque N est pair.

Au chapitre 4, nous introduisons, pour les conditions aux limites périodiques, la matrice de transfert $T_N(\lambda, \nu)$ et son hamiltonien \mathcal{H} , qui sont des éléments d'une algèbre de Temperley-Lieb élargie $\mathcal{E}TLP_N(\beta, \alpha)$. Nous introduisons deux types de représentations de cette algèbre : la représentation ρ et les représentations ω_d , qui dépendent d'un paramètre de torsion ν . Les modèles XXZ admettent aussi une représentation qui dépend de ce paramètre de torsion. Nous montrons qu'il est possible de construire un isomorphisme \tilde{i}_N^d entre la représentation ω_d en $\beta = -(q+q^{-1})$ et la représentation du modèle XXZ à $S^z = d/2$. Nous calculons le déterminant de \tilde{i}_N^d et trouvons que cette transformation est un isomorphisme sauf pour certaines courbes dans le plan (q, ν) . Lorsque \tilde{i}_N^d est un isomorphisme, $\omega_d(\mathcal{H})$ n'a pas de blocs de Jordan et, dans le cas contraire, nous construisons, pour une famille infinie de modèles sur les courbes critiques (q_c, ν_c) , des vecteurs composant la cellule de Jordan. Enfin, nous appliquons la méthode développée au chapitre 2 pour trouver les blocs de Jordan de $\rho(T_N(\lambda, \nu))$ entre secteurs d et d' .

Finalement, nous faisons au chapitre 5 une synthèse des résultats trouvés et une discussion des questions qui demeurent ouvertes. Certaines pourront être attaquées à l'aide des techniques développées dans cette thèse.

CHAPITRE 2: LA STRUCTURE DE JORDAN DES MODÈLES DE BOUCLES SUR LE RUBAN

Objectifs et méthodologie

La matrice de transfert du modèle de boucles sur le ruban, $D_N(\lambda, u)$, est l'analogue pour le modèle de Fortuin-Kasteleyn des matrices de transfert de spins \mathcal{T}_N pour les modèles d'Ising et de Potts. Elle n'est pas hermitienne, mais des simulations numériques indiquent que son spectre est réel. Au lieu d'agir sur un espace de spins comme \mathcal{T}_N , elle agit plutôt sur des états de connectivités, étiquetés par leur nombre de défauts d . Dans un article de Pearce, Rasmussen et Zuber [45], la non diagonalisabilité de $D_N(\lambda, u)$ pour des petites tailles du système N a été observée.

Dans cet article, nous démontrons comment la matrice de transfert $D_N(\lambda, u)$ entre dans le calcul des fonctions de partition des modèles de Fortuin-Kasteleyn (et de Potts), avec $\sqrt{Q} = 2 \cos \lambda$, pour deux types de conditions aux frontières au haut et au bas du réseau : périodiques (sur le ruban) ou libres (sur le rectangle). L'objectif principal est cependant l'étude approfondie de la structure de Jordan. Le résultat principal est la preuve de l'existence de blocs de Jordan dans $\rho(D_N(\lambda, u))$ pour toute grandeur N et l'identification des conditions sur λ , N et d qui assurent leur existence (voir les propositions 2.4.9 et 2.4.10). Lorsque ces conditions ne sont pas satisfaites, nous montrons que $\rho(D_N(\lambda, u))$ est diagonalisable. Voici un résumé des étapes utilisées pour y parvenir :

- $D_N(\lambda, u)$ est développé en une série de Fourier en la variable d'anisotropie u .
- Le dernier coefficient de cette série, F_N , est beaucoup plus simple à étudier que la matrice de transfert au complet. Nous montrons que les cellules de Jordan de F_N sont partagées par $D_N(\lambda, u)$.
- Nous trouvons que F_N est central dans l'algèbre de Temperley-Lieb, obtenons ses valeurs propres et calculons certaines composantes de ses vecteurs propres.
- Nous montrons que F_N possède des blocs de Jordan si et seulement si λ est tel que ses composantes sont divergentes. Ces blocs sont de rang 2.

Cet article a été publié dans le *Journal of Statistical Mechanics : Theory and Experiment*. En voici la référence complète :

→ A. Morin-Duchesne, Y. Saint-Aubin, *The Jordan Structure of Two Dimensional Loop Models*, J. Stat. Mech. **P04007** (2011) 65 p. ; arXiv : 1101.2885v4 [math-ph].

Comme premier auteur, ma contribution à cet article comprend notamment :

- Les calculs menant aux expressions des fonctions de partition de Potts et d’Ising en termes de $D_N(\lambda, u)$ sur le ruban et le rectangle (sections 2.2.3 à 2.2.5) ;
- L’identification du plus haut coefficient de Fourier F_N en termes d’une limite de la matrice de transfert $D_N(\lambda, u)$ connue sous le nom de *braid limit* (section 2.3.1) ;
- Le calcul des éléments de matrice de $\rho(F_N)$ et le calcul de ses valeurs propres (sections 2.B et 2.3.1) ;
- L’analyse des contraintes sur λ , d et N où des singularités apparaissent dans ces composantes (section 2.4.3) ;
- Les lemmes techniques de l’appendice 2.A caractérisant la singularité du vecteur $|P^r v^r\rangle$. C’est l’outil-clé du calcul.

The Jordan structure of two dimensional loop models

Alexi Morin-Duchesne

Département de physique

Université de Montréal, C.P. 6128, succ. centre-ville, Montréal

Québec, Canada, H3C 3J7

Yvan Saint-Aubin

Département de mathématiques et de statistique

Université de Montréal, C.P. 6128, succ. centre-ville, Montréal

Québec, Canada, H3C 3J7

Abstract

We show how to use the link representation of the transfer matrix D_N of loop models on the lattice to calculate partition functions, at criticality, of the Fortuin-Kasteleyn model with various boundary conditions and parameter $\beta = 2 \cos(\pi(1 - a/b))$, $a, b \in \mathbb{N}$ and, more specifically, partition functions of the corresponding Q-Potts spin models, with $Q = \beta^2$. The braid limit of D_N is shown to be a central element $F_N(\beta)$ of the Temperley-Lieb algebra $TL_N(\beta)$, its eigenvalues are determined and, for generic β , a basis of its eigenvectors is constructed using the Wenzl-Jones projector. To any element of this basis is associated a number of defects d , $0 \leq d \leq N$, and the basis vectors with the same d span a sector. Because components of these eigenvectors are singular when $b \in \mathbb{Z}^*$ and $a \in 2\mathbb{Z} + 1$, the link representations of F_N and D_N are shown to have Jordan blocks between sectors d and d' when $d - d' < 2b$ and $(d + d')/2 \equiv b - 1 \pmod{2b}$ ($d > d'$). When a and b do not satisfy the previous constraint, D_N is diagonalizable.

Keywords : Lattice models in two dimensions, loop models, logarithmic minimal models, conformal field theory, Jordan structure, indecomposable representations, Ising model, percolation, Potts models.

2.1 Introduction

Which are the representations of the Virasoro algebra involved in the thermodynamical limit of the Fortuin-Kasteleyn description of lattice spin models? This is such a natural question that it is somewhat surprising that the answer is not known precisely.

In the spin description of various two dimensional lattice models, like the Ising model, the answer is known. Thanks to early work by Onsager [12] and others [18, 8, 17], the spectrum of the transfer matrix of many models is known for various boundary conditions. To probe the hypothesis of conformal invariance of critical phenomenon [16] put forward in 1984, it was imperative to tie the lattice description to one of the conformal field theories (CFT). For that the transfer matrix, properly scaled, was identified to the generator L_0 of the Virasoro algebra. The possibility to use the characters of its three irreducible representations at $c = \frac{1}{2}$, with conformal dimensions 0, 1/2 and 1/16, to reproduce Onsager's spectrum of the Ising model was maybe the most compelling evidence for this hypothesis. The CFT description of rational models, denoted $\mathcal{M}(a, b)$, with $a, b \in \mathbb{N}$ ($b > a$), and central charge given by

$$c = c_{a,b} = 1 - \frac{6(b-a)^2}{ab} \quad (2.1.1)$$

is of particular interest, as the Ising model and 3-Potts model belong to this family, as $\mathcal{M}(3, 4)$ and $\mathcal{M}(4, 5)$ respectively. For models whose spectrum was not found analytically, the hypothesis of conformal invariance was later supported by strong numerical evidence, leading to many conjectures ([2], [26], [48], [49]), some of which were proven recently ([7], [50]).

In the Fortuin-Kasteleyn description (FK) of lattice models [51, 23, 52] (or simply loop models), the partition function is a sum over graphs instead of a sum over spin configurations like in the spin description. Each graph corresponds to many configurations, each spin configuration to many graphs. A transfer matrix D_N for the loop models is also available (see for example [53]) and much effort has been dedicated to the understanding of its spectrum and ground-state in particular situations ([54], [46]). But, in standard representations, the spin and loop transfer matrices of the same model on a given finite lattice do not have the same size. How can they possibly lead to the same partition function? Will they have the same spectrum in the thermodynamical limit? If not, the Virasoro representations involved in either limit are likely to be different. In the continuum limit, a similar problem arises and

Read and Saleur [36] wrote partition functions on the torus in terms of partition functions of free fields. Jacobsen and Richard [55] later proved that similar formulae hold for finite lattices. But partition functions reveal only a small part of the underlying representations.

It has been argued that multi-point correlation functions of these loop models exhibit logarithmic behavior [43]. This new feature does not fit well with the standard description of rational CFT's. Indeed, the differential equations obtained from singular vectors have logarithmic solutions, but the correlation functions of rational theories do not have logarithmic behavior. Of course, an extended paradigm, logarithmic conformal field theories (LCFT), is already available and allows these logarithmic functions. In these theories, a new field, the logarithmic partner of the stress energy tensor T , appears and is coupled to it in the operator product expansion, yielding the required logarithmic dependence for correlation functions [56, 41]. At the level of the Virasoro algebra, this translates into a generator L_0 that is no longer diagonalizable, but whose restriction to a fixed conformal weight subspace has Jordan blocks. One might also want to characterize the properties of a CFT based on indecomposable Virasoro representations, independently of the existence of such a logarithmic partner of T .

To probe the question raised at the very beginning, we shall use the loop transfer matrix D_N , $N \geq 1$, as introduced in [45]. This matrix was introduced earlier, of course, but the authors' observations indicate that the answer might be quite subtle for this particular form. In their notation D_N is an element of the Temperley-Lieb algebra $\mathbb{T}_N(\beta)$ whose parameter $\beta = 2 \cos(\lambda)$ is related to the central charge $c_{a,b}$ by $\lambda = (b - a)\pi/b$. In the given representation, the link representation, the element D_N acts on a vector space naturally broken into sectors. Pearce, Rasmussen and Zuber first provided numerical evidence that the eigenvalues of D_N , restricted to any of these sectors, reproduce the first highest weights of some highest weight representations of the Virasoro algebra. And second they showed that, on some examples and for some boundary conditions, the matrix D_N has Jordan blocks between some of the sectors, a telltale indication of logarithmic structure. Consequently they named *logarithmic minimal models* $\mathcal{LM}(a, b)$ the thermodynamical limit of these lattice loop models. We shall use simpler boundary conditions than theirs. Ours will be shown to correspond to free boundary conditions on a strip in the corresponding spin description.

Not surprisingly, the formulation in term of loop models owes much to the

Temperley-Lieb algebra $\mathcal{TL}_N(\beta)$ and its representations. This algebra is not semi-simple for all values of β . Actually it fails to be semi-simple precisely for the β corresponding to the rational models. Its representation theory, at these values, is much more involved than for generic β and its principal indecomposable modules were classified by Goodman and Wenzl [57], and Martin [58]. We shall use some of their tools in our study.

The goal of this paper is two-fold : to show how the spectrum of D_N relates to the spin models and to describe the Jordan structure of the double-row matrix, for all N , and at the critical values of β (or λ). Would D_N contain Jordan blocks, this would be a clear indication that the thermodynamical limit of the FK description requires indecomposable representations of the Virasoro algebra.

The introductory question has also been attacked from a different standpoint, that of conformal field theory. Percolation, the Q-Potts model with $Q = 1$, can be used as an example. It is believed that the thermodynamical limit of percolation is described by a theory with central charge $c = 0$. (A historical presentation of the difficulties arising in setting percolation within the context of CFT is given in the introduction of [59].) However, if only irreducible representations of the Virasoro algebra are used, the theory is trivial. One *must* introduce indecomposable representations, leading naturally to a logarithmic conformal field theory [56, 41]. The operator product expansion is then used to probe which representations should appear. However there exist more than one well-defined CFT at $c = 0$ and physical arguments will be needed to pick the right one for percolation. Studying the original problem on a finite lattice, as here, is a first step. But, to describe crossing probabilities, changes in boundary conditions will need to be included, a step that we have not considered.

Here is the layout of the paper. Section 2.2 makes explicit the relation between Q-Potts models at criticality and the double-row matrix D_N . After a quick reminder of definitions of the Temperley-Lieb algebras \mathcal{TL}_N and its link representation ρ , we introduce a trace τ on \mathcal{TL}_N and show that it is equivalent to a weighted trace on diagonal blocks of the representation ρ . Partition functions for the Q-Potts spin models on the cylinder are then expressed in terms of $\rho(D_N)$ on the cylinder. Extensions to various boundary conditions for the spin models are also given. In section 2.3, we study C_{2N} , the top Fourier coefficient of D_N , and show that it is central in \mathcal{TL}_N . (Appendix 2.B provides a simple method for calculating elements of $\rho(C_{2N})$ using 2×2 matrices.) Using the Wenzl-Jones projector, we find a basis of eigenvectors of $\rho(C_{2N})$

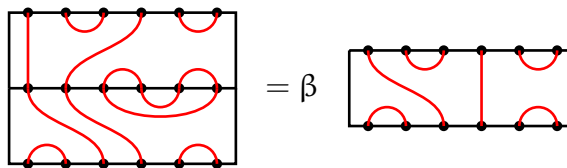
for non-critical λ . The critical λ s are studied in section 2.4. The singularities of the eigenvectors obtained in the previous section are identified. (Appendix 2.A gives the main lemmas with their technical proofs.) This singular behavior translates to a non-trivial Jordan structure of $\rho(C_{2N})$. More precisely, we find that when $\lambda = \frac{(b-a)\pi}{b}$, with $b \in \mathbb{Z}^*$ and $a \in 2\mathbb{Z} + 1$, the matrix $\rho(C_{2N})$ has Jordan blocks linking sectors d and d' ($d > d'$) when $d - d' < 2b$ and $\frac{d+d'}{2} \equiv b - 1 \pmod{2b}$. An extension of this to $\rho(D_N)$ exists and is our main result.

2.2 Transfer matrices of Q-Potts and loop models

2.2.1 The Temperley-Lieb algebra as an algebra of connectivities

We introduce the Temperley-Lieb algebra $\mathcal{TL}_N(\beta)$ in a slightly uncommon way. (See [60] for a longer description of this approach.) Let N be a positive integer and draw a rectangle with $2N$ marked points on it, N on its upper side, N on the bottom. A *connectivity diagram*, or simply a *connectivity*, is a pairwise pairing of all points by non-crossing curves drawn within the rectangular box. There are C_N distinct connectivities, where $C_N = \frac{1}{N+1} \binom{2N}{N}$ is the Catalan number. Let \mathcal{A}_N be the set of formal linear combinations over \mathbb{C} of these connectivities. It is a vector space of dimension C_N .

Choose now $\beta \in \mathbb{C}$. We define a product between two connectivities. If c and d are two such connectivities, their β -product cd is obtained by drawing their two rectangles one above the other, d being on top, and looking how the points of the top side of d and those on the bottom side of c are connected by the curves of c and d . The β -product cd is the resulting connectivity multiplied by a factor of β for each closed loop in the diagram with the two rectangles on top of each other. For example here is the product of two connectivities with $N = 6$.



This product between connectivities is extended to \mathcal{A}_N linearly on both entries. It is associative, non-commutative and it has a unit element, namely the connectivity that pairs points on the same vertical line. This element is written as id .

DEFINITION 2.2.1 *The Temperley-Lieb algebra $\mathcal{TL}_N(\beta)$ is the vector space \mathcal{A}_N endowed with the β -product just defined.*

The connectivities e_i , $i = 1, \dots, N - 1$, play an important role. Let the points be labeled from left to right. The connectivity e_i pairs all $2N$ points like the unit id does, except those in positions i and $i + 1$ on both top and bottom sides; the points i and $i + 1$ on the top are paired together, so are those on the bottom. It is easily shown that, as an algebra, $\mathbb{T}_N(\beta)$ is generated by the connectivities e_i , $i = 1, \dots, N - 1$. It is usual in the literature to define $\mathbb{T}_N(\beta)$ using the generators e_i together with the relations between them, namely

$$\begin{aligned} e_i^2 &= \beta e_i, \\ e_i e_j &= e_j e_i, \quad \text{for } |i - j| > 1 \\ e_i e_{i \pm 1} e_i &= e_i \quad \text{when } i, i \pm 1 \in \{1, 2, \dots, N - 1\}. \end{aligned}$$

For every $\beta \in (0, 2)$, there is a one-parameter family of elements in $\mathbb{T}_N(\beta)$ that has been studied by many because of its relationship with statistical physics. We use the notation of the double-row transfer matrix $D_N(\lambda, u)$ introduced in [45]. It is defined graphically by

$$D_N(\lambda, u) = \begin{array}{c} \overbrace{\hspace{10em}}^N \\ \begin{array}{|c|c|c|c|} \hline \bullet & \bullet & \dots & \bullet \\ \hline \lambda - u & \lambda - u & & \lambda - u \\ \hline u & u & & u \\ \hline \bullet & \bullet & \dots & \bullet \\ \hline \end{array} \end{array}$$

where each box stands for the sum

$$\boxed{u} = \sin(\lambda - u) \begin{array}{|c|} \hline \text{red arcs} \\ \hline \end{array} + \sin u \begin{array}{|c|} \hline \text{red arcs} \\ \hline \end{array} = \boxed{\lambda - u}$$

with $\beta = 2 \cos \lambda$, $\lambda \in (0, \frac{\pi}{2})$ and $u \in [0, \lambda]$ is the anisotropy parameter and will be given a physical interpretation in section 2.2.4. (A global factor to the weights of the two states does not change the physics; our factor differs from that of [45].) The matrix $D_N(\lambda, u)$ is therefore defined by $2N$ sums over the two states. As for the β -product of connectivities, any closed loop gives rise to a factor β . The simplest case is for $N = 2$. There are 2^4 configurations, each contributing to one of the two connectivities:

$$D_2(\lambda, u) = a_1 \begin{array}{|c|c|} \hline \bullet & \bullet \\ \hline \text{red arcs} \\ \hline \bullet & \bullet \\ \hline \end{array} + a_2 \begin{array}{|c|c|} \hline \bullet & \bullet \\ \hline \text{red arcs} \\ \hline \bullet & \bullet \\ \hline \end{array}$$

where

$$\begin{aligned} a_1 &= \left(\beta(\sin^4 u + \sin^2 u \sin^2(\lambda - u)) \right. \\ &\quad \left. + \sin^4(\lambda - u) + 2(\sin^3 u \sin(\lambda - u) + \sin u \sin^3(\lambda - u)) \right), \\ a_2 &= (2\beta(\sin^3 u \sin(\lambda - u) + \sin u \sin^3(\lambda - u)) + (4 + \beta^2) \sin^2 u \sin^2(\lambda - u)). \end{aligned} \tag{2.2.1}$$

The most important property of the double-row matrix $D_N(\lambda, u)$ is the following (for the proof, see [63]) :

$$[D_N(\lambda, u), D_N(\lambda, v)] = 0, \quad u, v \in [0, \lambda]. \quad (2.2.2)$$

It is a direct consequence of the Yang-Baxter equation. If some coefficient of $D_N(\lambda, u)$, for a fixed λ , is interpreted as a Hamiltonian, then the above equation leads to a family of constants of motion for this dynamical system. When there is no confusion, the dependence upon λ and u of $D_N(\lambda, u)$ and the β in $\mathbb{T}L_N(\beta)$ will be omitted.

2.2.2 The link representation of $\mathbb{T}L_N(\beta)$

Several representations are useful to study $\mathbb{T}L_N(\beta)$. Since $\mathbb{T}L_N(\beta)$ is itself a vector space, it comes with a natural representation on $\mathbb{C}^{\mathbb{C}^N}$. Another one that appears naturally in spin systems acts on the tensor product $(\mathbb{C}^2)^{\otimes N}$ and Goodman and Wenzl [57] have shown that it is a faithful representation. Following [45], we will use yet another representation, that on link states. (See also [64].) A *N-link state* is a set of non-crossing curves, drawn above a horizontal segment, pairing N points among themselves or to infinity (more than one point can be connected to infinity). In the latter case, we draw the curve as a vertical segment and call *defects* such pairings to infinity. The number of defects of a link state u will be denoted $d(u)$. The set of all N -link states is denoted by B_N and we shall order B_N such that the number of defects is increasing. (The actual order among link states of a given defect number will not play a role.) Formal linear combinations over \mathbb{C} of elements of B_N form the vector space V_N . It is of dimension $\binom{N}{\lfloor N/2 \rfloor}$. Subspaces V_N^d are those spanned by link states with d defects. Their dimension is $\dim V_N^d = \binom{N}{(N-d)/2} - \binom{N}{(N-d)/2-1}$ and $V_N = \bigoplus_{0 \leq d \leq N} V_N^d$. Note that V_N^d is non-trivial only if d and N have the same parity. As an example, there are six link states for $N = 4$:

$$B_4 = \left\{ \begin{array}{c} \text{---} \bullet \text{---} \bullet \text{---} \bullet \text{---} \bullet \text{---} \\ \text{---} \bullet \text{---} \bullet \text{---} \bullet \text{---} \bullet \text{---} \\ \text{---} \bullet \text{---} \bullet \text{---} \bullet \text{---} \bullet \text{---} \\ \text{---} \bullet \text{---} \bullet \text{---} \bullet \text{---} \bullet \text{---} \\ \text{---} \bullet \text{---} \bullet \text{---} \bullet \text{---} \bullet \text{---} \\ \text{---} \bullet \text{---} \bullet \text{---} \bullet \text{---} \bullet \text{---} \end{array} \right\}.$$

To each N -connectivity c corresponds a matrix $\rho(c) \in \text{End}(V_N)$. Let $v \in B_N$. To determine $\rho(c)$, we draw v on top of c (and denote the resulting diagram cv) and read how the bottom sites of c are connected among each other or to infinity. The result is a link state w in B_N . Any closed loop gives a factor of β . The column v in $\rho(c)$ contains therefore a single non-zero matrix element at position w and its value

is the product of all β factors.

$$= \beta^2 \quad \text{(2.2.3)}$$

Note that the action of c on a link state cannot increase its number of defects and, if $v \in V_N^d$, then $cv \in \bigoplus_{d' \leq d} V_N^{d'}$. We extend ρ linearly to the algebra $\mathbb{T}L_N(\beta)$.

LEMMA 2.2.1 $\rho : \mathbb{T}L_N(\beta) \rightarrow \text{End } \mathbb{C}^{\binom{N}{\lfloor N/2 \rfloor}}$ is a representation.

PROOF The only thing to check is whether $\rho(cd) = \rho(c)\rho(d)$ for all connectivities c, d . The product of cd is, up to a power of β , a connectivity. As noted before, a single element is non-zero in each column of $\rho(c)$, $\rho(d)$ and $\rho(cd)$. Fix a link state $u \in B_N$ and let $v, w \in B_N$ be such that $(\rho(d))_{vu}$ and $(\rho(cd))_{wu}$ are non-zero. Because the process of reading the pairs connected in the diagram cdu is associative, that is $(cd)u = c(du)$, then $(\rho(c))_{wv}$ must be non-zero. Therefore the only thing to check is whether the factors β in $(\rho(cd))_{wu}$ and $(\rho(c))_{wv}(\rho(d))_{vu}$ are the same. (Note that there is no sum on v .) These factors are indeed equal. They are both the number of closed loops in the diagram with, from top to bottom, the link state u , the connectivity d and then c . The two expressions count the number of loops in a different order however. For example, the term $(\rho(cd))_{wu}$ counts first the loops that are closed when the connectivities c and d are glued, and then the additional loops when the link u is added. \square

We shall refer to ρ as the link representation.

2.2.3 Traces in the link representation

We will be interested in making contacts between elements of $\mathbb{T}L_N(\beta)$ and partition functions $\tilde{\Lambda}$ of Q-Potts models. In section 2.2.4, the partition function $Z_{N \times M}$ is obtained as the trace of some powers of the transfer matrix $\tilde{\Lambda}$. Similar questions were already addressed for some models and representations of $\mathbb{T}L_N$. Our argument to answer this question is similar to that of Jacobsen and Richard [55]. Their computation is however done for a representation of dimension C_N , much larger than ours, and has to identify some of the degeneracies among the representations that constitute the starting one. The link representation avoids some of these difficulties and it is therefore useful to give the shorter computation for this case. A similar calculation, in the link basis, can be found in [61].

We now introduce an operation akin the trace on the algebra $\mathbb{T}L_N(\beta)$.

DEFINITION 2.2.2 *If c is an N -connectivity, the trace of c , noted $\tau(c)$, is $\beta^{\#(c)}$ where $\#(c)$ is the number of loops closed by the process of identifying the points on the top with those on the bottom of the rectangle. The trace $\tau : \mathbb{T}_N(\beta) \rightarrow \mathbb{C}$ is the linear extension of the trace of connectivities to the whole algebra.*

Note that τ is not a representation.

The double-row matrix $D_N(\lambda, u)$ is an element of $\mathbb{T}_N(\beta)$ and can then be written as $D_N = \sum_c \alpha_c c$ where the sum is over connectivities and $\alpha_c \in \mathbb{C}$. Note that any power D_N^M , seen as an element of $\mathbb{T}_N(\beta)$, is also of the same form $D_N^M = \sum_{c,M} \alpha_{c,M} c$ with $\alpha_{c,M} \in \mathbb{C}$. It will be shown in section 2.2.4 that, for the Potts models, β^2 equals $Q = 1, 2, 3$ or 4 and their partition function is related to $\tau(D_N^M)$ when N is even by

$$Z_{N \times M} \propto \sum_c \alpha_{c,M} \beta^{\#(c)} = \sum_c \alpha_{c,M} \tau(c) = \tau(D_N^M). \quad (2.2.4)$$

A natural question is then to relate $\tau(D_N^M)$ and $\text{tr } \rho(D_N^M)$ or, for any $C \in \mathbb{T}_N(\beta)$, to relate $\tau(C)$ and $\text{tr } \rho(C)$. We therefore turn to the (usual) trace $\text{tr } \rho(e)$, for a connectivity $e \in \mathbb{T}_N(\beta)$. Because $\rho(e)$ has a single element per column, its trace will be the sum of eigenvalues of link states that are eigenvectors of $\rho(e)$. Another important number characterizing connectivities is the following.

DEFINITION 2.2.3 *Let $\delta(c)$ be the maximum number of defects of link states among those that are eigenvectors of $\rho(c)$:*

$$\delta(c) = \max_{u \in B_N, \rho(c)_{uu} \neq 0} \{d(u)\}.$$

Note that $\#(c) \geq \delta(c)$.

This allows to count the number of eigenstates of $\rho(c)$ in B_N .

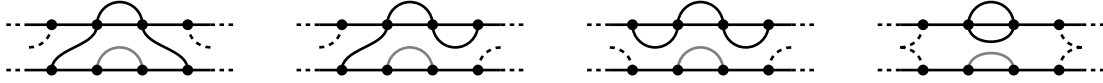
LEMMA 2.2.2 *The number of link states with d defects that are eigenstates of $\rho(c)$ is*

$$\dim V_{\delta(c)}^d = \binom{\delta(c)}{(\delta(c) - d)/2} - \binom{\delta(c)}{(\delta(c) - d)/2 - 1}.$$

PROOF The unit element id has $\delta(\text{id}) = N$ and all link states are eigenvectors of $\rho(\text{id}) = \text{id}_{\dim V_N}$. The numbers given in the statement are then the dimensions of the V_N^d .

Let c be a connectivity that is not the unit. We construct its link eigenstates as follows. Since $c \neq \text{id}$, there are for sure two points on the bottom of the rectangle that are paired. Among all pairs of joined points on the bottom, choose one such

that the points are contiguous. Such a pairing must also occur in any eigenstate of $\rho(c)$. Consider the diagram of the connectivity c to which an arc has been added to its top connecting the same pair. One of the following diagrams, where the original pairing is in gray, represents the extended curve thus created.



For simplicity, any arcs between the gray and black curves were omitted. There could be some. By adding this curve on top of the diagram, one of the following situations occurs : a pair of points on the bottom are joined, one point on the bottom and one of the top are joined, two on the tops are joined, a loop is closed. Since the points connected by the new arc are neighbors, the extended curve can be deformed, without crossing the others in c , into the corresponding diagram below



Note that the pairing between contiguous points on the bottom can be safely erased as long as we keep track that the link state under construction must have this arc.

The process has reduced by 2 the number of points on the top and bottom sides of the rectangle. If the new diagram is not the unit, the process is repeated. Suppose then that a unit has been reached and that this unit connects Δ pairs of points, $0 \leq \Delta \leq N$. Then the pairing of $(N - \Delta)$ points of the link has already been determined and all eigenstates of $\rho(c)$ in B_N will share these pairings. The remaining Δ points can be tied to infinity or among each other since the restriction of $\rho(c)$ to these points acts as the unit.

To get the maximum number of defects in an eigenstate, we connect the Δ remaining points to infinity. Then $\delta(c) = \Delta$ and there is precisely one link eigenstate u_c with this maximum number of defects. How many link eigenstates with d defects are there? It is simply the number of ways to connect $(\delta(c) - d)$ of the remaining $\delta(c)$ points of u_c , that is $\dim V_{\delta(c)}^d = \binom{\delta(c)}{(\delta(c)-d)/2} - \binom{\delta(c)}{(\delta(c)-d)/2-1}$. \square

Let $C = \sum_c \gamma_c c$. It is useful to split the sum over connectivities into sums over connectivities with a given number δ . Then

$$C_d = \sum_{c \text{ with } \delta(c) = d} \gamma_c c \quad \text{and} \quad C = \sum_{0 \leq d \leq N} C_d$$

and

$$\tau(C_d) = \sum_{c \text{ with } \delta(c) = d} \gamma_c \tau(c) = \sum_{c \text{ with } \delta(c) = d} \gamma_c \beta^{\#(c)} \quad \text{and} \quad \tau(C) = \sum_{0 \leq d \leq N} \tau(C_d).$$

Let N be even and fix a number of defects d with $0 \leq d \leq N$ and denote by $\text{tr}_d \rho(c)$ the trace of the diagonal block of $\rho(c)$ acting on the subspace V_N^d . All connectivities c with $\delta(c) = d$ have a single diagonal element in $\rho(c)$ contributing to $\text{tr}_d \rho(c)$. It comes from the eigenstate u_c constructed in the proof above. The proof has also shown that the connectivity c acts as the unit on $\delta(c)$ points. By definition $\tau(c) = \beta^{\#(c)}$ and therefore only $(\#(c) - \delta(c))$ loops are closed when the diagrams of u_c and c are joined. The eigenvalue of u_c must be $\beta^{\#(c) - \delta(c)}$. Such connectivities c , with $\delta(c) = d$, also contribute to $\text{tr}_{d'} \rho(C)$ with $d' < \delta(c)$. Equivalently $\text{tr}_d \rho(C)$ gets contribution from connectivities c that have their $\delta(c) > d$. If $d' \geq d$, then $\rho(c)$ with $\delta(c) = d'$ has precisely $(\dim V_{d'}^d)$ link eigenstates with d defects. The eigenvalue of these states can be obtained by an argument similar to the one above and is $\beta^{\#(c) - d'}$. Then let

$$\begin{aligned} \text{tr}_d \rho(C) &= \sum_{d' \geq d} \sum_{c \text{ with } \delta(c) = d'} \gamma_c \beta^{\#(c) - d'} \dim V_{d'}^d \\ &= \sum_{d' \geq d} \tau(C_{d'}) \beta^{-d'} \dim V_{d'}^d. \end{aligned}$$

The numbers of defects d and d' have the same parity as N and are thus even. They take $(\frac{N}{2} + 1)$ possible values. Let M be a $(\frac{N}{2} + 1) \times (\frac{N}{2} + 1)$ matrix whose elements are labeled by numbers of defects

$$M_{dd'} = \begin{cases} \beta^{-d'} \dim V_{d'}^d, & d' \geq d, \\ 0, & d' < d. \end{cases} \quad (2.2.5)$$

Then $\text{tr}_d \rho(C) = \sum_{d'} M_{dd'} \tau(C_{d'})$. The quantities of interest are the $\tau(C_d)$. The inverse of M can be computed. (The expression is given at the end of this section.)

Then

$$\tau(C_d) = \sum_{d'} (M^{-1})_{dd'} \text{tr}_{d'} \rho(C)$$

and

$$\tau(C) = \sum_{0 \leq d, d' \leq N} (M^{-1})_{dd'} \text{tr}_{d'} \rho(C).$$

The sum $\sum_d (M^{-1})_{dd'}$ will be done in another lemma below. This therefore proves the following relationship between $\tau(C)$ and the trace of $\rho(C)$.

PROPOSITION 2.2.3 *Let N be even and $W \in \text{End}(V_N)$ be the linear transformation that acts as a multiple of the identity on each V_N^d with $W|_{V_N^d} = \frac{\sin(d+1)\lambda}{\sin \lambda} \cdot \text{id}$ where $\beta = 2 \cos \lambda$. Then $\tau(C) = \text{tr}(\rho(C)W)$ for all $C \in \text{TL}_N(\beta)$.*

Here are the proofs of the announced lemmas.

LEMMA 2.2.4 *Let N be even. The inverse of the matrix M introduced in (2.2.5) is*

$$(M^{-1})_{dd'} = (-1)^{(d+d')/2} \beta^d \binom{(d+d')/2}{d}$$

if $d' \geq d$ and 0 otherwise.

PROOF Recall that the indices d and d' are even integers in the interval $[0, N]$. It is easier to work with integers i, j, \dots in the range $[0, \frac{N}{2}]$. With these indices we therefore have to prove that

$$\sum_{j=i}^l M_{ij}(M^{-1})_{jl} = \sum_{j=i}^l \frac{1}{\beta^{2j}} \left(\binom{2j}{j-i} - \binom{2j}{j-i-1} \right) (-1)^{j+l} \beta^{2j} \binom{j+l}{2j} = \delta_{il}$$

when $i \leq l$. (We use the convention that the binomial coefficient $\binom{a}{b}$ is zero if $b > a$ or if a or b are negative.) Using the two identities

$$\binom{r}{m} \binom{m}{k} = \binom{r}{k} \binom{r-k}{m-k} \quad \text{and} \quad \sum_{i=n-r}^{l-m} (-1)^i \binom{l}{m+i} \binom{r+i}{n} = (-1)^{l+m} \binom{r-m}{n-l}$$

that hold for integers $l \geq 0$ and any integers r, m, k, n (see eqs. (5.21) and (5.24) of [65] for proofs), we can compute the first sum

$$\sum_{j=i}^l (-1)^{j+l} \binom{2j}{j-i} \binom{j+l}{2j} = \sum_{j=i}^l (-1)^{j+l} \binom{l+i}{j+i} \binom{j+l}{l+i} = \binom{l-i}{0}.$$

The second sum is done similarly and we find

$$\sum_{j=i}^l M_{ij}(M^{-1})_{jl} = \binom{l-i}{0} - \binom{l-i-1}{0}.$$

As long as both $l-i$ and $l-i-1$ are non-negative, they are both 1 and $(MM^{-1})_{il} = 0$ when $i < l$. But when $i = l$, the second binomial coefficient above is zero and $(MM^{-1})_{ii} = 1$ as claimed. \square

LEMMA 2.2.5 *Again, let N be even. With the above notation,*

$$w_d = \sum_{d' \leq d} (M^{-1})_{d'd} = \sin \lambda (d+1) / \sin \lambda$$

for $\beta = 2 \cos \lambda$.

PROOF Again we use integers j, l, \dots in the range $[0, \frac{N}{2}]$ instead of the even numbers d, d' . We therefore compute

$$w_j \sin \lambda = \sum_{l=0}^j (-1)^{l+j} \binom{l+j}{2l} \sin \lambda (2 \cos \lambda)^{2l}.$$

By expanding both trigonometric functions of the right-hand side into exponentials and regrouping into a sum of sine functions, we obtain

$$w_j \sin \lambda = \sum_{l=0}^j (-1)^{l+j} \binom{l+j}{2l} \sum_{k=0}^l \left(\binom{2l}{k+l} - \binom{2l}{k+l+1} \right) \sin \lambda (2k+1).$$

Exchanging the order of the two sums we find again sums involving products of two binomial coefficients. These are very similar to those in the previous proof and, indeed, using again (5.21) and (5.24) of [65], we can bring these sums to the form

$$w_j \sin \lambda = \sum_{k=0}^j \left(\binom{j-k}{0} - \binom{j-k-1}{0} \right) \sin \lambda (2k+1).$$

As before both binomial coefficients are equal to one for all k , except for $k = j$ when the second one vanishes. The only term left is therefore $\sin \lambda (2j+1)$ as expected. \square

2.2.4 Q-Potts models with cylindrical boundary conditions

For this section and the next one, N is even.

The Q-Potts spin models, $Q \in \{1, 2, 3, 4\}$, are closely related to the double row matrix $D_N(\lambda, u)$ with $\beta^2 = (2 \cos \lambda)^2 = Q$. This section and the next detail this relationship.

Let a lattice of spins drawn on a $N \times (2M)$ rectangle, with N even, as shown in Figure 2.1 (a). The spins occupy the sites marked by dots. Nearest neighbors are indicated by gray bonds. The lattice is closed by periodic boundary conditions in the vertical direction, that is, the spins in the bottom line are identified to those on the top one. The spins on the leftmost and rightmost columns have only two

nearest neighbors. As all other spins, they may take any of the Q states available, so that free boundary conditions hold in the horizontal direction. A configuration σ is a choice, for each spin, of one of the Q states. Allowing for anisotropy, we define the energy of that configuration to be $E_\sigma = -J \sum_{\langle i,j \rangle (J)} \delta_{\sigma_i \sigma_j} - K \sum_{\langle i,j \rangle (K)} \delta_{\sigma_i \sigma_j}$ where $\sum_{\langle i,j \rangle (J)}$ stands for a sum over all nearest-neighbors pairs i, j with i an odd column and j in the next. These bonds are represented by dots in Figure 2.1 (a). Dashed lines are used for the K bonds. The Boltzmann weight of σ is $e^{-E_\sigma/k_B T}/Z$ with the normalization constant (the partition function) $Z = \sum_\sigma e^{-E_\sigma/k_B T}$.

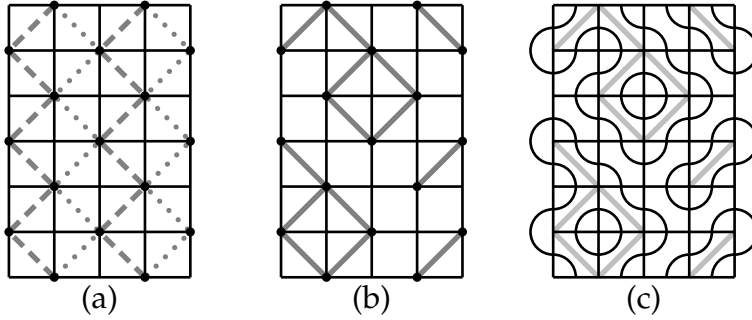


FIGURE 2.1 – A $N \times (2M)$ grid with $N = 4$ and $M = 3$ with a spin lattice at 45° : (a) with all vertices and bonds drawn, (b) a graph \mathcal{G} and (c) the corresponding loop configuration.

Let μ and ν be the restriction of σ to two neighboring lines containing $\frac{N}{2}$ spins. These are then separated by a line with $\frac{N}{2} + 1$ spins. Let ρ be the states of the spins on this intermediary line. It is customary to define the (spin) transfer matrix $\tilde{\Lambda}$, a $Q^{N/2} \times Q^{N/2}$ real matrix, by

$$\tilde{\Lambda}_{\mu,\nu} = \sum_{\rho} \prod_{\langle i,j \rangle (J)} \exp(\gamma_J (\delta_{\mu_i \rho_j} + \delta_{\rho_j \nu_i})) \prod_{\langle i,j \rangle (K)} \exp(\gamma_K (\delta_{\mu_i \rho_j} + \delta_{\rho_j \nu_i}))$$

where \sum_{ρ} is the sum over all intermediary states and the pairs $\langle i, j \rangle$ are restricted to the bonds between the lines described by μ and ν . The positive constant γ_X is the ratio of the interaction constant $X \in \{J, K\}$ and the temperature in dimensionless unit. The spectrum of $\tilde{\Lambda}$ is known for $Q = 2$ at critical temperature (see for example [17]) and the partition function is $Z = Z_{N \times M} = \text{tr } \tilde{\Lambda}^M$.

The partition function $Z_{N \times M}$ can also be expressed in terms of a sum over Fortuin-Kasteleyn graphs. The exponential $e^{-E_\sigma/k_B T}$ that occurs in the Boltzmann weight of σ can be written as

$$\prod_{\langle i,j \rangle (J)} (1 + v_J \delta_{\sigma_i \sigma_j}) \prod_{\langle i,j \rangle (K)} (1 + v_K \delta_{\sigma_i \sigma_j})$$

where $v_X = e^{\gamma_X} - 1$. Therefore

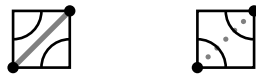
$$Z_{N \times M} = \sum_{\sigma} \prod_{(i,j) \in (J)} (1 + v_J \delta_{\sigma_i \sigma_j}) \prod_{(i,j) \in (K)} (1 + v_K \delta_{\sigma_i \sigma_j}) = \sum_{\mathcal{G}} \sum_{\sigma | \mathcal{G}} v_J^{N_{bJ}} v_K^{N_{bK}}.$$

In the last line, the sum $\sum_{\mathcal{G}}$ stands for the sum over possible graphs. The set of vertices is common to all these graphs and coincides with the set of spins. The sum $\sum_{\mathcal{G}}$ is therefore over the possible sets of bonds and N_{bX} is the number of X -bonds in \mathcal{G} . The inner sum $\sum_{\sigma | \mathcal{G}}$ is over all possible configurations σ compatible with the graph \mathcal{G} . To have the equality with the previous expression, we define a configuration σ to be compatible with \mathcal{G} if the states of two spins coincide when there is a bond in \mathcal{G} between them. The sum $\sum_{\sigma | \mathcal{G}}$ amounts then to a factor of Q for each connected component of \mathcal{G} . Then

$$Z_{N \times M} = \sum_{\mathcal{G}} v_J^{N_{bJ}} v_K^{N_{bK}} Q^{N_c}$$

where N_c is the number of connected components of \mathcal{G} . (The later expression has been known for many years [51].)

We represent a graph \mathcal{G} on the lattice by the diagram constructed as follows. Two corners of each box of Figure 2.1 (a) are occupied by spins, that is, vertices of \mathcal{G} . Each box is replaced by one where two quarter-circles are drawn with centers on opposite corners. If a bond exists in \mathcal{G} between the two vertices of \mathcal{G} , the centers are chosen so that the two quarter-circles do not touch the bond. If there is no bond, the quarter-circles cross the diagonal where the bond would have been. The two states for quarter-circles are shown below. In the first the full diagonal indicates the existence of a bond in \mathcal{G} , in the second the dotted diagonal its absence.

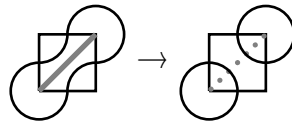


In Figure 2.1 (b) a graph \mathcal{G} is shown with its bonds drawn in gray. In (c) the same graph is represented with delimiting quarter-circles, instead of gray bonds. It is clear that representations with bonds (b) and with loops (c) are in one-to-one correspondence. If half-circles are added at the boundary of the grid as shown in (c), all loops formed by the quarter-circles are closed and it is possible to express the partition function in terms of data of the loop configurations only. (For the example of the Figure, $N_{bJ} = 6$, $N_{bK} = 8$, $N_b = N_{bJ} + N_{bK} = 14$, $N_c = 3$ and $\#(\mathcal{G}) = 5$.) This can be done using the following lemma, a variation of Euler's formula for triangulations.

LEMMA 2.2.6 *The relation $N_c = \frac{1}{2}(\#(\mathcal{G}) + N_s - N_b)$ holds for any graph \mathcal{G} on the strip with $N \times (2M)$ boxes. Here the number of spins $N_s = (N + 1) \times M$ is independent of \mathcal{G} , but the number of bonds N_b , the number of closed loops $\#(\mathcal{G})$ and the number of connected components N_c depend on \mathcal{G} .*

PROOF The formula holds when \mathcal{G} is the graph with all possible bonds. Then there is a single connected component ($N_c = 1$), the number of closed loops is $2+(N-1)M$ and the number of bonds $2NM$. Then $\frac{1}{2}(\#(\mathcal{G}) + N_s - N_b) = 1 = N_c$ as claimed. It is then sufficient to prove that, if the relationship holds for a graph \mathcal{G} , it also holds for any \mathcal{G}' obtained from \mathcal{G} by removal of a single bond. Three cases have to be studied : (i) the bond being removed is in itself a whole connected subgraph, (ii) the subgraph containing the bond remains connected after its removal and (iii) the subgraph is broken into two connected components by its removal.

In the case (i), the removal of the bond creates two connected components out of the single one and two closed loops from the one circumscribing the bond :

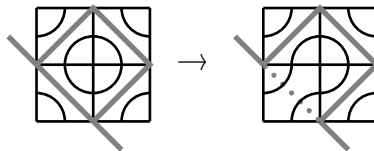


Then $N_c(\mathcal{G}') = N_c(\mathcal{G}) + 1$, $\#(\mathcal{G}') = \#(\mathcal{G}) + 1$ and $N_b(\mathcal{G}') = N_b(\mathcal{G}) - 1$ and

$$N_c(\mathcal{G}') = N_c(\mathcal{G}) + 1 = \frac{1}{2}(\#(\mathcal{G}) + N_s - N_b(\mathcal{G})) + 1 = \frac{1}{2}(\#(\mathcal{G}') + N_s - N_b(\mathcal{G}'))$$

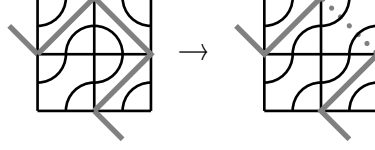
as before.

In case (ii), the subgraph of \mathcal{G} remains connected after the removal of the bond. This means that the two vertices tied by the bond are also tied to the component by other bonds. In other words, it is possible to go from one vertex to the other by visiting bonds of the subgraph other than the one being removed. The subgraph thus contains a cycle.



The removal of the bond will therefore decrease the number of loops : $\#(\mathcal{G}') = \#(\mathcal{G}) - 1$. Since $N_b(\mathcal{G}') = N_b(\mathcal{G}) - 1$ and $N_c(\mathcal{G}') = N_c(\mathcal{G})$, the identity is again easily verified. (Note that (ii) includes the case of a subgraph that winds non-trivially around the strip.)

In case (iii), the two quarter-circles on each side of the bond must belong to the same closed loop if its removal breaks the subgraph in two.



The data associated to \mathcal{G}' are $N_c(\mathcal{G}') = N_c(\mathcal{G}) + 1$, $\#(\mathcal{G}') = \#(\mathcal{G}) + 1$ and $N_b(\mathcal{G}') = N_b(\mathcal{G}) - 1$. Again an easy check shows that the identity is preserved. Note that the case (i) is in fact a particular case of (iii). \square

The critical temperature of Q-Potts models is known to be such that $v_J v_K = Q$ [8]. We will use the parametrization $\sqrt{Q} = 2 \cos \lambda$, $v_J / \sqrt{Q} = \sin(\lambda - u) / \sin(u)$, where $\lambda \in (0, \frac{\pi}{2})$ and $u \in [0, \lambda]$ is the anisotropy parameter. The previous lemma allows to write the partition function at criticality as

$$\begin{aligned} Z_{N \times M} &= \sum_{\mathcal{G}} v_J^{N_{bJ}} v_K^{N_{bK}} Q^{N_c} = \sum_{\mathcal{G}} Q^{(\#(\mathcal{G}) + N_s)/2} \left(\frac{\sin(\lambda - u)}{\sin(u)} \right)^{N_{bJ}} \left(\frac{\sin(u)}{\sin(\lambda - u)} \right)^{N_{bK}} \\ &= \frac{Q^{N_s/2}}{(\sin(u) \sin(\lambda - u))^{NM}} \sum_{\mathcal{G}} Q^{\#(\mathcal{G})/2} \sin^{N_{bJ}}(\lambda - u) \sin^{NM - N_{bJ}}(u) \\ &\quad \times \sin^{N_{bK}}(u) \sin^{NM - N_{bK}}(\lambda - u) \end{aligned}$$

which is the form (2.2.4) up to the overall factor κ^M , where

$$\kappa = (Q^{(N+1)/2} / (\sin(u) \sin(\lambda - u))^N).$$

Moreover, the weight given to every graph in $Z_{N \times M}$ is precisely the one in the definition of D_N . If we define $\Lambda = \tilde{\Lambda} / \kappa$, the Proposition 2.2.3 leads to a relationship between the traces of Λ and of D_N :

$$\boxed{\text{tr } \Lambda^M = \text{tr}(\rho(D_N^M)W), \quad \text{for all } M \in \mathbb{N}.} \quad (2.2.6)$$

The matrix $\rho(D_N^M)$ is block-triangular, that is, the blocks acting from V_N^d to $V_N^{d'}$ are zero if $d < d'$. The set of eigenvalues of $\rho(D_N^M)$ are then the union of those of the diagonal blocks of $\rho(D_N^M)$. Let δ be an eigenvalue of the diagonal block of $\rho(D_N)$ acting from V_N^d to V_N^d . On V_N^d , the matrix W acts as a multiple of the identity. Let w be this factor. Then, because W is diagonal, $\delta^M w$ is an eigenvalue of $\rho(D_N^M)W$. Let the eigenvalues of Λ be in decreasing order of absolute values : $|\lambda_1| \geq |\lambda_2| \geq \dots$

Similarly, let the eigenvalues of $\rho(D_N)$ be ordered as $|\delta_1| \geq |\delta_2| \geq \dots$. The identity (2.2.6) can be written as

$$\sum_i \lambda_i^M = \sum_j \delta_j^M w_j, \quad M \in \mathbb{N}. \quad (2.2.7)$$

The factors w_j are determined, for each eigenvalue δ_j , as described above. The first sum contains $Q^{N/2}$ eigenvalues, the second $\binom{N}{N/2}$. Note that, if an eigenvalue δ_j is degenerate, the various copies might have different weights w_j . Write $w(\delta)$ for the sum of the weights w_j over all eigenvalues equal to δ .

Let Δ be $\max\{|\lambda_1|, |\delta_1|\}$. Suppose for the time being that no other eigenvalues of Λ share the absolute value of λ_1 ; suppose, similarly, that the same statement holds for the spectrum of $\rho(D_N)$ and the absolute value of δ_1 . By dividing (2.2.7) by Δ^M and taking the limit $M \rightarrow \infty$, one can see that $|\lambda_1| > |\delta_1|$ is impossible. One can have $|\delta_1| > |\lambda_1|$ however, if $w(\delta_1)$ is zero. Finally one can have $|\delta_1| = |\lambda_1|$ and then the multiplicity $\text{mult } \lambda_1$ of the eigenvalue of the spin matrix must be equal to $w(\delta_1)$. One can then subtract from both members of (2.2.7) the contribution $\delta_1 w(\delta_1)$ of the maximum eigenvalue. The previous argument can then be repeated with the new sums.

What happens when some of the eigenvalues in either spectrum have the same absolute values but are distinct? Suppose that all eigenvalues with absolute values larger than a given $r > 0$ have been subtracted from the sum in (2.2.7). And suppose that several λ_i and δ_j have the same absolute value r and let $S = \{\alpha_1, \alpha_2, \dots, \alpha_n\}$ be the set of distinct phases. The equality (2.2.7) has then the form

$$\sum_{\alpha \in S} c_\alpha e^{i\alpha M} = v_M / r^M, \quad M \in \mathbb{N} \quad (2.2.8)$$

where v_M is the sum over all eigenvalues with absolute value less than r in either spectrum. For large M , the right-hand side is therefore small. The coefficient c_α in the left-hand side is

$$c_\alpha = \begin{cases} \text{mult}(re^{i\alpha}), & \text{if } re^{i\alpha} \text{ is an eigenvalue of only } \Lambda, \\ -w(re^{i\alpha}), & \text{if } re^{i\alpha} \text{ is an eigenvalue of only } \rho(D_M), \\ \text{mult}(re^{i\alpha}) - w(re^{i\alpha}), & \text{if } re^{i\alpha} \text{ is an eigenvalue of both.} \end{cases} \quad (2.2.9)$$

Let n be the number of (distinct) elements of S and consider n consecutive equations (2.2.8) with index $M, M+1, \dots, M+n-1$. The system of equations has the form $A_{MC} = w_M$ where c is the vector containing the c_α and w_M the vector of

components $v_M/r^M, v_{M+1}/r^{M+1}, \dots$. The matrix A_M is

$$\begin{pmatrix} e^{i\alpha_1 M} & e^{i\alpha_2 M} & \dots & e^{i\alpha_n M} \\ e^{i\alpha_1 (M+1)} & e^{i\alpha_2 (M+1)} & \dots & e^{i\alpha_n (M+1)} \\ \vdots & \vdots & \ddots & \vdots \\ e^{i\alpha_1 (M+n-1)} & e^{i\alpha_2 (M+n-1)} & \dots & e^{i\alpha_n (M+n-1)} \end{pmatrix}$$

and, after extracting a global phase $\prod_{\alpha \in S} e^{i\alpha M}$, is a Vandermonde matrix. The determinant of A is therefore the product of a phase that depends on M with the Vandermonde determinant that is independent of it. So the vector c is given by $A_M^{-1} w_M$ and this should hold independently of M . When M is taken to infinity, $A_M^{-1} w_M$ goes to zero and the vector c is therefore zero. The fact that c_α is zero for all elements of S has different consequences depending on the case in (2.2.9). The first case cannot happen : if $re^{i\alpha}$ is in the spectrum of Λ only, then $\text{mult } re^{i\alpha} > 0$. Consequently, all eigenvalues of Λ must be eigenvalues of $\rho(D_M)$. The second case may happen. It then forces the corresponding $\delta = re^{i\alpha}$ to have a $w(\delta) = 0$. And, in the third case, some eigenvalues λ and δ are equal and $\text{mult } \lambda = w(\delta)$. We have then proved the following result.

PROPOSITION 2.2.7 *Define the Q-Potts model ($Q = \beta^2 \in \{1, 2, 3\}$) on a lattice $\mathbb{N} \times (2M)$ as in Figure 2.1 with free boundary conditions on the left and right sides, and periodic boundary conditions in the vertical direction.*

- (i) *The partition function of the model is given by $Z_{\mathbb{N} \times M} = \kappa^M \text{tr}(\rho(D_N^M)W)$, for all $M \in \mathbb{N}$. W has been defined in Proposition 2.2.3*
- (ii) *The eigenvalues λ of the spin transfer matrix Λ of the Q-Potts model belong to the spectrum of the link representation $\rho(D_N)$ of the double-row transfer matrix and $\text{mult } \lambda$ in Λ is equal to the weight $w(\lambda)$, that is the sum of factors w_j of λ in $\rho(D_N)$.*
- (iii) *If an eigenvalue δ of $\rho(D_N)$ does not belong to the spectrum of Λ_N , the sum $w(\delta)$ of its weights is zero.*

2.2.5 Q-Potts models with fixed, free and mixed boundary conditions

The trace of the spin transfer matrix $\text{tr } \tilde{\Lambda}$ is the partition function for the lattice with periodic boundary condition in the vertical direction and free on the left and right sides. Of course there is more information in $\tilde{\Lambda}$ than just this particular partition function. Other partition functions, for spins at the top and bottom of the lattice (see Figure 2.2 (a)) in fixed, free or mixed boundary conditions while those

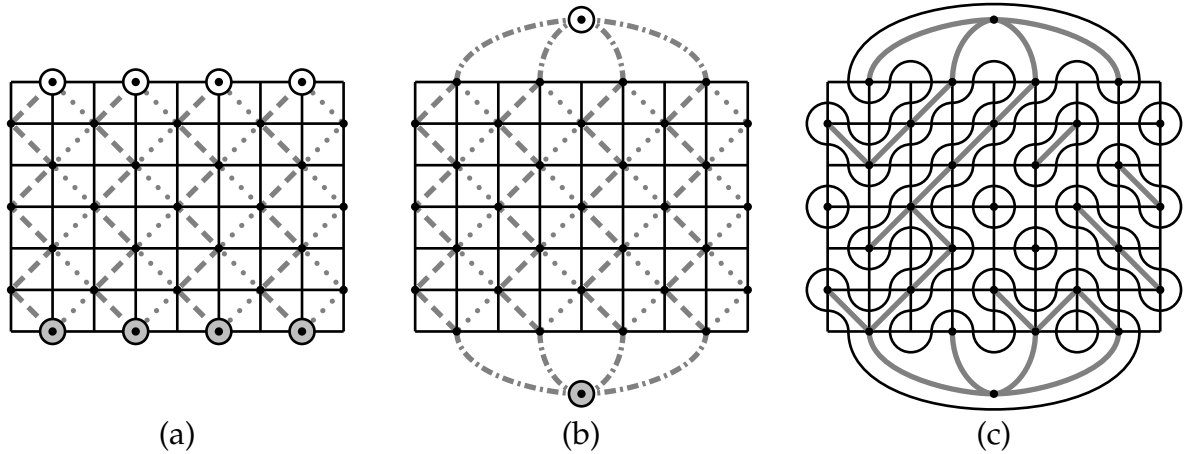


FIGURE 2.2 – The states of spins marked by white or gray circles in (a) are specified by boundary conditions. To obtain fixed boundary conditions, the spins are tied to a spurious spin in the desired state like in (b) and the interaction between the new spin and those at the boundary is sent to infinity. Again K bonds are represented by dashed lines, J bonds by dotted lines and L bonds by alternating dots and dashes. In (c) a FK graph (with $N_c^* = 7$) with the fixed boundary conditions on the top and bottom edges of the lattice. Note that this configuration contributes to the partition function $Z^{(b)}$, but is excluded from $Z^{(a)}$.

(iv) \odot is free, \bullet is fixed :

$$Z_{N \times M}^{(d)} = K(\beta, u) \beta^{-N/2-1} \langle \overbrace{\bullet \bullet \dots \bullet}^{\text{top}} | D_N^M(\lambda, u) \underbrace{\bullet \bullet \dots \bullet}_{\text{bottom}} \rangle_G \quad (2.2.13)$$

where

$$K(\beta, u) = \frac{\beta^{N_s}}{(\sin(u) \sin(\lambda - u))^{NM}} \quad \text{and} \quad N_s = (N + 1)M + \frac{1}{2}N.$$

PROOF The condition (i) that boundary spins be all fixed to a single value is implemented as in Figure 2.2 (b) : all spins from the top are connected to a spurious spin with fixed value. The same is done for those on the bottom. By putting a factor $e^{-N\gamma_L}$ and sending the interaction L of these bonds to infinity, we get the desired partition function :

$$Z_{N \times M}^{(a)} = \lim_{L \rightarrow \infty} e^{-N\gamma_L} \sum_{\bar{\sigma}} e^{-E_{\bar{\sigma}}/k_B T}, \quad E_{\bar{\sigma}} = -J \sum_{\langle i,j \rangle (J)} \delta_{\bar{\sigma}_i \bar{\sigma}_j} - K \sum_{\langle i,j \rangle (K)} \delta_{\bar{\sigma}_i \bar{\sigma}_j} - L \sum_{\langle i,j \rangle (L)} \delta_{\bar{\sigma}_i \bar{\sigma}_j}$$

where $\bar{\sigma}$ is the set of all spin configurations in Figure 2.2 (b), with \odot and \ominus fixed to distinct states.

$$\begin{aligned}
Z_{N \times M}^{(a)} &= \lim_{L \rightarrow \infty} e^{-N\gamma_L} \sum_{\bar{\sigma}} e^{-E_{\bar{\sigma}}/k_B T} \\
&= \lim_{L \rightarrow \infty} e^{-N\gamma_L} \sum_{\bar{\sigma}} \prod_{\langle i,j \rangle (J)} (1 + v_J \delta_{\bar{\sigma}_i \bar{\sigma}_j}) \prod_{\langle i,j \rangle (K)} (1 + v_K \delta_{\bar{\sigma}_i \bar{\sigma}_j}) \prod_{\langle i,j \rangle (L)} (1 + v_L \delta_{\bar{\sigma}_i \bar{\sigma}_j}) \\
&= \sum_{\sigma} \prod_{\langle i,j \rangle (J)} (1 + v_J \delta_{\sigma_i \sigma_j}) \prod_{\langle i,j \rangle (K)} (1 + v_K \delta_{\sigma_i \sigma_j}) \\
&= \sum_{\sigma} \sum_{\mathcal{G}|\sigma} v_J^{N_{bJ}} v_K^{N_{bK}}.
\end{aligned}$$

The first sum is now on spin configurations σ with \odot and \ominus of Figure 2.2 (a) fixed, and $\mathcal{G}|\sigma$ represents the Fortuin-Kasteleyn loop configurations that are in the restricted set compatible with σ . Inverting the sums, the restriction on σ is moved to the set of FK configurations ; it becomes the set \mathcal{G}^a of all graphs that do not contain a subgraph connecting the top and bottom edges of the lattice. The partition function is then

$$Z_{N \times M}^{(a)} = \sum_{\mathcal{G}_a} \sum_{\sigma|\mathcal{G}_a} v_J^{N_{bJ}} v_K^{N_{bK}} = \sum_{\mathcal{G}_a} v_J^{N_{bJ}} v_K^{N_{bK}} Q^{N_c^*}. \quad (2.2.14)$$

At the last step, we summed over all σ compatible with a given graph in \mathcal{G}_a . Since the clusters touching the boundary have fixed spin, the resulting weight is $Q^{N_c^*}$ where N_c^* is the number of closed components not touching the top and lower boundaries, that is, $N_c^* = N_c - 2$. Lemma 2.2.6 was proved for a lattice drawn on the geometry of a ribbon. In the present case, the lattice is drawn on a rectangle, but the relationship remains $N_c = \frac{1}{2}(\#\mathcal{G}) + N_s^* - N_b^*$ when N_s^* and N_b^* include the spurious sites and the bonds joining them to the lattice. This relation is proved using the same arguments. In terms of N_s and N_b , the numbers without the spurious sites and bonds, one gets $N_c^* = \frac{1}{2}(\#\mathcal{G}) + N_s - N_b - N - 2$. At the critical temperature and for the parametrization of the interactions used before, the partition function is now

$$Z_{N \times M}^{(a)} = \frac{K(\beta, \mathbf{u})}{\beta^{N+2}} \sum_{\mathcal{G}_a} \underbrace{\beta^{\#\mathcal{G}} \sin^{N_{bJ}}(\lambda - \mathbf{u}) \sin^{NM - N_{bJ}}(\mathbf{u}) \sin^{N_{bK}}(\mathbf{u}) \sin^{NM - N_{bK}}(\lambda - \mathbf{u})}_{X(\mathcal{G})}. \quad (2.2.15)$$

To perform the final sum, we write $\mathcal{G}^a \cup \mathcal{G}_{cr} = \mathcal{G}$ where the subscript \mathcal{G}_{cr} is the set of crossing graphs. The two sets \mathcal{G}_a and \mathcal{G}_{cr} are disjoint. The only way to close the loops arriving at the horizontal edges that is compatible with the bonds ending at one of

the spurious sites is by adding the set of arcs $\overbrace{\text{---}}^{\text{---}}$ on the top and the bottom of the lattice. Therefore $\sum_{\mathcal{G}} \chi(\mathcal{G}) = \langle \overbrace{\text{---}}^{\text{---}} | D_N^M(\lambda, u) \overbrace{\text{---}}^{\text{---}} \rangle_{\mathcal{G}}$. Note that the Gram product adds the proper power of β to account for the loops that are closed by adding the arcs at the lower boundary. The argument for $\sum_{\mathcal{G}_{cr}} \chi(\mathcal{G})$ is similar. This time, the Gram product of $D_N^M(\lambda, u) \downarrow \text{---} \dots \text{---} \downarrow$ with $\downarrow \text{---} \dots \text{---} \downarrow$ excludes any non-crossing graph. Moreover each graph contributing to the latter Gram product also appears in $\langle \overbrace{\text{---}}^{\text{---}} | D_N^M(\lambda, u) \overbrace{\text{---}}^{\text{---}} \rangle_{\mathcal{G}}$, but with a weight that has an additional factor β for the outer loop that is left open here. Adding by hand a factor of β to the second sum yields (2.2.10).

The steps leading to (i) can be used for (ii) and carry through up to (2.2.14), with \mathcal{G}_a replaced with $\mathcal{G}_b = \mathcal{G}$. Here, however, N_c^* is $N_c - 1$ when a crossing occurs and $N_c - 2$ when none exists :

$$\begin{aligned} Z_{N \times M}^{(b)} &= \left(\sum_{\mathcal{G}_a} + \sum_{\mathcal{G}_{cr}} \right) v_j^{N b_j} v_k^{N b_k} Q^{N_c^*} = Z_{N \times M}^{(a)} + \frac{\beta^{N_s - N}}{(\sin(u) \sin(\lambda - u))^{NM}} \sum_{\mathcal{G}_{cr}} \chi(\mathcal{G}) \\ &= Z_{N \times M}^{(a)} + K(\beta, u) \beta^{1-N} \langle \downarrow \text{---} \dots \text{---} \downarrow | D_N^M(\lambda, u) \downarrow \text{---} \dots \text{---} \downarrow \rangle_{\mathcal{G}} \end{aligned}$$

and the result follows.

Cases (iii) and (iv) are simpler. Their proofs do not require any new idea and are omitted. \square

By the last remark of Definition 4.5, any element of the form $\langle v | D_N^M w \rangle_{\mathcal{G}}$ can be expressed as $\sum_y G_{vy} \rho(D_N^M)_{yw}$: the information on $Z_{N \times M}$ is contained in $\rho(D_N^M)$ as suggested earlier.

2.3 A central element of $\mathbb{T}\mathbb{L}_N(\beta)$

Let λ be fixed. The element $D_N(\lambda, u) \in \mathbb{T}\mathbb{L}_N$ is a homogeneous polynomial in $\sin u$ and $\sin(\lambda - u)$ of order $2N$. Its coefficients are elements of $\mathbb{T}\mathbb{L}_N$. Moreover, since $D_N(\lambda, u) = D_N(\lambda, u + \pi)$ and $D_N(\lambda, u) = D_N(\lambda, \lambda - u)$ (see [63]), the double-row matrix $D_N(\lambda, u)$ can be written as a Fourier series in $v = u - \lambda/2$ ($v = 0$ is then the isotropic case) :

$$D_N(\lambda, v + \lambda/2) = \frac{1}{2} C_0 + \sum_{i=1}^N C_{2i}(\lambda) \cos(2iv) \quad (2.3.1)$$

where the Fourier coefficients $C_{2i}(\lambda)$ are again elements of $\mathbb{T}\mathbb{L}_N$. The commutation relation $[D_N(\lambda, u), D_N(\lambda, v)] = 0$ implies that $[D_N(\lambda, u), C_{2i}(\lambda)] = 0$ for all i or simply $[C_{2i}(\lambda), C_{2j}(\lambda)] = 0$ for all i, j . One of these Fourier coefficients is easier than the

others to study since it is a central element of $\mathbb{T}\mathbb{L}_N$. Even though it is central, we shall see in the present and following sections that it carries much of the information about the Jordan structure. We start our analysis by this coefficient.

2.3.1 The last Fourier coefficient of $D_N(\lambda, u)$

DEFINITION 2.3.1 *The braid 2-box (see for example [45]) is defined as :*

$$\begin{aligned} \begin{array}{|c|} \hline \text{---} \\ \hline \text{---} \\ \hline \end{array} &= -ie^{-i\lambda/2} \lim_{u \rightarrow -i\infty} \frac{1}{\sin(\lambda - u)} \begin{array}{|c|} \hline \text{---} \\ \hline \text{---} \\ \hline \end{array} \begin{array}{|c|} \hline u \\ \hline \end{array} = ie^{i\lambda/2} \begin{array}{|c|} \hline \text{---} \\ \hline \text{---} \\ \hline \end{array} - ie^{-i\lambda/2} \begin{array}{|c|} \hline \text{---} \\ \hline \text{---} \\ \hline \end{array}, \\ \begin{array}{|c|} \hline \text{---} \\ \hline \text{---} \\ \hline \end{array} &= ie^{i\lambda/2} \lim_{u \rightarrow +i\infty} \frac{1}{\sin(\lambda - u)} \begin{array}{|c|} \hline \text{---} \\ \hline \text{---} \\ \hline \end{array} \begin{array}{|c|} \hline u \\ \hline \end{array} = -ie^{-i\lambda/2} \begin{array}{|c|} \hline \text{---} \\ \hline \text{---} \\ \hline \end{array} + ie^{i\lambda/2} \begin{array}{|c|} \hline \text{---} \\ \hline \text{---} \\ \hline \end{array}. \end{aligned}$$

We define the double-row braid matrix :

$$F_N(\lambda) = \begin{array}{c} \overbrace{\hspace{10em}}^N \\ \begin{array}{|c|c|c|c|c|} \hline \bullet & \bullet & \dots & \bullet & \bullet \\ \hline \text{---} & \text{---} & \dots & \text{---} & \text{---} \\ \hline \bullet & \bullet & \dots & \bullet & \bullet \\ \hline \end{array} \end{array}.$$

Note that $\begin{array}{|c|} \hline \text{---} \\ \hline \text{---} \\ \hline \end{array}$ and $\begin{array}{|c|} \hline \text{---} \\ \hline \text{---} \\ \hline \end{array}$ can be obtained from one another by a simple rotation by $\frac{\pi}{2}$ of the connectivity boxes. Consequently one gets rid of the small arc giving the orientation of the box. Note also that the weights of one are the complex conjugate of those of the other.

Let c be an element of $\mathbb{T}\mathbb{L}_N$. We shall denote by $\rho(c)_{d',d}$ the submatrix of its link representation containing lines associated with basis elements in $B_N^{d'}$ and columns with those in B_N^d . Because $\rho(c)$ never increases the number of defects, $\rho(c)_{d',d} = 0$ whenever $d' > d$.

LEMMA 2.3.1 (i) *The last Fourier coefficient of $D_N(\lambda, u)$ is given by*

$$C_{2N}(\lambda) = 2^{-2N+1} F_N(\lambda).$$

(ii) *The diagonal submatrices $\rho(F_N)_{d,d}$ are*

$$\rho(F_N(\lambda))_{d,d} = 2(-1)^d \cos(\lambda(d+1)) \text{id}_{\dim V_N^d}. \quad (2.3.2)$$

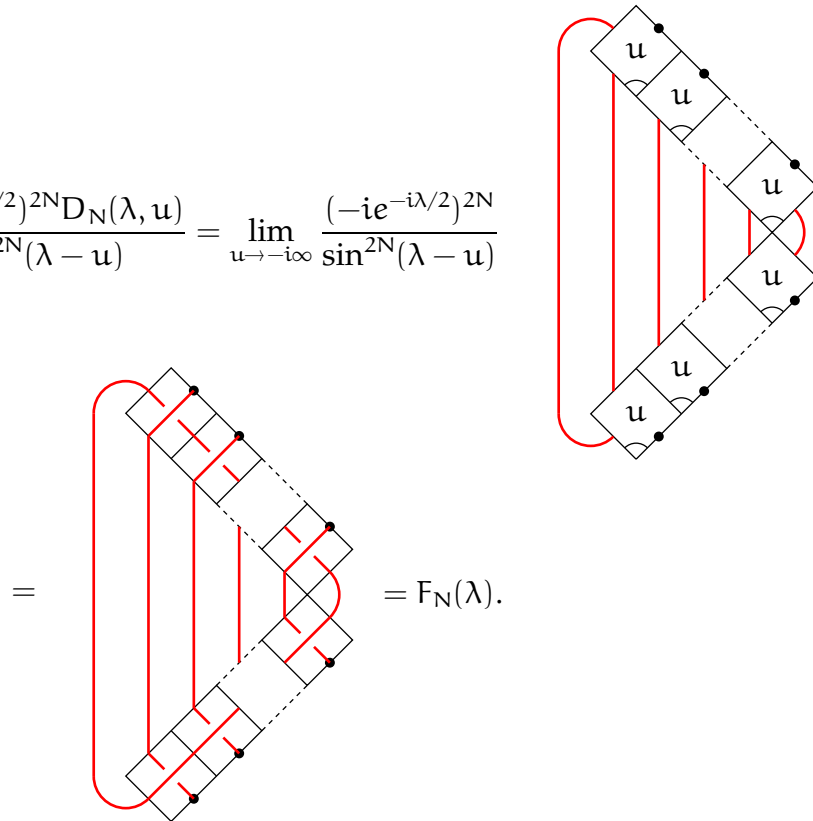
(iii) *$F_N(\lambda)$ is in the center of $\mathbb{T}\mathbb{L}_N(\beta)$ with $\beta = 2 \cos \lambda$.*

PROOF To prove (i), the limit of

$$D_N(\lambda, v + \lambda/2) = \frac{1}{2}C_0 + \sum_{j=1}^N C_{2j}(\lambda) \cos(2jv) = \frac{1}{2} \sum_{-N \leq j \leq N} C_{|2j|} e^{2ijv}$$

is taken with the appropriate power of the factor defining the braid box. The limit of the left-hand side gives

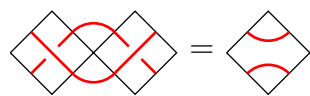
$$\lim_{u \rightarrow -i\infty} \frac{(-ie^{-i\lambda/2})^{2N} D_N(\lambda, u)}{\sin^{2N}(\lambda - u)} = \lim_{u \rightarrow -i\infty} \frac{(-ie^{-i\lambda/2})^{2N}}{\sin^{2N}(\lambda - u)}$$



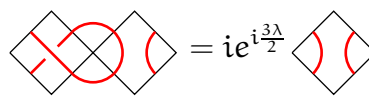
That of the right-hand side is

$$(-ie^{-i\lambda/2})^{2N} \lim_{u \rightarrow -i\infty} \frac{1}{2} \sum_{-N \leq j \leq N} C_{|2j|} \frac{e^{2ij(u-\lambda/2)}}{\sin^{2N}(\lambda - u)} = 2^{2N-1} C_{2N}.$$

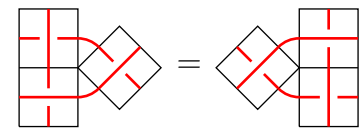
To prove (ii) and do other computations, several identities will be used. The following identities are well-known and proved for example in [45] :



(a) Inversion relation



(b) Twist relation



(c) Yang-Baxter equation

The next one characterizes the action of two braid boxes on an arc :

$$\begin{array}{|c|c|c|} \hline & \text{arc} & \\ \hline \hline \hline \\ \hline \hline \hline \\ \hline \end{array} = \begin{array}{|c|c|c|} \hline & \text{arc} & \\ \hline \hline \hline \\ \hline \hline \hline \\ \hline \end{array} = \begin{array}{|c|c|c|} \hline & \text{arc} & \\ \hline \hline \hline \\ \hline \hline \hline \\ \hline \end{array} . \tag{2.3.3}$$

It can be verified by direct computation. Therefore, when $F_N(\lambda)$ acts on a link state, the arcs of the state propagate down the diagrammatic representation of F_N . For instance :

$$\begin{array}{|c|c|c|c|c|c|c|c|} \hline & \text{arc} & & \text{arc} & & \text{arc} & & \text{arc} \\ \hline \hline \hline \hline \\ \hline \hline \hline \hline \\ \hline \end{array} = \begin{array}{|c|c|c|c|c|c|c|c|} \hline & \text{arc} & & \text{arc} & & \text{arc} & & \text{arc} \\ \hline \hline \hline \hline \\ \hline \hline \hline \hline \\ \hline \end{array} = \begin{array}{|c|c|c|c|c|c|c|c|} \hline & \text{arc} & & \text{arc} & & \text{arc} & & \text{arc} \\ \hline \hline \hline \hline \\ \hline \hline \hline \hline \\ \hline \end{array} . \tag{2.3.4}$$

This simple observation proves that $\rho(F_N(\lambda))_{d,d}$ will be a constant times the identity : the arcs in the incoming link state are carried through and are part of the outgoing one, and if any pair of entering defects annihilates, the image is not in V_N^d . When an arc goes through the transfer matrix, it forces one of the two states for each box it visits, and it creates equal numbers of both box states so that the factors $ie^{i\lambda/2}$ and $-ie^{-i\lambda/2}$ cancel. All the boxes whose state has been forced by the arc can then be removed since they contribute globally by a factor of 1. The matrix block $\rho(F_N(\lambda))_{d,d}$ is therefore a multiple of the identity matrix and the factor is obtained by calculating the action of $F_d(\lambda)$ on the link state with d defects. The sum in the top left box is first done explicitly :

$$\begin{array}{|c|c|c|c|} \hline & \text{arc} & & \text{arc} \\ \hline \hline \hline \hline \\ \hline \hline \hline \hline \\ \hline \end{array} = -ie^{-i\lambda/2} \begin{array}{|c|c|c|c|} \hline & \text{arc} & & \text{arc} \\ \hline \hline \hline \hline \\ \hline \hline \hline \hline \\ \hline \end{array} + ie^{i\lambda/2} \begin{array}{|c|c|c|c|} \hline & \text{arc} & & \text{arc} \\ \hline \hline \hline \hline \\ \hline \hline \hline \hline \\ \hline \end{array} .$$

Because only the diagonal element is of interest, states with a smaller number of defects are not considered. In the following equalities, the “ d ” over the equal sign

stresses the fact that equalities are up to states whose number of defects is smaller than d . In many braid boxes, this constraint chooses one of the two states. The first term above is

$$\begin{aligned}
 & (-ie^{-i\lambda/2}) \text{ [diagram]} \stackrel{d}{=} (-ie^{-i\lambda/2})^2 \text{ [diagram]} \\
 & \stackrel{d}{=} (-ie^{-i\lambda/2})^{(2d-1)} \text{ [diagram]} \\
 & = (-1)^d e^{-i\lambda(d+1)} \text{ [diagram]} .
 \end{aligned}$$

We have used the twist relation to obtain the last equality. The second term is computed as follows.

$$\begin{aligned}
 & (ie^{i\lambda/2}) \text{ [diagram]} \stackrel{d}{=} (ie^{i\lambda/2})^2 \text{ [diagram]} \\
 & \quad + \text{ [diagram]} \\
 & \stackrel{d}{=} (ie^{i\lambda/2})^d \text{ [diagram]} = (ie^{i\lambda/2})^{(d+1)} e^{i\lambda} \text{ [diagram]} \\
 & \stackrel{d}{=} (-1)^d e^{i\lambda(d+1)} \text{ [diagram]} .
 \end{aligned}$$

The last term of the first line does not contribute to $\rho(F_N(\lambda))_{d,d}$ because (2.3.3) causes the arc to propagate downwards to the bottom, decreasing the number of defects by 2. The sum of the two contributions is the constant in (2.3.2). (Another proof of this identity is given in Appendix 2.B.) To prove statement (iii), that F_N is a central element in \mathbb{T}_N , it is sufficient to verify that F_N commutes with the generators e_i . This is a direct consequence of the identity (2.3.3) and an easy computation. For example

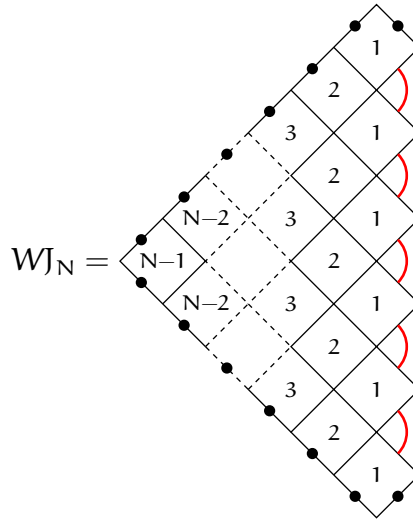
$$F_N e_2 = \begin{array}{c} \begin{array}{|c|c|c|c|} \hline \bullet & \bullet & \bullet & \bullet \\ \hline \bullet & \bullet & \bullet & \bullet \\ \hline \bullet & \bullet & \bullet & \bullet \\ \hline \bullet & \bullet & \bullet & \bullet \\ \hline \bullet & \bullet & \bullet & \bullet \\ \hline \bullet & \bullet & \bullet & \bullet \\ \hline \bullet & \bullet & \bullet & \bullet \\ \hline \end{array} \\ = \begin{array}{c} \begin{array}{|c|c|c|c|} \hline \bullet & \bullet & \bullet & \bullet \\ \hline \bullet & \bullet & \bullet & \bullet \\ \hline \bullet & \bullet & \bullet & \bullet \\ \hline \bullet & \bullet & \bullet & \bullet \\ \hline \bullet & \bullet & \bullet & \bullet \\ \hline \bullet & \bullet & \bullet & \bullet \\ \hline \bullet & \bullet & \bullet & \bullet \\ \hline \bullet & \bullet & \bullet & \bullet \\ \hline \end{array} \\ = \begin{array}{c} \begin{array}{|c|c|c|c|} \hline \bullet & \bullet & \bullet & \bullet \\ \hline \bullet & \bullet & \bullet & \bullet \\ \hline \bullet & \bullet & \bullet & \bullet \\ \hline \bullet & \bullet & \bullet & \bullet \\ \hline \bullet & \bullet & \bullet & \bullet \\ \hline \bullet & \bullet & \bullet & \bullet \\ \hline \bullet & \bullet & \bullet & \bullet \\ \hline \bullet & \bullet & \bullet & \bullet \\ \hline \end{array} = e_2 F_N. \end{array} \quad \square$$

Even though equation (2.3.3) was introduced as a tool to prove the previous lemma, it implies that $\rho(F_N(\lambda))$ can be computed recursively with minimal cost. In fact, the knowledge of $\rho(F_n(\lambda))$, $n < N$, determines with no further computation all columns of $\rho(F_N(\lambda))$ except the last one. This can be seen easily. Let v be any vector in B_N that has at least one arc, that is, any basis vector except the last one that has N defects. Then, when $F_N(\lambda)$ acts on v , all boxes under the arcs of v are fixed by (2.3.3) and only the boxes of $F_N(\lambda)$ under defects of v remain to be summed. Moreover these boxes are connected horizontally by the arcs of v that have moved downward into $F_N(\lambda)$. All boxes that have been fixed by the arcs can be removed and the remaining columns of $F_N(\lambda)$ glued together. If $v \in B_N^d$, then the action of $F_N(\lambda)$ on v is obtained by the action of $F_d(\lambda)$ on the vector with d defects. Since $d < N$, this information is contained in the last column of $\rho(F_d(\lambda))$ and, to obtain the components of the vector $F_N(\lambda)v$, one has simply to insert back the arcs into the basis vectors that correspond to non-zero elements of this last column. This observation that allows for a recursive computation of $\rho(F_N(\lambda))$ can be completed by an efficient algorithm to compute the last column of $\rho(F_N(\lambda))$. This algorithm is described in Appendix 2.B.

2.3.2 The Wenzl-Jones Projector

A family of linear transformations P^d will play a central role in the rest of this paper. They are constructed from the Wenzl-Jones projectors which we first introduce.

DEFINITION 2.3.2 For each $N \geq 1$, define $WJ_N \in \mathbb{T}L_N(\beta)$ to be $WJ_1 = \text{id}$ and, for $N > 1$,



and each box stands for

$$\begin{array}{c} \diamond \\ k \end{array} = \underbrace{\begin{array}{c} \diamond \\ \text{red arcs} \end{array}}_{\text{id}} + \frac{S_k}{S_{k+1}} \underbrace{\begin{array}{c} \diamond \\ \text{red arcs} \end{array}}_{e_{N-k}} = \frac{(-1)^k}{S_{k+1}} \begin{array}{c} \diamond \\ -k\lambda \end{array} \tag{2.3.5}$$

where the following compact notation is used from now on :

$$S_k = \sin(k\Lambda), \quad C_k = \cos(k\Lambda), \quad \Lambda = \pi - \lambda.$$

Note that with this notation, $\beta = -2C_1 = -S_2/S_1$ and $\Lambda \in (\frac{\pi}{2}, \pi)$. Throughout the next sections, we will relax this last constraint and take $\Lambda \in \mathbb{R}$ even though the corresponding loop model is unphysical, having negative Boltzmann weights.

This diagrammatic definition appears in [53] and, more recently, in [45]. But the object itself has been known to mathematicians for a long time (see [66], [67], [60]). Note that, due to the factors $S_{k+1} = \sin(\Lambda(k+1))$ in the denominator, the WJ_N may fail to exist in certain of the algebras $\mathbb{T}L_N(\beta)$. A closer look will be given to this difficulty starting in the following subsections.

PROPOSITION 2.3.2 The WJ_N are non-zero elements and satisfy the following properties :

- (i) $WJ_N e_i = e_i WJ_N = 0$ for $N \geq 2$ and $i = 1, 2, \dots, N-1$;
- (ii) $(WJ_N)^2 = WJ_N$.

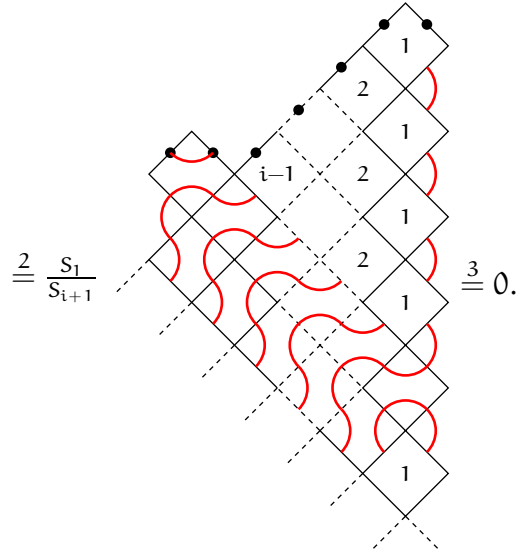
PROOF To prove statement (i), the following two identities are needed :

$$\begin{aligned}
 \begin{array}{|c|} \hline k \\ \hline \hline k+1 \\ \hline \end{array} &= \frac{S_k}{S_{k+1}} \begin{array}{|c|} \hline \hline \hline \hline \end{array} + \begin{array}{|c|} \hline \hline \hline \hline \end{array} + \frac{S_k}{S_{k+2}} \begin{array}{|c|} \hline \hline \hline \hline \end{array} + \frac{S_{k+1}}{S_{k+2}} \begin{array}{|c|} \hline \hline \hline \hline \end{array} \\
 &= \frac{S_k}{S_{k+1}} \begin{array}{|c|} \hline \hline \hline \hline \end{array} + \underbrace{\left(1 + \frac{S_k}{S_{k+2}} - \frac{S_2 S_{k+1}}{S_1 S_{k+2}}\right)}_0 \begin{array}{|c|} \hline \hline \hline \hline \end{array} = \frac{S_k}{S_{k+1}} \begin{array}{|c|} \hline \hline \hline \hline \end{array},
 \end{aligned}$$


$$\begin{array}{|c|} \hline 1 \\ \hline \end{array} = \begin{array}{|c|} \hline \hline \hline \hline \end{array} + \frac{S_1}{S_2} \begin{array}{|c|} \hline \hline \hline \hline \end{array} = \left(1 - \frac{S_2 S_1}{S_1 S_2}\right) \begin{array}{|c|} \hline \hline \hline \hline \end{array} = 0. \tag{2.3.6}$$

Note that the second identity is just $WJ_2 e_1 = 0$. For $N > 2$,

$$WJ_N e_{r-i} = \begin{array}{c} \text{[Lattice diagram with red arcs on bottom edges]} \end{array} = \frac{1}{S_{i+1}} \begin{array}{c} \text{[Lattice diagram with red loop on top edge and red arcs on bottom edges]} \end{array}$$



Here, the first identity has been used once after equality 1 and $i - 1$ more times after equality 2, allowing bubbles to propagate in the lower right direction. Finally, the second identity has been used after equality 3 and the bubble vanishes. To obtain the relation $e_{r-i}WJ_N = 0$, the generator e_{r-i} is applied from below, and the bubbles propagate in the upper right direction.

Statement (ii) is trivially true for WJ_1 . Now let $G \in \mathbb{T}L_N(\beta)$. It can be written as $G = \alpha_{id}(G) id + \sum_{\{c\}^*} \alpha_c(G)c$ where $\{c\}^*$ is the set of all connectivities in $\mathbb{T}L_N(\beta)$ (as described in section 2.2.1), excluding the identity. Since every connectivity in $\{c\}^*$ is a finite product of the e_{is} , $(\sum_{\{c\}^*} \alpha_c c) \times WJ_N = 0$ and $GWJ_N = \alpha_{id}(G)WJ_N$. Choosing $G = WJ_N$, it only remains to show that $\alpha_{id}(WJ_N) = 1$. This is indeed true, as the only configuration giving the identity is the one where every box is chosen to be . The normalization of the boxes in eq. (4.5.5) ensures that the total weight $\alpha_{id}(WJ_N)$ is 1. \square

Kauffman and Lins [60] introduce the family of $WJ_N \in \mathbb{T}L_N$ recursively and they show that there is a unique non-zero element in $\mathbb{T}L_N$ that has the two properties stated in the above proposition. The two definitions, theirs and the present, must therefore coincide. The element of $\mathbb{T}L_N$ obtained by reflecting the diagram defining WJ_N along a vertical axis also has the properties of Proposition 2.3.2; by unicity it must also coincide with WJ_N .

To introduce the family of linear transformations P^d , the following subspaces of the link space will be needed. Let $UpTo_d$ be the span of $\cup_{e \leq d} B_N^e$ where B_N^e is the link basis of the subspace of vectors with precisely e defects. Therefore $UpTo_d$ is the subspaces of all vectors whose components have up to d defects. The subspaces

UpTo_d depend also on N ; we chose not to add the label N to the notation. The natural filtration of the link space and the fact that connectivities $c \in \mathbb{T}_N$ do not increase the number of defects are formulated easily in terms of these subspaces : if N is even

$$\text{UpTo}_0 \subset \text{UpTo}_2 \subset \dots \subset \text{UpTo}_N = V_N \quad \text{and} \quad \rho(c)\text{UpTo}_d \subset \text{UpTo}_d, \quad \text{for all } d$$

and similarly for N odd. We also define $\text{UpTo}_{-1} = \text{UpTo}_{-2} = \{0\}$.

DEFINITION 2.3.3 *The linear transformation $P^d : \text{UpTo}_d \rightarrow \text{UpTo}_d, 0 \leq d \leq N$ with N and d of the same parity, is defined by $P^0 = \text{id}$ and $P^1 = \text{id}$ and, for $d \geq 2$, by its action on the basis $\cup_{e \leq d} B_N^e$:*

- (i) $P^d v = 0$ if $v \in B_N^e$ with $e < d$;
- (ii) for $v \in B_N^d$, the following procedure is followed : first, all arcs are removed from v , leaving its d defects ; second, the action of $\rho(WJ_d)$ on these d defects is computed ; and finally, the arcs of v are then reinserted, unchanged and in their original positions, into each vectors of the linear combination obtained from $\rho(WJ_d)v^d$.

The definition of P^d on the elements of B_N^d is somewhat awkward. But it has a diagrammatic representation that is easy to work with, namely the action of P^d on $v \in B_N^d$ is drawn from top to bottom as first the projector WJ_d acting on d defects followed by the insertion of the arcs between the defects coming out WJ_d . Here is the action of P^2 on two vectors of V_4^2 , given first in the form $P^2 v$, second diagrammatically, and last, as a linear combination of basis elements :

$$\begin{aligned}
 P^2(\downarrow \downarrow \curvearrowright) &= \begin{array}{c} \diamond 1 \\ \downarrow \downarrow \curvearrowright \end{array} = \downarrow \downarrow \curvearrowright + \frac{S_1}{S_2} \curvearrowright \curvearrowright, \\
 P^2(\downarrow \curvearrowright \downarrow) &= \begin{array}{c} \diamond 1 \\ \downarrow \curvearrowright \downarrow \end{array} = \downarrow \curvearrowright \downarrow + \frac{S_1}{S_2} \curvearrowright \curvearrowright.
 \end{aligned}$$

Even though the P^d s are similar to the WJ_N , they are different by one property, namely statement (i) of Proposition 2.3.2 does not make sense for P^d . The product $e_i WJ_N$ amounts to closing two neighboring defects coming out of WJ_N . But, for vectors in B_N^d , defects are not necessarily contiguous since they may be separated by arcs. Still one sees, in the second example above, that a generalization of this property can be proposed. Indeed, if c is any connectivity that ties positions 1 and

4, then $cP^2(\downarrow \curvearrowright \downarrow)$ will be zero :

$$cP^2(\downarrow \curvearrowright \downarrow) = \boxed{\downarrow \curvearrowright \downarrow} - \frac{1}{\beta} \boxed{\downarrow \curvearrowright \downarrow} = 0.$$

This observation can be generalized.

PROPOSITION 2.3.3 *The linear transformations P^d have the following properties.*

- (i) P^d is a projector.
- (ii) Let $v \in B_N^d$ and i, j be positions of two contiguous defects of v . If c is a connectivity in \mathbb{T}_N that join i and j , then $cP^d v = 0$.
- (iii) The restriction $\rho(F_N(\lambda))|_{\text{UpTo}_d}$ commutes with P^d and, on UpTo_d ,

$$\rho(F_N(\lambda))P^d = -2C_{d+1}P^d.$$

PROOF If $v \in \text{UpTo}_e$ with $e < d$, then $P^d v = 0$ and therefore $(P^d)^2 v = P^d v$. If $v \in B_N^d$, then $P^d v = v + w$ for some $w \in \text{UpTo}_{d-2}$ and therefore $P^d w = 0$. Then $(P^d)^2 v = P^d(v + w) = P^d v$.

The second statement is the equivalent of the property $e_i W_N = 0$ proved in Proposition 2.3.2 and is actually an immediate consequence of it. The action of P^d on V_N^d cannot be written as the action of a given element of \mathbb{T}_N as it was for W_N . However the proof of (i) in the previous proposition is purely in terms of connectivities. For example, the two first identities opening the proof do not state on which defects they act; they are statements about connectivities only. If a connectivity c closes two adjacent defects of v , then $cP^d v$ will contain an arc, from i to j , encircling whichever arcs that lie between positions i and j . These arcs will have to be closed by c and, for the purpose of studying connectivities, the loops closed that way can be forgotten. The tie between i and j will introduce therefore the same connectivity as that introduced by e_i in the proof of Proposition 2.3.2, leading to $cP^d v = 0$.

For (iii), note first that, if $v \in B_N^e$, $e < d$, then $\rho(F_N)P^d v = 0$. But, because $\rho(F_N)\text{UpTo}_e \subset \text{UpTo}_e$ for all e , $\rho(F_N)v \in \text{UpTo}_e$ and $P^d(\rho(F_N)v) = 0$. If $v \in B_N^d$, then statement (ii) of Lemma 2.3.1 shows that $\rho(F_N)v = -2C_{d+1}v + w$ for some $w \in \text{UpTo}_{d-2}$. Therefore $P^d(\rho(F_N)v) = -2C_{d+1}P^d v$. The fact that $\rho(F_N)(P^d v) = -2C_{d+1}P^d v$ follows from (2.3.3). The latter identity allows to push $\rho(F_N)$ upward

through all arcs in v as the following example shows.

$$\rho(F_8)(P^2v) = \begin{array}{c} \text{Diagram 1} \\ \text{Diagram 2} \\ \text{Diagram 3} \end{array} = -2C_3P^2v.$$

To understand the third equality, note that the only boxes of $\rho(F_N)$ remaining to be summed over are those directly under the defects of v and that these boxes are connected as if the columns containing them were glued to one another. The arcs between them either connect these columns or they reproduce on the bottom line the original arcs of v . One can therefore draw the remaining boxes together, without the connecting arcs, but one then has to add the original arcs below. The last equality follows from the fact that $F_d(\lambda)$ commutes with WJ_d and that $\rho(F_d(\lambda))_{d,d} = -2C_{d+1} \text{id}$. This closes both the proof of the commutativity of P^d and of $\rho(F_N)|_{\text{UpTo}_d}$ and that of the eigenvalue of $\rho(F_N)$ on the subspace onto which P^d projects. \square

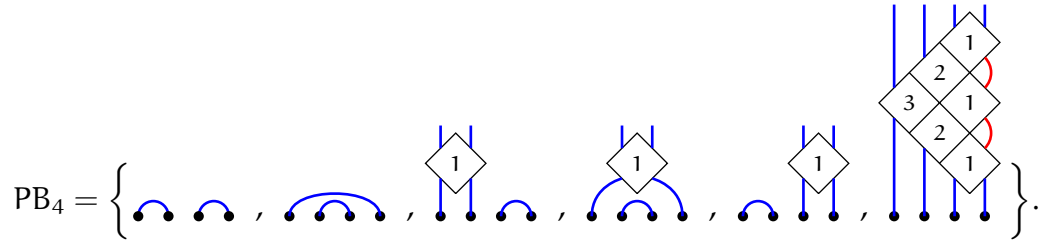
2.3.3 Eigenvectors of $\rho(F_N(\lambda))$ for non-critical λ s

The previous proposition has shown that $P^d v, v \in B_N^d$, is an eigenvector of $\rho(F_N(\lambda))$. Therefore one may hope that the projectors P^d , whenever they exist, can diagonalize $\rho(F_N(\lambda))$.

DEFINITION 2.3.4 *The number λ (or Λ) is said to be critical for N if $e^{i\Lambda} = e^{i(\pi-\lambda)}$ is a (2ι) -th root of unity, for some ι in the range $2 \leq \iota \leq N$. Otherwise, λ is said non-critical or generic (for N).*

Let N be fixed and λ non-critical for this N . Let PB_N^d be the set $PB_N^d = \{P^d v \mid v \in B_N^d\}$. Because, for any such $v \in B_N^d$, $P^d v = v + w$ for some $w \in \text{UpTo}_{d-2}$, the set $\cup_{e \leq d} PB_N^e$ is a basis for UpTo_d and $PB_N = \cup_{0 \leq d \leq N} PB_N^d$ a basis for V_N . We shall keep

on writing, somewhat abusively, that PB_N^d , like B_N^d , spans the sector with d defects. Here is PB_4 as an example :



As an immediate consequence of Proposition 2.3.3 (iii), we get the following result.

PROPOSITION 2.3.4 For λ generic, PB_N is a basis of eigenvectors of $F_N(\lambda)$.

The first few WJ_N are

$$WJ_1 = \text{id}, \quad WJ_2 = \text{id} + \frac{S_1}{S_2}e_1, \quad WJ_3 = \text{id} + \frac{S_2}{S_3}(e_1 + e_2) + \frac{S_1}{S_3}(e_1e_2 + e_2e_1).$$

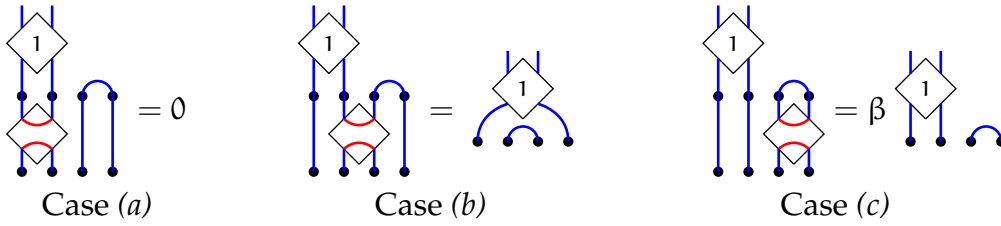
Even though these and other WJ_N s may be singular at some critical λ_c , the limit $\lim_{\lambda \rightarrow \lambda_c} P^d v$ might exist. For instance, the projector WJ_3 is singular at $\Lambda_c = 2\pi/3$ in the range $\Lambda \in (\frac{\pi}{2}, \pi)$. However, $\lim_{\Lambda \rightarrow \Lambda_c} P^3(\downarrow \downarrow \downarrow) = \downarrow \downarrow \downarrow - \frac{1}{2}(\downarrow \curvearrowright + \curvearrowleft \downarrow)$. The value $\Lambda_c = 2\pi/3$ is the one for percolation. It is clear that the condition of genericity on λ is somewhat too restrictive. We shall come back to this in the next section.

PROPOSITION 2.3.5 Let λ be generic for N . Then

- (i) the subspace spanned by PB_N^d is stable under $\mathbb{T}L_N$;
- (ii) in the basis PB_N , the matrix $\rho(D_N(\lambda, u))$ is block diagonal, each block corresponding to a sector spanned by PB_N^d , $0 \leq d \leq N$.

PROOF The second statement follows from the first. For the latter, it is sufficient to study the action of the generators e_i s on each element $v \in PB_N^d$ of the basis. (The examples drawn below may help.) Three cases occur :

- (a) the arc of e_i connects two defects leaving P^d and the result is 0 by Proposition 2.3.3;
- (b) it connects one defect leaving P^d and one arc of v . The resulting link state is different from the original one, but is still an element of PB_N^d ;
- (c) it connects no defects leaving P^d . The resulting link state is also an element of PB_N^d , up to a possible factor β . □



Note that, in view of the example given just before the proposition, the hypothesis that λ be generic may be replaced by the less stringent hypothesis that all vectors in PB_N exist or be obtained by the limit process described earlier.

2.4 The Jordan structure of $\rho(D_N(\lambda, u))$

2.4.1 Jordan blocks and families of linear transformations

The singularity of WJ_N and of the projectors P^d at critical values of λ may appear as a weakness of these tools. However it is exactly this singular behavior that allows to probe the Jordan structure of $\rho(F_N(\lambda))$ and, eventually, of $\rho(D_N(\lambda, u))$.

The study of the Jordan structure of $\rho(F_N(\lambda))$ as a function of λ is an example of the study of linear operators depending on parameters. In the early chapters of his book [68], Kato gives examples of each possible singular behaviors of such families. The one that interests us here is given by linear transformations that, in a basis $\{e_1, e_2\}$, have the form of the simple 2×2 matrix

$$m(\lambda) = \begin{pmatrix} \lambda & 1 \\ 0 & 0 \end{pmatrix}.$$

Its eigenvectors, when $\lambda \neq 0$, are

$$v_1 = e_1 \quad \text{and} \quad v_2 = e_2 - \frac{e_1}{\lambda}.$$

Note that the change of basis $\{e_1, e_2\} \rightarrow \{v_1, v_2\}$ is singular at the critical value $\lambda_c = 0$. The similarity with $\rho(F_N(\lambda))$ and the change of basis $B_N \rightarrow PB_N$ is revealing. Let us draw the parallel as follows :

$$\begin{aligned} \text{span } e_1 &\leftrightarrow \text{UpTo}_e \\ \text{span } \{e_1, e_2\} &\leftrightarrow \text{UpTo}_d, \quad \text{with } e < d \\ \{e_1, e_2\} \rightarrow \{v_1, v_2\} &\leftrightarrow B_N \rightarrow PB_N \end{aligned}$$

One notices that the component of v_2 in the subspace $\mathbb{C}e_2$ is constant and equal to one, exactly like the vector $P^d v$, for $v \in \text{UpTo}_d$, whose component in V_N^d remains v for all λ . The singularity, in both v_2 and $P^d v$, occurs in the subspaces $\mathbb{C}e_1 \leftrightarrow \text{UpTo}_e$. Finally, because $v_2 = v_2(\lambda)$ has a simple pole, it can be written as a Laurent polynomial around its singular point $\lambda_c = 0$:

$$v_2(\lambda) = r + \frac{s}{\lambda - \lambda_c}$$

and this form is unique if $r, s \in \mathbb{C}^2$ are chosen to be constant vectors. Then, the matrix $m(\lambda)$ at $\lambda = \lambda_c$ has a 2×2 Jordan block with eigenvalue $\mu = 0$ and

$$\begin{aligned} m(\lambda)r &= \mu r + \text{constant} \times s, \\ m(\lambda)s &= \mu s. \end{aligned}$$

(A rescaling of s might be necessary to change the constant to the usual 1 in the Jordan block.) The fact that the regular and singular parts of v_2 are proportional to the vectors that form the Jordan block is not a coincidence. This will be the case for $F_N(\lambda)$ and it is the goal of this section to prove it.

We end this subsection by recalling basic properties of the Jordan structure of block triangular matrices. Let $A \in \mathbb{C}^{n \times n}$ and let $\text{sp } A$ be the set of distinct eigenvalues of A . Let T be the matrix that puts A into its Jordan form. (The Jordan form is unique only up to a permutation of its Jordan block. We shall refer to it nonetheless as *the* Jordan form of A .) Then $T^{-1}AT$ is block diagonal with each of its blocks being of the form

$$\begin{pmatrix} \mu & 1 & & & \\ 0 & \mu & 1 & & \\ & & \ddots & \ddots & \\ & & & \mu & 1 \\ & & & & \mu \end{pmatrix}$$

for some $\mu \in \text{sp } A$. For each $\mu \in \text{spec } A$, define the subspace

$$V_A(\mu) = \{v \in \mathbb{C}^n \mid (A - \mu \text{id})^n v = 0\}.$$

Clearly $\mathbb{C}^n = \bigoplus_{\mu \in \text{spec } A} V_A(\mu)$. Moreover $A|_{V_A(\mu)} = \mu \times \text{id} + n$ where n is a nilpotent matrix.

LEMMA 2.4.1 (i) *Let $A, B \in \mathbb{C}^{n \times n}$ such that $[A, B] = 0$. Then $BV_A(\mu) \subset V_A(\mu)$ for all $\mu \in \text{sp } A$.*

(ii) Let $\{A_i, 1 \leq i \leq m\}$ be a set of $n \times n$ commuting matrices. Let $\mu_i \in \text{spec } A_i$ be a choice of m eigenvalues, one for each A_i . Then $W(\{\mu_1, \mu_2, \dots, \mu_m\}) = \bigcap_{1 \leq i \leq m} V_{A_i}(\mu_i)$ is stable under all A_j . Moreover, if W_1, W_2, \dots, W_l is a list of all non-trivial subspaces obtained by such intersections, then $\mathbb{C}^n = \bigoplus_{1 \leq j \leq l} W_j$.

PROOF For (i), let $v \in V_A(\mu)$. Then $(A - \mu I)^n(Bv) = B(A - \mu I)^n v = 0$ and $Bv \in V_A(\mu)$.

For the stability of the $W(\{\mu_i\})$, note simply that $A_j W(\{\mu_i\}) = \bigcap_{1 \leq i \leq m} A_j V_{A_i}(\mu_i) \subset W(\{\mu_i\})$ by (i). Clearly, if the two ordered sets $\{\mu_i\}$ and $\{\nu_i\}$ are distinct, then $W(\{\mu_i\}) \cap W(\{\nu_i\}) = \{0\}$ since, for at least one j , the eigenvalues μ_j and ν_j are distinct and $V_{A_j}(\mu_j) \cap V_{A_j}(\nu_j) = \{0\}$. Therefore, if W_1, W_2, \dots, W_l correspond to different choices of eigenvalues, their pairwise intersections are trivial. Because $\mathbb{C}^n = \bigoplus_{\mu \in \text{spec } A_i} V_{A_i}(\mu)$ and $V_{A_i}(\mu) = \sum'_{\mu_j \in \text{spec } A_j} W(\{\mu_1, \mu_2, \dots\})$, where \sum' means that μ_i is fixed to μ , the sum of W_1, W_2, \dots, W_l must be \mathbb{C}^n . \square

Let M be a matrix $\in \mathbb{C}^{n \times n}$ and let $n_i, 1 \leq i \leq m$, be positive numbers with $\sum_{1 \leq i \leq m} n_i = n$. We say that M is a *block-triangular matrix* if it is partitioned in blocks $m_{ij}, 1 \leq i, j \leq m$ where m_{ij} is a $n_i \times n_j$ submatrix and all $m_{ij} = 0$ when $i > j$. We now make three observations that will be useful for the study of block triangular matrices.

The most obvious one is $\text{spec } M = \bigcup_{i=1}^m \text{spec } m_{ii}$. This has already been used in section 2.2.4.

The second property allows for the identification of non-trivial Jordan blocks using submatrices of a block triangular matrix. Let μ be an eigenvalue of M whose degeneracy is larger than 1. Suppose that μ is an eigenvalue of more than a single diagonal block m_{kk} and let i and j be the indices of the first and last diagonal blocks that have μ as an eigenvalue and suppose $i < j$. Let $M_{\text{top}}, M_{\text{mid}}$ and M_{bot} the submatrices of M along its diagonal that gather all blocks with indices smaller than i for M_{top} , between i and j (included) for M_{mid} and larger than j for M_{bot} . In other words

$$M = \begin{pmatrix} M_{\text{top}} & X & Y \\ 0 & M_{\text{mid}} & Z \\ 0 & 0 & M_{\text{bot}} \end{pmatrix}$$

for certain blocks X, Y, Z . Let v be a vector in $V_M(\mu)$ and let $v = (v_1, v_2, \dots, v_m)$, each v_i having n_i components. This vector v solves the equation $(M - \mu)^p v = 0$ for some

p , and we start the study of this equation with its bottom part, namely the equation

$$(M_{\text{bot}} - \mu \text{id})^p \begin{pmatrix} v_{j+1} \\ \vdots \\ v_m \end{pmatrix} = 0.$$

Since μ is not an eigenvalue of any of the diagonal blocks of M_{bot} by hypothesis, then $M_{\text{bot}} - \mu \text{id}$ is non-singular, so are its powers, and all the v_k , $k > j$ must be zero. Recall now that the number of eigenvectors associated to μ is given by $\dim \ker(M - \mu \text{id})$. We have just seen that solving $Mv = \mu v$ is equivalent to solving

$$\begin{pmatrix} M_{\text{top}} & X \\ 0 & M_{\text{mid}} \end{pmatrix} \begin{pmatrix} v_1 \\ \vdots \\ v_j \end{pmatrix} = \mu \begin{pmatrix} v_1 \\ \vdots \\ v_j \end{pmatrix}.$$

The number of eigenvectors associated to μ is therefore

$$\sum_{1 \leq k \leq j} n_k - \text{rank} \left(\begin{pmatrix} M_{\text{top}} & X \\ 0 & M_{\text{mid}} \end{pmatrix} - \mu \text{id} \right).$$

But M_{top} does not have μ as eigenvalue by hypothesis and $M_{\text{top}} - \mu \text{id}$ is non-singular. So the first $\sum_{1 \leq k < i} n_k$ columns are of maximal rank. Therefore the number of eigenvectors of M associated to μ is

$$\sum_{i \leq k \leq j} n_k - \text{rank} (M_{\text{mid}} - \mu \text{id}) = \dim \ker(M_{\text{mid}} - \mu \text{id}).$$

We therefore conclude that *the number of eigenvectors of M associated to μ is the number of eigenvectors of M_{mid} associated to μ .*

DEFINITION 2.4.1 (i) Let V_i , $1 \leq i \leq N$ be a filtration of subspaces $V_1 \subset V_2 \subset \dots \subset V_N = \mathbb{C}^n$. Set $V_n = \{0\}$ for $n \leq 0$. A vector v is said to belong strictly to V_i if $v \in V_i$ but $v \notin V_{i-1}$. We then write $v \overset{\circ}{\in} V_i$.

(ii) For such a filtration let $A : \mathbb{C}^n \rightarrow \mathbb{C}^n$ be a linear transformation such that $AV_i \subset V_i$ for all i . The linear transformation A is said to have a Jordan block between V_i and V_j , $i > j$, if there exists $\mu \in \text{spec } A$ and two vectors v and w in $V_A(\mu)$ such that $v \overset{\circ}{\in} V_i$, $w \overset{\circ}{\in} V_j$ and $(A - \mu \text{id})v = w$.

By this definition, a vector v strictly in V_i is always non-zero. The second part of the definition is fairly intuitive, but it helps in formulating the third property. Suppose as before that M is a block triangular matrix. Set V_1 to be the subspace of vectors

whose components after the n_1 first ones are all zero. Similarly the vectors in V_j have their components zero if they are after the first $(n_1 + n_2 + \dots + n_j)$ ones. Because M is block triangular, it satisfies $MV_i \subset V_i$. Suppose now that the diagonal blocks A_{ii} and A_{jj} , $i < j$, both share the eigenvalues μ and let M_{mid} as before. Then, an argument similar to the previous one shows that M has a Jordan block between V_i and V_j if and only if M_{mid} does.

The following lemma is an easy consequence of the definitions and properties just introduced.

LEMMA 2.4.2 *The matrix $\rho(D_N(\lambda, \mathbf{u}))$ has no Jordan blocks between two subspaces UpTo_d and $\text{UpTo}_{d'}$ with defects d and d' if $\cos(\lambda(d+1)) \neq \cos(\lambda(d'+1))$.*

PROOF The block $\rho(F_N(\lambda))_{d,d}$ has a unique, degenerate eigenvalue $\mu_d = 2(-1)^d \cos(\lambda(d+1))$. Its subspaces $V_{F_N}(\mu_d)$ are therefore spanned by vectors strictly in some $\text{UpTo}_{d'}$'s whose d' satisfies $\cos(\lambda(d+1)) = \cos(\lambda(d'+1))$. Since F_N and D_N commute, $\rho(D_N(\lambda, \mathbf{u}))$ must share the same property by Lemma 2.4.1. \square

As a consequence, for λ/π irrational, $\rho(D_N(\lambda, \mathbf{u}))$ will never have any Jordan blocks.

2.4.2 The singularities of P^d

To carry through the program outlined in the previous paragraph, the first task is to identify the singularities of all $P^d \mathbf{v}$, $\mathbf{v} \in B_N^d$. This is somewhat simplified by the fact that, for $\mathbf{v} \in B_N^d$, the computation of $P^d \mathbf{v}$ starts by that of the action of WJ_d on the vector with d defects. This vector will be denoted $\mathbf{v}^d \in B_d^d$. Any singularities of $P^d \mathbf{v}$ for $\mathbf{v} \in B_N^d$ are therefore readable from those of $WJ_d \mathbf{v}^d$. This simplification is welcome as the explicit computation of $WJ_d \mathbf{v}^d$ is itself difficult. The aim could be to give all components of this vector explicitly. We tried that for a while, but realized that a more modest goal is sufficient. It is enough to calculate a few well-chosen coefficients and relate all others to these. The following two lemmas give all the information needed to proceed with our goal. Their proof is highly technical and done in Appendix 2.A.

Since only the coefficients of $WJ_d \mathbf{v}^d$ are needed, we shall denote them as P_w^d where w is some link basis vectors. Therefore P_w^d is the matrix element of P^d at position (w, \mathbf{v}^d) . Let $\{m^m\}$ denote the basis vector with m concentric arcs joining together the first $2m$ points, all other being joined to defects.

LEMMA 2.4.3 *Concentric bubbles in leftmost position.*

$$P_{\{m^m\}}^d = \frac{1}{(2S_{1/2})^m} \prod_{i=0}^{m-1} \frac{S_{(d-m-i)/2}}{C_{(d-i)/2}},$$

where, again, the following compact notation has been used : $S_k = \sin(k\Lambda)$, $C_k = \cos(k\Lambda)$, $\Lambda = \pi - \lambda$.

These basis vectors $w = \{m^m\}$ are well-chosen as their components contain all possible singularities of P^d .

LEMMA 2.4.4 *Let w be any link state with k arcs. Then*

$$P_w^d = \sum_{i=1}^k \alpha_i P_{\{i\}}^d$$

for some functions α_i analytic in Λ . Therefore

$$\{\Lambda \in \mathbb{R} \mid P_w^d \text{ diverges at } \Lambda\} \subset \bigcup_{i=1}^k \{\Lambda \in \mathbb{R} \mid P_{\{i\}}^d \text{ diverges at } \Lambda\} \subset \bigcup_{i=0}^{k-1} \{\Lambda \in \mathbb{R} \mid C_{(d-i)/2} = 0\}. \quad (2.4.1)$$

2.4.3 Jordan blocks of $\rho(F_N(\lambda))$

We first study the coefficient $P_{\{m^m\}}^d$ as a function of $q = e^{i\lambda} = e^{i(\pi-\Lambda)}$.

LEMMA 2.4.5 *Let $\Lambda_c = \pi a/b$ with a, b coprime integers, b non-zero and $q_c = e^{i(\pi-\Lambda_c)}$. Then*

– for m in the range $1 \leq m < b$, the coefficient $P_{\{m^m\}}^d$ has a pole at q_c if

$$C_{(d-m+1)/2} \Big|_{q=q_c} = 0;$$

– if $m = m_1 b + m_2$ with $m_1 > 0$ and $b > m_2 \geq 0$, then one of $P_{\{m^m\}}^d \pm P_{\{m_2^{m_2}\}}^d / (2S_{1/2})^{m_1 b}$ is regular at q_c ;

– all poles of $P_{\{m^m\}}^d(q)$, $m > 0$, are simple.

Note that the lemma does not preclude singularities of $P_{\{m^m\}}^d$ other than the zeroes of $C_{(d-m+1)/2}$. In fact, $P_{\{m^m\}}^d$ will have in general poles at zeroes of some of the $C_{(d-i)/2}$ with $0 \leq i < m - 1$.

PROOF : The following properties characterize the number $C_{n/2}$ and $S_{n/2}$, $n \in \mathbb{Z}$, at $\Lambda = \Lambda_c$. First, if a is even, then $C_{n/2}$, $n \in \mathbb{Z}$, is never zero. Indeed the argument of

$C_{n/2} = \cos(\pi a n / 2b)$ is π times a fraction whose denominator is odd. This argument can never be of the form $(2i+1)\pi/2$. From now on, we assume that a is odd. Second, at $\Lambda = \Lambda_c$, $C_{(n+2b)/2} = -C_{n/2}$ and the values taken by $|C_{n/2}|$, $n \in \mathbb{Z}$, belong to any set of $2b$ consecutive C_i s, namely to any set $\{|C_{j/2}|, |C_{(j+1)/2}|, \dots, |C_{(j+2b-1)/2}|\}$ for any j . The values $|S_{n/2}|$ have the same property. Third, for all n , $|C_{(n+b)/2}| = |S_{n/2}|$. And finally, for any $j \in \mathbb{Z}$, the sets $\{C_{(j+i)/2}, 0 \leq i < 2b\}$ (and therefore $\{S_{(j+i)/2}, 0 \leq i < 2b\}$) contain precisely one zero. To prove this, clearly $C_{b/2} = \cos \pi a / 2 = 0$ as a is odd. Moreover, if $C_{i/2} = C_{j/2} = 0$ with $|j - i| < 2b$, then $\Lambda_c i / 2 = (2k - 1)\pi/2$ and $\Lambda_c j / 2 = (2l - 1)\pi/2$ for some $k, l \in \mathbb{Z}$ and $a(i - j) = 2(l - k)b$. Since a is odd and a, b are coprimes, $(i - j)$ must be a multiple of $2b$ and the constraint $|j - i| < 2b$ implies that $i = j$.

We now study $C_{n/2} = C_{n/2}(q)$ in a neighborhood of q_c . If $\cos \Lambda_c n / 2 = 0$, then

$$\begin{aligned} \cos \Lambda n / 2 &= \cos(\Lambda - \Lambda_c + \Lambda_c)n / 2 = \pm \sin(\Lambda - \Lambda_c)n / 2 \\ &= \pm \frac{i}{2} \frac{(q - q_c)}{(q q_c)^{n/2}} \sum_{j=0}^{n-1} q^j q_c^{n-1-j} \end{aligned}$$

where $q = e^{i(\pi - \Lambda)}$ and $C_{n/2}(q)$ goes to zero linearly in $(q - q_c)$ as q goes to q_c .

The formula

$$P_{\{m^m\}}^d = \frac{1}{(2S_{1/2})^m} \prod_{i=0}^{m-1} \frac{S_{(d-m-i)/2}}{C_{(d-i)/2}}$$

reveals that the only possible poles of $P_{\{m^m\}}^d$ are at the zeroes of the cosine functions $C_{(d-i)/2}$. There will be a singularity of $P_{\{m^m\}}^d$ at a zero of a given cosine of the denominator if and only if this zero is not cancelled by a zero of one of the sine functions of the numerator. Therefore $P_{\{m^m\}}^d$ will have a pole at zeroes of $C_{(d-m+1)/2}$ if no sine functions of the numerator are equal, up to a sign, to $S_{(d-(m+b-1))/2}$. There is no such cancellation because the hypothesis $m < b$ implies that $d - (m + b - 1) < d - (2m - 1)$ and therefore that $d - (m + b - 1)$ is not in the range $[d - (2m - 1), d - m]$ of the index of the sine functions.

Suppose now that $m = m_1 b + m_2$ with $m_1 \geq 1$ and $b > m_2 \geq 0$. If m_1 is even, the last $m_1 b$ terms of the product (corresponding to the values of the index $m_2 \leq i \leq m_1 b + m_2 - 1$) contain $m_1/2$ complete sets of the possible absolute values of both the sine and cosine functions. The product of these $m_1 b$ terms is therefore

± 1 . Using the periodicity of the sine, one gets

$$\begin{aligned} P_{\{m^m\}}^d &= \pm \frac{1}{(2S_{1/2})^m} \prod_{i=0}^{m_2-1} \frac{S_{(d-m_1 b-m_2-i)/2}}{C_{(d-i)/2}} + \mathcal{O}((q - q_c)^0) \\ &= \pm \frac{1}{(2S_{1/2})^{m_1 b}} P_{\{m_2^{m_2}\}}^d + \mathcal{O}((q - q_c)^0). \end{aligned}$$

If m_1 is odd, the terms of the product are split as follows. The m_2 first cosines are gathered with the last m_2 sines in a first product, and all the remaining sines and cosines in a second :

$$P_{\{m^m\}}^d = \frac{1}{(2S_{1/2})^m} \prod_{i=0}^{m_2-1} \frac{S_{(d-2m_1 b-m_2-i)/2}}{C_{(d-i)/2}} \prod_{i=0}^{m_1 b-1} \frac{S_{(d-m_1 b-m_2-i)/2}}{C_{(d-m_2-i)/2}}.$$

Because m_1 is odd, $S_{(d-m_1 b-m_2-i)/2} = \pm C_{(d-m_2-i)/2}$ at $q = q_c$ and the last product is ± 1 . Again the periodicity of trigonometric functions gives the same result as for m_1 even.

Thus the coefficient $P_{\{n^n\}}^b$ with $n \geq b$ has the same singularities as $P_{\{m^m\}}^d$ with $m \equiv n \pmod{b}$, $0 \leq m < b$. But the denominator of $P_{\{m^m\}}^d$, $1 \leq m < b-1$, has less than b cosine functions among $\{C_{d/2}, C_{(d-1)/2}, \dots, C_{(d-(b-2))/2}\}$ and at most one of these can vanish for a given Λ_c . Hence poles of $P_{\{m^m\}}^d$, $m \geq 1$, are simple. \square

LEMMA 2.4.6 *Let $\Lambda_c = \pi - \lambda_c = \pi a/b$ with a, b coprime integers and b non-zero and set $q_c = e^{i(\pi - \Lambda_c)}$. Then*

- if a is even : $P^d(q)(v^d)$ is not singular at $\Lambda_c = \pi a/b$;
- if a is odd : $P^d(q)(v^d)$ has a singularity at $\Lambda_c = \pi a/b$ if and only if there exists d' satisfying

$$\boxed{d - d' < 2b \quad \text{and} \quad \frac{1}{2}(d + d') \equiv b - 1 \pmod{2b}.} \quad (2.4.2)$$

d' is the largest integer for which there exists a $w \in B_N^{d'}$ such that the coefficient P_w^d is singular. (By definition of P^d , d' is strictly smaller than d .) In the following, d' will retain this definition.

PROOF : The only poles of $P^d(q)(v^d)$ are at zeroes of $C_{(d-i)/2}$, $1 \leq i < b-1$. But if a is even, and b is therefore odd, then none of these cosines vanish at $\Lambda = \Lambda_c$.

Let then a be odd. In order for d' to be the largest defect number with some of the P_w^d , $w \in B_N^{d'}$, singular, one must have that P_v^d is regular for any $v \in B_N^e$, $e > d'$. This means that all $P_{\{n^n\}}^d$ with $n < m = \frac{1}{2}(d-d')$ are regular. Because of the inclusion

of sets of singularities of Lemma 2.4.4, the coefficient $P_{\{m^m\}}^d$ must be singular. Hence the definition of the number d' is equivalent to the requirement that all $P_{\{n^n\}}^d$ with $n < m = \frac{1}{2}(d - d')$ be regular and $P_{\{m^m\}}^d$ be singular at Λ_c . This Λ_c must therefore be a zero of $C_{(d-m+1)/2}$, that is $d - m + 1 = (2k + 1)b$ for some $k \in \mathbb{Z}$ or, equivalently, $\frac{(d+d')}{2} \equiv b - 1 \pmod{2b}$. \square

Let $\Lambda_c = \pi a/b$, with a, b coprimes and b non-zero, $q_c = e^{i(\pi - \Lambda_c)}$, the pair (d, d') solving (2.4.2) and $v \in B_N^d$. Because the poles of $P^d(q)(v^d)$ are simple, the vector $P^d(q)v$ can be written as

$$P^d(q)v = r_{q_c}(q, v) + \frac{s_{q_c}(v)}{q - q_c}$$

where $s_{q_c}(v)$ is the residue of $P^d(q)v$ at q_c . As a function of q , the vector $r_{q_c}(q, v)$ is then analytic in a neighborhood of q_c .

Recall that $\text{UpTo}_d = \bigoplus_{e \leq d} V_N^e$ is the subspace spanned by basis vectors with at most d defects. Our next goal is to study the action of $F_N(\lambda)$ on the projections of r_{q_c} and s_{q_c} on the quotient $\text{UpTo}_d/\text{UpTo}_{d'-2}$. Let $v \in \text{UpTo}_d$ and denote by $v_{[d', d]}$ the subset of its components along the link basis vectors with defect number in the range $[d', d]$. Clearly the coordinate vectors $v_{[d', d]}, v \in B_N^d$, and the projected vectors $\pi(v) \in \text{UpTo}_d/\text{UpTo}_{d'-2}$ are in one-to-one correspondence. (Here π denotes the canonical projection $\text{UpTo}_d \rightarrow \text{UpTo}_d/\text{UpTo}_{d'-2}$.) Let $M : V_N \rightarrow V_N$ be a linear transformation and denote by $M_{[d', d]}$ the diagonal block of its matrix form in the link basis that includes lines and columns in sectors d' to d . Because $F_N(\lambda)$ is upper triangular, $(F_N(\lambda)v)_{[d', d]} = F_N(\lambda)_{[d', d]}v_{[d', d]}$ for $v \in \text{UpTo}_d$. (In other words, there is a natural action of $F_N(\lambda)$ on the quotient $\text{UpTo}_d/\text{UpTo}_{d'-2}$.)

LEMMA 2.4.7 *Let (d', d) be a solution of (2.4.2). With the notation above, if $\hat{r} = (r_{q_c}(q_c, v))_{[d', d]}$ and $\hat{s} = (s_{q_c}(v))_{[d', d]}$, then*

$$\begin{aligned} (F_N(\lambda_c))_{[d', d]} \hat{r} &= \mu_d \hat{r} + \alpha \hat{s}, \\ (F_N(\lambda_c))_{[d', d]} \hat{s} &= \mu_d \hat{s} \end{aligned}$$

where $\alpha \in \mathbb{C}^\times$ and $\mu_d = (-1)^d (q_c^{(d+1)} + q_c^{-(d+1)})$.

In other words \hat{r} and \hat{s} are part of a Jordan block under the natural action of $F_N(\lambda)$ on $\text{UpTo}_d/\text{UpTo}_{d'-2}$.

PROOF : We write $F_N(q)$ instead of $F_N(\lambda)$, with $q = e^{i\lambda}$, to stress the dependency upon q and compute the action of $F_N(q)$ for q in a neighborhood of q_c , but distinct

of it :

$$\begin{aligned} F_N(\mathbf{q})_{[d',d]}(\mathbf{r}_{q_c}(\mathbf{q}, \mathbf{v}))_{[d',d]} &= F_N(\mathbf{q})_{[d',d]} \left((P^d(\mathbf{q})\mathbf{v})_{[d',d]} - \frac{s_{q_c}(\mathbf{v})_{[d',d]}}{\mathbf{q} - \mathbf{q}_c} \right) \\ &= \mu_d(\mathbf{q})(P^d(\mathbf{q})\mathbf{v})_{[d',d]} - \mu_{d'}(\mathbf{q}) \frac{\hat{\mathbf{s}}}{\mathbf{q} - \mathbf{q}_c} \end{aligned}$$

because $P^d(\mathbf{q})\mathbf{v}$ is an eigenvector of $F_N(\mathbf{q})$ for generic \mathbf{q} with eigenvalue $\mu_d(\mathbf{q}) = 2(-1)^d \cos(\lambda(d+1)) = (-1)^d(q^{(d+1)} + q^{-(d+1)})$ and $s_{q_c}(\mathbf{v})_{[d',d]} = \hat{\mathbf{s}}$ has components only in $V_N^{d'}$ and is therefore an eigenvector with eigenvalue $\mu_{d'}(\mathbf{q})$. Then

$$= \mu_d(\mathbf{r}_{q_c}(\mathbf{q}, \mathbf{v}))_{[d',d]} + \left(\frac{\mu_d(\mathbf{q}) - \mu_{d'}(\mathbf{q})}{\mathbf{q} - \mathbf{q}_c} \right) \hat{\mathbf{s}}.$$

The limit $\mathbf{q} \rightarrow \mathbf{q}_c$ of the first term is simply $\mu_d(\mathbf{q}_c)\hat{\mathbf{r}}$, since both factors are smooth at \mathbf{q}_c . Since d and d' have the same parity, the difference $(\mu_d(\mathbf{q}) - \mu_{d'}(\mathbf{q}))$ can be written up to a sign as

$$\cos \lambda(d+1) - \cos \lambda(d'+1) = -2 \sin \frac{\lambda}{2}(d-d') \sin \frac{\lambda}{2}(d+d'+2).$$

If (d, d') is a solution of (2.4.2), then $d+d'+2 = 2b(2k+1)$ for some integer k and $\sin \frac{\lambda}{2}(d+d'+2)$ has a simple zero at $\lambda = \lambda_c$. Could $\sin \frac{\lambda}{2}(d-d')$ also vanish at $\lambda = \lambda_c$? This would mean that both $\lambda_c(d+1)$ and $\lambda_c(d'+1)$ are integer multiples of π . Because a and b are coprimes, this implies that $2b$ divides both $(d+1)$ and $(d'+1)$. The requirement that $|d-d'| < 2b$ implies that there are no such pair (d, d') with distinct d and d' . The limit $\alpha = \lim_{\mathbf{q} \rightarrow \mathbf{q}_c} (\mu_d(\mathbf{q}) - \mu_{d'}(\mathbf{q})) / (\mathbf{q} - \mathbf{q}_c)$ therefore exists and is non-zero. The second equation of the statement follows from the previous observation that $\hat{\mathbf{s}}$ is an eigenvector of $F_N(\lambda)_{[d',d]}$ and its eigenvalue coincides with $\mu_d(\mathbf{q}_c)$ when $\mathbf{q} \rightarrow \mathbf{q}_c$. \square

Because the constant α is non-zero, it can be absorbed in the definition of $\hat{\mathbf{s}}$. By the discussion in section 2.4.1, the previous lemma implies that $\rho(F_N(\lambda_c))$ has a Jordan block between the subspace UpTo_d and $\text{UpTo}_{d'}$. The next result provides the linear condition determining the size of the Jordan block.

LEMMA 2.4.8 *Let λ_c be fixed and note F_N for $F_N(\lambda_c)$. Let $\hat{\mathbf{x}}_0$ and $\hat{\mathbf{x}}_1$ be two vectors in $\text{UpTo}_d / \text{UpTo}_{d'-2}$ that are respectively projections of some vectors strictly in UpTo_d and $\text{UpTo}_{d'}$. The two following statements are equivalent.*

– $\hat{\mathbf{x}}_0$ and $\hat{\mathbf{x}}_1$ satisfy

$$(F_N)_{[d',d]}\hat{\mathbf{x}}_0 = \mu\hat{\mathbf{x}}_0 + \hat{\mathbf{x}}_1$$

$$(F_N)_{[d',d]}\hat{\mathbf{x}}_1 = \mu\hat{\mathbf{x}}_1;$$

– there exists $\{x_0, x_1, \dots, x_i\} \subset V_N, i \geq 1$, such that

$$\begin{aligned} F_N x_j &= \mu x_j + x_{j+1}, & 0 \leq j \leq i-1 \\ F_N x_i &= \mu x_i \end{aligned}$$

where $x_j \in \mathring{\text{UpTo}}_{d_j}$ with $d_{j+1} < d_j$ and $(x_0)_{[d',d]} = \hat{x}_0$ and $(x_1)_{[d',d]} = \hat{x}_1$.

PROOF : Due to the block-triangular structure of F_N , the statement \Leftarrow is immediate. To prove the statement \Rightarrow , we solve recursively on the number of defects $e < d'$. Suppose that a partial solution has been obtained for the components in sectors $e+2$ to d of $l+1$ vectors :

$$\begin{aligned} (F_N x_j)_{[e+2,d]} &= \mu(x_j)_{[e+2,d]} + (x_{j+1})_{[e+2,d]}, & 0 \leq j < l \\ (F_N x_l)_{[e+2,d]} &= \mu(x_l)_{[e+2,d]}. \end{aligned}$$

The next step is to determine the components of these vectors along the basis vectors in B_N^e . The block matrix $(F_N)_{[e,e]}$ is a multiple of the identity, say by the factor σ . If $\alpha = \sigma - \mu$ is non-zero, then the system of equations for the components in B_N^e is

$$\begin{aligned} \alpha(x_j)_{[e,e]} + X_e(x_j)_{[e+2,d]} &= (x_{j+1})_{[e,e]}, & 0 \leq j < l \\ \alpha(x_l)_{[e,e]} + X_e(x_l)_{[e+2,d]} &= 0 \end{aligned}$$

where the rectangular matrix X_e contains the parts of the lines of F_N to the right of the block $(F_N)_{[e,e]}$. The solution to this system is unique and can be found by solving first the last equation, labeled by l , then the previous, and so on.

If $\alpha = \sigma - \mu = 0$, then the system is different and might not have a solution. It is

$$X_e(x_j)_{[e+2,d]} = (x_{j+1})_{[e,e]}, \quad 0 \leq j < l \quad (2.4.3)$$

$$X_e(x_l)_{[e+2,d]} = 0. \quad (2.4.4)$$

The last equation is actually a constraint on the components of x_l that have already been fixed. If it is not satisfied, a new vector x_{l+1} has to be introduced in the Jordan block. Its components in B_N^e are $(x_{l+1})_{[e,e]} = X_e(x_l)_{[e+2,d]}$. Then the j -th equation can be used to determine $(x_{j+1})_{[e,e]}$ for $1 < j \leq l$. Finally one can set $(x_0)_{[e,e]}$ to zero. This determines the components in $\cup_{e \leq f \leq d} B_N^f$ of all the vectors in this extended Jordan block. Repeating the process until $e = 0$ is reached leads to the second statement. \square

The constraint (2.4.4) will not be satisfied in general if \hat{x}_0 is chosen from the regular part of $P^d(v)$ for some $v \in B_N^d$. But, of course, a linear combination of vectors

in PB_N^d might. Therefore the number of Jordan blocks connecting the sectors d and d' is likely to be smaller than the dimension of V_N^d .

The following proposition determines between which sectors the central element F_N has Jordan blocks. It is an immediate consequence of the three previous lemmas.

PROPOSITION 2.4.9 *Let $\Lambda_c = \pi - \lambda_c = \pi a/b$, with a, b coprimes and b non-zero. Then*

- *if a is even, $F_N(\lambda_c)$ has no Jordan blocks ;*
- *let a be odd and $|d - d'| < 2b$. Then $F_N(\lambda_c)$ has a Jordan block between the sectors d and d' if and only if*

$$\frac{1}{2}(d + d') \equiv b - 1 \pmod{2b}.$$

2.4.4 Jordan blocks of $\rho(D_N(\lambda, u))$

PROPOSITION 2.4.10 – *If $P^d(q = e^{i\lambda})(v^d)$ is regular at λ , then, for all u and N , the matrix $\rho(D_N(\lambda, u))$ has no Jordan blocks between the sectors d and d' , for any $d' < d$.*

- *If $P^d(q = e^{i\lambda})(v^d)$ is singular at some $\lambda = \lambda_c$ and the pair (d, d') satisfies (2.4.2), then, for all u , but a finite number of values, and all $N (\geq d)$, there are some vectors $\overset{\circ}{\in} \text{UpTo}_d$ that form Jordan blocks of $\rho(D_N(\lambda_c, u))$ with vectors in UpTo_d . Moreover, if the diagonal block $\rho(D_N)_{d,d}$ is diagonalizable, then $\rho(D_N(\lambda_c, u))$ has a Jordan block between sectors d and d' , for all u except a finite number of values.*

PROOF : If $P^d(e^{i\lambda})(v^d)$ is regular at λ , then all vectors in PB_N^d are strictly in UpTo_d and their projections on $\text{UpTo}_d/\text{UpTo}_{d-2}$ form a basis of this quotient. The subspace spanned by PB_N^d in UpTo_d is stable under the action of the generators of the Temperley-Lieb algebra and, therefore, of $D_N(\lambda, u)$. This set PB_N^d can be completed into a basis of UpTo_d by a set B of vectors strictly in UpTo_e , for some $e < d$. In this basis $D_N(\lambda, u)$ has no matrix elements between the two subspaces spanned by PB_N^d and B respectively.

Expand $\rho(D_N(\lambda_c, u))$ as a trigonometric polynomial of u as in (2.3.1). There are at most $N + 1$ linearly independent coefficients in this polynomial, the last one is $\rho(F_N)$ up to a non-zero constant, and they all commute by (2.2.2). Denote by $d_i, 0 \leq i \leq N$, their restrictions to UpTo_d . These d_i are therefore linear transformations of UpTo_d . As shown in Lemma 2.4.1, the vector space UpTo_d can be written as a direct sum of subspaces $W(\{\mu_i\}) = \bigcap_{0 \leq i \leq N} V_{d_i}(\mu_i)$ where $\{\mu_i\}$ represents a choice of one eigenvalue μ_i for each d_i . The subspaces $W(\{\mu_i\})$ are stable under all d_j s.

Suppose now that one of them, say d_N , has a Jordan block between the sectors d and d' . Let μ be the eigenvalue of this block. Since the Jordan form of d_N contains a Jordan block of size at least 2, there exists a choice $\{\mu_i\}$ with $\mu_N = \mu$ such that the restriction of d_N to $W_0 = W(\{\mu_i\})$ has a non-trivial Jordan block. The restrictions of the d_i s to this subspace W_0 are of the form $\mu_i \cdot \text{id}_{W_0} + n_i$ where n_i is nilpotent. Because the d_i s commute, so do the n_i s. Hence, on this subspace W_0 , the matrix $\rho(D_N(\lambda_c, u))|_{W_0} = f(u) \cdot \text{id}_{\dim W_0} + n(u)$ where $f(u)$ is a trigonometric polynomial and $n(u)$ is a nilpotent matrix. (Recall that the sum of two commuting nilpotent matrices is nilpotent.) Because n_N is non-zero, the matrix $n(u)$ is itself a non-zero trigonometric polynomial. It can vanish only at a finite number of values of u and, generically, $\rho(D_N)|_{\text{UpTo}_d}$ has Jordan blocks.

To see if $\rho(D_N(\lambda_c, u))$ has a Jordan block between UpTo_d and $\text{UpTo}_{d'}$, it is sufficient, by the last property of section 2.4.1, to see if its action on the quotient $\text{UpTo}_d/\text{UpTo}_{d'-2}$ has such a block. Suppose now that the diagonal block $\rho(D_N(\lambda_c, u))_{d,d}$ is diagonalizable and pick W_0 as above. Then W_0 is stable under $\rho(D_N)$ and $\rho(D_N)$ preserves the filtration $\dots \subset W_0 \cap \text{UpTo}_{d'} \subset \dots \subset W_0 \cap \text{UpTo}_d \subset \dots$. However the action of $\rho(D_N)$ on $(W_0 \cap \text{UpTo}_d)/(W_0 \cap \text{UpTo}_{d'-2})$ cannot have a Jordan block since $\rho(D_N)_{d,d}$ is diagonalizable. But $\rho(D_N)$ can only have Jordan blocks between sectors upon which F_N has the same eigenvalues by Lemma 2.4.2. Because $|d' - d| < 2b$, the sectors d and d' are two such consecutive sectors. Therefore the actions of both $\rho(F_N)$ and $\rho(D_N)$ on $(W_0 \cap \text{UpTo}_d)/(W_0 \cap \text{UpTo}_{d'-2})$ must have a Jordan block between the projections of $W_0 \cap \text{UpTo}_d$ and $W_0 \cap \text{UpTo}_{d'}$. The last statement follows, again by the last property of section 2.4.1. \square

Both the diagonalizability of the diagonal blocks $\rho(D_N)_{d,d}$ and the reality of their spectrum are delicate questions. A natural way to settle both questions is to find a scalar product on V_N^d with respect to which $\rho(D_N)_{d,d}$ is self-adjoint. We found such a scalar product, for all β and $N \leq 12$, using a computer. In the basis B_N , the elements of the matrix representing the scalar products are polynomials in β . But we could not guess its form for general N . The situation is to be paralleled to the same two questions for the XXZ Hamiltonian with the specific boundary conditions introduced in [34]. With these boundary conditions, H_{XXZ} is invariant under $U_q(\mathfrak{sl}(2))$ [35]. Because $U_q(\mathfrak{sl}(2))$ has indecomposable representations when q is a root of unity, it is not surprising that, at these values, this Hamiltonian is not diagonalizable. Korff and Weston [69] identified a subspace to which the restriction of H_{XXZ} is self-adjoint with respect to some scalar product. Due to the link between

loop transfer matrices and the Hamiltonian H_{XXZ} , we had hoped their efforts would answer rigorously our questions for $\rho(D_N)$. However the subspace constructed in [69] is too small to contain the image of the diagonal blocks of $\rho(D_N)$, even for the N for which our computation answers affirmatively the questions of diagonalizability and of the reality of the spectrum.

2.5 Conclusion

The results of this paper show the existence of Jordan blocks between sectors d and d' for certain λ s. For example, for the transfer matrices $\rho(D_N)$ related to critical polymers, the Ising and the 3-Potts models by Proposition 2.2.7, the sectors tied by a line in Figure 2.3 are joined by Jordan blocks.

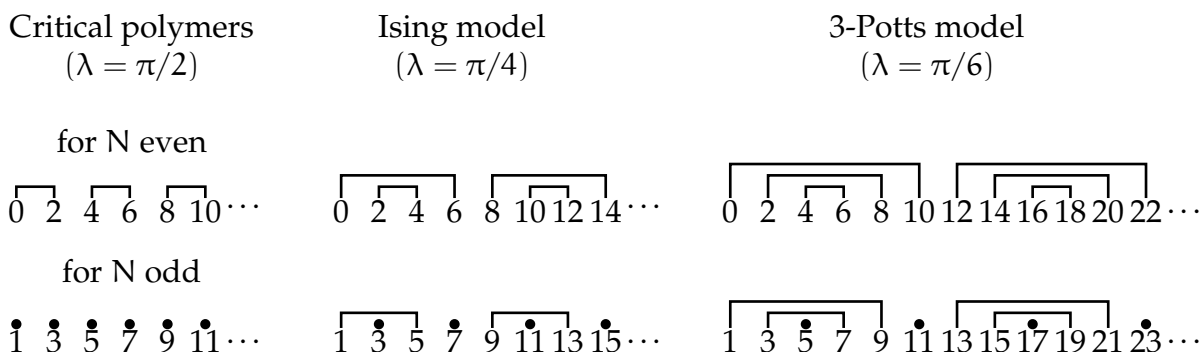


FIGURE 2.3 – The pattern of Jordan blocks of $\rho(D_N(\lambda, u))$ for $\lambda = \pi/2$ (critical polymers), $\lambda = \pi/4$ (Ising) and $\lambda = \pi/6$ (3-Potts).

However the transfer matrix $\rho(D_N(\lambda = \pi/3, u))$ that is tied with percolation has no Jordan blocks for any N . This particular result for $\lambda = \pi/3$ was suggested by Dubail, Jacobsen and Saleur [70], based on their exploration for small N s.

A few questions remain unanswered. The first concerns the order of the Jordan cells : our numerics suggest that all Jordan blocks are of size 2, though a proof remains unknown, even for F_N . In the case of critical polymers ($\lambda = \pi/2$), an inversion equation for D_N is known [45] and yields $F_N^2 = 0$ for N even (and Jordan blocks all have size 2), but $(F_N - 2 \text{id})(F_N + 2 \text{id}) = 0$ for N odd (no Jordan blocks). The size of the Jordan cells for $\rho(D_N)$ might be an even harder problem and we have not been able to prove that they are of size 2 for any non-trivial cases. Another related ques-

tion is that of possible Jordan blocks connecting sectors d and d' when $|d - d'| \geq 2b$. These have not been ruled out by Propositions 2.4.9 and 2.4.10. Indeed, consider a non-zero linear combination of vectors in $\text{UpTo}_{d'}$ that are partners in Jordan blocks of vectors strictly in UpTo_d . Such a linear combination could fail to be strictly in $\text{UpTo}_{d'}$. It will then be strictly in $\text{UpTo}_{d''}$, with $d'' < d' < d$. Of course the eigenvalues of F_N in the sectors d , d' and d'' should all be equal. For example, a Jordan block for $\lambda = \frac{\pi}{4}$ could exist between sectors $d = 12$ and $d'' = 2$. Though limited to small N , our numerics have ruled out any such Jordan blocks.

The goal of the computation was to decide whether, for simple boundary conditions corresponding to open ones on spin lattices, representations of the Virasoro algebra other than irreducible highest weight ones could appear in the thermodynamical limit. Our result is that this is indeed the case. One would probably like to count, for each eigenvalue of the limit operator L_0 , how many Jordan blocks appear. Such information cannot be retrieved from our method, at least in the present state.

One may still wonder what type of representations occur in the limit. Let $\mathcal{H}_N \propto \frac{1}{2} \frac{\partial}{\partial u} D_N(\lambda, u)|_{u=0}$ where the proportionality factor is a power of $\sin \lambda$. Once the finite size corrections are properly handled, the large N limit of the matrix $\rho(\mathcal{H}_N)$ is linked to L_0 . It was argued in [45], with strong numerical support, that the spectrum of the diagonal block of $\rho(\mathcal{H}_N)$ in the sector with d defects reproduces the character of some highest weight modules associated with the central charge $c_{a,b}$ (see (2.1.1)) and highest weight $\Delta_{1,d+1} = (ad^2 - 2d(b-a))/4b$. (Their numerical analysis allows to fix precisely the first few eigenvalues of L_0 , but does not go deep enough to suggest whether the highest weight representation is irreducible.) If this is the case, then a pair (d, d') solving $\frac{1}{2}(d + d') \equiv b - 1 \pmod{2b}$ will lead to a pair of highest weights such that $\Delta_{1,d'+1} - \Delta_{1,d+1} \in \mathbb{Z}$. Therefore staggered modules, a large family of which was recently classified in [40], are likely candidates for the representations of the Virasoro algebra appearing in the thermodynamical limit of the models we have studied.

We hope that the methods introduced here to probe the Jordan structure can be used for other boundary conditions as those introduced in [45] and in [71]. Both these sets are stated algebraically, in a way therefore that might help to extend the present results, and they might actually match one another. Moreover the latter were given a direct interpretation in terms of classical spin models. Indeed these conditions amount, for the Q-Potts models, to restrict spins on the boundaries to take values only in a subset $\{Q_1, Q_2, \dots, Q_s\}$ of the Q possible values. Of course,

for these new boundary conditions, the Jordan cell structure could be very different from the one found here (see, for example, [72]).

Acknowledgements

AMD holds a scholarship and YSA a grant of the Canadian Natural Sciences and Engineering Research Council. This support is gratefully acknowledged. We have benefitted greatly from discussions with Paul Pearce and Jørgen Rasmussen and from David Ridout's many remarks and explanations. Discussions with Jesper Jacobsen and Philippe di Francesco are also gratefully acknowledged.

Appendices

2.A The main lemmas

2.A.1 Labeling link states and matrix elements

In this section, we introduce a new notation for link states in B_N and for matrix elements of linear transformations on V_N , both of which will prove useful in later sections.

To describe $w \in B_N^{N-2k}$ a link state with $N - 2k$ defects and k arcs, we label by k integers n_i , ranging from 1 to $N - 1$, the halfway points between points which w connects : $w \rightarrow v_{n_1, n_2, \dots, n_k}^r$. We usually write the n_i s, from left to right in the order the arcs need to be closed, going from the inner to the outer ones. Even with this ordering, there may be many $v_{n_1, n_2, \dots, n_k}^r$ for a given w , but they all determine w completely. For example,

$$\begin{aligned}
 v_{3,7}^{10} &= \bullet_1 \downarrow \bullet_2 \downarrow \bullet_3 \curvearrowright \bullet_4 \downarrow \bullet_5 \downarrow \bullet_6 \curvearrowright \bullet_7 \downarrow \bullet_8 \downarrow \bullet_9, & v_{2,2,7,7}^{10} &= \bullet_1 \curvearrowright \bullet_2 \downarrow \bullet_3 \downarrow \bullet_4 \downarrow \bullet_5 \downarrow \bullet_6 \curvearrowright \bullet_7 \downarrow \bullet_8 \downarrow \bullet_9, \\
 v_{2,6,8,7}^{10} &= \bullet_1 \downarrow \bullet_2 \curvearrowright \bullet_3 \downarrow \bullet_4 \downarrow \bullet_5 \curvearrowright \bullet_6 \downarrow \bullet_7 \curvearrowright \bullet_8 \downarrow \bullet_9, & v_{3,5,4,8,5}^{10} &= \bullet_1 \downarrow \bullet_2 \downarrow \bullet_3 \downarrow \bullet_4 \downarrow \bullet_5 \downarrow \bullet_6 \downarrow \bullet_7 \downarrow \bullet_8 \downarrow \bullet_9.
 \end{aligned}$$

As in section 2.4 the link state with N defects and no arcs is labelled v^N . We shall also shorten the notation whenever there are several arcs sharing the same halfpoints by writing n_i^m for a group of m successive identical n_i s. For example $v_{2,2,7,7}^r$ could also be written as $v_{2^2, 7^2}^r$. Finally, we shall call a 1-bubble a half-arc that encloses no other half-arc, a 2-bubble a half-arc that encloses 1-bubbles and an n -bubble a half arc that

contains at least one $(n - 1)$ -bubble. So $v_{3,7}^{10}$ has 1-bubbles only, $v_{2,2,7,7}^{10}$ drawn above has 1-bubbles and 2-bubbles and $v_{3,5,4,8,5}^{10}$ has a 3-bubble.

The linear transformations on V_N , like F_N and P^d , will often be expressed in the basis B_N . To refer to a given matrix element of the linear transformation $\rho(A) : V_N \rightarrow V_N$ (or on one of the subspaces UpTo_d), we shall use the bra-ket notation. Therefore the matrix element $\rho(A)_{v,w}$, for $v, w \in B_N$, will be written as $\langle v | Aw \rangle$. (This is equivalent to introducing a scalar product on V_N for which B_N is an orthonormal basis.) As most of the computations will be done graphically, it is useful to develop tools to quickly select a given matrix element. To depict $\langle v | Aw \rangle$, we draw the “incoming” state w with full line and usually on the top of the diagram. The “outgoing” state v is depicted with dashed ones and usually on the bottom. The matrix elements of the identity are all zero unless $v = w$. For instance,

$$\langle v_{2,6,8,7}^{10} | \text{id} v_{3,7,7}^{10} \rangle = \text{diagram} = 0$$

In some computations the arcs or defects of the incoming state will cross the diagram representing the linear transformation A . When this occurs, a partial comparison of the incoming and outgoing states is possible and the patterns can be replaced by either 1 or 0. In the latter case, this means that this particular contribution to A is vanishing and can be ignored. Here are the patterns :

$$\text{diagram} = \text{diagram} = 1 \quad \text{diagram} = \text{diagram} = \text{diagram} = \text{diagram} = 0 \quad (2.A.1)$$

and their images through a vertical mirror.

By definition, the computation of $P^d : \text{UpTo}_d \rightarrow \text{UpTo}_d$, for a vector in $B_N^d \subset \text{UpTo}_d \subset V_N$, starts by the removal of all arcs, leaving only its d defects. The singularities of any matrix elements $\langle v | P^d w \rangle$ can therefore be deduced from those of $\langle v' | P^d v^d \rangle$ for some v' and for $v^d \in B_d^d$, the vector with all defects in V_d . We found useful to use another letter for the number of defects to underline the fact that $v^d \in V_d$ belongs to a vector space in general distinct from V_N . We shall therefore compute matrix elements of P^r in the column corresponding to v^r . These are the only matrix elements that are really needed and they will be labelled in any of the two following forms, the second being defined by the first that was just introduced :

$$\langle v_{n_1, \dots, n_k}^r | P^r v^r \rangle = P_{\{n_1, \dots, n_k\}}^r$$

The extreme case P_{\emptyset}^r stands for $\langle v^r | P^r v^r \rangle$ which is equal to 1. We are now ready to give explicit expressions for some matrix elements $P_{w'}^r$.

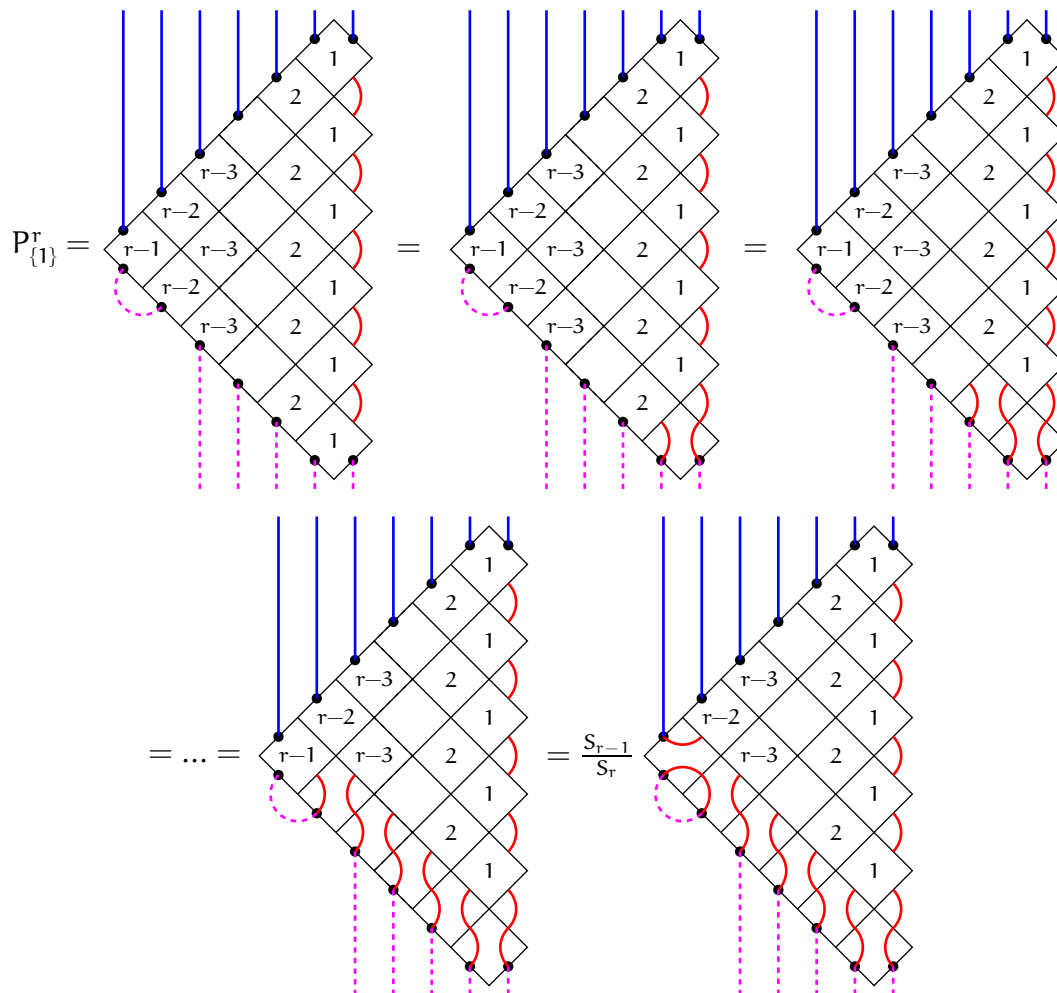
2.A.2 $P_{\{m^m\}}^r$ and its singularities

The singularities of all the matrix elements of P^r will be understood from those of the $P_{\{m^m\}}^r$ for some m . We start by computing these key elements.

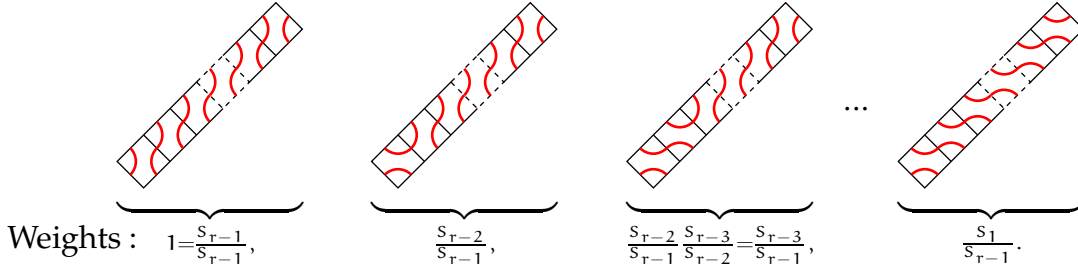
LEMMA 2.A.1 *Single bubble in first position :*

$$P_{\{1\}}^r = \frac{S_{(r-1)/2}}{2S_{1/2}C_{r/2}}.$$

PROOF The strategy is to start with the first lower diagonal row of boxes, applying eqs. (4.5.5) and (2.A.1). To understand the first step below, note that the sum represented by the lowest box, labelled by "1", gives two terms. The first draws an arc between the two outgoing defects and is therefore zero by (2.A.1). Therefore the only non-vanishing contribution comes from the second which is drawn. The other steps are similar.



We now sum the boxes of the upper diagonal row. Only $r - 1$ of the 2^{r-2} terms contribute, namely :



Other box configurations produce half arcs, which propagate down and eventually annihilate with $\diamond 1$. Therefore the sums of the upper diagonal row lead to the downward propagation, by one box, of all incoming defects and to an overall weight of

$$\sum_{i=1}^{r-1} \frac{S_i}{S_{r-1}} = \frac{S_{(r-1)/2} S_{r/2}}{S_{r-1} S_{1/2}}.$$

Finally,

$$P_{\{1\}}^r = \frac{S_{r-1} S_{(r-1)/2} S_{r/2}}{S_r S_{r-1} S_{1/2}} = \frac{S_{(r-1)/2}}{2 S_{1/2} C_{r/2}}.$$

$$= \langle v^{r-2} | P^{r-2} v^{r-2} \rangle = 1$$

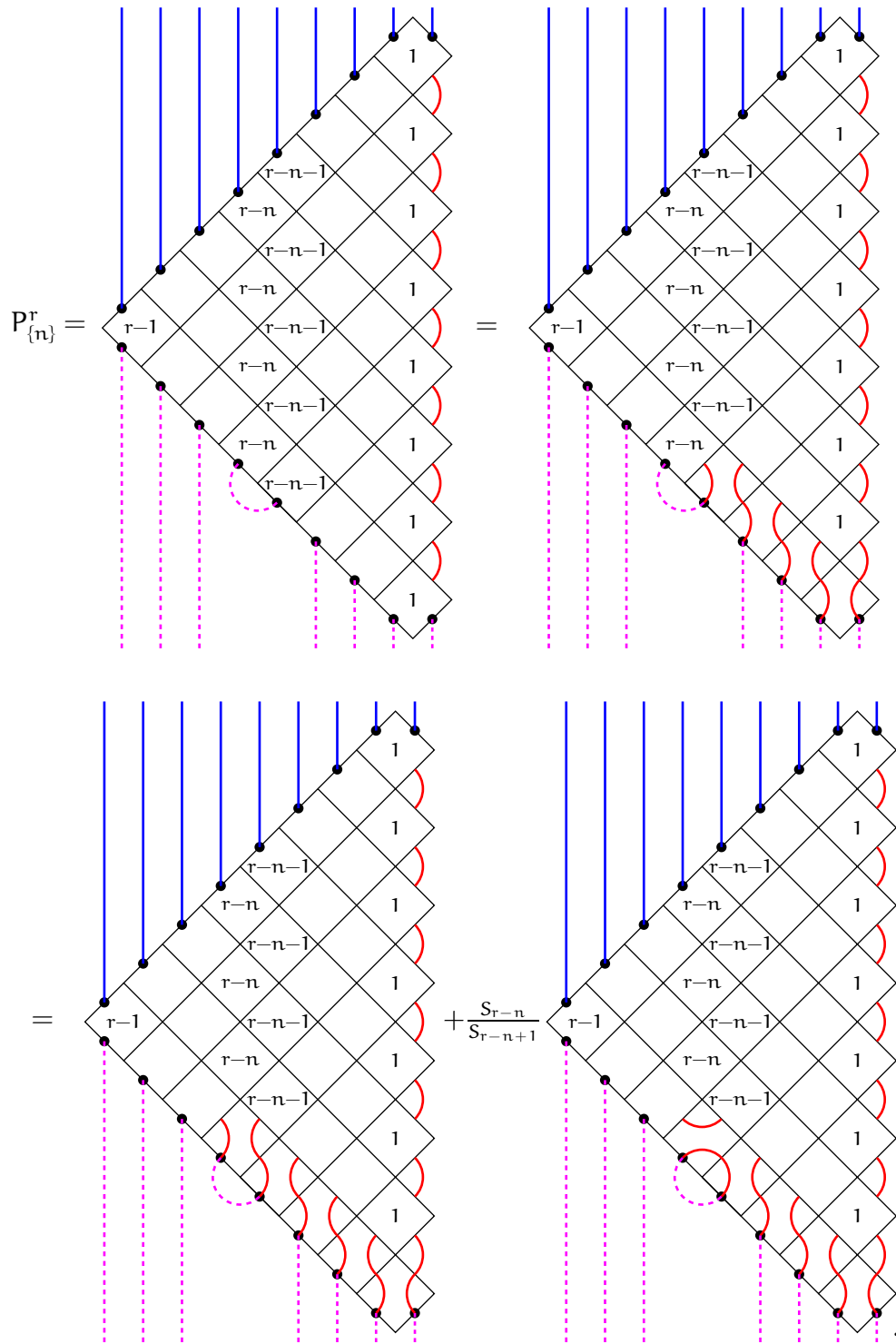
□

LEMMA 2.A.2 *The single bubble in general position :*

$$P_{\{n\}}^r = \frac{S_{(r-n)/2} S_{n/2}}{2 (S_{1/2})^2 C_{r/2}} \quad \text{for } n = 1, \dots, r - 1.$$

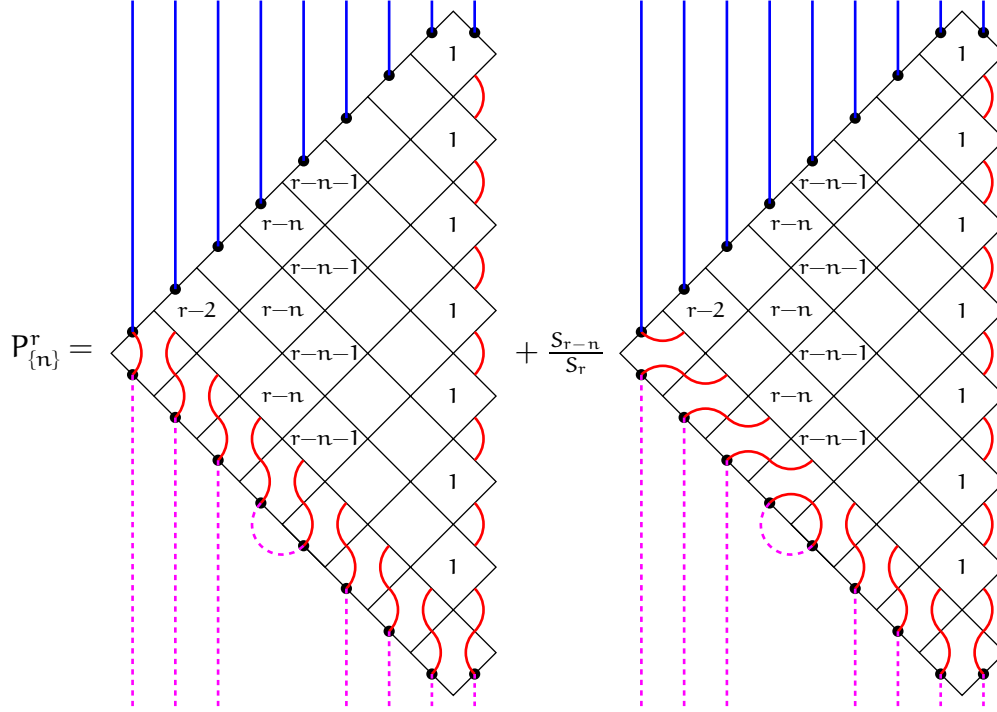
PROOF The expression given for $P_{\{n\}}^r$ certainly works for $n = 1$ and all r . The rest of the proof will be by induction. Using the same strategy as before, we build a

recursion relation for $P_{\{n\}}^r$:



Summing the lower diagonal row of boxes has yielded two terms. For the second, the remaining $n-1$ boxes of the first lower diagonal row must all be \diamond . Otherwise,

a half-arc is formed, propagates in the upper right direction and annihilates.



The first term is $P_{\{n-1\}}^{r-1}$. For the second, the upper diagonal of boxes is summed in the same fashion as in the proof of Lemma 2.A.1. The desired recurrence relation is :

$$P_{\{n\}}^r = P_{\{n-1\}}^{r-1} + \frac{S_{r-n}}{4S_{1/2}C_{r/2}C_{(r-1)/2}}. \tag{2.A.2}$$

To complete the proof, we suppose the proposition is true for $r - 1$ and verify that the recurrence relation yields the correct answer for r :

$$\begin{aligned} P_{\{n-1\}}^{r-1} + \frac{S_{r-n}}{4S_{1/2}C_{r/2}C_{(r-1)/2}} &= \frac{S_{(r-n)/2}S_{(n-1)/2}}{2(S_{1/2})^2 C_{(r-1)/2}} + \frac{S_{r-n}}{4S_{1/2}C_{r/2}C_{(r-1)/2}} \\ &= \frac{S_{(r-n)/2}}{2(S_{1/2})^2 C_{r/2}C_{(r-1)/2}} (S_{(n-1)/2}C_{r/2} + S_{1/2}C_{(r-n)/2}) \\ &= \frac{S_{(r-n)/2}S_{n/2}}{2(S_{1/2})^2 C_{r/2}}. \end{aligned}$$

□

The invariance of P^r under reflection appears through $P_{\{n\}}^r = P_{\{r-n\}}^r$. Note also that (2.A.2) holds for $n = 1$ if we impose the unphysical condition $P_{\{0\}}^{r-1} = 0$. This will become the initial condition in recursion arguments in propositions to come.

The presence of $C_{r/2}$ in the denominator will cause $P_{\{n\}}^r$ to diverge for specific values of Λ , but for all n . We now direct our interest to m concentric bubbles, starting with all the defects sitting at the right end of the link state.

LEMMA 2.A.3 *Concentric bubbles in leftmost position :*

$$P_{\{m^m\}}^r = \frac{1}{(2S_{1/2})^m} \prod_{i=0}^{m-1} \frac{S_{(r-m-i)/2}}{C_{(r-i)/2}}.$$

PROOF The proof does not require new ideas. Using the graphical representation, one finds the following recurrence relation :

$$P_{\{m^m\}}^r = \frac{S_{r-m}}{4C_{r/2}C_{(r-1)/2}S_{1/2}} P_{\{(m-1)^{m-1}\}}^{r-2}. \quad (2.A.3)$$

The proposed $P_{\{m^m\}}^r$ certainly fits the initial condition, $m = 1$, given in Lemma 2.A.1. Proving the induction is straightforward. \square

A little more work would also yield :

$$P_{\{n^m\}}^r = \frac{1}{(2S_{1/2})^m} \prod_{i=0}^{m-1} \frac{S_{(r-n-i)/2}S_{(n-i)/2}}{C_{(r-i)/2}S_{(i+1)/2}}. \quad (2.A.4)$$

Since the $S_{(r-n-i)/2}/S_{1/2}$ are analytic in Λ on \mathbb{R} , the set of singularities of $P_{\{m^m\}}^r$ is contained in the set $\cup_{i=0}^{m-1} \{\Lambda \mid C_{(r-i)/2} = 0\}$. The singularities of $P_{\{n^m\}}^r$ could be worked out from the above expression, but the analysis would be more tedious because zeroes of the denominator could be cancelled by zeroes of the numerator. Similar difficulties arise when one studies w with more complicated patterns of arcs. This is why the analysis in the next subsection turns to expressing the general matrix elements in terms of some already computed, instead of giving new explicit expressions.

2.A.3 $P_{\{n_1, n_2, \dots, n_k\}}^r$ with non trivial bubble patterns

This section shows how to express the matrix elements P_w^r for any link state w in terms of a sum of $P_{\{m^m\}}^r$. This is done by two basic operations : the removal of the leftmost defects and the replacement of a cluster of arcs by a cluster of concentric ones.

The operation of shifting a pattern of arcs by removing the defect at position "1" will be denoted by " \leftarrow ". It is an operation from B^r to $B^{r-1} \cup \{0\}$. If w does not start with a defect, the result \overleftarrow{w} is zero. For example, $v_{2,6,8,7}^{10} = v_{1,5,7,6}^9$ but $v_{2,2,7,7}^{10} = 0$.

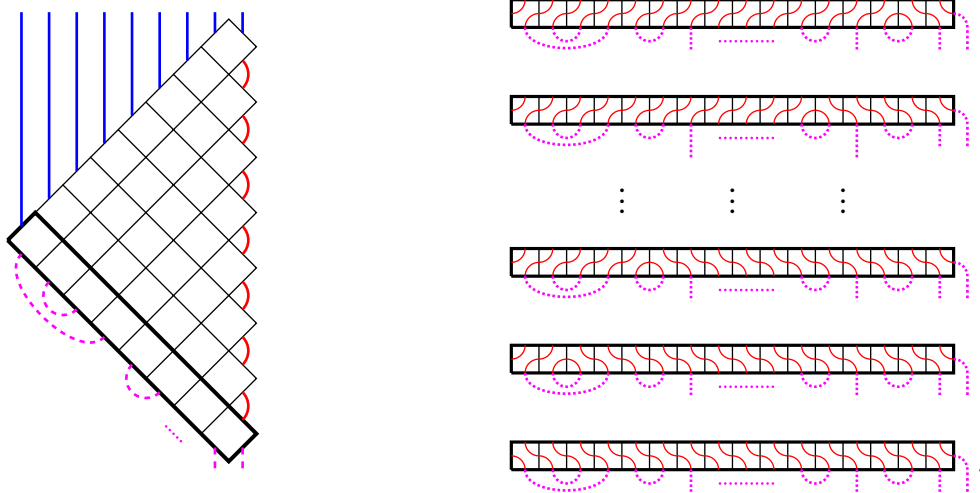
We also define the operation, from B^r to B^{r-2} , of removing the j -th 1-bubble from w . The result is noted $w \setminus \{j\}$. For example, $v_{2,6,8,7}^{10} \setminus \{1\} = v_{4,6,5}^8$ and $v_{2,6,8,7}^{10} \setminus \{2\} = v_{2,6,6}^8 = v_{2,6,8,7}^{10} \setminus \{3\}$.

LEMMA 2.A.4 *Left shift of arcs.* Let $w \in B^r$ any link state, with b 1-bubbles, labelled by j and centered at n_j (see section 2.A.1). The matrix element P_w^r satisfies the following recursion equation :

$$P_w^r = P_{\overleftarrow{w}}^{r-1} + \frac{1}{4S_{1/2}C_{r/2}C_{(r-1)/2}} \sum_{j=1}^b S_{r-n_j} P_{w \setminus \{j\}}^{r-2} \tag{2.A.5}$$

It also holds when $\overleftarrow{w} = 0$ if we define $P_{\overleftarrow{w}=0}^{r-1} = 0$.

PROOF This is a generalization of (2.A.2) and (2.A.4). Summing the first lower diagonal row of boxes of P_w^r , only $b + 1$ configurations have non zero contributions. For example,



All other configurations have zero weight, either because of (2.A.1) or because bubbles formed in this lower diagonal will propagate in the upper right direction to form an arc attached to a braid box labelled by a “1”, leading to zero contribution by (2.3.6). In the configurations drawn above, the last one has weight 1 and is simply a translation of the link state towards the left, giving rise to $P_{\overleftarrow{w}}^{r-1}$. (When the link state has a bubble in first position, it has weight zero.) The other configurations all remove a 1-bubble from w . Removing the j -th 1-bubble yields a weight S_{r-n_j}/S_r . Since the first box is always , the first upper right row can be summed, as was done in the proof of Lemma 2.A.1. The result is

$$\frac{S_{(r-1)/2}S_{r/2}}{S_{r-1}S_{1/2}} \frac{S_{r-n_j}}{S_r} P_{w \setminus \{j\}}^{r-2} = \frac{S_{r-n_j} P_{w \setminus \{j\}}^{r-2}}{4S_{1/2}C_{r/2}C_{(r-1)/2}},$$

$m \leq r/2$, that is, for $m = 1$. Suppose it is valid for $r - 1$ and $r - 2$, then

$$\begin{aligned} P_w^r &= \left(\prod_{i=1}^m \frac{S_i}{S_1} \right) P_{\bar{u}}^{r-1} + \frac{S_{r-m-a_0}}{4S_{1/2}C_{r/2}C_{(r-1)/2}} \frac{S_m}{S_1} \left(\prod_{i=1}^{m-1} \frac{S_i}{S_1} \right) P_{u \setminus \{1\}}^{r-2} \\ &= \left(\prod_{i=1}^m \frac{S_i}{S_1} \right) \left(P_{\bar{u}}^{r-1} + \frac{S_{r-m-a_0} P_{u \setminus \{1\}}^{r-2}}{4S_{1/2}C_{r/2}C_{(r-1)/2}} \right) \\ &= \left(\prod_{i=1}^m \frac{S_i}{S_1} \right) P_u^r \end{aligned}$$

as required. Since (2.A.6) is true for the fictitious initial conditions introduced earlier, after Lemma 2.A.2, the proof is complete.

We now define the operation $\mathcal{O}_{b,x}$ that acts on link state w by removing b 1-bubbles centered on x and replacing them with $(b - 1)$ 1-bubbles, circumscribed by a large 2-bubble :

The diagram shows two examples of the operation $\mathcal{O}_{b,x}$. In the first example, $\mathcal{O}_{2,4}$ is applied to a link state with 4 1-bubbles centered at $x=4$. The result is a link state with 3 1-bubbles and a large 2-bubble. In the second example, $\mathcal{O}_{3,7}$ is applied to a link state with 7 1-bubbles centered at $x=7$. The result is a link state with 4 1-bubbles and a large 2-bubble.

The action of $\mathcal{O}_{b,x}$ is not defined for all w , but any link state $w \in B_N$ with $\zeta(w) = [a_0](k_1 k_2 \dots k_m)[a_1]$ can be written as

$$[a_0](k_1 k_2 \dots k_m)[a_1] = \left(\prod_i \mathcal{O}_{b_i, x_i} \right) [a_0](\underbrace{11 \dots 1}_m)[a_1]$$

for some b_i and x_i . For instance, the right-hand sides of the above examples are

$$[2](2, 1, 2, 1)[2] = \mathcal{O}_{2,8} \mathcal{O}_{2,4} [2](1111)[2],$$

$$[0](6, 1, 4, 3, 1, 1)[0] = \mathcal{O}_{3,7} \mathcal{O}_{4,7} \mathcal{O}_{6,6} [0](111111)[0].$$

Let w_1 and w_2 be two link states such that $w_2 = \mathcal{O}_{b,x} w_1$. If we can show that

$$P_{w_1}^r = \frac{S_b}{S_1} P_{w_2}^r, \quad (2.A.7)$$

then the proof of the proposition will be complete. Note first that this relation holds (somewhat trivially) for $r = 3$. For $r = 4$ the relation is non-trivial only for $w_1 = v_{1,3}^4$, $w_2 = v_{2,2}^4$ and $\mathcal{O}_{2,2}$. The element $P_{w_2}^4$ has been calculated in Lemma 2.A.3; $P_{w_1}^4$ can

be obtained from (2.A.5) and it agrees with (2.A.7). We now use (2.A.5) for such a pair w_1 and $w_2 = \mathcal{O}_{b,x}w_1$. For w_1 we partition the sum over j into the set G_1 of b 1-bubbles modified by the action $\mathcal{O}_{b,x}$ and its complement :

$$\begin{aligned} P_{w_1}^r &= P_{w_1}^{r-1} + \frac{1}{4S_{1/2}C_{r/2}C_{(r-1)/2}} \left(\sum_{j \in G_1^c} S_{r-n_j} P_{w_1 \setminus \{j\}}^{r-2} + \sum_{j \in G_1} S_{r-n_j} P_{w_1 \setminus \{j\}}^{r-2} \right) \\ &= P_{w_1}^{r-1} + \frac{1}{4S_{1/2}C_{r/2}C_{(r-1)/2}} \left(\sum_{j \in G_1^c} S_{r-n_j} P_{w_1 \setminus \{j\}}^{r-2} + \left(\sum_{j=1}^b S_{r-(x-b+2j-1)} \right) P_{w_1 \setminus \{g_1\}}^{r-2} \right) \\ &= P_{w_1}^{r-1} + \frac{1}{4S_{1/2}C_{r/2}C_{(r-1)/2}} \left(\sum_{j \in G_1^c} S_{r-n_j} P_{w_1 \setminus \{j\}}^{r-2} + \left(\frac{S_b S_{r-x}}{S_1} \right) P_{w_1 \setminus \{g_1\}}^{r-2} \right) \end{aligned}$$

where g_1 is the first 1-bubble in G_1 . The same can be carried out for w_2 :

$$\begin{aligned} P_{w_2}^r &= P_{w_2}^{r-1} + \frac{1}{4S_{1/2}C_{r/2}C_{(r-1)/2}} \left(\sum_{j \in G_1^c} S_{r-n_j} P_{w_2 \setminus \{j\}}^{r-2} + \left(\sum_{j=1}^{b-1} S_{r-(x-b+2j)} \right) P_{w_2 \setminus \{g_2\}}^{r-2} \right) \\ &= P_{w_2}^{r-1} + \frac{1}{4S_{1/2}C_{r/2}C_{(r-1)/2}} \left(\sum_{j \in G_1^c} S_{r-n_j} P_{w_2 \setminus \{j\}}^{r-2} + \left(\frac{S_{b-1} S_{r-x}}{S_1} \right) P_{w_2 \setminus \{g_2\}}^{r-2} \right) \end{aligned}$$

where again g_2 is the position of the first 1-bubble in the complement in w_2 of G_1^c . If (2.A.7) is true for $r-1$ and $r-2$,

$$P_{w_1}^{r-1} = \frac{S_b}{S_1} P_{w_2}^{r-1}, \quad P_{w_1 \setminus \{j\}}^{r-2} = \frac{S_b}{S_1} P_{w_2 \setminus \{j\}}^{r-2} \quad \forall j \in G_1^c, \quad P_{w_1 \setminus \{g_1\}}^{r-2} = \frac{S_{b-1}}{S_1} P_{w_2 \setminus \{g_2\}}^{r-2},$$

and then for r :

$$\begin{aligned} P_{w_1}^r &= \frac{S_b}{S_1} P_{w_2}^{r-1} + \frac{1}{4S_{1/2}C_{r/2}C_{(r-1)/2}} \left(\sum_{j \in G_1^c} \frac{S_b S_{r-n_j}}{S_1} P_{w_2 \setminus \{j\}}^{r-2} + \left(\frac{S_b S_{r-x}}{S_1} \right) \frac{S_{b-1}}{S_1} P_{w_2 \setminus \{g_2\}}^{r-2} \right) \\ &= \frac{S_b}{S_1} \left(P_{w_2}^{r-1} + \frac{1}{4S_{1/2}C_{r/2}C_{(r-1)/2}} \left(\sum_{j \in G_1^c} S_{r-n_j} P_{w_2 \setminus \{j\}}^{r-2} + \left(\frac{S_{b-1} S_{r-x}}{S_1} \right) P_{w_2 \setminus \{g_2\}}^{r-2} \right) \right) \\ &= \frac{S_b}{S_1} P_{w_2}^r. \end{aligned}$$

□

The definition of the pattern $\zeta(w)$ can be extended to link states w with more than one cluster of bubbles. Clusters of defects and clusters of bubbles are noted,

respectively, in $[\]$ and $()$:

$$\zeta(w) = [a_0] \left(\prod_j (k_{1,j} k_{2,j} \dots k_{m_j,j}) [a_j] \right)$$

where the product over j is over the clusters of bubbles.

LEMMA 2.A.6 *For a general link state w , the result of the previous lemma extends to*

$$P_w^r = \left(\prod_j \prod_{i=1}^{m_j} \frac{S_i}{S_{k_{i,j}}} \right) P_u^r$$

where

$$\zeta(u) = [a_0] \left(\prod_j (m_j \ m_j - 1 \dots 2 \ 1) [a_j] \right)$$

is a state that has only clusters of concentric bubbles.

PROOF The definition of $\mathcal{O}_{b,x}$ was not restricted to link states with only one cluster of defects. Multiple-cluster link states can then be created by successive applications of \mathcal{O}_{b_i,x_i} on link states with only 1-bubbles, changing one cluster at a time. The result will follow if (2.A.7) still holds for states with multiple clusters. This is indeed the case because, in the previous proof, the fact that the 1-bubbles of G_1^c were in a single cluster was not used. The rest of the argument goes through. \square

2.A.4 Singular points of $P_{\{n_1, n_2, \dots, n_k\}}^r$

The goal of this section is to show that

$$\begin{aligned} \{\Lambda \in \mathbb{R} \mid P_{\{n_1, n_2, \dots, n_k\}}^r \text{ diverges at } \Lambda\} &\subset \cup_{i=1}^k \{\Lambda \in \mathbb{R} \mid P_{\{i\}}^r \text{ diverges at } \Lambda\} \\ &\subset \cup_{i=0}^{k-1} \{\Lambda \in \mathbb{R} \mid C_{(r-i)/2} = 0\}. \end{aligned}$$

We start by investigating the singularities of $P_{\{n_1, n_2, \dots, n_k\}}^r$ when $w = v_{n_1, n_2, \dots, n_k}^r$ has only 1-bubbles, and will show that

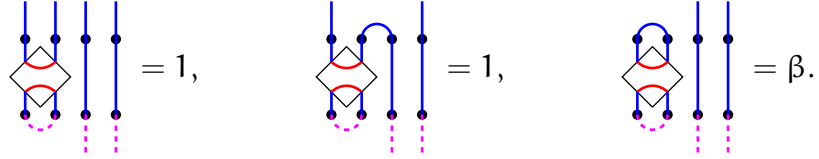
$$P_{\{n_1, n_2, \dots, n_k\}}^r = \sum_{i=0}^k a_i P_{\{i\}}^r \quad (2.A.8)$$

where a_i s are analytic functions of $\Lambda \in \mathbb{R}$ and the term $i = 0$ is for P_{\emptyset}^r .

LEMMA 2.A.7 *Moving a single bubble to position "1".*

$$P_{\{n\}}^r = \frac{S_n}{S_1} P_{\{1\}}^r - \frac{S_{n/2} S_{(n-1)/2}}{S_{1/2} S_{2/2}} P_{\emptyset}^r. \quad (2.A.9)$$

PROOF The trick is to start by calculating $\langle v_1^r | e_1 P^r v^r \rangle$. The only link states $w \in B^r$ satisfying $\langle v_1^r | e_1 w \rangle \neq 0$ are v^r , v_1^r and v_2^r and



Since $e_1 P^r$ is zero whenever $r \geq 2$,

$$0 = \langle v_1^r | e_1 P^r v^r \rangle = P_{\emptyset}^r \langle v_1^r | e_1 v^r \rangle + P_{\{1\}}^r \langle v_1^r | e_1 v_1^r \rangle + P_{\{2\}}^r \langle v_1^r | e_1 v_2^r \rangle = P_{\emptyset}^r - \frac{S_2}{S_1} P_{\{1\}}^r + P_{\{2\}}^r,$$

that is

$$P_{\{2\}}^r = \frac{S_2}{S_1} P_{\{1\}}^r - P_{\emptyset}^r$$

and the proposed $P_{\{n\}}^r$ is correct for $n = 1$ and 2 . For $n > 2$, we calculate $\langle v_{n-1}^r | e_{n-1} P^r v^r \rangle$ and use induction. Four link states carry non-zero contributions :

$$\begin{aligned} 0 &= \langle v_{n-1}^r | e_{n-1} P^r v^r \rangle \\ &= P_{\emptyset}^r \langle v_{n-1}^r | e_{n-1} v^r \rangle + P_{\{n-2\}}^r \langle v_{n-1}^r | e_{n-1} v_{n-2}^r \rangle + P_{\{n-1\}}^r \langle v_{n-1}^r | e_{n-1} v_{n-1}^r \rangle + P_{\{n\}}^r \langle v_{n-1}^r | e_{n-1} v_n^r \rangle \\ &= P_{\emptyset}^r + P_{\{n-2\}}^r - \frac{S_2}{S_1} P_{\{n-1\}}^r + P_{\{n\}}^r. \end{aligned}$$

If eq. (2.A.9) is valid for $n - 1$ and $n - 2$, then

$$\begin{aligned} P_{\{n\}}^r &= \frac{S_2}{S_1} P_{\{n-1\}}^r - P_{\{n-2\}}^r - P_{\emptyset}^r \\ &= \frac{S_2}{S_1} \left(\frac{S_{n-1}}{S_1} P_{\{1\}}^r - \frac{S_{(n-1)/2} S_{(n-2)/2}}{S_{1/2} S_{2/2}} P_{\emptyset}^r \right) - \left(\frac{S_{n-2}}{S_1} P_{\{1\}}^r - \frac{S_{(n-2)/2} S_{(n-3)/2}}{S_{1/2} S_{2/2}} P_{\emptyset}^r \right) - P_{\emptyset}^r \\ &= Y_n P_{\{1\}}^r - Z_n P_{\emptyset}^r \end{aligned}$$

where

$$Y_n = \frac{S_2 S_{n-1} - S_{n-2} S_1}{S_1^2}, \quad Z_n = \frac{S_2 S_{(n-1)/2} S_{(n-2)/2}}{S_{1/2} S_{2/2}^2} - \frac{S_{(n-2)/2} S_{(n-3)/2}}{S_{1/2} S_{2/2}} + 1.$$

Trigonometric identities can be used to bring Y_n and Z_n onto the forms proposed for the coefficients of $P_{\{1\}}$ and P_{\emptyset} respectively. \square

LEMMA 2.A.8 Let $\{n, X\}$ be a set of 1-bubbles such that the positions m_1, m_2, \dots, m_k represented by X are all to the right of the first bubble at n . Then,

$$P_{\{n, X\}}^r = \frac{S_n}{S_1} P_{\{1, X\}}^r - \frac{S_{n/2} S_{(n-1)/2}}{S_{1/2} S_{2/2}} P_{\{X\}}^r.$$

PROOF Reading the previous proof, one sees that X acts as a spectator. For instance, the same four terms will appear in $\langle v_{n-1}^r | e_{n-1} P^r v^r \rangle$ and none others, even when the bubbles at n and m_1 are immediate neighbors. In other words, the proof is identical.

□

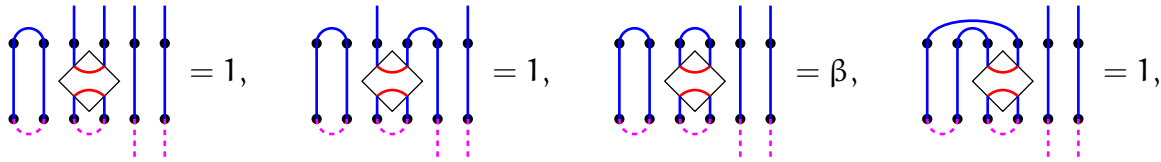
The ultimate objective is to write $P_{\{n_1, \dots, n_k\}}^r$ as a linear combination of the form (2.A.8). The previous lemma allows to move the first bubble to the extreme left, or make it disappear. We now show how this can be done with the remaining bubbles.

LEMMA 2.A.9 Moving bubbles to the leftmost available position.

$$P_{\{1, 3, \dots, 2b-3, n, X\}}^r = \frac{S_{n-b+1}}{S_b} P_{\{1, 3, \dots, 2b-3, 2b-1, X\}}^r - \frac{S_{(n-2b+2)/2} S_{(n-2b+1)/2}}{S_{1/2} S_{2/2}} P_{\{1, 3, \dots, 2b-3, X\}}^r. \quad (2.A.10)$$

The previous lemma is just the case $b = 1$.

PROOF In this proof, X plays no role and will be omitted. We start with the case of two 1-bubbles. The element $\langle v_{1,3}^r | e_3 P^r v^r \rangle$ has four contributions :



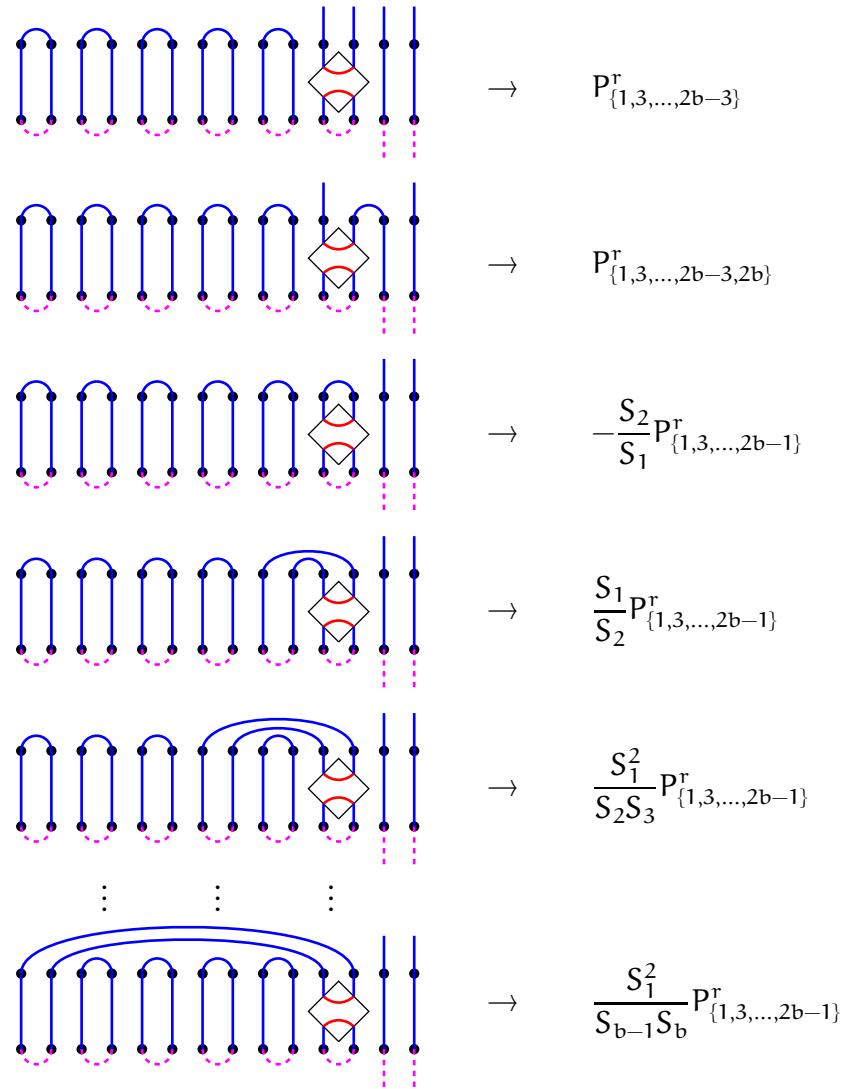
so that

$$P_{\{1,4\}}^r = \frac{S_2}{S_1} P_{\{1,3\}}^r - P_{\{2,2\}}^r - P_{\{1\}}^r = \left(\frac{S_2}{S_1} - \frac{S_1}{S_2} \right) P_{\{1,3\}}^r - P_{\{1\}}^r = \frac{S_3}{S_2} P_{\{1,3\}}^r - P_{\{1\}}^r,$$

where Lemma 2.A.5 was used for $P_{\{2,2\}}^r$. When the second bubble is at $n > 4$, the equation $0 = \langle v_{1,n-1}^r | e_{n-1} P^r v^r \rangle$ and induction yield

$$P_{\{1,n\}}^r = \frac{S_2}{S_1} P_{\{1,n-1\}}^r - P_{\{1,n-2\}}^r - P_{\{1\}}^r = \frac{S_{n-1}}{S_2} P_{\{1,3\}}^r - \frac{S_{(n-2)/2} S_{(n-3)/2}}{S_{1/2} S_{2/2}} P_{\{1\}}^r.$$

More generally, when the b -th bubble is at position $2b$, we compute the matrix element $\langle v_{1,3,\dots,2b-1}^r | e_{2b-1} P^r v^r \rangle$. The following contributions



are obtained using, among others, (2.A.7). Overall,

$$P_{\{1,3,\dots,2b-3,2b\}}^r = \underbrace{\left(\frac{S_2}{S_1} - \sum_{i=1}^{b-1} \frac{S_1^2}{S_i S_{i+1}} \right)}_{A_b} P_{\{1,3,\dots,2b-1\}}^r - P_{\{1,3,\dots,2b-3\}}^r$$

The factor A_b satisfies $A_b = A_{b-1} - S_1^2/(S_b S_{b-1})$ and the initial condition $A_1 = S_2/S_1$. An induction confirms that $A_b = S_{b+1}/S_b$. When the b -th bubble is placed in $n > 2b$,

only four terms contribute to $\langle v_{1,3,\dots,2b-3,n-1}^r | e_{n-1} P^r v^r \rangle$, and

$$\begin{aligned} P_{\{1,3,\dots,2b-3,n\}}^r &= \frac{S_2}{S_1} P_{\{1,3,\dots,2b-3,n-1\}}^r - P_{\{1,3,\dots,2b-3,n-2\}}^r - P_{\{1,3,\dots,2b-3\}}^r \\ &= \frac{S_{n-b+1}}{S_b} P_{\{1,3,\dots,2b-3,2b-1\}}^r - \frac{S_{(n-2b+2)/2} S_{(n-2b+1)/2}}{S_{1/2} S_{2/2}} P_{\{1,3,\dots,2b-3\}}^r \end{aligned}$$

where a last induction, on n , was used to obtain the last line. \square

LEMMA 2.A.10 *Let $w = v_{n_1, n_2, \dots, n_k}^r$ a link state with only 1-bubbles. Then*

$$\{\Lambda \in \mathbb{R} \mid P_w^r \text{ diverges at } \Lambda\} \subset \cup_{i=1}^k \{\Lambda \in \mathbb{R} \mid P_{\{i\}}^r \text{ diverges at } \Lambda\}.$$

PROOF By repeated use of (2.A.10), it is certainly possible to express P_w^r as :

$$P_{\{n_1, n_2, \dots, n_k\}}^r = \sum_{i=0}^k \alpha_i P_{\{1,3,\dots,2i-1\}}^r$$

where the α_i are functions independent of r and the term $i = 0$ is for P_{\emptyset}^r . Due to the S_b in the denominator of the first term of (2.A.10), the α_i s may be divergent for some values of Λ . More precisely, α_i may carry at most one factor S_j , for any j in $1 < j \leq i$, in its denominator. (The coefficient of the second term of (2.A.10) is analytic for $\Lambda \in \mathbb{R}$.) However, from (2.A.6),

$$P_{\{n_1, n_2, \dots, n_k\}}^r = \sum_{i=0}^k \left(\alpha_i \prod_{j=1}^i \frac{S_j}{S_1} \right) P_{\{i\}}^r$$

and the terms in the denominator of α_i are cancelled by the product $\prod_{1 \leq j \leq i} S_j/S_1$. The coefficients of $P_{\{i\}}^r$ are therefore analytic for $\Lambda \in \mathbb{R}$. \square

LEMMA 2.A.11 *Let $w = v_{n_1, n_2, \dots, n_k}^r$ be any link state. Then*

$$P_w^r = \sum_{i=0}^k \alpha_i P_{\{i\}}^r$$

for some functions α_i analytic in Λ . Therefore

$$\{\Lambda \in \mathbb{R} \mid P_w^r \text{ diverges at } \Lambda\} \subset \cup_{i=1}^k \{\Lambda \in \mathbb{R} \mid P_{\{i\}}^r \text{ diverges at } \Lambda\} \subset \cup_{i=0}^{k-1} \{\Lambda \in \mathbb{R} \mid C_{(r-i)/2} = 0\}. \quad (29)$$

PROOF Let $w_1, w_2 \in B_r^d$ and let $\Delta_{1,2}$ and $\Delta_{2,1}$ be the set of bubbles of w_1 and w_2 respectively that are not shared by both. These sets are noted in the form $\Delta_{1,2} =$

$\{p_1, p_2, \dots, p_k\}$ and $\Delta_{2,1} = \{q_1, q_2, \dots, q_k\}$ where k is the number of distinct bubbles and the p_i s ($p_i < p_{i+1}$) are the end points of the bubbles in w_1 that do not appear in w_2 . For example

$$\begin{aligned} w_1 &= \text{[diagram of w}_1 \text{]} , & \Delta_{1,2} &= \{6, 8, 15\} \\ w_2 &= \text{[diagram of w}_2 \text{]} , & \Delta_{2,1} &= \{7, 8, 10\}. \end{aligned}$$

A partial order “ $<$ ” is defined on the link basis B_r by setting $w_1 < w_2$ if w_1 has less bubbles than w_2 and, if w_1, w_2 have the same number of bubbles, then $w_1 < w_2$ if $p_k < q_k$. For the above example, $w_2 < w_1$.

Each subset B_r^d contains several minimal elements for this order, namely all elements whose arcs are all bunched up on the left. (The number of minimal elements in B_r^d is $\dim V_d^0$.) The proof of the lemma is by induction on this order. More precisely, we first prove the statement for all minimal elements. Then we construct an iterative procedure that expresses P_w^r as a sum $\sum_{y < w} \beta_y P_y^r$ with β_y s analytic in Λ .

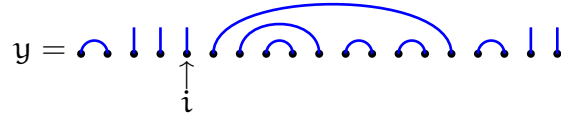
The first step is actually given by Lemma 2.A.5. If $w \in B_r^d$ is minimal, then $\zeta(w) = [0](k_1, k_2, \dots, k_m)[d]$ for $m = (r - d)/2$ and

$$P_w^r = P_{\{m^m\}}^r \left(\prod_{1 \leq i \leq m} \frac{S_i}{S_{k_i}} \right).$$

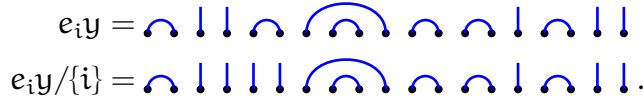
The analyticity of $\prod_i S_i/S_{k_i}$ will follow if all zeroes of the denominator are canceled by zeroes in the numerator. Those of the denominator originate from $S_k = 0$, that is $e^{2ik\Lambda} = 1$, and they are therefore all of the form $\pi\alpha/b$, with $1 \leq b \leq m$ and α, b coprimes. Because all S_k have 2π as a period, the integer α can be restricted to $0 \leq \alpha < 2b$. Moreover the multiplicities of the zero at $\Lambda = 0$ of both numerator and denominator are identical and the case $\alpha = 0$ can be forgotten. Fix now a zero $\pi\alpha/b$ of the denominator, $\alpha \neq 0$. Its multiplicity will depend of the k_i s. This multiplicity is never larger than when the k_i s contain as many b as possible. The largest multiplicity of $\pi\alpha/b$ in the denominator is therefore $\lfloor m/b \rfloor$. But each term in the numerator whose index is a multiple of b has also $\pi\alpha/b$ among its zeroes and there are precisely $\lfloor m/b \rfloor$ of those. So $\prod_i S_i/S_{k_i}$ is not singular at $\pi\alpha/b$ and is therefore analytic.

Suppose now that y is not minimal. This means that there are some defects on the left of some bubbles. We study the leftmost patch of defects and divide the remaining argument depending on whether this patch contains a single defect or

many. We assume first that this patch contains more than one defect, as in



Note that the patch of defects might not be preceded on the left by any arcs. Let i be the position of the last defect on the right of this patch and consider the matrix element $\langle e_i y | e_i P^r v^r \rangle$ which is zero because $e_i P^r = 0$. Several terms of the linear combination $P^r v^r$ will contribute. First the following coefficients will appear : P_y^r , $P_{e_i y}^r$ and $P_{e_i y / \{i\}}^r$ where $e_i y / \{i\}$ stands for the link state obtained from $e_i y$ by replacing the 1-bubble starting at i by two defects. For example, for the y above



Second, because there is a defect at position $i - 1$, the generator e_i can be used to exchange this defect with a 1-bubble starting at i and $P_{e_{i-1} e_i y}^r$ will also contribute. Finally, some link states with a pattern of bubbles on the right of the defect i will also contribute. If the notation $P^r(w)$ is used for P_w^r , the contributions for the example are

$$0 = \langle e_i y | e_i P^r v^r \rangle = P_y^r + \beta P^r(\text{diagram}) + P^r(\text{diagram}) + P^r(\text{diagram}) + P^r(\text{diagram}) + P^r(\text{diagram}) + P^r(\text{diagram})$$

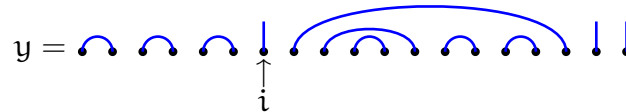
The terms in the last line are reminiscent of those appearing in the proof of Lemma 2.A.9. Each term in this line is accounted as follows. Let a closed cluster be a cluster that contains n bubbles of which one contains all the others. All 1-bubbles are closed clusters and, in the above y , a closed cluster with $n = 5$ starts at position $i + 1 = 6$. Consider the closed cluster to the right of the patch of defects. If this is not a 1-bubble, it contains itself a certain number n_c of closed clusters. (In the example, $n_c = 3$.) The state $e_i y$ breaks this closed cluster and introduces an arc joining $i \leftrightarrow i + 1$, itself followed by the n_c smaller closed clusters that were included in the larger original one. Choose one of these n_c closed clusters and let p_1 and p_2 be the beginning and end positions of its exterior bubble. In $e_i y$, replace the arcs $i \leftrightarrow i + 1$ and $p_1 \leftrightarrow p_2$ by the arcs $i \leftrightarrow p_2$ and $i + 1 \leftrightarrow p_1$. The resulting state y' is such that $e_i y' = e_i y$; it is one of the n_c terms in the last line. Note that if the closed cluster at the right of the defect in y is a 1-bubble, then $n_c = 0$ and the last line of

the above example would have been empty. One more feature of $e_i y$ needs to be underlined. The breaking of the exterior loop of the closed cluster has left a new defect at the end point $i' = i + 2n$ of this loop. Any arc or defect to the right of this new defect appears without change in each term contributing to the matrix element under study. The matrix element is thus

$$0 = P_y^r + \beta P_{e_i y}^r + P_{e_i y / \{i\}}^r + P_{e_{i-1} e_i y}^r + \sum_{y'} P_{y'}^i \tag{2.A.11}$$

and allows to express P_y^r in terms of the other P_{w}^r s. Note that $e_i y$, $e_i y / \{i\}$, $e_{i-1} e_i y$ and the n_c terms y' of the sum all share the new defect at position i' and they are therefore all smaller than y for the partial order. Since $\beta = -S_2/S_1 = -2 \cos \Lambda$ is analytic, the statement follows. Note, before closing this case, that the expression (2.A.11) also holds for link vectors y that have a single defect at position 1 followed by a bubble starting at position 2 (setting $P_{e_{i-1} e_i y}^r$ to 0).

We now study the case where the leftmost patch of defects is actually a single defect at position i . (Note that this i is always odd.) Because the previous case covered the possibility of $i = 1$, we can now assume that a cluster starts at position 1. Given such a link state Y , we replace the leftmost cluster by 1-bubbles, using Lemma 2.A.5. The factor $\prod_i S_i/S_{k_i}$ that this lemma introduces is set aside and will be dealt with later. Here is an example of the resulting state y :



with



Again a vanishing matrix element is computed : $\langle e_i y | e_i P^r v^r \rangle$. The components of $P^r v^r$ that contribute to this matrix element are of several types. Again P_y^r , $P_{e_i y}^r$ and $P_{e_i y / \{i\}}^r$ will appear, as well as a sum $\sum_{y'}$ over states constructed as previously from the n_c closed clusters inside the large closed cluster to the right of the defect. (Again the present y has $n_c = 3$.) Besides these, a sum appears over states y'' obtained from $e_i y$ by replacing the arcs $i \leftrightarrow i + 1$ and $2j - 1 \leftrightarrow 2j$ with $2j < i$ by arcs $i \leftrightarrow 2j$ and $i + 1 \leftrightarrow 2j - 1$. There are $(i - 1)/2$ terms of this type. Here are all the terms for the

above y . The three terms y'' are contained in the first parenthesis.

$$\begin{aligned}
0 &= \langle \text{diagram} | e_i P^r v^r \rangle \\
&= P_y^r + \beta P^r(e_i y = \text{diagram}) \\
&+ \left(P^r(\text{diagram}) + P^r(\text{diagram}) + P^r(\text{diagram}) \right) \\
&+ P^r(e_i y / \{i\} = \text{diagram}) \\
&+ \left(P^r(\text{diagram}) + P^r(\text{diagram}) + P^r(\text{diagram}) \right)
\end{aligned}$$

Using Lemma 2.A.5, all terms of type y'' can be brought down to $P_{e_i y}^r$. Their sum, with $\beta P_{e_i y}^r$ included, is

$$P_{e_i y}^r \left(-\frac{S_2}{S_1} + \frac{S_1^2}{S_1 S_2} + \cdots + \frac{S_1^2}{S_{(i-1)/2} S_{(i+1)/2}} \right) = -P_{e_i y}^r A_{(i+1)/2}$$

where the coefficients $A_b = S_{b+1}/S_b$ was introduced in Lemma 2.A.9. The equation for the matrix elements is therefore

$$0 = P_y^r - P_{e_i y}^r A_{(i+1)/2} + P_{e_i y / \{i\}}^r + \sum_{y'} P_{y'}^r$$

and allows to express P_y^r as a function of coefficients in $P^r v^r$ of the states $e_i y$, $e_i y / \{i\}$ and y' which are all smaller than y for the partial order $<$.

Now is the time to address the factor $\prod_i S_i / S_{k_i}$ left aside at the beginning. The states $e_i y / \{i\}$ and y' start on the left with the same number of bubbles as y does. Through the use of Lemma 2.A.5, the left cluster of the original state Y can be reconstructed using this product; the coefficients of the corresponding terms will be 1 and the new states are smaller than Y . The state $P_{e_i y}^r$ contains an additional 1-bubble joining i and $i+1$. A large bubble from 1 to $i+1$ is first drawn to get rid of the denominator $S_{(i+1)/2}$ in $A_{(i+1)/2}$. Then, within it, the original left cluster of the state Y is reconstructed, taking care of $\prod_i S_i / S_{k_i}$. The corresponding state has an analytic factor, namely $S_{(i+1)/2+1}$, and is smaller than Y . So, as claimed, $P_Y^r = \sum_{w < Y} \beta_w P_w^r$ form some analytic $\beta_w s$.

The example given above has only two clusters separated by one defect. What if, to the right of the second cluster, there are others? As for the case with a patch with more than one defects, the other clusters are left untouched by the procedure above. Only the cluster starting at 1 and the *closed* cluster starting at $i+1$ are transformed by the computation of $\langle e_i y | e_i P^r v^r \rangle$. Because the other clusters remain as they are in the starting state y , all new terms produced during the computation are smaller than y as required. \square

2.B Matrix elements of $\rho(F_N(\lambda))$

In this appendix, we describe a method for calculating any matrix element of $\rho(F_N(\lambda))$. From the simple graphical identity (2.3.3), we know that every half arc in $u = v_{n_1, n_2, \dots, n_k}^N$ propagates down through $F_N(\lambda)$. The only w s for which the matrix element $\langle w | F_N(\lambda) u \rangle$ does not vanish are those that contain all arcs in u and, maybe, additional ones. They are then of the form $w = v_{n_1, n_2, \dots, n_k, m_1, m_2, \dots, m_j}^N$. (The notation introduced in 2.A.1 is used throughout this appendix.) Calculating off-diagonal elements of $\rho(F_N(\lambda))$ amounts to calculating the last column of $\rho(F_r(\lambda))$ for all r smaller or equal to N , but with the same parity, or more specifically, $\langle v_{\ell_1, \ell_2, \dots, \ell_n}^r | F_r(\lambda) v^r \rangle$ where, again, v^r stands for the link vector with r defects ($\in B_r^r$).

The result is expressed in terms of another notation for the link vector. To each element $w \in B_N$ is associated a set $\eta(w)$ of N integers $\in \{-1, 0, 1\}$. Going from left to right along the N entries of the link state w , we assign a “0” for a defect, a “1” for the beginning of a bubble and a “-1” for the end of bubble. The examples given in section 2.A.1 have the following notation η :

$$\begin{aligned}\eta(v_{3,7}^{10}) &= \{0, 0, 1, -1, 0, 0, 1, -1, 0, 0\}, \\ \eta(v_{2,2,7,7}^{10}) &= \{1, 1, -1, -1, 0, 1, 1, -1, -1, 0\}, \\ \eta(v_{2,6,8,7}^{10}) &= \{0, 1, -1, 0, 1, 1, -1, 1, -1, -1\}, \\ \eta(v_{3,5,4,8,5}^{10}) &= \{1, 1, 1, -1, 1, -1, -1, 1, -1, -1\}.\end{aligned}$$

PROPOSITION 2.B.1 *Let $w \in B^r$. Then the matrix element of $\rho(F_r(\lambda))$ between w and v^r is*

$$\langle w | F_r(\lambda) v^r \rangle = I^\dagger \left(\prod_{1 \leq k \leq r} N_{\eta(w)_k} \right) G I \quad (2.B.1)$$

where the matrices in the product are ordered from left to right as k increases, the vector I is

$$I = \begin{pmatrix} 1 \\ 0 \\ 0 \\ \vdots \\ 0 \end{pmatrix} \text{ and the matrices } G, N_i, i \in \{-1, 0, 1\} \text{ are}$$

$$N_0 = \begin{pmatrix} -e^{i\lambda} & 1 - e^{-2i\lambda} & 0 & 0 & 0 & 0 & 0 & 0 \\ 0 & -e^{-i\lambda} & 0 & 1 & 0 & 0 & 0 & 0 \\ -e^{i\lambda} & 1 - e^{-i\lambda} & 1 & 0 & 0 & 0 & 0 & 0 \\ 0 & 0 & 0 & 1 & 0 & 0 & 0 & 0 \\ 0 & 0 & 0 & 0 & 0 & 0 & 0 & 0 \\ 0 & 0 & 0 & 0 & 0 & 0 & 0 & 0 \\ 0 & 0 & 0 & 0 & 0 & 0 & 0 & 0 \\ 0 & -e^{-i\lambda} & 0 & 0 & 0 & 0 & 0 & 0 \end{pmatrix}, N_1 = \begin{pmatrix} 0 & 0 & 0 & 0 & 1 - e^{-2i\lambda} & 0 & 0 & 0 \\ 0 & 0 & 0 & 0 & -e^{-i\lambda} & 1 & 0 & 0 \\ 0 & 0 & 0 & 0 & 1 - e^{-i\lambda} & 0 & 0 & 0 \\ 0 & 0 & 0 & 0 & 0 & 1 & 0 & 0 \\ 0 & 0 & 0 & 0 & 0 & 0 & 1 & 0 \\ 0 & 0 & 0 & 0 & 0 & 0 & 0 & 1 \\ 0 & 0 & 0 & 0 & 0 & 0 & 0 & 0 \\ 0 & 0 & 0 & 0 & -e^{-i\lambda} & 0 & 0 & 0 \end{pmatrix},$$

$$N_{-1} = \begin{pmatrix} 0 & 0 & 0 & 0 & 0 & 0 & 0 & 0 \\ 0 & 0 & 0 & 0 & 0 & 0 & 0 & 0 \\ 0 & 0 & 0 & 0 & 0 & 0 & 0 & 0 \\ 0 & 0 & 0 & 0 & 0 & 0 & 0 & 0 \\ -e^{i\lambda} & 0 & 1 & 0 & 0 & 0 & 0 & 1 \\ -e^{i\lambda} & 1 & 0 & 0 & 0 & 0 & 0 & 1 \\ 0 & 0 & 0 & 0 & 1 & 0 & 0 & 0 \\ 0 & 0 & 0 & 0 & 0 & 0 & 0 & 0 \end{pmatrix}, G = \begin{pmatrix} 2 \cos(\lambda) & 1 & 1 & 0 & 0 & 0 & 0 & 1 \\ 1 & 0 & 1 & 0 & 0 & 0 & 0 & 0 \\ 1 & 1 & 1 & 1 & 0 & 0 & 0 & 0 \\ 0 & 0 & 1 & 0 & 0 & 0 & 0 & 0 \\ 0 & 0 & 0 & 0 & 1 & 1 & 0 & 0 \\ 0 & 0 & 0 & 0 & 1 & 0 & 0 & 0 \\ 0 & 0 & 0 & 0 & 0 & 0 & 1 & 0 \\ 1 & 0 & 0 & 0 & 0 & 0 & 0 & 0 \end{pmatrix}.$$

PROOF The strategy will be to sum the braid boxes in F_r from left to right, using this identity :

The matrix element $\langle v_2^4 | F_4(\lambda) v^4 \rangle$ will serve as an example. Using the previous identity on the first two boxes, we obtain :

Summing the first two boxes of $F_r(\lambda)$, we obtain a linear combination of new objects made of $(r - 1) \times 2$ boxes, with different boundary condition on the left side. If we repeat the process on the second term, two terms are found to be zero due to eq. (2.A.1) and we get :

We are now left with a combination of $(r - 2) \times 2$ boxes. The incoming straight lines (or curves) represent the defects of v^r and the dashed ones represent where the defects and arcs of w are. The same procedure can be repeated until all the sums in the braid boxes are performed. At each step, the pattern of straight and dashed

lines (or curves) entering the leftmost pair of braid boxes is one of the following eight “vectors” :

$$\mathcal{L} = \left\{ \begin{array}{c} \text{red arc} \\ \text{blue U-arc} \\ \text{blue U-arc} \\ \text{dashed red arc} \\ \text{blue U-arc} \\ \text{dashed red arc} \\ \text{dashed red arc} \\ \text{dashed red arc} \end{array} \right\}.$$

The dashed curves represent the states of w , either a defect if it ends as a line or an arc if it is a half-circle. One can understand the leftmost pair of braid boxes as acting linearly on one of these eight basis vectors of the basis \mathcal{L} . This action depends on the states entering this new pair of braids and three linear transformations must be distinguished :

$$N_0 = \begin{array}{|c|} \hline \bullet \\ \hline \text{---} \\ \hline \text{---} \\ \hline \bullet \\ \hline \end{array}, \quad N_1 = \begin{array}{|c|} \hline \bullet \\ \hline \text{---} \\ \hline \text{---} \\ \hline \bullet \\ \hline \end{array} \quad \text{and} \quad N_{-1} = \begin{array}{|c|} \hline \bullet \\ \hline \text{---} \\ \hline \text{---} \\ \hline \bullet \\ \hline \end{array}.$$

The three linear transformations can be expressed in the basis \mathcal{L} , with the action given by right multiplication on a row vector of components. The two examples (2.B.2) and (2.B.3) have computed one line of each N_0 and N_1 in this basis :

- eq. (2.B.2) is $(1 \ 0 \ 0 \ 0 \ 0 \ 0 \ 0 \ 0) \cdot N_0 = (-e^{i\lambda} \ 1 - e^{-2i\lambda} \ 0 \ 0 \ 0 \ 0 \ 0 \ 0)$;
- eq. (2.B.3) is $(0 \ 1 \ 0 \ 0 \ 0 \ 0 \ 0 \ 0) \cdot N_1 = (0 \ 0 \ 0 \ 0 \ -e^{-i\lambda} \ 1 \ 0 \ 0)$.

A direct computation gives the three matrices in the statement. After the procedure has been applied r times, the row vector is $I^\dagger \left(\prod_{1 \leq k \leq r} N_{\eta(w)_k} \right)$. All boxes have been summed and it remains to connect the state on left and with the half-circle on the right, using the rules (2.A.1) as in

$$\begin{array}{|c|} \hline \bullet \\ \hline \text{---} \\ \hline \bullet \\ \hline \end{array} \text{red circle} = 2 \cos(\lambda), \quad \begin{array}{|c|} \hline \text{blue U-arc} \\ \hline \text{red arc} \\ \hline \text{dashed red arc} \\ \hline \end{array} = 1, \quad \begin{array}{|c|} \hline \text{blue U-arc} \\ \hline \text{blue U-arc} \\ \hline \text{red arc} \\ \hline \end{array} = 1, \quad \begin{array}{|c|} \hline \text{dashed red arc} \\ \hline \text{red arc} \\ \hline \text{dashed red arc} \\ \hline \end{array} = 0, \quad \dots$$

This pairing of elements in the basis elements \mathcal{L} with the mirror image of the first element can be extended to the mirror images of all elements, thus defining the symmetric bilinear form G given in the proposition. But for the specific boundary condition represented by the first vector of \mathcal{L} , only the first column of G is needed and one gets $\langle w | F_r(\lambda) v^r \rangle = I^\dagger \left(\prod_{1 \leq k \leq r} N_{\eta(w)_k} \right) G I$ as claimed. \square

To end the example started in the proof, we can use the formula to express the matrix element $\langle v_2^4 | F_4(\lambda) v^4 \rangle$ as $I^\dagger N_0 N_1 N_{-1} N_0 G I = -2^5 \cos \lambda \sin^2 \lambda \sin^2 \lambda / 2$. A few remarks are in order. It is impossible to create 3-bubbles with only two rows of braid-boxes. Consequently $\langle w | F_N(\lambda) v^N \rangle$ is always zero if w has n -bubbles, with $n \geq 3$ and the two matrices N_1 and N_{-1} are nilpotent of degree 3: $(N_{-1})^3 = (N_1)^3 = 0$. The previous proposition allows for another proof of the eigenvalue (2.3.2) of $\rho(F_N)$ in the sector d (Lemma 2.3.1). This eigenvalue is $\langle v^d | F_d(\lambda) v^d \rangle = I^\dagger N_0^d G I$. The powers of N_0 are obtained by diagonalization: $N_0 = S n_0 S^{-1}$ with

$$n_0 = \begin{pmatrix} 0 & 0 & 0 & 0 & 0 & 0 & 0 & 0 & 0 \\ 0 & 0 & 0 & 0 & 0 & 0 & 0 & 0 & 0 \\ 0 & 0 & 0 & 0 & 0 & 0 & 0 & 0 & 0 \\ 0 & 0 & 0 & 0 & 0 & 0 & 0 & 0 & 0 \\ 0 & 0 & 0 & 0 & 1 & 0 & 0 & 0 & 0 \\ 0 & 0 & 0 & 0 & 0 & 1 & 0 & 0 & 0 \\ 0 & 0 & 0 & 0 & 0 & 0 & -e^{-i\lambda} & 0 & 0 \\ 0 & 0 & 0 & 0 & 0 & 0 & 0 & -e^{i\lambda} & 0 \end{pmatrix}, \quad (2.B.4)$$

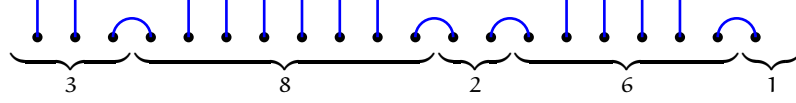
$$S = \begin{pmatrix} 0 & 0 & 0 & 0 & -1 + e^{-i\lambda} & 0 & e^{-i\lambda} & 1 + e^{-i\lambda} \\ 0 & 0 & 0 & 0 & -e^{i\lambda} & 0 & 1 & 0 \\ 0 & 0 & 0 & 0 & 0 & 1 & \frac{1}{1+e^{i\lambda}} & 1 \\ 0 & 0 & 0 & 0 & -1 - e^{i\lambda} & 0 & 0 & 0 \\ 0 & 0 & 0 & 1 & 0 & 0 & 0 & 0 \\ 0 & 0 & 1 & 0 & 0 & 0 & 0 & 0 \\ 0 & 1 & 0 & 0 & 0 & 0 & 0 & 0 \\ 1 & 0 & 0 & 0 & 0 & 0 & 1 & 0 \end{pmatrix}.$$

With these, it is now trivial to verify that $I^\dagger S (n_0)^d S^{-1} G I = 2(-1)^d \cos(\lambda(d+1))$. As a last remark, note that in the proof of the previous proposition, we have summed 2-boxes from left to right. We could very well have started from the right, summing 2-boxes from right to left. Simple matrix products yield $N_k G = G N_{-k}^\dagger$. This allows to move the matrix G in (2.B.1) anywhere within $\prod_k N_{\eta(w)_k}$. In particular,

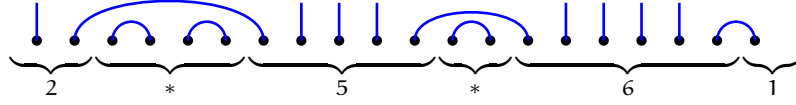
$$\langle w | F_r(\lambda) v^r \rangle = I^\dagger G \left(\prod_{1 \leq k \leq r} N_{-\eta(w)_k}^\dagger \right) I.$$

Our last expression for the matrix elements of $\rho(F_N)$ is given in yet another notation. Let $w \in B_N^d$ be a link state with only 1-bubbles and let $n_1 = (N - d)/2$ be their number. We associate with w a set of $(N - d)/2 + 1$ positive integers $\mu(w) = [m_0, m_1, \dots, m_{n_1}]$, where m_i is the number of points separating the middle of bubbles i and $(i + 1)$ -th, for $i = 1, \dots, n_1 - 1$. Then m_0 counts the points before the

middle of the first bubble and m_{n_1} those after the middle of the last. For instance, $\mu(v_{3,11,13,19}^{20}) = [3, 8, 2, 6, 1]$:



With this definition, $\sum_i m_i = N$. Now let w be a link state with 1-bubbles and 2-bubbles. Again we associate with w the set $\mu(w) = [m_0, m_1, \dots, m_L]$, with $L = n_1 + 2n_2$, where n_2 is the number of 2-bubbles and n_1 , the number of 1-bubbles that are not circumscribed by 2-bubbles. This time, m can either be an integer (and counts defects between bubbles including the first or last point of delimiting arcs, as before), or an asterisk to denote all points within a 2-bubble. For instance, $\mu(v_{3,5,4,12,12,19}^{20}) = [2, *, 5, *, 6, 1]$:



LEMMA 2.B.2 *Let $w \in B_\tau$ be a link state with $\mu(w) = [m_0, m_1, \dots, m_L]$. Then*

$$\langle w | F_\tau(\lambda) v^r \rangle = V(m_0)^T \left(\prod_{i=1}^{L-1} W(m_i) \right) G' V(m_L)$$

with

$$\begin{aligned} V(m) &= 2 \begin{pmatrix} S_m \\ S_{\frac{m-1}{2}} S_{\frac{m}{2}} / S_{\frac{1}{2}} \end{pmatrix}, & W(*) &= \begin{pmatrix} 1 & 0 \\ 1 & 0 \end{pmatrix}, \\ W(m) &= \begin{pmatrix} S_{\frac{2m-1}{2}} / S_{\frac{1}{2}} & S_{\frac{m}{2}} S_{\frac{m-2}{2}} / S_{\frac{1}{2}}^2 \\ 2 C_{m-1} & S_{\frac{2m-3}{2}} / S_{\frac{1}{2}} \end{pmatrix}, & G' &= \begin{pmatrix} 1 & 1 \\ 1 & 0 \end{pmatrix}, \end{aligned} \quad (2.B.5)$$

where the notation of Definition 2.3.2 was used.

PROOF We start with w s that have no 2-bubbles. The product of eq. (2.B.1) can be rearranged by displacing G to the left until it comes across the first bubble, that is, until it passes the rightmost N_{-1} . The matrices on the left of G can then be gathered in groups labelled by the subscript $i = 1, \dots, n_1 - 1$. Each group starts with N_{-1} , followed by $m_i - 2$ occurrences of N_0 , and ends with N_{-1} . The result is

$$\langle w | F_N(\lambda) v^N \rangle = \left(I^\dagger (N_0)^{m_0-1} N_1 \right) \left(\prod_{i=1}^{n_1-1} \left(N_{-1} (N_0)^{m_i-2} N_1 \right) \right) G (N_1^\dagger (N_0^\dagger)^{m_{n_1}-1} I). \quad (2.B.6)$$

Using the diagonal form (2.B.4) of N_0 , we are able to compute $I^\dagger (N_0)^{m-1} N_1$ and $N_{-1} (N_0)^{m-2} N_1$:

$$I^\dagger S n_0^{m-1} S^{-1} N_1 = -2ie^{i\Lambda} \begin{pmatrix} 0 & 0 & 0 & 0 & S_m & S_{\frac{m}{2}} S_{\frac{m-1}{2}} / S_{\frac{1}{2}} & 0 & 0 \end{pmatrix}$$

$$N_{-1} S n_0^{m-2} S^{-1} N_1 = \begin{pmatrix} 0 & 0 & 0 & 0 & 0 & 0 & 0 & 0 \\ 0 & 0 & 0 & 0 & 0 & 0 & 0 & 0 \\ 0 & 0 & 0 & 0 & 0 & 0 & 0 & 0 \\ 0 & 0 & 0 & 0 & 0 & 0 & 0 & 0 \\ 0 & 0 & 0 & 0 & S_{\frac{2m-1}{2}} / S_{\frac{1}{2}} & S_{\frac{m}{2}} S_{\frac{m-2}{2}} / S_{\frac{1}{2}}^2 & 0 & 0 \\ 0 & 0 & 0 & 0 & 2 C_{m-1} & S_{\frac{2m-3}{2}} / S_{\frac{1}{2}} & 0 & 0 \\ 0 & 0 & 0 & 0 & 0 & 0 & 0 & 0 \\ 0 & 0 & 0 & 0 & 0 & 0 & 0 & 0 \end{pmatrix}.$$

Hence, $I^\dagger (N_0)^{m_0} N_1$ belongs to the subspace spanned by

$$\{(0, 0, 0, 0, 1, 0, 0, 0), (0, 0, 0, 0, 0, 1, 0, 0)\},$$

which is also stable under the action of both $N_{-1} (N_0)^{m_i} N_1$ and G . The products in (2.B.6) can therefore be restricted to this subspace. Note that the two factors $(-ie^{i\Lambda})$ and $(ie^{-i\Lambda})$ coming from the extreme factors cancel.

The same rearrangement can be carried out on the product of (2.B.1) when link states carry 2-bubbles. When they do, $(N_1 N_{-1})^p$ appears between $N_{-1} (N_0)^{m_i} N_1$ and $N_{-1} (N_0)^{m_i+2} N_1$. Here p is the number of 1-bubbles enclosed in the 2-bubble. But the 2-dimensional subspace used above is also stable under

$$N_1 N_{-1} = \begin{pmatrix} e^{-i\Lambda} - e^{i\Lambda} & 0 & 1 - e^{-2i\Lambda} & 0 & 0 & 0 & 0 & 1 - e^{-2i\Lambda} \\ 1 - e^{i\Lambda} & 1 & -e^{-i\Lambda} & 0 & 0 & 0 & 0 & 1 - e^{-i\Lambda} \\ 1 - e^{i\Lambda} & 0 & 1 - e^{-i\Lambda} & 0 & 0 & 0 & 0 & 1 - e^{-i\Lambda} \\ -e^{i\Lambda} & 1 & 0 & 0 & 0 & 0 & 0 & 1 \\ 0 & 0 & 0 & 0 & 1 & 0 & 0 & 0 \\ 0 & 0 & 0 & 0 & 1 & 0 & 0 & 0 \\ 0 & 0 & 0 & 0 & 0 & 0 & 0 & 0 \\ 1 & 0 & -e^{-i\Lambda} & 0 & 0 & 0 & 0 & -e^{-i\Lambda} \end{pmatrix}.$$

The fact that the restriction $W(*)$ of this matrix to the subspace is idempotent shows that the contribution of 2-bubbles is independent of p . This concludes the proof. \square

CHAPITRE 3: LES RÈGLES DE SÉLECTION DU MODÈLE DE POLYMÈRES DENSES CRITIQUE SUR LE RUBAN

Objectifs et méthodologie

En 2007, Pearce et Rasmussen [46] montrent qu'en $\beta = 0$ ($\lambda = \pi/2$), la matrice de transfert à deux colonnes, introduite aux sections 1.4.2 et 2.2.1, satisfait l'équation

$$D_N(\pi/2, u)D_N(\pi/2, u + \pi/2) = \left(\frac{\cos^{4N}(u) - \sin^{4N}(u)}{\cos^2(u) - \sin^2(u)} \right)^2 \text{id.}$$

Cela leur permet de trouver un ensemble de valeurs propres possibles pour la matrice de transfert dans chacune des représentations de lien. Ils émettent une conjecture à propos des *règles de sélection* pour les valeurs propres dans $\rho(D_N(\lambda, u))|_d$, c'est-à-dire la règle qui indique, dans l'ensemble des valeurs possibles, lesquelles sont présentes dans le spectre de $\rho(D_N(\lambda, u))$ dans le secteur à d défauts, de même que leurs dégénérescences. Le présent article est consacré à la preuve de cette conjecture, qui utilise une autre représentation de l'algèbre de Temperley-Lieb, celle du modèle XXZ. Il permettra notamment de calculer la forme de Jordan non triviale de l'hamiltonien XXZ en $q = i$ et de montrer que $\rho(\mathcal{H})|_d$ est toujours diagonalisable. Cet article pavera également le chemin pour le chapitre 4, où l'utilisation du modèle XXZ permettra de sonder la structure de Jordan de la matrice de transfert de boucles avec conditions aux limites périodiques.

Voici un résumé de la méthode utilisée et des résultats trouvés :

- Le premier terme du développement en série de Taylor de $D_N(\lambda, u)$ autour de $u = 0$ fait intervenir \mathcal{H} , l'hamiltonien de boucles, qui est plus simple que $D_N(\lambda, u)$. La conjecture des règles de sélection de Pearce et de Rasmussen est aussi une conjecture pour les valeurs propres de $\rho(\mathcal{H})|_d$.
- Les matrices e_j du modèle XXZ engendrent des représentations de l'algèbre de Temperley-Lieb, étiquetées par la valeur propre de S^z . Ces représentations agissent sur des états de spin plutôt que sur des vecteurs de connectivités.

- Lorsque $\beta = -q - q^{-1}$, nous montrons qu'il existe un isomorphisme entre le module des vecteurs de connectivités à d défauts et le noyau $\ker S^+$ dans le sous-espace du module XXZ avec $S^z = d/2$. Cela implique notamment que le spectre est le même dans les deux représentations.
- Nous calculons les valeurs propres de l'hamiltonien dans la représentation XXZ en $q = i$ grâce à une transformation de Jordan-Wigner. Nous trouvons que cet hamiltonien est diagonalisable lorsque N est impair, mais pas lorsque N est pair, où il a des blocs de Jordan de rang 2. Aussi, le noyau $\ker S^+$ est un sous-module invariant sous l'action des matrices e_j dans lequel H n'a jamais de bloc de Jordan, propriété qui, vu l'isomorphisme, est partagée par $\rho(\mathcal{H})|_{\mathfrak{d}}$.
- Nous démontrons la conjecture de Pearce et Rasmussen [46].

Cet article a été publié en 2011 dans le *Journal of Physics A : Mathematical and Theoretical*. La référence complète est :

→ A. Morin-Duchesne, *A proof of selection rules for critical dense polymers*, J. Phys. A : Math. Theor. **44** 495003 (2011) 32 p. ; arXiv : math-ph/1109.6397.

A proof of selection rules for critical dense polymers

Alexi Morin-Duchesne

Département de physique

Université de Montréal, C.P. 6128, succ. centre-ville, Montréal

Québec, Canada, H3C 3J7

Abstract

Among the lattice loop models defined by Pearce, Rasmussen and Zuber (2006), the model corresponding to critical dense polymers ($\beta = 0$) is the only one for which an inversion relation for the transfer matrix $D_N(u)$ was found by Pearce and Rasmussen (2007). From this result, they identified the set of possible eigenvalues for $D_N(u)$ and gave a conjecture for the degeneracies of its relevant eigenvalues in the link representation, in the sector with d defects. In this paper, we set out to prove this conjecture, using the homomorphism of the $\mathbb{T}_N(\beta)$ algebra between the loop model link representation and that of the XXZ model for $\beta = -(q + q^{-1})$.

Keywords : Lattice models in two dimensions, loop models, critical dense polymers, Heisenberg model, XXZ model, Jordan-Wigner transformation.

3.1 Introduction

This paper proves a recent conjecture by Pearce and Rasmussen [46] for the model of critical dense polymers on the strip, by using the relation between this model and the Heisenberg spin model. The Heisenberg model (or XXZ model) is a long studied family of Hamiltonians of N interacting spins on a chain. The models depend upon a spectral parameter q , which controls the z interaction between neighboring spins. The Hamiltonian H_{XXZ} acts on $(\mathbb{C}^2)^{\otimes N}$ (every spin is $\frac{1}{2}$) and commutes with S^z . The spectrum of the XXX Hamiltonian ($q = 1$) for the periodic chain was computed by Bethe [73] long ago and his method, the Bethe ansatz, has since allowed for solutions of the more general XXZ problem on various geometries ([74], [75]). In this paper, we focus on the case where the chain is finite and the Hamiltonian has very particular boundary terms for which the model is invariant under $U_q(\mathfrak{sl}_2)$ [35]. This symmetry will play an important role. We shall be particularly

interested in the case $q = i$, for which the z coupling in the Hamiltonian is absent (known as the XX-model). Though the Bethe ansatz solution is known, the spectrum of this Hamiltonian can be found using the simpler technique of Jordan-Wigner transformation [76].

The loop models introduced in [45] are two dimensional lattice models on the strip that obey Yang-Baxter relations and are, in this sense, integrable. The transfer matrix $D_N(u)$ and Hamiltonian \mathcal{H}_N of the model are elements of the Temperley-Lieb algebra $\mathbb{T}_N(\beta)$ and depend on one free parameter, the fugacity β of the loops. The action of $\mathbb{T}_N(\beta)$ connectivities on link states (i.e. on V_N , the space they generate) defines a representation ρ of $\mathbb{T}_N(\beta)$. For a given connectivity c , the matrix $\rho(c)$ is upper block-triangular (the number of defects, d , is a non increasing quantity) and its spectrum $\rho(c)$ is the union of the spectra of the diagonal blocks, indexed by d , the number of defects. Moreover, the partition functions of Potts models and Fortuin-Kasteleyn models can be computed from the eigenvalues of $\rho(D_N(u))$ of the loop models for specific values of β ([55], [61], [77]).

These models have attracted much interest because the ρ representation of the Hamiltonian and transfer matrix exhibit non trivial Jordan cells ([45], [77], [78]). The corresponding representations of the Virasoro algebra should then be indecomposable and the underlying conformal field theory, logarithmic [45]. On the finite lattice, the diagonal blocks $\rho(D_N)|_d$ have been conjectured to be diagonalizable for $\beta \in [-2, 2]$ for all d . Non trivial Jordan cells do occur, but they tie eigenvalues belonging to sectors with different numbers of defects. This structure appears for specific values of the fugacity $\beta = -(q + q^{-1})$ when q is a root of unity.

The case $\beta = 0$ is somewhat special, as an inversion relation for the transfer matrix was found [46] : $D_N(u)D_N(u + \frac{\pi}{2})$ is a scalar multiple of the identity. From this, one can identify the set of all possible eigenvalues, and the degeneracies of each of these in a given sector d was conjectured by Pearce and Rasmussen through selection rules [46].

The two models introduced previously are known to be related (for example in [79], [80] and [78]). Namely, there exists a \mathbb{T}_N -homomorphism i_N^d from V_N^d to $(\mathbb{C}^2)^{\otimes N}|_{S^z=d/2}$ (the restriction of $(\mathbb{C}^2)^{\otimes N}$ to spin configurations with $n = (N - d)/2$ down spins). The Heisenberg Hamiltonians can be expressed in terms of some matrices e_{iS} that act on $i_N^d(V_N^d)$ in the same way the Temperley-Lieb generators U_i act on V_N^d for $\beta = -(q + q^{-1})$ (except that the number of defects is conserved). For any q and β satisfying this relation and any $c \in \mathbb{T}_N(\beta)$, the spectrum of $\rho(c)$ is contain-

ned in the spectrum of $X(c)$, the representation of c in the XXZ model. We will use the homomorphism to compute the degeneracies of $\rho(\mathcal{H}_N)$ and show they are those predicted by Pearce and Rasmussen [46].

The outline of the paper is as follows. In section 3.2, we review the definition of Temperley-Lieb algebra and of the transfer matrix for critical dense polymers. We recall the selection rules conjectured in [46] and translate these in terms of eigenvalue degeneracies of the Hamiltonian. In section 3.3, we perform the Jordan-Wigner transformation on the XX Hamiltonian and write it in terms of creation and annihilation operators. For N odd, we find H_{XX} to be diagonalizable, but not for N even, for which we provide its Jordan form (some technical details for N even are given in appendix 3.A). The Hamiltonian H_{XXZ} is invariant under $U_q(\mathfrak{sl}_2)$ and, in section 3.4, we write down the generators of the $U_{q=i}(\mathfrak{sl}_2)$ algebra in terms of the creation and annihilation operators of section 3.3. In section 3.5, we construct the homomorphism i_N^d between V_N^d and $(\mathbb{C}^2)^{\otimes N}|_{S^z=d/2}$, the vector space generated by spin configurations with $\frac{N-d}{2}$ down spins. We show that i_N^d sends link states to $(\mathbb{C}^2)^{\otimes N}|_{S^z=d/2} \cap \ker(S^+)$. Because this homomorphism is injective, one can find the spectrum of any element of $\mathbb{T}_N(\beta)$ by looking at its corresponding matrix in the XXZ representation. This is the goal of section 3.6 : we find a set of eigenvectors that complement those in $i_N^d(V_N^d)$ and prove in appendix 3.B that these states are indeed independent. From this we can identify degeneracies in the XX Hamiltonian of eigenvectors $\in \ker(S^+)$ and show they reproduce the spectrum given by the selection rules in section 3.2.

3.2 Critical dense polymers and selection rules

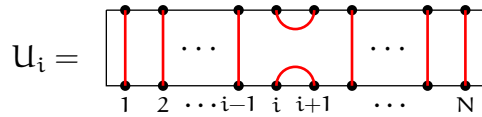
3.2.1 The algebra $\mathbb{T}_N(\beta)$ and the double-row matrix

We start this section by recalling known definitions and results for the Temperley-Lieb algebra and its transfer matrices. The Temperley-Lieb algebra $\mathbb{T}_N(\beta)$ is a finite algebra, with generators $\text{id}, U_1, \dots, U_{N-1}$ satisfying the relations

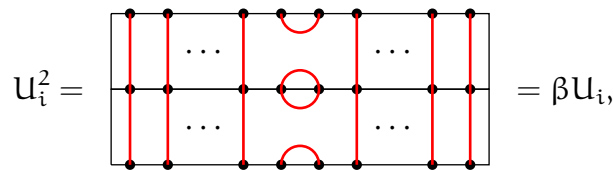
$$\begin{aligned} U_i^2 &= \beta U_i, \\ U_i U_j &= U_j U_i, & \text{for } |i-j| > 1, \\ U_i U_{i\pm 1} U_i &= U_i, & \text{when } i, i\pm 1 \in \{1, 2, \dots, N-1\}. \end{aligned} \tag{3.2.1}$$

The algebra $\mathbb{T}_N(\beta)$ is sometimes referred to as a connectivity algebra. A connectivity is a diagram made of a rectangular box with N marked points on the top

segment and as many marked points on the bottom. Inside the box, the $2N$ points are connected pairwise by non intersecting curves. To the generator U_i , we associate the connectivity

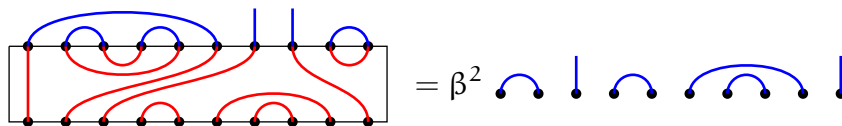


Diagrammatically, the product $U_i U_j$ amounts to gluing the diagram of U_j over the diagram of U_i . The resulting connectivity is obtained by reading the connections between the top and bottom marked points. With this identification, the first equation of (3.2.1) is



so that the free parameter β is the weight given to loops closed in the process. The other two equations in (3.2.1) have similar interpretations. Any connectivity can be obtained by a product of the generators, and the product of any two connectivities c_1 and c_2 in $\mathbb{T}L_N(\beta)$ is given by the same concatenation rule. The algebra $\mathbb{T}L_N(\beta)$ is the algebra of connectivities endowed with the product just described and is of dimension $\frac{1}{n+1} \binom{2n}{n}$.

A useful representation is the representation ρ on *link states* (or *link patterns*). A link pattern is a set of N marked points on a horizontal segment. The points are connected pairwise, or to infinity, by non intersecting curves that lay above the segment. Points connected to infinity are called *defects*. The set of link states of length N with d defects is denoted B_N^d and their linear span by V_N^d , with $\dim(V_N^d) = \binom{N}{(N-d)/2} - \binom{N}{(N-d-2)/2}$. The set of all link states of size N is noted B_N (and V_N the corresponding vector space). Let $v \in B_N$ and c a connectivity. The product cv is obtained by connecting the marked points of v to the top marked points of c , by reading the resulting link pattern given by the new connections at the bottom of c , and by adding a multiplicative factor of β for each closed loop. Here is an example :



The matrix representing c in the link representation is denoted $\rho(c)$. It is of size $\dim(V_N)$ and obtained by acting on c with all the link patterns of B_N . Because the

number of defects can never increase, $\rho(c)$ is upper block-triangular and we will note by $\rho(c)|_d$ the blocks on the diagonal of $\rho(c)$, that restrict the domain and image to elements in V_N^d . The matrices $\rho(c)|_d$ also generate representations of $\mathcal{TL}_N(\beta)$.

We introduce the double-row matrix $D_N(u)$ as an element of $\mathcal{TL}_N(\beta = 0)$. It is defined diagrammatically by

$$D_N(u) = \frac{1}{\sin 2u} \begin{array}{c} \overbrace{\hspace{10em}}^N \\ \begin{array}{|c|c|c|c|} \hline \bullet & \bullet & \cdots & \bullet \\ \hline \frac{\pi}{2} - u & \frac{\pi}{2} - u & & \frac{\pi}{2} - u \\ \hline u & u & & u \\ \hline \bullet & \bullet & \cdots & \bullet \\ \hline \end{array} \end{array}$$

where each box is given by

$$\boxed{u} = \cos u \begin{array}{|c|} \hline \text{red arcs} \\ \hline \end{array} + \sin u \begin{array}{|c|} \hline \text{red arcs} \\ \hline \end{array} = \boxed{\frac{\pi}{2} - u}$$

and $u \in [0, \frac{\pi}{2}]$ is the anisotropy parameter (for a definition of $D_N(u)$ for general β , see [45]). From the definition, it can easily be shown that $D_N(u) = D_N(\pi/2 - u)$ and $D_N(0) = D_N(\pi/2) = \text{id}$ are satisfied, where id is the unique connectivity connecting every point on top to the corresponding point on the bottom. In [46], it is also shown that $D_N(u)$ satisfies the following inversion identity :

$$D_N(u)D_N(u + \frac{\pi}{2}) = \left(\frac{\cos^{2N} u - \sin^{2N} u}{\cos^2 u - \sin^2 u} \right)^2 \text{id},$$

from which is it possible to retrieve a closed expression for the eigenvalues of $D_N(u)$, which we note $d_N(u)$:

$$\text{N odd : } d_N(u) = \frac{1}{2^{N-1}} \prod_{j=1}^{\frac{N-1}{2}} \left(\frac{1}{\sin \frac{(2j-1)\pi}{2N}} + \epsilon_j \sin 2u \right) \left(\frac{1}{\sin \frac{(2j-1)\pi}{2N}} + \mu_j \sin 2u \right), \quad (3.2.2)$$

$$\text{N even : } d_N(u) = \frac{N}{2^{N-1}} \prod_{j=1}^{\frac{N-2}{2}} \left(\frac{1}{\sin \frac{j\pi}{N}} + \epsilon_j \sin 2u \right) \left(\frac{1}{\sin \frac{j\pi}{N}} + \mu_j \sin 2u \right), \quad (3.2.3)$$

where $\epsilon_j, \mu_j = \pm 1$ for every j . Fixing values for each ϵ_j and each μ_j , the set of zeroes of $d_N(u)$ is

$$\{u | d_N(u) = 0\} = \bigcup_{\nu=\epsilon, \mu} \bigcup_j \left\{ (2 + \nu_j) \frac{\pi}{4} \pm \frac{i}{2} \ln \tan \frac{t_j}{2} + \pi k, \quad k \in \mathbb{Z} \right\}$$

where

$$\text{N odd : } \quad t_j = \frac{(2j-1)\pi}{2N},$$

$$\text{N even : } \quad t_j = \frac{j\pi}{N}.$$

Given a fixed $d_N(u)$, every zero in the above set appears 0, 1 or 2 times, and the number of zeroes with imaginary value $i/2 \ln \tan t_j/2$ is always 2. There are $N-1$ zeroes for N odd and $N-2$ for N even, which results in a total of 2^{N-1} and 2^{N-2} choices, respectively, for the eigenvalues $d_N(u)$. The set of possible solutions for eigenvalues of $\rho(D_N(u))$ is too large and one must identify which ones are *relevant*. This will be the subject of the next section.

$D_N(u)$ can be developed in a Taylor series around the point $u = 0$, yielding

$$D_N(u) = \text{id} + 2u\mathcal{H}_N + \mathcal{O}(u^2) \quad \text{with} \quad \mathcal{H}_N = \sum_{i=1}^{N-1} u_i. \quad (3.2.4)$$

To understand and prove the selection rules, we will calculate the eigenvalues of \mathcal{H}_N . Using the expansions of (3.2.2) and (3.2.3) around $u = 0$, and using $d_N(0) = 1$, i.e.

$$\frac{1}{2^{N-1}} \prod_{j=1}^{\frac{N-1}{2}} \frac{1}{\sin^2 \frac{(2j-1)\pi}{2N}} = 1 \quad \text{and} \quad \frac{N}{2^{N-1}} \prod_{j=1}^{\frac{N-2}{2}} \frac{1}{\sin^2 \frac{j\pi}{N}} = 1$$

for N odd and N even respectively, one finds that eigenvalues of \mathcal{H}_N , denoted h_N , are

$$\text{N odd : } \quad h_N = \sum_{j=1}^{\frac{N-1}{2}} \cos \left(\frac{\pi j}{N} \right) (\epsilon_{\frac{N+1}{2}-j} + \mu_{\frac{N+1}{2}-j}), \quad (3.2.5)$$

$$\text{N even : } \quad h_N = \sum_{j=1}^{\frac{N-2}{2}} \cos \left(\frac{\pi j}{N} \right) (\epsilon_{\frac{N}{2}-j} + \mu_{\frac{N}{2}-j}), \quad (3.2.6)$$

and the ϵ_j s and μ_j s are those of $d_N(u)$.

3.2.2 Two-column configurations

The selection rules given in [46] have been formulated in terms of column configurations. This section is a quick review of their definitions.

DEFINITION 3.2.1 *A one-column configuration of height M is a configuration of M sites disposed in a column and labeled from 1 to M , starting from the top. In a column configuration, every site is either occupied or unoccupied and we define its signature, $S =$*

$\{S_1, S_2, \dots, S_m\}$, where the S_i s are the labels of the occupied sites in ascending order (and $m \leq M$ is their number and will be called the length of the signature). We identify unoccupied sites with white circles “○” and occupied sites with blue circles “●”.

DEFINITION 3.2.2 A two-column configuration of height M is a pair of one-column configurations, both of height M , and is usually depicted as in Figure 3.1. Its signature is $S = (L, R)$, where L and R are the respective signatures of the left and right column configurations and may have different lengths m and n . A two-column configuration will be said to be admissible if $0 \leq m \leq n \leq M$ and $L_i \geq R_i$ for all $i = 1, \dots, m$. We denote by $A_{m,n}^M$ the set of admissible two-column configurations of height M and signature lengths m and n . When m, n and M are such that the previous constraint is violated, $A_{m,n}^M \equiv \emptyset$.

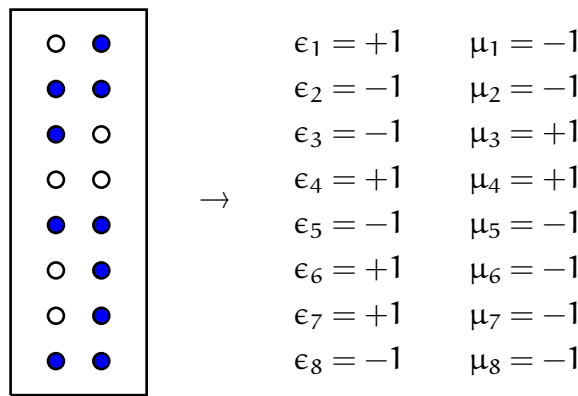


FIGURE 3.1 – An admissible two-column configuration in $A_{4,6}^8$ with $L = (2, 3, 5, 8)$ and $R = (1, 2, 5, 6, 7, 8)$: blue sites are occupied and white sites unoccupied. To its right, the corresponding values of the ϵ_j s and μ_j s.

The graphical interpretation of this last definition is simple. Fix a two-column configuration. To see if it is admissible, we draw on the two-column configuration segments connecting sites with label L_i from the left column to sites with label R_i from the right column, for $i = 1, \dots, m$ (the remaining sites at positions R_j with $m < j \leq n$ are not connected to any other site). If all the segments have positive or null slopes, the configuration is admissible.

DEFINITION 3.2.3 The reduced set $\tilde{A}_{x,y}^{x+y}$ of admissible two-column configurations is the subset of configurations of $A_{x,y}^{x+y}$ that have one and only one excitation for every j .

Evaluating $|\tilde{A}_{x,y}^{x+y}|$ is simple, as there exists bijections between reduced configurations in $\tilde{A}_{x,y}^{x+y}$, Dyck paths $\vec{x} \in DP_{y-x}^{x+y}$ (see definition 3.5.2) and link states in V_{x+y}^{y-x} :

- From an element of $\tilde{A}_{x,y}^{x+y}$, we set $\epsilon_j = +1$ if the site of the left one-column configuration at height j is unoccupied, and -1 otherwise. $\vec{x} = (\epsilon_1, \dots, \epsilon_{x+y})$ is a Dyck path of length $x + y$ as, from the definition of reduced admissible configurations, $\sum_{i=1}^k \epsilon_i \geq 0$ for every k in $1, \dots, x + y$. Since there are, in total, y “+1”s and x “-1”s, the endpoint of the Dyck Path is at $y - x$. This transformation is bijective.
- The bijection between Dyck paths and link states is given by the following. To each of the entries of the link state, we associate the integer j in $1, \dots, N$ from left to right and build pairings (j', j) (the positions where the bubbles connect). Starting from the left, for every $x_j = -1$, we pair j to the closest available j' such that $x_{j'} = +1$ and $j > j'$. When every j with $x_j = -1$ is paired, the remaining $y - x$ unpaired sites are chosen to be defects. The link state v obtained from a given Dyck path \vec{x} by the previous procedure will be noted $v = \mathcal{B}(\vec{x})$.

From this bijection,

$$|\tilde{A}_{x,y}^{x+y}| = \dim V_{x+y}^{y-x} = \binom{x+y}{x} - \binom{x+y}{x-1}. \tag{3.2.7}$$

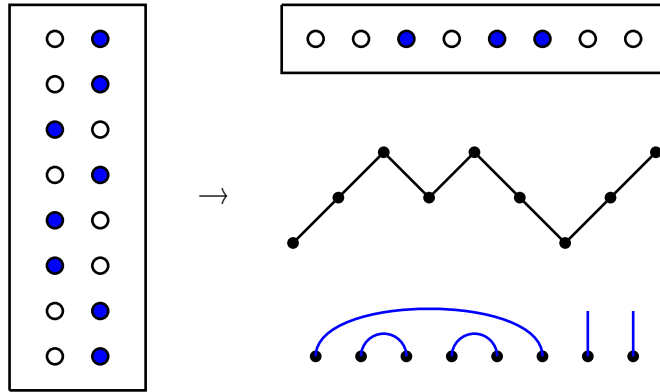


FIGURE 3.2 – A two-column admissible configuration in $\tilde{A}_{3,5}^8$ and, to the right, the corresponding Dyck path $\in DP_2^8$ and link state $\in V_8^2$.

3.2.3 Conjectured degeneracies and selection rules

In this section, we state the conjecture of [46] and use the definitions of $A_{m,n}^M$ to translate it in terms of degeneracies in the spectrum of $\rho(\mathcal{H}_N(u))$. To each two-

column configuration corresponds a choice of ϵ_j and μ_j . The rules are the following :

- A white circle “○” corresponds to +1 and a blue circle “●” to a –1.
- The left column corresponds to ϵ excitations, and the right to μ excitations.
- As before, j grows from top to bottom.

Pearce and Rasmussen [46] give the following conjecture :

CONJECTURE 3.2.1 *In the sector with d defects, the set of choices of the ϵ_j s and μ_j s belonging to*

$$\text{N odd : } \bigcup_{p=0}^{\frac{N-d}{2}} A_{p, p+\frac{d-1}{2}}^{\frac{N-1}{2}}, \quad \text{N even : } \bigcup_{p=0}^{\frac{N-d}{2}} \left(A_{p, p+\frac{d-2}{2}}^{\frac{N-2}{2}} \cup A_{p, p+\frac{d}{2}}^{\frac{N-2}{2}} \right), \quad (3.2.8)$$

forms the spectra of $\rho(D_N(\mathbf{u}))$ and $\rho(\mathcal{H}_N)$.

Recall that when some indices of $A_{m,n}^M$ do not satisfy the constraint $0 \leq m \leq n \leq M$, the set $A_{m,n}^M$ is empty. In this sense, the case $d = 0$ is special, as the selection rule reduces to

$$\bigcup_{p=0}^{\frac{N-2}{2}} A_{p,p}^{\frac{N-2}{2}}. \quad (3.2.9)$$

DEFINITION 3.2.4 *The set of eigenvalues of $\rho(\mathcal{H}_N)$ in the sector with d defects, as given by the selection rules (3.2.8) and eqs (3.2.5) and (3.2.6), will be noted H_N^d . An eigenvalue λ will be said to belong to $A_{m,n}^M$ if it can be obtained by a choice of ϵ_j s and μ_j s represented by an element of $A_{m,n}^M$. For N even, we distinguish between $H_{N,0}^d$ and $H_{N,1}^d$, the sets of eigenvalues λ obtained from admissible two-column configurations in $\bigcup_{p=0}^{\frac{N-d}{2}} A_{p, p+\frac{d-2}{2}}^{\frac{N-2}{2}}$ and $\bigcup_{p=0}^{\frac{N-d}{2}} A_{p, p+\frac{d}{2}}^{\frac{N-2}{2}}$ respectively.*

In the following, the cases N odd and N even will often be treated separately. In preparation, we give the following two definitions.

DEFINITION 3.2.5 *Let $\delta = 0, 1$, we define the set Λ_δ^N of λ s given by*

$$\lambda = 2 \sum_{i=1}^m \eta_{k_i} \cos \frac{\pi k_i}{N}, \quad \text{where} \quad (3.2.10)$$

- $\eta_i = \pm 1$ for all i ;
- m may take all values satisfying both $0 \leq m \leq n$ and $n - m \equiv \delta \pmod{2}$;
- $k_i \in \mathbb{N}$, $1 \leq k_1 < k_2 < \dots < k_m \leq F(N)$ with $F(N) = \begin{cases} (N-1)/2, & \text{N odd,} \\ (N-2)/2, & \text{N even.} \end{cases}$

Let $\lambda \in \Lambda_8^n$. We also define

- K^+ : the set of ks in $\{k_1, \dots, k_m\}$ with $\eta_{k_i} = +1$,
- K^- : the set of ks in $\{k_1, \dots, k_m\}$ with $\eta_{k_i} = -1$,
- K^c : the set of ks in $\{1, \dots, F(N)\}$ that are neither in K^+ nor K^- .

To each $\lambda \in \Lambda_8^n$ we associate the smallest number m such that λ can be written as (3.2.10), ignoring accidental cancellations. For instance, with $N = 9$, $\lambda_1 = 0$ has $m = 0$ and $\lambda_2 = 2 \cos \pi/9 - 2 \cos 2\pi/9 - 2 \cos 4\pi/9$ has $m = 3$, even though λ_2 evaluates to 0. The accidental degeneracies like the one given previously will not be considered, as they are degeneracies of $\rho(\mathcal{H}_N)$, but not of $\rho(D_N(u))$.

3.2.4 N odd

PROPOSITION 3.2.2 *The two sets H_N^d and $\Lambda_0^{(N-d)/2}$ are equal.*

PROOF First, let $h \in H_N^d$. It is obvious that h can be written as (3.2.10), for a certain $0 \leq m \leq (N-1)/2$. Here are the rules : if at level j

- (a) there are two white circles, put k_j in K^+ ;
- (b) there are two blue circles, put k_j in K^- ;
- (c) there is one white and one blue circle, put k_j in K^c .

To prove that $h \in \Lambda_0^{(N-d)/2}$, one must show two things : that the top bound for m can be lowered from $(N-1)/2$ to $(N-d)/2$, and that $n - m = 0 \pmod{2}$. To do this, note first that if $h \in A_{p, p+(d-1)/2}^{(N-1)/2}$, the maximal number of elements in K^- and K^+ are p and $(N-d)/2 - p$ respectively (and these two events occur simultaneously). The maximal value of $m \equiv |K^+ \cup K^-|$ is $(N-d)/2$; it never goes beyond n . The values m takes make jumps of 2 and are $n, n-2, n-4, \dots, 0$: $n - m = 0 \pmod{2}$ as expected.

Second, let $\lambda \in \Lambda_0^n$ with m fixed. We show that $\lambda \in H_N^{N-2n}$. The rule is the following :

- (a) if $k_j \in K^+$, put two white circles at level j ;
- (b) if $k_j \in K^-$, put two blue circles at level j ;
- (c) if $k_j \in K^c$, put one circle of each color at level j .

One must then choose carefully the position of the pairs of colored circles in (c), to ensure that the two-column configuration is admissible and that it is in $A_{p, p+(d-1)/2}^{(N-1)/2}$ for some p . Among all k_j in K^c , one must put a_1 blue circles in the left column and a_2 in the right column, and impose that $a_1 + a_2 = |K^c| = (N-1)/2 - m$ and $a_2 - a_1 = (N-1)/2 - n$. This is always possible, with the choice $a_1 = (n-m)/2$ and $a_2 = (N-n-m-1)/2$ (note that a_1 and a_2 are integers). λ is then contained

in $\Lambda_{p,p+(d-1)/2}^{(N-1)/2}$ with $p = |K^-| + (n - m)/2$. \square

From the previous proof, all the eigenvalues of $\rho(\mathcal{H}_N)$ are in Λ_0^n , and we need not worry about values in Λ_1^n . For a given element of Λ_0^n , we can now calculate its degeneracy in $\rho(\mathcal{H}_N)$ in the sector with d defects, as given by the selection rules. The following statement is therefore equivalent to conjecture 3.2.1 for N odd (omitting accidental degeneracies) :

CONJECTURE 3.2.3 *Let $\lambda \in \Lambda_0^n$ with a fixed value of m (and $n - m \equiv 0 \pmod{2}$). Its degeneracy in $\rho(\mathcal{H}_N)$ in the sector with $N - 2n$ defects, as conjectured in [46], is*

$$\text{deg}_{\mathcal{H}}(\lambda) = \binom{\frac{N-1}{2} - m}{\frac{n-m}{2}} - \binom{\frac{N-1}{2} - m}{\frac{n-m-2}{2}}, \quad 0 \leq m \leq n. \quad (3.2.11)$$

PROOF In the second part of the previous proof, for every k_j in K^c , there was a freedom in the choice of admissible configurations. To count the degeneracies, one has to count these possible choices, as a pair of occupied and unoccupied sites at height j gives contribution 0 to eigenvalues of $\rho(\mathcal{H}_N)$, regardless of j . For a given two-column configuration, whether it is admissible does not depend on levels with two blue circles or two white circles. These can be removed. The configuration resulting from this operation is in the reduced set $\tilde{\Lambda}_{(n-m)/2, (N-1-n-m)/2}^{(N-1)/2-m}$ whose dimension, given by (3.2.7), is the desired result (3.2.11). \square

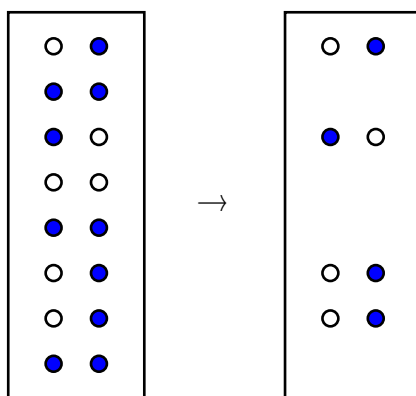


FIGURE 3.3 – A two-column admissible configuration in $\Lambda_{4,6}^8$ and its corresponding reduced configuration in $\tilde{\Lambda}_{1,3}^4$. It corresponds to the eigenvalue $-2 \cos \pi/17 - 2 \cos 4\pi/17 + 2 \cos 5\pi/17 - 2 \cos 7\pi/17$ of $\rho(\mathcal{H}_{N=17})$ and has degeneracy 3.

3.2.5 N even

The case N even is analogous to the case N odd, though the selection rule is more complicated.

PROPOSITION 3.2.4 *Let $\delta = 0, 1$. Then $H_{N,\delta}^d = \Lambda_\delta^{(N-d)/2}$.*

PROOF We start by showing that for $\delta = 0, 1$, $H_{N,\delta}^d \subset \Lambda_\delta^{(N-d)/2}$. The beginning of this proof is identical to that of proposition 3.2.2. The arguments for lowering the upper bound for m from $(N-2)/2$ to $(N-d)/2$ and for the parity of $n-m$ must be repeated. (Note that in the case $d=0$, it seems that this raises the upper bound, but since the selection rule is given in (3.2.9), this is not the case.) For $\delta=0$, K^- has at most p elements and K^+ , at most $(N-d)/2 - p$. Then, $m = |K^+ \cup K^-|$ is at most $n = (N-d)/2$ and m takes values $n, n-2, \dots$; this is the case $n-m \equiv 0 \pmod{2}$. For $\delta=1$, $\max m = \max |K^-| = p$, $\max |K^+| = (N-d)/2 - p - 1$, $\max(|K^+ \cup K^-|) = (N-d)/2 - 1 = n-1$, and $n-m \equiv 1 \pmod{2}$.

In the other direction, we show that $\Lambda_0^{(N-d)/2} \subset H_{N,0}^d$. The rules are those of proposition 3.2.2. The positions of the pairs in K^c is as follows :

- If $\lambda \in \Lambda_0^n$, the constraints are $a_1 + a_2 = (N-2)/2 - m$ and $a_2 - a_1 = (N-2)/2 - n$. Among the k_j s in K^c , we put $a_1 = (n-m)/2$ excitations in the left column and $a_2 = (N-n-m-2)/2$ in the right column.
- If $\lambda \in \Lambda_1^n$, the constraints are $a_1 + a_2 = (N-2)/2 - m$ and $a_2 - a_1 = N/2 - n$. Among the k_j s in K^c , we put $a_1 = (n-m-1)/2$ excitations in the left column and $a_2 = (N-n-m-1)/2$ in the right column.

□

For N even, the following is the translation of the conjecture 3.2.1 :

CONJECTURE 3.2.5 *The conjectured degeneracy of $\lambda \in \Lambda_\delta^n$, m fixed (and $n-m \equiv \delta \pmod{2}$), in the sector $d = N - 2n$, is given by*

$$\delta = 0 : \quad \text{deg}_{\mathcal{H}}(\lambda) = \binom{\frac{N-2}{2} - m}{\frac{n-m}{2}} - \binom{\frac{N-2}{2} - m}{\frac{n-m-2}{2}}, \quad 0 \leq m \leq n, \quad (3.2.12)$$

$$\delta = 1 : \quad \text{deg}_{\mathcal{H}}(\lambda) = \binom{\frac{N-2}{2} - m}{\frac{n-m-1}{2}} - \binom{\frac{N-2}{2} - m}{\frac{n-m-3}{2}}, \quad 0 \leq m \leq n-1. \quad (3.2.13)$$

The proof is identical to that of 3.2.3 and left to the reader. One can also verify that these formulae are valid for $d=0$ and that $\text{deg}_{\mathcal{H}}(\lambda) = 0$ for $\delta=0$, as expected. The

results of the conjectures 3.2.3 and 3.2.5 are statements equivalent to (3.2.8) : they provide a conjecture for degeneracies of eigenvalues of $\rho(\mathcal{H}_N)$ in the sector with $d = N - 2n$ defects (in fact, the statement is not as strong because of the accidental degeneracies due to exceptional trigonometric identities, but these will be ignored). To prove the selection rules, we will show that degeneracies of $\rho(\mathcal{H}_N)$ are indeed given by eqs (3.2.11), (3.2.12) and (3.2.13).

3.3 The XXZ Hamiltonian

On the finite (non-periodic) lattice, the well-studied [35] XXZ Hamiltonian for spin- $\frac{1}{2}$ particles is

$$H_{\text{XXZ}}^q = \frac{1}{2} \left(\sum_{j=1}^{N-1} (\sigma_j^x \sigma_{j+1}^x + \sigma_j^y \sigma_{j+1}^y + \frac{q + q^{-1}}{2} \sigma_j^z \sigma_{j+1}^z) - \frac{q - q^{-1}}{2} (\sigma_1^z - \sigma_N^z) \right), \quad (3.3.1)$$

where

$$\sigma_j^a = \underbrace{\text{id}_2 \otimes \text{id}_2 \otimes \cdots \otimes \text{id}_2}_{j-1} \otimes \sigma^a \otimes \underbrace{\text{id}_2 \otimes \text{id}_2 \otimes \cdots \otimes \text{id}_2}_{N-j}.$$

This Hamiltonian acts on $(\mathbb{C}^2)^{\otimes N}$ and can also be written as

$$H_{\text{XXZ}}^q = \sum_{j=1}^{N-1} \left(\frac{q + q^{-1}}{4} I + e_j \right), \quad \text{where}$$

$$\begin{aligned} e_j &= \frac{1}{2} \left(\sigma_j^x \sigma_{j+1}^x + \sigma_j^y \sigma_{j+1}^y + \frac{q + q^{-1}}{2} (\sigma_j^z \sigma_{j+1}^z - \text{id}) - \frac{q - q^{-1}}{2} (\sigma_j^z - \sigma_{j+1}^z) \right) \\ &= \underbrace{\text{id}_2 \otimes \text{id}_2 \otimes \cdots \otimes \text{id}_2}_{j-1} \otimes \tilde{e} \otimes \underbrace{\text{id}_2 \otimes \text{id}_2 \otimes \cdots \otimes \text{id}_2}_{N-j-1} \end{aligned} \quad (3.3.2)$$

$$\text{and} \quad \tilde{e} = \begin{pmatrix} 0 & 0 & 0 & 0 \\ 0 & -q & 1 & 0 \\ 0 & 1 & -q^{-1} & 0 \\ 0 & 0 & 0 & 0 \end{pmatrix}. \quad (3.3.3)$$

The matrices e_j s form a representation of $\mathbb{T}L_N(\beta)$ with $\beta = -(q + q^{-1})$. We will be interested in diagonalizing this Hamiltonian when $q = i$. More precisely, we will show that $H_{\text{XXZ}}^{q=i}$ can be diagonalized when N is odd, but not when N is even, in which case we shall give its Jordan form. We start with

$$H \equiv H_{\text{XXZ}}^{q=i} = \frac{1}{2} \left(\sum_{j=1}^{N-1} (\sigma_j^x \sigma_{j+1}^x + \sigma_j^y \sigma_{j+1}^y) - i (\sigma_1^z - \sigma_N^z) \right).$$

3.3.1 Free fermions

Ideas in this section are similar to those found in [81], [82] and [83]. The Hamiltonian H can be transformed by writing σ_j^x , σ_j^y and σ_j^z in terms of $\sigma_j^\pm = (\sigma_j^x \pm i\sigma_j^y)/2$:

$$H = \sum_{j=1}^{N-1} (\sigma_j^+ \sigma_{j+1}^- + \sigma_j^- \sigma_{j+1}^+) - i(\sigma_1^+ \sigma_1^- - \sigma_N^+ \sigma_N^-).$$

We perform the celebrated Jordan-Wigner transformation by passing to creation and annihilation operators c_j and c_j^\dagger ,

$$\begin{aligned} c_j &= \left(\prod_{k=1}^{j-1} (-\sigma_k^z) \right) \sigma_j^-, & \sigma_j^- &= \left(\prod_{k=1}^{j-1} (-\sigma_k^z) \right) c_j, \\ c_j^\dagger &= \left(\prod_{k=1}^{j-1} (-\sigma_k^z) \right) \sigma_j^+, & \sigma_j^+ &= \left(\prod_{k=1}^{j-1} (-\sigma_k^z) \right) c_j^\dagger, \end{aligned}$$

which satisfy the usual anti-commutation relations for fermions,

$$\{c_j^\dagger, c_{j'}\} = \delta_{j,j'}, \quad \{c_j, c_{j'}\} = \{c_j^\dagger, c_{j'}^\dagger\} = 0.$$

The c_j and c_j^\dagger are real matrices and are indeed conjugate to one another. With this transformation,

$$H = \sum_{j=1}^{N-1} (c_j^\dagger c_{j+1} + c_{j+1}^\dagger c_j) - i(c_1^\dagger c_1 - c_N^\dagger c_N),$$

which can also be written as

$$H = \sum_{k_1, k_2} c_{k_1}^\dagger c_{k_2} \mathcal{N}_{k_1, k_2}, \quad (3.3.4)$$

where

$$\mathcal{N} = \begin{pmatrix} -i & 1 & 0 & 0 & \dots & 0 & 0 & 0 \\ 1 & 0 & 1 & 0 & \dots & 0 & 0 & 0 \\ 0 & 1 & 0 & 1 & \dots & 0 & 0 & 0 \\ 0 & 0 & 1 & 0 & \dots & 0 & 0 & 0 \\ \vdots & \vdots & \vdots & \vdots & \ddots & \vdots & \vdots & \vdots \\ 0 & 0 & 0 & 0 & \dots & 0 & 1 & 0 \\ 0 & 0 & 0 & 0 & \dots & 1 & 0 & 1 \\ 0 & 0 & 0 & 0 & \dots & 0 & 1 & i \end{pmatrix}$$

is a symmetric matrix (but not a hermitian matrix) of size N . We want to perform a Bogoliubov transformation

$$b_n = \sum_j f_n^j c_j^\dagger, \quad a_n = \sum_j g_n^j c_j, \quad (3.3.5)$$

that will make H as simple as possible in terms of these new operators. We also require that the a_n s and b_n s satisfy the fermionic anticommutation relations

$$\{b_n, a_{n'}\} = \delta_{n,n'}, \quad \{b_n, b_{n'}\} = \{a_n, a_{n'}\} = 0. \quad (3.3.6)$$

To this intent, we want to diagonalize \mathcal{N} . Define the matrix \mathcal{K}_L , of dimensions $L \times L$

$$\mathcal{K}_L = \begin{pmatrix} 0 & 1 & 0 & 0 & \dots & 0 & 0 & 0 \\ 1 & 0 & 1 & 0 & \dots & 0 & 0 & 0 \\ 0 & 1 & 0 & 1 & \dots & 0 & 0 & 0 \\ 0 & 0 & 1 & 0 & \dots & 0 & 0 & 0 \\ \vdots & \vdots & \vdots & \vdots & \ddots & \vdots & \vdots & \vdots \\ 0 & 0 & 0 & 0 & \dots & 0 & 1 & 0 \\ 0 & 0 & 0 & 0 & \dots & 1 & 0 & 1 \\ 0 & 0 & 0 & 0 & \dots & 0 & 1 & 0 \end{pmatrix}.$$

Also, let $\tilde{\mathcal{N}} = \mathcal{N} - \xi \text{id}_N$ and $\tilde{\mathcal{K}}_L = \mathcal{K}_L - \xi \text{id}_L$. The eigenvalues of \mathcal{N} are ξ s for which $\det(\tilde{\mathcal{N}}) = 0$. Summing over the first and last line, we find

$$\det(\tilde{\mathcal{N}}) = (\xi^2 + 1) \det(\tilde{\mathcal{K}}_{N-2}) + 2\xi \det(\tilde{\mathcal{K}}_{N-3}) + \det(\tilde{\mathcal{K}}_{N-4})$$

and, similarly,

$$\det(\tilde{\mathcal{K}}_L) = -\xi \det(\tilde{\mathcal{K}}_{L-1}) - \det(\tilde{\mathcal{K}}_{L-2})$$

with initial conditions $\det(\tilde{\mathcal{K}}_1) = -\xi$ and $\det(\tilde{\mathcal{K}}_2) = \xi^2 - 1$ (or, more simply, $\det(\tilde{\mathcal{K}}_0) = 1$). These are Chebyshev polynomials of the second type, with recursion relations

$$U_{k+1}(x) = 2xU_k(x) - U_{k-1}(x)$$

and initial conditions $U_0 = 1$ and $U_1(x) = 2x$. They can be written in a simple closed form :

$$U_k(\cos v) = \frac{\sin(k+1)v}{\sin v}.$$

With $\xi = -2 \cos v$, one finds $\det(\tilde{\mathcal{K}}_L) = \sin(L+1)v / \sin v$ and

$$\begin{aligned} \det(\tilde{\mathcal{N}}) &= \frac{(4 \cos^2 v + 1) \sin(N-1)v}{\sin v} - \frac{4 \cos v \sin(N-2)v}{\sin v} + \frac{\sin(N-3)v}{\sin v} \\ &= \frac{2 \cos v \sin Nv}{\sin v}. \end{aligned} \quad (3.3.7)$$

Eigenvalues of \mathcal{N} satisfy one of the two conditions :

- $\sin Nv / \sin v = 0$. Solutions for ξ are $\xi_n = 2 \cos \pi n / N$ with $n = 1, \dots, N-1$. (The minus sign has disappeared because we changed $n \leftrightarrow N-n$.) The values $n = 0$ and $n = N$ are absent because of the $\sin v$ in the denominator of (3.3.7).

– $\cos v = 0$, with solution $\xi_{N/2} = 0$ (even when N is not even).

When N is odd, $v_n = \pi n/N$ is never $\pi/2$. All eigenvalues are distinct and \mathcal{N} is diagonalizable. When N is even however, the eigenvalue $\xi = 0$ appears twice.

For a fixed value of n in the interval $1, \dots, N-1$, we now look for $u_n = (u_n^1, \dots, u_n^N)$, the eigenvector of \mathcal{N} with eigenvalue ξ_n . Its components satisfy the constraints

$$\begin{aligned} (-i - \xi_n)u_n^1 + u_n^2 &= 0, \\ u_n^j - \xi_n u_n^{j+1} + u_n^{j+2} &= 0, \quad \text{for } j = 1, \dots, N-2, \\ u_n^{N-1} + (i - \xi_n)u_n^N &= 0. \end{aligned}$$

Let x_n be such that $\xi_n = x_n + x_n^{-1}$ (and $x_n = e^{i\pi n/N}$). One can easily verify that the ansatz

$$u_n^j = K_n(\alpha_n x_n^j + \gamma_n x_n^{-j}) \quad \text{with} \quad \alpha_n = -(1 + ix_n^{-1}) \quad \text{and} \quad \gamma_n = 1 + ix_n \quad (3.3.8)$$

satisfies all three constraints. For reasons that will be soon clear, when $n \neq N/2$, we fix the constant K_n to $(2\alpha_n \gamma_n N)^{-1/2}$ ensuring that $u_n^\top u_n = 1$. Indeed,

$$\begin{aligned} u_n^\top u_n &= \sum_{j=1}^N (u_n^j)^2 = \frac{1}{2\alpha_n \gamma_n N} \sum_{j=1}^N (\alpha_n x_n^j + \gamma_n x_n^{-j})^2 \\ &= 1 + \frac{\alpha_n^2}{2\alpha_n \gamma_n N} \frac{x_n^2(1 - x_n^{2N})}{1 - x_n^2} + \frac{\gamma_n^2}{2\alpha_n \gamma_n N} \frac{x_n^{-2}(1 - x_n^{-2N})}{1 - x_n^{-2}} = 1, \end{aligned}$$

because $x_n^{\pm 2N} = 1$. Notice that we have

$$\alpha_n \gamma_n = -i(x_n + x_n^{-1}) = -i\xi_n.$$

For the states with $\xi = 0$, the cases N odd and N have to be treated separately.

3.3.2 N odd

For the eigenvector with $\xi = 0$, the ansatz (3.3.8) still works with $x = i$. Then, $\gamma_n = 0$, $\alpha_n = -2$ and we can write $u_{N/2}^j = K'_{N/2} i^j$.

$$u_{N/2}^\top u_{N/2} = (K'_{N/2})^2 \sum_{j=1}^N (-1)^j = -(K'_{N/2})^2$$

and $K'_{N/2} = i$ is the correct choice. When N is odd, \mathcal{N} is diagonalizable and from (3.3.5), H can be written as $H = \sum_{k=0}^{N-1} \Lambda_k b_k a_k$, and

$$[H, a_m] = \sum_{k=0}^{N-1} \Lambda_k [b_k a_k, a_m] = -\Lambda_m a_m, \quad \{c_i^\dagger, [H, a_m]\} = -\Lambda_m \sum_j g_m^j \{c_i^\dagger, c_j\} = -\Lambda_m g_m^i,$$

but because of (3.3.4), we also have

$$[\mathbf{H}, \mathbf{a}_m] = \sum_{k_1, k_2} \sum_j \mathcal{N}_{k_1, k_2} g_m^j [c_{k_1}^\dagger c_{k_2}, c_j] = - \sum_{k_1, k_2} \mathcal{N}_{k_1, k_2} g_m^{k_1} c_{k_2},$$

$$\{c_i^\dagger, [\mathbf{H}, \mathbf{a}_m]\} = - \sum_{k_1, k_2} \mathcal{N}_{k_1, k_2} g_m^{k_1} \{c_i, c_{k_2}\} = - \sum_{k_1} \mathcal{N}_{i, k_1} g_m^{k_1},$$

where we used $\mathcal{N}_{i, j} = \mathcal{N}_{j, i}$. We can write

$$\mathcal{N} \vec{g}_m = \Lambda_m \vec{g}_m, \quad \text{where} \quad \vec{g}_m = \begin{pmatrix} g_m^1 \\ g_m^2 \\ \vdots \\ g_m^N \end{pmatrix}. \quad (3.3.9)$$

The g_m^j s are the components of the eigenvectors of \mathcal{N} and the Λ_m s, its eigenvalues. The same process can be carried out for the \mathbf{b}_m s, yielding

$$\mathcal{N} \vec{f}_m = \Lambda_m \vec{f}_m, \quad \text{where} \quad \vec{f}_m = \begin{pmatrix} f_m^1 \\ f_m^2 \\ \vdots \\ f_m^N \end{pmatrix}. \quad (3.3.10)$$

The labeling of the \mathbf{a} s and \mathbf{b} s is as follows.

- For $n = 1, \dots, N-1$, we choose $\Lambda_n = \xi_n$ and $f_n^j = g_n^j = u_n^j$. This gives

$$\mathbf{a}_n = K_n \sum_{j=1}^N (\alpha_n x_n^j + \gamma_n x_n^{-j}) c_j, \quad \mathbf{b}_n = K_n \sum_{j=1}^N (\alpha_n x_n^j + \gamma_n x_n^{-j}) c_j^\dagger, \quad (3.3.11)$$

with K_n , α_n and γ_n given previously.

- For the eigenvector with eigenvalue zero, $\Lambda_0 = \xi_{N/2} = 0$, $f_0^j = g_0^j = u_{N/2}^j = i^{j+1}$, and

$$\mathbf{a}_0 = \sum_{j=1}^N i^{j+1} c_j, \quad \mathbf{b}_0 = \sum_{j=1}^N i^{j+1} c_j^\dagger. \quad (3.3.12)$$

Because f_k^j has a non zero imaginary part and $f_k^j = g_{k'}^j$, $\mathbf{b}_n \neq \mathbf{a}_n^\dagger$. Instead, $c_j^\dagger = c_j^\top$ gives $\mathbf{b}_n = \mathbf{a}_n^\top$. In terms of f_k^j and $g_{k'}^j$, the constraint given by the anticommutation relation is

$$\delta_{n, n'} = \{\mathbf{b}_n, \mathbf{a}_{n'}\} = \sum_{j, j'} g_n^j g_{n'}^{j'} \{c_j^\dagger, c_{j'}\} = \sum_j g_n^j g_{n'}^j = \vec{g}_n^\top \vec{g}_{n'}.$$

When $n \neq n'$, this is trivial, because

$$0 = \vec{g}_n^\top (\mathcal{N} - \mathcal{N}^\top) \vec{g}_{n'} = \vec{g}_n^\top \vec{g}_{n'} (\xi_{n'} - \xi_n) \quad \text{and} \quad \xi_n \neq \xi_{n'}.$$

However when $n = n'$, $\vec{g}_n^T \vec{g}_n = 1$ explains our previous choice for the K_n s. Finally, one finds that H can be written as $H = 2 \sum_{k=1}^{N-1} \cos(\pi k/N) b_k a_k$. If we denote by $|0\rangle$ the state $|\uparrow\uparrow \dots \uparrow\rangle$ with all spins up, then eigenvectors of H in the sector $S^z = N/2 - n$ are

$$|\gamma\rangle = a_{k_1} a_{k_2} \dots a_{k_n} |0\rangle, \quad (3.3.13)$$

where the k_1, \dots, k_n are in the interval $0, \dots, N-1$ and appear at most once. When the a_0 excitation is present, we decide to set it at the end, $k_n = 0$. With this convention, the eigenvalue of $|\gamma\rangle$ is

$$\gamma = \begin{cases} 2 \sum_{i=1}^n \cos(\pi k_i/N), & \text{if } k_n \neq 0, \\ 2 \sum_{i=1}^{n-1} \cos(\pi k_i/N), & \text{if } k_n = 0. \end{cases}$$

3.3.3 N even

For N even, the eigenvalue 0 appears twice and \mathcal{N} is not diagonalizable. To show this, we study \mathcal{N}^2 :

$$\mathcal{N}^2 = \begin{pmatrix} 0 & -i & 1 & 0 & 0 & 0 & \dots & 0 & 0 & 0 & 0 & 0 & 0 \\ -i & 2 & 0 & 1 & 0 & 0 & \dots & 0 & 0 & 0 & 0 & 0 & 0 \\ 1 & 0 & 2 & 0 & 1 & 0 & \dots & 0 & 0 & 0 & 0 & 0 & 0 \\ 0 & 1 & 0 & 2 & 0 & 1 & \dots & 0 & 0 & 0 & 0 & 0 & 0 \\ 0 & 0 & 1 & 0 & 2 & 0 & \dots & 0 & 0 & 0 & 0 & 0 & 0 \\ 0 & 0 & 0 & 1 & 0 & 2 & \dots & 0 & 0 & 0 & 0 & 0 & 0 \\ \vdots & \vdots & \vdots & \vdots & \vdots & \vdots & \ddots & \vdots & \vdots & \vdots & \vdots & \vdots & \vdots \\ 0 & 0 & 0 & 0 & 0 & 0 & \dots & 2 & 0 & 1 & 0 & 0 & 0 \\ 0 & 0 & 0 & 0 & 0 & 0 & \dots & 0 & 2 & 0 & 1 & 0 & 0 \\ 0 & 0 & 0 & 0 & 0 & 0 & \dots & 1 & 0 & 2 & 0 & 1 & 0 \\ 0 & 0 & 0 & 0 & 0 & 0 & \dots & 0 & 1 & 0 & 2 & 0 & 1 \\ 0 & 0 & 0 & 0 & 0 & 0 & \dots & 0 & 0 & 1 & 0 & 2 & i \\ 0 & 0 & 0 & 0 & 0 & 0 & \dots & 0 & 0 & 0 & 1 & i & 0 \end{pmatrix}$$

and check that

$$w_1^j = i^j \left\lfloor \frac{N-j-1}{2} \right\rfloor \quad \text{and} \quad w_2^j = i^j \left\lfloor \frac{N-j+1}{2} \right\rfloor$$

are two independent eigenvectors of \mathcal{N}^2 with eigenvalue 0. The eigenvector $u_{N/2}^j = K'_{N/2} i^j$ of \mathcal{N} is given by the linear combination $w_2^j - w_1^j = i^j$ (though the constant $K'_{N/2}$ will be different from the N odd constant). Also,

$$(\mathcal{N}w_1)^j = i^{j-1}, \quad (\mathcal{N}w_2)^j = i^{j-1}, \quad (3.3.14)$$

and any linear combination $w = \beta_1 w_1 + \beta_2 w_2$ satisfies $\mathcal{N}w \propto u_{N/2}$; \mathcal{N} is therefore not diagonalizable. Nevertheless, it is possible to write H in the following manner :

$$H = b_0 a_{-1} + \sum_{\substack{n=1 \\ n \neq N/2}}^{N-1} \Lambda_n b_n a_n \quad (3.3.15)$$

where all the a s and b s obey (3.3.6). The identification for N even is slightly modified :

- For the $N - 2$ eigenvectors with $\xi \neq 0$, (3.3.9) and (3.3.10) stay valid and the same identification is made : $\Lambda_n = \xi_n = 2 \cos \pi n/N$ and $f_n^j = g_n^j = u_n^j$ (for $n = 1, 2, \dots, N - 1$, except $n = N/2$). The operators a and b are then given by the solution (3.3.11).
- For the two remaining modes, a new feature appears :

$$\begin{aligned} 0 = -[H, a_{-1}] &= \sum_{k_1, k_2} g_{-1}^{k_1} \mathcal{N}_{k_1, k_2} c_{k_2} \rightarrow \mathcal{N} \vec{g}_{-1} = 0, \\ a_{-1} = -[H, a_0] &= \sum_{k_1, k_2} g_0^{k_1} \mathcal{N}_{k_1, k_2} c_{k_2} \rightarrow \mathcal{N} \vec{g}_0 = \vec{g}_{-1}, \\ 0 = [H, b_0] &= \sum_{k_1, k_2} f_0^{k_1} \mathcal{N}_{k_1, k_2} c_{k_2} \rightarrow \mathcal{N} \vec{f}_0 = 0, \\ b_0 = [H, b_{-1}] &= \sum_{k_1, k_2} f_{-1}^{k_1} \mathcal{N}_{k_1, k_2} c_{k_2} \rightarrow \mathcal{N} \vec{f}_{-1} = \vec{f}_0, \end{aligned}$$

where the equations on the right are obtained by anti-commuting the equations on the left with c_i and writing the result as matrix products. The result is $f_0^j = g_{-1}^j = u_{N/2}^j = K'_{N/2} i^j$ and $f_{-1}^j = g_0^j = w^j = \beta_1 w_1^j + \beta_2 w_2^j$, where $K'_{N/2}$, β_1 and β_2 are constants that remain to be fixed. The relation $\mathcal{N}w = u_{N/2}$, along with the commutation relations (3.3.6), fixes these constants (this is done in appendix 3.A). The final result is

$$\begin{aligned} a_0 &= \sum_{j=1}^N (\beta_1 w_1^j + \beta_2 w_2^j) c_j, & b_0 &= K'_{N/2} \sum_{j=1}^N i^j c_j^\dagger, \\ a_{-1} &= K'_{N/2} \sum_{j=1}^N i^j c_j, & b_{-1} &= \sum_{j=1}^N (\beta_1 w_1^j + \beta_2 w_2^j) c_j^\dagger, \end{aligned} \quad (3.3.16)$$

with $K'_{N/2} = (2i/N)^{1/2}$, $\beta_1 = \frac{-1}{2K'_{N/2}}$ and $\beta_2 = -\frac{N-4}{N} \beta_1$. The new feature here is the pairing $a_0^\dagger = b_{-1}$ and $a_{-1}^\dagger = b_0$.

Finally, the canonical expression for the Hamiltonian is

$$H = b_0 a_{-1} + 2 \sum_{\substack{k=1 \\ k \neq N/2}}^{N-1} \cos(\pi k/N) b_k a_k.$$

In the sector $S^z = N/2 - n$, the states $|\gamma\rangle$ given in eq. (3.3.13) are tied to the eigenvalues

$$\gamma = \begin{cases} 2 \sum_{i=1}^n \cos(\pi k_i/N), & \text{if } a_0 \text{ and } a_{-1} \text{ are absent,} \\ 2 \sum_{i=1}^{n-1} \cos(\pi k_i/N), & \text{if only one of } a_0 \text{ or } a_{-1} \text{ is present,} \\ 2 \sum_{i=1}^{n-2} \cos(\pi k_i/N), & \text{if both } a_0 \text{ and } a_{-1} \text{ are present.} \end{cases}$$

All the k_i s are in the set $\{-1, 0, \dots, N-1\} \setminus \{N/2\}$ and, as in the N odd case, the a_0 and a_{-1} are always set to the last k_i s when present. Not all the states $|\gamma\rangle$ are eigenstates of H . The generalized eigenvectors are those with the a_0 excitation, but not a_{-1} . In total, there are 2^{N-2} such states, while all others are eigenvectors.

3.4 The algebra $U_q(\mathfrak{sl}_2)$

The algebra $U_q(\mathfrak{sl}_2)$ is generated by the three generators q^{S^z} , S^+ and S^- that satisfy the relations

$$q^{S^z} S^\pm q^{-S^z} = q^{\pm 1} S^\pm \quad \text{and} \quad [S^+, S^-] = \frac{q^{2S^z} - q^{-2S^z}}{q - q^{-1}}.$$

PROPOSITION 3.4.1 *The representation*

$$\begin{aligned} q^{S^z} &= q^{\sigma^z/2} \otimes q^{\sigma^z/2} \otimes \dots \otimes q^{\sigma^z/2} = \prod_{j=1}^N q^{\sigma_j^z/2}, \\ S^z &= \sum_{j=1}^N \sigma_j^z/2, \\ S^\pm &= \sum_{j=1}^N S_j^\pm = \sum_{j=1}^N q^{-\sigma^z/2} \otimes \dots \otimes q^{-\sigma^z/2} \otimes \sigma^\pm \otimes q^{\sigma^z/2} \otimes \dots \otimes q^{\sigma^z/2} \\ &= \sum_{j=1}^N \left(\prod_{k=1}^{j-1} q^{-\sigma_k^z/2} \right) \sigma_j^\pm \left(\prod_{k'=j+1}^N q^{\sigma_{k'}^z/2} \right) \end{aligned}$$

of $U_q(\mathfrak{sl}_2)$ commutes with the e_i matrices given in (3.3.2).

PROOF The commutation of q^{S^z} , S^+ and S^- with e_i arises from the relations

$$[\tilde{e}, q^{\sigma^z/2} \otimes q^{\sigma^z/2}] = 0 \quad \text{and} \quad [\tilde{e}, q^{-\sigma^z/2} \otimes \sigma^\pm + \sigma^\pm \otimes q^{\sigma^z/2}] = 0,$$

where \tilde{e} is the 4×4 matrix given in (3.3.3). \square

This property, first noticed in [35], will be used thoroughly. Note also that $S^- = (S^+)^T$. Some particularities occur when $q^{2P} = 1$. Let q_c be a $2P$ -th root of unity. Then

$(S^\pm)^P|_{q=q_c} = 0$. For these values q_c , the generators $(S^\pm)^P$ can be replaced by ([84], [35]):

$$S^{\pm(P)} \equiv \lim_{q \rightarrow q_c} \frac{(S^\pm)^P}{[P]_q!}, \quad \text{where} \quad [n]_q! = \prod_{k=1}^n [n]_q \quad \text{and} \quad [n]_q = \frac{q^n - q^{-n}}{q - q^{-1}}.$$

For $q = q_c$ a root of unity, $S^{\pm(P)}$ is non zero and commutes with e_i , because

$$[S^{\pm(P)}, e_i] = \lim_{q \rightarrow q_c} \frac{[(S^\pm)^P, e_i]}{[P]_q} = \lim_{q \rightarrow q_c} \frac{0}{[P]_q} = 0.$$

We are interested in the case $q_c = i$, $P = 2$, and calculate $S^{\pm(2)}$. The square of S^\pm is

$$(S^\pm)^2 = \sum_{j_1, j_2} S_{j_1}^\pm S_{j_2}^\pm = \left(\sum_{j_1 < j_2} + \sum_{j_2 < j_1} \right) S_{j_1}^\pm S_{j_2}^\pm = \sum_{j_1 < j_2} (S_{j_1}^\pm S_{j_2}^\pm + S_{j_2}^\pm S_{j_1}^\pm).$$

When $j_1 < j_2$,

$$\begin{aligned} S_{j_1}^\pm S_{j_2}^\pm &= \left(\prod_{k_1=1}^{j_1-1} q^{-\sigma_{k_1}^\pm} \right) \sigma_{j_1}^\pm q^{-\sigma_{j_1}^\pm/2} q^{\sigma_{j_2}^\pm/2} \sigma_{j_2}^\pm \left(\prod_{k_2=j_2+1}^N q^{\sigma_{k_2}^\pm} \right) \\ &= q^{\pm 1} \left(\prod_{k_1=1}^{j_1-1} q^{-\sigma_{k_1}^\pm} \right) \sigma_{j_1}^\pm \sigma_{j_2}^\pm \left(\prod_{k_2=j_2+1}^N q^{\sigma_{k_2}^\pm} \right), \end{aligned}$$

but

$$S_{j_2}^\pm S_{j_1}^\pm = q^{\mp 1} \left(\prod_{k_1=1}^{j_1-1} q^{-\sigma_{k_1}^\pm} \right) \sigma_{j_1}^\pm \sigma_{j_2}^\pm \left(\prod_{k_2=j_2+1}^N q^{\sigma_{k_2}^\pm} \right)$$

and finally,

$$\frac{(S^\pm)^2}{[2]_q} = \sum_{j_1 < j_2} \underbrace{\left(\prod_{k_1=1}^{j_1-1} q^{-\sigma_{k_1}^\pm} \right) \sigma_{j_1}^\pm \sigma_{j_2}^\pm \left(\prod_{k_2=j_2+1}^N q^{\sigma_{k_2}^\pm} \right)}_{S_{j_1, j_2}^{\pm(2)}(q)}.$$

3.4.1 S^\pm and $S^{\pm(2)}$ for free fermions

The next step is to write S^\pm and $S^{\pm(2)}$ first in terms of operators c_j and c_j^\dagger , and then of the a_{nS} and b_{nS} calculated in section 3.3 (Deguchi *et al.* did this for the

periodic case [82]). We start with S^+ and S^- ,

$$\begin{aligned}
S^\pm &= \left(\prod_{k=1}^N q^{\sigma_k^z/2} \right) \sum_{j=1}^N \left(\prod_{k=1}^{j-1} q^{-\sigma_k^z} \right) q^{-\sigma_j^z/2} \sigma_j^\pm \\
&= q^{S^z} q^{\mp 1/2} \sum_{j=1}^N \left(\prod_{k=1}^{j-1} q^{-\sigma_k^z} \right) \sigma_j^\pm \\
&= i^{S^z \mp 1/2} \sum_{j=1}^N \left(\prod_{k=1}^{j-1} -i \sigma_k^z \right) \sigma_j^\pm \\
&= i^{S^z \mp 1/2 - 1} \sum_{j=1}^N i^j \left(\prod_{k=1}^{j-1} -\sigma_k^z \right) \sigma_j^\pm
\end{aligned}$$

and this yields

$$S^+ = i^{S^z - 3/2} \sum_{j=1}^N i^j c_j^\dagger = \frac{i^{S^z - 3/2}}{K'_{N/2}} \sum_{j=1}^N u_{N/2}^j c_j^\dagger, \quad S^- = i^{S^z - 1/2} \sum_{j=1}^N i^j c_j = \frac{i^{S^z - 1/2}}{K'_{N/2}} \sum_{j=1}^N u_{N/2}^j c_j. \quad (3.4.1)$$

We can repeat the computation for $S^{+(2)}$ and $S^{-(2)}$:

$$S^{+(2)} = i^{-1} (-1)^{S^z} \sum_{j_1 < j_2} i^{j_1 + j_2} c_{j_1}^\dagger c_{j_2}^\dagger, \quad S^{-(2)} = -i^{-1} (-1)^{S^z} \sum_{j_1 < j_2} i^{j_1 + j_2} c_{j_1} c_{j_2}.$$

Though it is less apparent than before, both $S^- = (S^+)^T$ and $S^{-(2)} = (S^{+(2)})^T$ still hold. Our ultimate goal is to write $S^{+(2)}$ and $S^{-(2)}$ as

$$S^{+(2)} = \sum_{k_1, k_2} A(k_1, k_2) b_{k_1} b_{k_2}, \quad S^{-(2)} = - \sum_{k_1, k_2} A(k_1, k_2) b_{k_1}^T b_{k_2}^T,$$

where $A(k_1, k_2) = -A(k_2, k_1)$. To do this calculation, we need to find the inverse formula

$$c_j^\dagger = \sum_k d_j^k b_k, \quad c_j = \sum_k e_j^k a_k.$$

To do so, we calculate $\{c_j^\dagger, a_k\}$ and $\{c_j, b_k\}$ in the two possible ways, to find $d_j^k = e_j^k = g_k^j$. This allows us to pursue the computation,

$$\begin{aligned}
S^{+(2)} &= \frac{i^{-1} (-1)^{S^z}}{2} \sum_{j_1 < j_2} i^{j_1 + j_2} (c_{j_1}^\dagger c_{j_2}^\dagger - c_{j_2}^\dagger c_{j_1}^\dagger) \\
&= \frac{i^{-1} (-1)^{S^z}}{2} \sum_{k_1, k_2} b_{k_1} b_{k_2} \underbrace{\left(\sum_{j_1 < j_2} i^{j_1 + j_2} (g_{k_1}^{j_1} g_{k_2}^{j_2} - g_{k_1}^{j_2} g_{k_2}^{j_1}) \right)}_{B(k_1, k_2)}
\end{aligned}$$

and $B(k_1, k_2)$ can be calculated directly. For any k_1, k_2 with $\xi \neq 0$,

$$\begin{aligned} B(k_1, k_2) &= K_{k_1} K_{k_2} \sum_{j_1 < j_2} i^{j_1 + j_2} \left(\alpha_{k_1} \alpha_{k_2} (x_{k_1}^{j_1} x_{k_2}^{j_2} - x_{k_1}^{j_2} x_{k_2}^{j_1}) + \gamma_{k_1} \gamma_{k_2} (x_{k_1}^{-j_1} x_{k_2}^{-j_2} - x_{k_1}^{-j_2} x_{k_2}^{-j_1}) \right. \\ &\quad \left. + \alpha_{k_1} \gamma_{k_2} (x_{k_1}^{j_1} x_{k_2}^{-j_2} - x_{k_1}^{j_2} x_{k_2}^{-j_1}) + \alpha_{k_2} \gamma_{k_1} (x_{k_1}^{-j_1} x_{k_2}^{j_2} - x_{k_1}^{-j_2} x_{k_2}^{j_1}) \right) \\ &= K_{k_1} K_{k_2} (g(x_{k_1}, x_{k_2}) + g(x_{k_1}^{-1}, x_{k_2}^{-1}) - g(x_{k_1}, x_{k_2}^{-1}) - g(x_{k_1}^{-1}, x_{k_2})) \end{aligned}$$

where $g(z, w) = (f(z, w) - f(w, z))(1 + iz^{-1})(1 + iw^{-1})$ and $f(z, w) = \sum_{j_1 < j_2} (iz)^{j_1} (iw)^{j_2}$. After simplification, one finds

$$g(z, w) = ((iz)^N - (iw)^N) + \frac{(iw - iz)(1 - (-zw)^N)}{1 + zw}$$

and

$$\begin{aligned} B(k_1, k_2) &= \frac{i(-1)^N K_{k_1} K_{k_2}}{(x_{k_2} + x_{k_1})(1 + x_{k_2} x_{k_1})(x_{k_2} x_{k_1})^N} \\ &\quad \times ((x_{k_1}^{2N} - x_{k_2}^{2N})(1 - x_{k_1}^2 x_{k_2}^2) + (1 - x_{k_2}^{2N} x_{k_1}^{2N})(x_{k_2}^2 - x_{k_1}^2)) \end{aligned} \quad (3.4.2)$$

Because $x_{k_i} = e^{i\tau k_i/N}$, $x_{k_i}^{2N} = 1$ and $B(k_1, k_2) = 0$ in general. There is an exception when $x_{k_1} x_{k_2} = -1$, i.e. when $k_1 + k_2 = N$. $B(k_1, N - k_1)$ is calculated by taking the limit

$$B(k_1, N - k_1) = \lim_{x_{k_2} \rightarrow -1/x_{k_1}} B(k_1, k_2).$$

The first term of (3.4.2) is zero, but not the second,

$$B(k, N - k) = -2NiK_k K_{N-k} (x_k + x_k^{-1}) = -2NiK_k K_{N-k} \xi_k.$$

This simplifies even more, because when $k < N/2$,

$$K_k K_{N-k} = \frac{1}{2N(\alpha_k \gamma_k \alpha_{N-k} \gamma_{N-k})^{1/2}} = \frac{1}{2N(-\xi_k \xi_{N-k})^{1/2}} = \frac{1}{2N\xi_k},$$

and finally,

$$B(k_1, k_2) = \begin{cases} -i\delta_{k_1+k_2, N} & k_1 < N/2, \\ i\delta_{k_1+k_2, N} & k_1 > N/2. \end{cases} \quad (3.4.3)$$

3.4.2 N odd

From (3.3.12) and (3.4.1), one finds directly

$$S^+ = i^{S_z + 3/2} b_0 \quad \text{and} \quad S^- = i^{S_z - 3/2} a_0. \quad (3.4.4)$$

For $S^{+(2)}$, $B(k_1, k_2)$ has been calculated except when $k_1 = 0$. The result (3.4.2) for $B(k_1, k_2)$ is also valid for $k_1 = 0$ (as the eigenstate is still given by (3.3.8)); replacing $x_{k_1} = i$ gives $B(0, k) = 0$ for all values of k in $1, \dots, N-1$, and

$$S^{+(2)} = \frac{(-1)^{S^z+1}}{2} \left(\sum_{k=1}^{(N-1)/2} b_k b_{N-k} - \sum_{k=(N+1)/2}^{N-1} b_k b_{N-k} \right) = (-1)^{S^z+1} \sum_{k=1}^{(N-1)/2} b_k b_{N-k}, \quad (3.4.5)$$

$$S^{-(2)} = \frac{(-1)^{S^z}}{2} \left(\sum_{k=1}^{(N-1)/2} a_k a_{N-k} - \sum_{k=(N+1)/2}^{N-1} a_k a_{N-k} \right) = (-1)^{S^z} \sum_{k=1}^{(N-1)/2} a_k a_{N-k}.$$

Because the operators $b_k b_{N-k}$ and $a_k a_{N-k}$ commute with H , $S^{+(2)}$ and $S^{-(2)}$ also do, as expected.

3.4.3 N even

The case N even is again different because of the Jordan cell of size 2 in \mathcal{N} related to the eigenvalue 0. From (3.3.16) and (3.4.1),

$$S^+ = \frac{i^{S^z-3/2}}{K'_{N/2}} b_0, \quad S^- = \frac{i^{S^z-1/2}}{K'_{N/2}} a_{-1}. \quad (3.4.6)$$

For $S^{+(2)}$ and $S^{-(2)}$, $B(k_1, k_2)$ has been calculated for k_1, k_2 in $\{1, \dots, N-1\} \setminus \{N/2\}$ in (3.4.3). When $k = 0$ or -1 and $k' \in \{1, \dots, N-1\} \setminus \{N/2\}$, as before we can show that $B(0, k') = B(-1, k') = 0$. A quick argument consists in noticing that operators $b_0 b_{k'}$ and $b_{-1} b_{k'}$ do not commute with H and that $S^{+(2)}$ could not have a component along these operators. But there is a component $b_0 b_{-1}$:

$$B(0, -1) = K'_{N/2} \beta_1 \sum_{j_1 < j_2} (-1)^{j_1+j_2} \left(\left[\frac{N-j_1-1}{2} \right] - \frac{N-4}{N} \left[\frac{N-j_1+1}{2} \right] - \left[\frac{N-j_2-1}{2} \right] + \frac{N-4}{N} \left[\frac{N-j_2+1}{2} \right] \right).$$

To evaluate these sums (for N even), note that

$$\begin{aligned} \sum_{j_1 < j_2} (-1)^{j_1+j_2} \left[\frac{N-j_1-1}{2} \right] &= \sum_{j_1=1}^N (-1)^{j_1} \left[\frac{N-j_1-1}{2} \right] \sum_{j_2=j_1+1}^N (-1)^{j_2} \\ &= \sum_{j_1=1}^N (-1)^{j_1} \left[\frac{N-j_1-1}{2} \right] \delta_{1, j_1 \bmod 2} \\ &= - \sum_{j=1}^{N/2} (N/2 - j) = - \frac{N(N-2)}{8} \end{aligned}$$

and in a similar fashion,

$$\begin{aligned} \sum_{j_1 < j_2} (-1)^{j_1+j_2} \left\lfloor \frac{N-j_1+1}{2} \right\rfloor &= -\frac{N(N-2)}{8} - \frac{N}{2}, \\ \sum_{j_1 < j_2} (-1)^{j_1+j_2} \left\lfloor \frac{N-j_2-1}{2} \right\rfloor &= -\frac{N(N-2)}{8} + \frac{N}{2}, \\ \sum_{j_1 < j_2} (-1)^{j_1+j_2} \left\lfloor \frac{N-j_2+1}{2} \right\rfloor &= -\frac{N(N-2)}{8}. \end{aligned}$$

After simplification, $B(0, -1) = -2K'_{N/2}\beta_1 = 1$, and

$$\begin{aligned} S^{+(2)} &= \frac{(-1)^{S^z}}{2} \left(i(b_{-1}b_0 - b_0b_{-1}) - \sum_{k=1}^{(N-2)/2} b_k b_{N-k} + \sum_{k=(N+2)/2}^{N-1} b_k b_{N-k} \right) \\ &= (-1)^{S^z} \left(ib_{-1}b_0 - \sum_{k=1}^{(N-2)/2} b_k b_{N-k} \right), \\ S^{-(2)} &= (-1)^{S^z} \left(ia_{-1}a_0 + \sum_{k=1}^{(N-1)/2} a_k a_{N-k} \right). \end{aligned} \tag{3.4.7}$$

3.5 The relation between H and \mathcal{H}_N

In this section, we make explicit the relation between the XXZ model and the loop model. The results in this section hold for all q .

3.5.1 The homomorphism

We start by introducing a notation for link states. Let v be a link state in B_N^d with $n = (N-d)/2$ bubbles and let $\psi(v) = \{(p_1, q_1), (p_2, q_2), \dots, (p_n, q_n)\}$, where the p_i s are the positions where the bubbles of v start and q_i s the positions where they end. In $\psi(v)$, the (p_i, q_i) pairs are ordered in ascending order of p_i , though this choice will play no role.

DEFINITION 3.5.1 *The linear transformation $i_N^d : V_N^d \rightarrow (\mathbb{C}^2)^{\otimes N}|_{S^z=d/2}$ (the subset of $(\mathbb{C}^2)^{\otimes N}$ of spin configurations with $n = (N-d)/2$ down spins) is defined by its action on*

the basis elements of B_N^d ,

$$i_N^d(v) = \left(\prod_{(i,j) \in \psi(v)} T_{i,j} \right) |0\rangle, \quad \text{where} \quad T_{i,j} = w\sigma_j^- + w^{-1}\sigma_i^-, \quad (3.5.1)$$

$w = \sqrt{-q}$ and $|0\rangle = \binom{1}{0} \otimes \binom{1}{0} \otimes \cdots \otimes \binom{1}{0} = |\uparrow\uparrow \dots \uparrow\rangle$ as before.

This definition can seem complex, but its graphical interpretation is not. In the simplest cases,

$$i_2^0 \left(\begin{array}{c} \text{---} \\ \bullet \quad \bullet \\ \text{---} \end{array} \right) = w|\uparrow\downarrow\rangle + w^{-1}|\downarrow\uparrow\rangle, \quad i_1^1 \left(\begin{array}{c} \downarrow \\ \bullet \\ \downarrow \end{array} \right) = |\uparrow\rangle, \quad (3.5.2)$$

and when a link state v has more than one bubble or more than one defect, they are replaced recursively by the rule (3.5.2). For instance,

$$\begin{aligned} i_6^2 \left(\begin{array}{c} \downarrow \quad \text{---} \quad \downarrow \quad \text{---} \\ \bullet \quad \bullet \quad \bullet \quad \bullet \\ \downarrow \quad \text{---} \quad \downarrow \quad \text{---} \end{array} \right) &= w^2|\uparrow\uparrow\downarrow\uparrow\uparrow\downarrow\rangle + |\uparrow\downarrow\uparrow\uparrow\uparrow\downarrow\rangle + |\uparrow\uparrow\downarrow\uparrow\downarrow\uparrow\rangle + w^{-2}|\uparrow\downarrow\uparrow\uparrow\downarrow\uparrow\rangle, \\ i_6^2 \left(\begin{array}{c} \downarrow \quad \text{---} \quad \text{---} \quad \text{---} \quad \downarrow \\ \bullet \quad \bullet \quad \bullet \quad \bullet \quad \bullet \\ \downarrow \quad \text{---} \quad \text{---} \quad \text{---} \quad \downarrow \end{array} \right) &= w^2|\uparrow\uparrow\uparrow\downarrow\uparrow\uparrow\rangle + |\uparrow\uparrow\downarrow\uparrow\downarrow\uparrow\rangle + |\uparrow\downarrow\uparrow\downarrow\uparrow\uparrow\rangle + w^{-2}|\uparrow\downarrow\uparrow\uparrow\uparrow\rangle. \end{aligned}$$

The order of pairs (i, j) in $\psi(v)$ is unimportant, as indices in the product (3.5.1) are never repeated and $[T_{i,j}, T_{k,l}] = 0$ when i, j, k, l are all different.

PROPOSITION 3.5.1 *For any $c \in \mathbb{T}_N(-(q+q^{-1}))$ and any $v \in V_N^d$, $i_N^d(cv|_d) = X(c)i_N^d(v)$ where $X(c)$ is the matrix of c in the representation on $(\mathbb{C}^2)^{\otimes N}$ as given in (3.3.2), and where $|_d$ means that all components with less than d defects are set to 0.*

PROOF To prove the proposition, one must show that the action of the matrix e_i on $i_N^d(v)$ is equal to $i_N^d(U_i v|_d)$ for any $v \in B_N^d$. (We can also restrict to the U_i s and e_i s only, as other connectivities are products of these.) More precisely, let $Y(v) = \prod_{(m,n) \in \psi'(v)} T_{m,n}$ and $\psi'(v)$ be the subset of $\psi(v)$ that only contains positions of bubbles in v that do not touch the positions $i, i+1, j$ and k . We first give a list of properties sufficient to prove $i_N^d(cv|_d) = X(c)i_N^d(v)$ for any v . For each entry of the list, we give a diagrammatic property followed by the algebraic identity that needs to be checked.

$$\begin{aligned} 1) \quad X \left(\begin{array}{c} \text{---} \\ \bullet \quad \bullet \\ \text{---} \end{array} \right) i_N^d \left(\begin{array}{c} \downarrow \\ \bullet \\ \downarrow \end{array} \right) &= i_N^d \left(\begin{array}{c} \downarrow \\ \bullet \\ \downarrow \end{array} \right) \left(\begin{array}{c} \text{---} \\ \bullet \quad \bullet \\ \text{---} \end{array} \right) \Big|_d = 0 \\ &\rightarrow e_i Y(v) |0\rangle = 0, \end{aligned}$$

$$\begin{aligned}
2) & \ X \left(\begin{array}{c} \text{Diagram 2} \\ \vdots \\ \text{Diagram 2} \end{array} \right) i_N^d(\text{Diagram 2}) = -(q + q^{-1}) i_N^d(\text{Diagram 2}) \\
& \rightarrow e_i T_{i,i+1} Y(v) |0\rangle = -(q + q^{-1}) T_{i,i+1} Y(v) |0\rangle, \\
3) & \ X \left(\begin{array}{c} \text{Diagram 3} \\ \vdots \\ \text{Diagram 3} \end{array} \right) i_N^d(\text{Diagram 3}) = i_N^d(\text{Diagram 3}) \\
& \rightarrow e_i T_{i+1,j} Y(v) |0\rangle = T_{i,i+1} Y(v) |0\rangle, \\
4) & \ X \left(\begin{array}{c} \text{Diagram 4} \\ \vdots \\ \text{Diagram 4} \end{array} \right) i_N^d(\text{Diagram 4}) = i_N^d(\text{Diagram 4}) \\
& \rightarrow e_i T_{j,i} Y(v) |0\rangle = T_{i,i+1} Y(v) |0\rangle, \\
5) & \ X \left(\begin{array}{c} \text{Diagram 5} \\ \vdots \\ \text{Diagram 5} \end{array} \right) i_N^d(\text{Diagram 5}) = i_N^d(\text{Diagram 5}) \\
& \rightarrow e_i T_{i,k} T_{i+1,j} Y(v) |0\rangle = T_{i,i+1} T_{j,k} Y(v) |0\rangle, \\
6) & \ X \left(\begin{array}{c} \text{Diagram 6} \\ \vdots \\ \text{Diagram 6} \end{array} \right) i_N^d(\text{Diagram 6}) = i_N^d(\text{Diagram 6}) \\
& \rightarrow e_i T_{j,i} T_{i+1,k} Y(v) |0\rangle = T_{i,i+1} T_{j,k} Y(v) |0\rangle, \\
7) & \ X \left(\begin{array}{c} \text{Diagram 7} \\ \vdots \\ \text{Diagram 7} \end{array} \right) i_N^d(\text{Diagram 7}) = i_N^d(\text{Diagram 7}) \\
& \rightarrow e_i T_{j,i+1} T_{k,i} Y(v) |0\rangle = T_{i,i+1} T_{j,k} Y(v) |0\rangle.
\end{aligned}$$

We now verify that each algebraic identity holds. Since $Y(v)$ commutes with e_i and with $T_{i,j}$, $T_{i,k}$, ..., we can ignore it in our calculations. Because of (3.3.2), one can write

$$e_j = \sigma_j^- \sigma_{j+1}^+ + \sigma_j^+ \sigma_{j+1}^- + (q + q^{-1}) \sigma_j^+ \sigma_j^- \sigma_{j+1}^+ \sigma_{j+1}^- - q \sigma_j^+ \sigma_j^- - q^{-1} \sigma_{j+1}^+ \sigma_{j+1}^-.$$

Since $\sigma_j^+ \sigma_j^- |0\rangle = |0\rangle$ and $\sigma_j^+ |0\rangle = 0$, it is obvious that 1) is satisfied. As opposed to the ρ representation, here the number of defects is conserved, which explains the

restriction $|_d$ given in the proposition. Similarly, for 2), 3) and 5),

$$\begin{aligned}
e_i T_{i,i+1}|0\rangle &= (\omega(\sigma_i^- \sigma_{i+1}^+ \sigma_{i+1}^- - q \sigma_i^+ \sigma_i^- \sigma_{i+1}^-) + \omega^{-1}(\sigma_i^+ \sigma_{i+1}^- \sigma_i^- - q^{-1} \sigma_{i+1}^+ \sigma_{i+1}^- \sigma_i^-))|0\rangle \\
&= -(\omega + \omega^{-1})(\omega \sigma_{i+1}^- + \omega^{-1} \sigma_i^-)|0\rangle = -(\omega + \omega^{-1})T_{i,i+1}|0\rangle, \\
e_i T_{i+1,j}|0\rangle &= (\omega(0) + \omega^{-1}(\sigma_i^- \sigma_{i+1}^+ \sigma_{i+1}^- - q \sigma_i^+ \sigma_i^- \sigma_{i+1}^-))|0\rangle \\
&= (\omega^{-1} \sigma_i^- + \omega \sigma_{i+1}^-)|0\rangle = T_{i,i+1}|0\rangle, \\
e_i T_{i,k} T_{i+1,j}|0\rangle &= (\omega^2(0) + \omega^{-2}(0) + \omega^0(\sigma_{i+1}^- \sigma_j^- - q^{-1} \sigma_i^- \sigma_j^- + \sigma_i^- \sigma_k^- - q \sigma_k^- \sigma_{i+1}^-))|0\rangle \\
&= (\omega \sigma_{i+1}^- + \omega^{-1} \sigma_i^-)(\omega \sigma_k^- + \omega^{-1} \sigma_j^-)|0\rangle = T_{i,i+1} T_{j,k}|0\rangle.
\end{aligned}$$

The proofs of 4), 6) and 7) do not require any new ideas and are left to the reader. \square

The only difference between the action of the Temperley-Lieb algebra element c on V_N^d and that of the matrix $X(c)$ on $i_N^d(V_N^d)$ is that connected defects always give 0 in the second case. Nevertheless, for any connectivity c , the diagonal blocks of $\rho(c)|_d$ can be calculated from those of $X(c)|_{S^z=d/2}$. Any information in non diagonal blocks in the loop model is lost in the XXZ model.

3.5.2 The injectivity of i_N^d

DEFINITION 3.5.2 *Path, Dyck path and order.*

- (a) The set of paths with endpoint distance y , P_y^N , is the set of $\vec{x} = \{x_1, x_2, \dots, x_N\}$, where $x_i = \pm 1 \forall i$ and $\sum_{i=1}^N x_i = y$.
- (b) The set of Dyck paths with endpoint distance y , DP_y^N , is the subset of \vec{x} in P_y^N satisfying $\sum_{i=1}^k x_i \geq 0$ for all k in $\{1, \dots, N\}$.
- (c) We define an order for elements of $\vec{x} \in P_y^N$: $\vec{x}_1 < \vec{x}_2$ if $\mathcal{O}(\vec{x}_1) < \mathcal{O}(\vec{x}_2)$, with $\mathcal{O}(\vec{x}) = \sum_{i=1}^N 2^i \delta_{x_i, -1}$.

Dyck paths in DP_y^N are paths starting from $(0, 0)$ and ending at (N, y) using steps $(1, 1)$ and $(1, -1)$, that never venture in the lower half of the plane. The largest Dyck paths with respect to the ordering are those where the steps $(1, -1)$ are at the end of the path. One can easily be convinced that there are no \vec{x}_1, \vec{x}_2 in DP_y^N such that $\mathcal{O}(\vec{x}_1) = \mathcal{O}(\vec{x}_2)$ and $\vec{x}_1 \neq \vec{x}_2$.

Basis elements of $(\mathbb{C}^2)^{\otimes N}|_{S^z=N/2-n}$, labeled $|\alpha\rangle$, are vectors of length N with every component $\in \{+1, -1\}$, indicating up and down spins. There exists a simple bijection between elements \vec{x} in P_{N-2n}^N and spin configurations $|\alpha\rangle$. To each path \vec{x} , we associate a configuration $\mathcal{C}(\vec{x})$: the i -th spin is \uparrow when $x_i = +1$ and \downarrow when $x_i = -1$.

PROPOSITION 3.5.2 i_N^d is injective.

PROOF Let the v s be elements of $B_N^{d=N-2n}$ and the $|\alpha\rangle$ s as before. To show that i_N^d is injective, we must show that

$$P_{\alpha,v} = \langle \alpha | i_N^d(v) \rangle,$$

a rectangular matrix of dimensions $\binom{N}{n}$ by $\binom{N}{n} - \binom{N}{n-1}$ (and again $n = (N-d)/2$ is the number of bubbles), is of maximal rank. For this, we study a square matrix $\tilde{P}_{\alpha,v}$, of size $\binom{N}{n} - \binom{N}{n-1}$, with the same definition as $P_{\alpha,v}$, except we make a restriction on the spin configurations $|\alpha\rangle$. We will show that this matrix is of maximal rank. To this intent, we will order the v s of the link basis in decreasing order of their corresponding Dyck path, $\mathcal{O}(\mathcal{B}^{-1}(v))$ (\mathcal{B} has been introduced in definition 3.2.3). For the $|\alpha\rangle$ s, we choose the subset of spin configurations $|\alpha\rangle = \mathcal{C}(\vec{x})$ for \vec{x} in DP_N^d , and order them, again, in decreasing order of $\mathcal{O}(\vec{x})$.

For a given $v \in B_N^d$, $\mathcal{C}(\mathcal{B}^{-1}(v))$ is the state in $(\mathbb{C}^2)^{\otimes N}|_{S^z=d/2}$ whose component in $i_N^d(v)$ has the biggest power of $w : n$. Indeed, $\mathcal{C}(\mathcal{B}^{-1}(v))$ is the configuration obtained by replacing every bubble of v by $w \uparrow\downarrow$. All other components of $i_N^d(v)$ are obtained from the first by replacing certain pairs $\uparrow\downarrow$ by $\downarrow\uparrow$ and by diminishing the power of w by two for each pair changed. We conclude that in $\tilde{P}_{\alpha,v}$, every element on the diagonal is w^n and is non zero (except for $w = 0$, which is an unphysical case). Every component $|\alpha\rangle$ of $i_N^d(v)$ has a $\mathcal{O}(\mathcal{C}^{-1}(|\alpha\rangle))$ smaller or equal to $\mathcal{O}(\mathcal{B}^{-1}(v))$, and $\tilde{P}_{\alpha,v}$ matrix is therefore lower triangular. From the previous remark, the rank of $\tilde{P}_{\alpha,v}$, and therefore of $P_{\alpha,v}$, is maximal. □

For example, with $N = 5$, $n = 2$ and $d = 1$:

$$\begin{array}{l} \vec{x} \in DP_1^5 : \quad \begin{array}{ccccc} \text{↗↘} & \text{↗↘↗↘} & \text{↗↘↗↘} & \text{↗↘↘↗} & \text{↗↘↘↗} \end{array} \\ \mathcal{O}(\vec{x}) \quad \quad \quad 2^4 + 2^5 & 2^3 + 2^5 & 2^2 + 2^5 & 2^3 + 2^4 & 2^2 + 2^4 \\ \mathcal{B}(\vec{x}) \in V_5^1 : \quad \begin{array}{ccccc} | \text{↗↘} \rangle & | \text{↗↘↗↘} \rangle & | \text{↗↘↗↘} \rangle & | \text{↗↘↘↗} \rangle & | \text{↗↘↘↗} \rangle \end{array} \\ \mathcal{C}(\vec{x}) \in (\mathbb{C}^2)^{\otimes 5} : \quad | \uparrow\uparrow\uparrow\downarrow\downarrow \rangle & | \uparrow\uparrow\downarrow\uparrow\downarrow \rangle & | \uparrow\downarrow\uparrow\uparrow\downarrow \rangle & | \uparrow\uparrow\downarrow\downarrow\uparrow \rangle & | \uparrow\downarrow\uparrow\downarrow\uparrow \rangle \end{array}$$

$$\tilde{P}_{\alpha,v} = \begin{pmatrix} w^2 & 0 & 0 & 0 & 0 \\ 1 & w^2 & 0 & 0 & 0 \\ 0 & 1 & w^2 & 0 & 0 \\ 0 & 1 & 0 & w^2 & 0 \\ 1 & w^{-2} & 1 & 1 & w^2 \end{pmatrix}.$$

From propositions 3.5.1 and 3.5.2, $i_N^d(V_N^d)$ is a subspace of $\dim V_N^d$ of $(\mathbb{C}^2)^{\otimes N}|_{S^z=d/2}$, invariant under the action of the e_i s of XXZ. The eigenvectors of $\rho(\mathcal{H}_N)$ (for any β),

restricted to the sector with d defects, are in correspondence with eigenvectors of H_{XXZ} in the $S^z = d/2$ sector. For N odd, because i_N^d is injective and H has no Jordan blocks, $\rho(\mathcal{H}_N)|_d$ must share this property. We will find at the end of section 3.6.2 that $\rho(\mathcal{H}_N)|_d$ is also diagonalizable when N is even.

3.5.3 The relation between $U_q(\mathfrak{sl}_2)$ and $i_N^d(V_N^d)$

In this section, we establish the relation between the homomorphism i_N^d and the algebra $U_q(\mathfrak{sl}_2)$.

PROPOSITION 3.5.3 *For all $v \in V_N^d$, $i_N^d(v) \in \ker S^+$.*

PROOF We start by restricting the proof to link patterns with only simple bubbles, i.e. to vs for which every $(i, j) \in \psi(v)$ is of the form $(i, i+1)$. We notice that, in general, whenever k does not appear in any of the pairs (i, j) in $\psi(v)$, $S_k^+ i_N^d(v) = 0$. Indeed, when $i \neq j$,

$$S_i^+ \sigma_j^- = q^{s_{i,j}} \sigma_j^- S_i^+ \quad \text{where} \quad s_{i,j} = \begin{cases} +1, & \text{if } i > j, \\ -1, & \text{if } i < j. \end{cases}$$

and, when k is not in any of the pairs of $\psi(v)$,

$$\begin{aligned} S_k^+ i_N^d(v) &= S_k^+ \left(\prod_{(i,i+1) \in \psi(v)} (w \sigma_{i+1}^- + w^{-1} \sigma_i^-) \right) |0\rangle \\ &= \left(\prod_{(i,i+1) \in \psi(v)} (q^{s_{k,i+1}} w \sigma_{i+1}^- + q^{s_{k,i}} w^{-1} \sigma_i^-) \right) S_k^+ |0\rangle = 0. \end{aligned}$$

All that is left to calculate is $S^+ i_N^d(v) = \sum_{(k,k+1) \in \psi(v)} (S_k^+ + S_{k+1}^+) i_N^d(v)$,

$$\begin{aligned} (S_k^+ + S_{k+1}^+) i_N^d(v) &= \left(\prod_{\substack{(i,i+1) \in \psi(v) \\ i \neq k}} (q^{s_{k,i+1}} w \sigma_{i+1}^- + q^{s_{k,i}} w^{-1} \sigma_i^-) \right) S_k^+ (w \sigma_{k+1}^- + w^{-1} \sigma_k^-) |0\rangle \\ &\quad + \left(\prod_{\substack{(i,i+1) \in \psi(v) \\ i \neq k}} (q^{s_{k+1,i+1}} w \sigma_{i+1}^- + q^{s_{k+1,i}} w^{-1} \sigma_i^-) \right) S_{k+1}^+ (w \sigma_{k+1}^- + w^{-1} \sigma_k^-) |0\rangle \\ &= \left(\prod_{\substack{(i,i+1) \in \psi(v) \\ i \neq k}} q^{s_{k,i}} (w \sigma_{i+1}^- + w^{-1} \sigma_i^-) \right) (S_k^+ + S_{k+1}^+) (w \sigma_{k+1}^- + w^{-1} \sigma_k^-) |0\rangle. \end{aligned}$$

When v has only simple bubbles, $s_{k,i} = s_{k+1,i} = s_{k,i+1} = s_{k+1,i+1}$. This has been used at the last equality. Finally,

$$\begin{aligned}
(S_k^+ + S_{k+1}^+)(w\sigma_{k+1}^- + w^{-1}\sigma_k^-)|0\rangle &= w^{-1}S_k^+\sigma_k^-|0\rangle + wS_{k+1}^+\sigma_{k+1}^-|0\rangle \\
&= w^{-1}\left(\prod_{i=1}^{k-1}q^{-\sigma_i^z/2}\right)\sigma_k^+\sigma_k^-\left(\prod_{j=k+1}^Nq^{\sigma_j^z/2}\right)|0\rangle \\
&\quad + w\left(\prod_{i=1}^kq^{-\sigma_i^z/2}\right)\sigma_{k+1}^+\sigma_{k+1}^-\left(\prod_{j=k+2}^Nq^{\sigma_j^z/2}\right)|0\rangle \\
&= w^{-1}\left(q^{(N-2k+1)/2} + w^2q^{(N-2k-1)/2}\right)|0\rangle = 0.
\end{aligned}$$

For $w \in B_N^d$ with bubbles that are not simple, from proposition 3.5.1, one can write $i_N^d(w) = (\prod_{j \in J} e_j)i_n^d(v)$ for some set J and for v a link state with only simple bubbles. Since $[S^+, e_j] = 0$ by proposition 3.4.1, $S^+i_N^d(w) = 0$ for all $w \in B_N^d$. \square

From this proposition, it follows that for $q = q_c$ and $(q_c)^{2P} = 1$, $i_N^d(V_N^d)$ is also $\subset \ker S^{+(P)}$:

$$S^{+(P)}i_N^d(v) = \lim_{q \rightarrow q_c} \frac{(S^+)^P i_N^d(v)}{[P]_q} = \lim_{q \rightarrow q_c} \frac{0}{[P]_q} = 0.$$

3.6 The reduction of state space and the degeneracies

In the last sections, we found that the set of eigenvalues of $\rho(\mathcal{H}_N)$ in the sector with n bubbles was a subset of the eigenvalues of H in the sector $S^z = N/2 - n$. For $\beta = 0$, this will allow us to prove the selection rules of section 3.2 : we will calculate the degeneracies of every eigenvalue in H , remove those that are tied to eigenvectors not in $i_N^d(V_N^d)$ and show that the degeneracies obtained match those of the loop model, given by eqs (3.2.11), (3.2.12) and (3.2.13). The two corresponding vector spaces $(\mathbb{C}^2)^{\otimes N}|_{S^z=N/2-n}$ and V_N^{N-2n} have respective dimensions $\binom{N}{n}$ and $\binom{N}{n} - \binom{N}{n-1}$. To get only states in $i_N^d(V_N^{N-2n})$, we will need to remove $\binom{N}{n-1}$ independent states from $(\mathbb{C}^2)^{\otimes N}|_{S^z=N/2-n}$.

DEFINITION 3.6.1 Let $\mathcal{O} = \sum_{\vec{i}} \alpha_{\vec{i}} \mathcal{O}_{\vec{i}}$ with $\vec{i} = (i_1, i_2, \dots, i_{|\vec{i}|})$, where $\alpha_{\vec{i}} \in \mathbb{C}$ and $\mathcal{O}_{\vec{i}}$ is the product of some annihilation operators : $\mathcal{O}_{\vec{i}} = \prod_{k=1}^{|\vec{i}|} b_{i_k}$. We define \mathcal{O}' with the following two rules :

- $\mathcal{O}' = \sum_{\vec{i}} \alpha_{\vec{i}}^* \mathcal{O}'_{\vec{i}}$,
- $\mathcal{O}'_{\vec{i}} = \prod_{k=1}^{|\vec{i}|} a'_{i_{|\vec{i}|+1-k}}$,

where the product of non-commuting elements is always taken from left to right.

The sum over \vec{i} is a sum over multi-indexes that could potentially have different lengths, but the only \mathcal{O} s we will need have $\mathcal{O}_{\vec{i}}$ s with a unique fixed length. For example,

$$(b_3 b_6 b_1)' = a_1 a_6 a_3,$$

$$(3i b_2 + (5i + 1) b_7 b_4 + 12 b_0 b_2 b_1 b_{12})' = -3i a_2 + (-5i + 1) a_4 a_7 + 12 a_{12} a_1 a_2 a_0.$$

PROPOSITION 3.6.1 *Let an operator $\mathcal{O} \neq 0$ that satisfies $\mathcal{O} i_N^d(v) = 0$ for all $v \in V_N^d$. Then $\mathcal{O}'|0\rangle \notin i_N^d(V_N^d)$.*

PROOF There does not exist a set of constants γ_v s such that

$$\mathcal{O}'|0\rangle + \sum_{v \in V_N^d} \gamma_v i_N^d(v) = 0.$$

Indeed, multiplying this equation from the left with \mathcal{O} , the second term is zero by hypothesis and

$$\mathcal{O} \mathcal{O}'|0\rangle = \sum_{\vec{i}} |\alpha_{\vec{i}}|^2 |0\rangle = 0,$$

which contradicts the hypothesis $\mathcal{O} \neq 0$. \square

By proposition 3.5.3, the operators S^+ and $S^{+(2)}$ are two such operators \mathcal{O} satisfying $\mathcal{O} i_N^d(v) = 0, \forall v \in V_N^d$. To find eigenvectors of H not in $i_N^d(V_N^d)$ and that we will have to remove from all the states of the form $a_{i_1} a_{i_2} \dots a_{i_n} |0\rangle$ (with $n = (N - d)/2$), we look for operators $\mathcal{O} = \sum_{\vec{i}} \alpha_{\vec{i}} \mathcal{O}_{\vec{i}}$ for which every $\mathcal{O}_{\vec{i}}$ is a product of n annihilation operators. They are :

- $\mathcal{O} = S^+ b_{j_1} b_{j_2} \dots b_{j_{n-1}}$ where $j_k \neq 0$ for $k = 1, \dots, n - 1$ (b_0 is the generator corresponding to S^+ , see eqs (3.4.4) and (3.4.6), and \mathcal{O} must be non zero). Because $\{b_0, b_j\} = 0$ for all j , $\mathcal{O} i_N^d(v) = 0$ for all v . All the states $a_{j_{n-1}} a_{j_{n-2}} \dots a_{j_1} a_0 |0\rangle$ must be removed. They will be referred to as states *of the first kind*. There are $\binom{N-1}{n-1}$ such states.
- $\mathcal{O} = S^{+(2)} b_{k_1} b_{k_2} \dots b_{k_{n-2}}$, and $\mathcal{O} i_N^d(v) = 0$ for all v by the same argument. The states to be removed are of the form $a_{k_{n-2}} a_{k_{n-3}} \dots a_{k_1} (S^{+(2)})' |0\rangle$, where the a_{k_i} s can be any of the $N - 1$ remaining operators (not a_0 , as we want to avoid any overlap with states of the first kind). They will be referred to as states *of the second kind*. There are $\binom{N-1}{n-2}$ such states.

Of course, $\binom{N-1}{n-1} + \binom{N-1}{n-2} = \binom{N}{n-1}$, precisely the number of states we need to remove. That all these states are independent is non trivial and shown in appendix 3.B. Having succeeded in finding a rule that removes all eigenstates of H not in $i_N^d(V_N^d)$, we can now calculate the degeneracies.

3.6.1 N odd

As seen in section 3.3.2, when N is odd, the eigenvectors of H , restricted to the $S^z = N/2 - n$ sector, are of the form

$$|\gamma\rangle = \left(\prod_{i=1}^n \alpha_{k_i} \right) |0\rangle \quad (3.6.1)$$

for $k_i \in \{0, 1, \dots, N-1\}$. If one of the k_i s is 0, we put it at the end and set $\alpha_{k_n} = \alpha_0$. The eigenvalues are

(a) $\gamma = 2 \sum_{i=1}^n \cos(\pi k_i/N)$, if $k_n \neq 0$,

(b) $\gamma = 2 \sum_{i=1}^{n-1} \cos(\pi k_i/N)$, if $k_n = 0$.

We call Γ_0^n and Γ_1^n respectively the set of all γ s for (a) and (b).

PROPOSITION 3.6.2 $\Lambda_\delta^n = \Gamma_\delta^n$ for both $\delta = 0$ and 1.

PROOF Let $\gamma \in \Gamma_\delta^n$. To show that $\gamma \in \Lambda_\delta^n$, we construct the three subsets K^+ , K^- and K^c . For all $k \in \{1, \dots, (N-1)/2\}$,

(i) if $k \in \{k_1, \dots, k_n\}$ and $N-k \notin \{k_1, \dots, k_n\}$, we put k in K^+ ;

(ii) if $k \notin \{k_1, \dots, k_n\}$ and $N-k \in \{k_1, \dots, k_n\}$, we put k in K^- ;

(iii) if $k \in \{k_1, \dots, k_n\}$ and $N-k \in \{k_1, \dots, k_n\}$, we put k in K^c ;

(iv) if $k \notin \{k_1, \dots, k_n\}$ and $N-k \notin \{k_1, \dots, k_n\}$, we put k in K^c ;

We stress that when $k_n = 0$, 0 is not in any of K^+ , K^- or K^c , but for fixed n , its presence or absence changes the number of elements in $K^+ \cup K^-$. The case $\delta = 0$ is when the α_0 creation operator is absent : $n - m = n - |K^+ \cup K^-|$ counts the number of elements in (iii) and is even. When $\delta = 1$, the last momentum is $k_n = 0$ and the number of elements in (iii) is still even, but now given by $n - 1 - m$, so $n - m$ is odd.

Now, let $\lambda \in \Lambda_\delta^n$ with a fixed m . To see it is also in Γ_δ^n , we construct the set of momenta as follows

(i) if k is in K^+ , we put k in $\{k_1, \dots, k_n\}$, but not $N-k$;

(ii) if k is in K^- , we put $N-k$ in $\{k_1, \dots, k_n\}$, but not k ;

(iii) if $\delta = 1$, we set $k_n = 0$,

- (iv) For all the k s that are in K^c , we choose $(n-m-\delta)/2$ among the $(N-1)/2-m$ remaining values and put, for each, k and $N-k$ in $\{k_1, \dots, k_n\}$.

□

From the previous construction, an eigenvalue λ of H has eigenvector

$$\left(\prod_i a_{N-i} a_i \right) \left(\prod_{j \in K^-} a_{N-j} \right) \left(\prod_{k \in K^+} a_k \right) |0\rangle, \quad \text{if } \delta = 0, \quad (3.6.2)$$

$$\left(\prod_i a_{N-i} a_i \right) \left(\prod_{j \in K^-} a_{N-j} \right) \left(\prod_{k \in K^+} a_k \right) a_0 |0\rangle, \quad \text{if } \delta = 1. \quad (3.6.3)$$

where the product on i has $(n-m-\delta)/2$ terms, all different, with $i \in K^c$. The degeneracy comes from all the possibilities for the product on i , and is given by

$$\text{deg}_{\mathcal{H}}(\lambda) = \binom{\frac{N-1}{2} - m}{\frac{n-m-\delta}{2}}.$$

To obtain the degeneracies of these eigenvalues in $\rho(\mathcal{H}_N)$, we remove the states of (3.6.3) (they are all of the first kind) and from (3.6.2), all the states of the second kind,

$$\left(\prod_{i'} a_{N-i'} a_{i'} \right) \left(\prod_{j \in K^-} a_{N-j} \right) \left(\prod_{k \in K^+} a_k \right) \left(\sum_{l=1}^{(N-1)/2} a_l a_{N-l} \right) |0\rangle, \quad (3.6.4)$$

where the products on i' has $(n-m-2)/2$ terms and where the constant $(-1)^{S^z}$ of (3.4.5) has been dropped for convenience. For some λ with a fixed value of m , there are $\binom{\frac{N-1}{2}-m}{\frac{n-m-2}{2}}$ such possible choices, each corresponding to an eigenvector. The set of corresponding eigenvectors is linearly independent (see appendix 3.B) and the result is

- For $\lambda \in \Lambda_0^n$, $\text{deg}_{\mathcal{H}}(\lambda) = \binom{\frac{N-1}{2}-m}{\frac{n-m}{2}} - \binom{\frac{N-1}{2}-m}{\frac{n-m-2}{2}}$,
- For $\lambda \in \Lambda_1^n$, $\text{deg}_{\mathcal{H}}(\lambda) = 0$.

This is precisely the content of conjecture 3.2.3, which is now proved.

3.6.2 N even

As in section 3.3.2, eigenvectors and generalized eigenvectors of H , for $S^z = N/2 - n$, are given in (3.6.1), but with $k_i \in \{-1, 0, 1, \dots, N-1\} \setminus \{N/2\}$. When the a_0 and/or a_{-1} excitations are present, we set them to the last k_i s (k_n and k_{n-1} , when both are present). Eigenvalues are

- (a) $\gamma = 2 \sum_{i=1}^n \cos(\pi k_i/N)$ if a_0, a_{-1} are not in the a_i s;

- (b) $\gamma = 2 \sum_{i=1}^{n-1} \cos(\pi k_i/N)$ if
- (i) a_{-1} is not in the a_i s, but a_0 is;
 - (ii) a_0 is not in the a_i s, but a_{-1} is;
- (c) $\gamma = 2 \sum_{i=1}^{n-2} \cos(\pi k_i/N)$ if a_0 and a_{-1} are both among the a_i s.

We refer to the sets of eigenvalues in the cases (a), (b) and (c) as Γ_a^n , Γ_b^n and Γ_c^n .

PROPOSITION 3.6.3 *Based on the definition of 3.2.5 for Λ_0^n and Λ_1^n , $\Gamma_a^n = \Lambda_0^n$, $\Gamma_b^n = \Lambda_1^n$ and $\Gamma_c^n \subset \Lambda_0^n$.*

The proof is identical to the proof of proposition 3.6.2, with a few subtleties. The first is that whenever γ has the a_{-1} excitation, the a_0 excitation or both, their momenta are not in either K^+ , K^- or K^c , but their absence changes the number of elements in $K^+ \cup K^-$. The second concerns the fact that Γ_c^n is only a subset of Λ_0^n . Indeed, the elements of Λ_0^n with $m = n$ are not contained in Γ_c^n . The rest of the proof is not repeated. Note that the number of pairs $(k, N - k)$ to be fixed (among the $(N - 2)/2 - m$ possible choices) and the degeneracies of the eigenvalues are different for the three cases (a), (b) and (c) :

- (a) $(n - m)/2$ pairs to be fixed and $\deg_{\mathcal{H}}(\lambda) = \binom{\frac{N-2}{2}-m}{\frac{n-m}{2}}$;
- (b) $(n - m - 1)/2$ pairs to be fixed and $\deg_{\mathcal{H}}(\lambda) = \binom{\frac{N-2}{2}-m}{\frac{n-m-1}{2}}$;
- (c) $(n - m - 2)/2$ pairs to be fixed and $\deg_{\mathcal{H}}(\lambda) = \binom{\frac{N-2}{2}-m}{\frac{n-m-2}{2}}$.

States to be removed are those of the first kind, see (3.6.3), and those of the second kind,

$$\left(\prod_{i'} a_{N-i'} a_{i'} \right) \left(\prod_{j \in K^-} a_{N-j} \right) \left(\prod_{k \in K^+} a_k \right) \left(\sum_{l=1}^{(N-2)/2} a_l a_{N-l} \right) |0\rangle,$$

and the product on i' has $(n - m - 2)/2$ terms. The $a_0 a_{-1}$ contribution from $(S^{+(2)})'$ has been removed because this caused an overlap with states of the first kind. The degeneracies are

- (a) $\deg_{\mathcal{H}}(\lambda) = \binom{\frac{N-2}{2}-m}{\frac{n-m}{2}} - \binom{\frac{N-2}{2}-m}{\frac{n-m-2}{2}}$,
- (i) $\deg_{\mathcal{H}}(\lambda) = 0$,
- (b) (ii) $\deg_{\mathcal{H}}(\lambda) = \binom{\frac{N-2}{2}-m}{\frac{n-m-1}{2}} - \binom{\frac{N-2}{2}-m}{\frac{n-m-3}{2}}$,
- (c) $\deg_{\mathcal{H}}(\lambda) = 0$.

The cases (a) and (c) correspond to Λ_0^n , while (b) (i) and (b) (ii) correspond to Λ_1^n . This is the result of conjecture 3.2.5 and concludes the proof of the selection rules.

Note that Jordan partners were the states of (b) (i). Since they have all been removed, $\rho(\mathcal{H}_N)$ is diagonalizable.

3.7 Conclusion

In this paper, we proved that the degeneracies of the eigenvalues of $\rho(\mathcal{H}_N)$, as given by the selection rules, are correct. We must stress however that the proof ignored the problem of accidental degeneracies resulting from accidental trigonometric identities. Another problem is the case of loop models on other geometries. A recent paper [47] solved the model of critical dense polymers on the cylinder. An inversion relation was computed, eigenvalues were found and degeneracies conjectured by selection rules different from the ones here. The method proposed here might also lead to a proof of these conjectures.

Acknowledgements

The author thanks the NSERC for an Alexander Graham Bell graduate fellowship. The author would like to thank Yvan Saint-Aubin for fruitful discussions throughout the project and for reviewing his manuscript. He has benefitted from discussions with Jørgen Rasmussen and David Ridout, and would like to thank Michael Doob for sharing his knowledge of graph theory.

Appendices

3.A The computation of $K'_{N/2}$, β_1 and β_2 (for N even)

The goal of this section is to calculate the three constants $K'_{N/2}$, β_1 and β_2 that fix the two states (the eigenstate and its Jordan partner) tied to the eigenvalues $\xi = 0$ of \mathcal{N} . The anticommutation relations, in terms of $u_{N/2}$ and w , are rewritten as

$$\begin{aligned} \{b_{-1}, a_{-1}\} &= \vec{f}_{-1}^T \vec{g}_{-1} = \sum_{j=1}^N u_{N/2}^j w^j = 1, \\ \{b_0, a_{-1}\} &= \vec{f}_0^T \vec{g}_{-1} = \sum_{j=1}^N (u_{N/2}^j)^2 = 0, \\ \{b_{-1}, a_0\} &= \vec{f}_{-1}^T \vec{g}_0 = \sum_{j=1}^N (w^j)^2 = 0, \\ \{b_0, a_0\} &= \vec{f}_0^T \vec{g}_0 = \sum_{j=1}^N w^j u_{N/2}^j = 1. \end{aligned}$$

The second relation is trivially satisfied, since $\sum_{j=1}^N (-1)^j = 0$ for N even. The third constraint reads

$$\beta_1^2 w_1^\top w_1 + \beta_2^2 w_2^\top w_2 + 2\beta_1 \beta_2 w_1^\top w_2 = 0. \quad (3.A.1)$$

To calculate $w_1^\top w_1$,

$$\begin{aligned} w_1^\top w_1 &= \sum_{j=1}^N (-1)^j \left[\frac{N-j-1}{2} \right]^2 \\ &= \sum_{k=1}^{N/2} \left((-1)^{2k} \left[\frac{N-2k-1}{2} \right]^2 + (-1)^{2k-1} \left[\frac{N-2k}{2} \right]^2 \right) \\ &= \sum_{k=1}^{N/2} (N/2 - k - 1)^2 - \sum_{k=1}^{N/2} (N/2 - k)^2 = -N(N-4)/4, \end{aligned}$$

and one can also find $w_2^\top w_2 = -N^2/4$, $w_1^\top w_2 = -N(N-2)/4$, and, from (3.A.1), $\beta_2/\beta_1 = -(N-4)/N$. The second solution, $\beta_2/\beta_1 = -1$, is not retained, because it corresponds to the eigenvector $u_{N/2}^j = K'_{N/2}(w_2^j - w_1^j) = K'_{N/2}i^j$ that we already found. It remains to fulfill the first constraint (the fourth one is identical) :

$$\begin{aligned} 1 &= \sum_{j=1}^N u_{N/2}^j w^j = K'_{N/2} \beta_1 \left(-w_1^\top w_1 - \frac{N-4}{N} w_2^\top w_2 + \left(\frac{N-4}{N} + 1 \right) w_2^\top w_1 \right) \\ &= K'_{N/2} \beta_1 \left(\frac{N(N-4)}{4} + \frac{N(N-4)}{4} - \left(\frac{N-4}{N} + 1 \right) \frac{N(N-2)}{4} \right) = -2K'_{N/2} \beta_1 \end{aligned}$$

which gives $K'_{N/2} \beta_1 = -1/2$. Finally, a last constraint is obtained from $\mathcal{N} \vec{g}_0 = \vec{g}_{-1}$, which is equivalent to imposing that the coefficient in front of $b_0 a_{-1}$ is 1 in equation (3.3.15) :

$$\begin{aligned} K'_{N/2} i^j &= g_{-1}^j = (\mathcal{N} \vec{g}_0)^j = \beta_1 (\mathcal{N}(w_1 - w_2(N-4)/N))^j \\ &= \beta_1 i^{j-1} (1 - (N-4)/N) = \beta_1 i^j (-4i/N) \end{aligned}$$

where eq. (3.3.14) has been used at the fourth equality. This gives $K'_{N/2}/\beta_1 = -4i/N$ and the calculation of the three constants is complete.

3.B Independence of states not in $i_N^d(V_N^d)$

In section 3.6, we have identified states to be removed from $(\mathbb{C}^2)^{\otimes N}|_{S^z=d/2}$ and that should form a basis for the complement of $i_N^d(V_N^d)$. In this section, we show that these states are non zero and independant.

DEFINITION 3.B.1 *Let $|v_1\rangle$ and $|v_2\rangle$ be any vector that can be written as $\mathcal{O}_1|0\rangle$ and $\mathcal{O}_2|0\rangle$, where \mathcal{O}_1 and \mathcal{O}_2 are multi-indexes as in definition 3.6.1. We introduce a scalar product between such states by defining $(|v_1\rangle, |v_2\rangle) = \langle 0|\mathcal{O}'_1\mathcal{O}_2|0\rangle$. We will denote this scalar product by $\langle v_1|v_2\rangle$.*

The fact that states of the first kind $|w\rangle = a_{j_{n-1}}a_{j_{n-2}}\dots a_{j_1}a_0|0\rangle$ (with $j_1 < j_2 < \dots < j_{n-1}$) are independent and non zero is trivial, as the scalar product restricted to such states is just $\langle w_1|w_2\rangle = \delta_{w_1,w_2}$: they all have length one and are mutually orthogonal. There are $\binom{N-1}{n-1}$ such vectors.

The proof for vectors of the second kind is more involved. It requires the following definition ([85], [86]).

DEFINITION 3.B.2 *Let v and k be positive integers, with $v > k$. The Johnson graph $J(v, k)$ is the following :*

- *its vertices θ are the subsets of length k of $\{1, 2, \dots, v\}$, their number is $\binom{v}{k}$;*
- *two vertices θ_1 and θ_2 are connected by an edge if and only if $|\theta_1 \cap \theta_2| = k - 1$.*

The adjacency matrix $A(v, k)$ of the Johnson graph $J(v, k)$ is the matrix with entries

$$A(v, k)_{\theta_1, \theta_2} = \begin{cases} 1 & \text{if } \theta_1 \text{ and } \theta_2 \text{ are connected by an edge,} \\ 0 & \text{otherwise (even if } \theta_1 = \theta_2\text{).} \end{cases}$$

Johnson graphs have been thoroughly studied ([85], [86], [87]). In particular, the eigenvalues of $A(v, k)$ are $k(v-k) - j(v-j+1)$ with $j = 0, \dots, k$ with degeneracy $\binom{v}{j} - \binom{v}{j-1}$ [87]. Some pathologies occur when $v \leq 2k - 1$, as some of the degeneracies become negative or zero. We will see that in our cases, v will always be larger than $2k - 1$.

For N odd, we write in full generality the states of the second kind as

$$|w\rangle = \prod_{i \in I^w} a_i a_{N-i} \prod_{j_1 \in J_+^w} a_{j_1} \prod_{j_2 \in J_-^w} a_{N-j_2} \sum_{k \in K^w} a_k a_{N-k} |0\rangle = \sum_{k \in K^w} |w_k\rangle. \quad (3.B.1)$$

In the previous formula, I^w is the set of integers i in the interval $1, \dots, (N-1)/2$ such that w contains both the a_i and the a_{N-i} excitation. J_+^w (J_-^w) is the set of integers j_1 (j_2), also in the interval $1, \dots, (N-1)/2$, such that the a_{j_1} (a_{N-j_2}) excitation is present but the a_{N-j_1} (a_{j_2}) is not (in fact, the sets J_{\pm}^w are just the sets K^{\pm} in the definition 3.2.5). The sets I^w , J_+^w and J_-^w are all disjoint. Finally, the sum over k in (3.6.4), was over all integers in $1, \dots, (N-1)/2$, but since the square of any of the as

is zero, the sum really is on $K^w = \{1, \dots, (N-1)/2\} \setminus (I^w \cup J_+^w \cup J_-^w)$. We also define $L^w = \{1, \dots, (N-1)/2\} \setminus (J_+^w \cup J_-^w)$.

Not all states (3.B.1) are non zero. In fact, because $\langle w_k | w_{k'} \rangle = \delta_{k,k'}$, $\langle w | w \rangle = |K^w|$. If $I^w \cup J_+^w \cup J_-^w = \{1, \dots, (N-1)/2\}$, K^w is empty and the state is zero, as can be seen more easily on (3.6.4). Recall that we are interested in states that have at most $(N-1)/2$ excitations for N odd, as the number of excitations corresponds to the number of bubbles in the link states, n . This imposes that $2|I^w| + |J_+^w| + |J_-^w| + 2 = n \leq (N-1)/2$ (or equivalently, $|L| - 2|I| \geq 2$) and $I^w \cup J_+^w \cup J_-^w \neq \{1, \dots, (N-1)/2\}$.

Two states $|w_1\rangle$ and $|w_2\rangle$ are orthogonal unless $J_\pm^{w_1} = J_\pm^{w_2}$. We can restrict the study of independence to sets of states with $J_\pm^{w_1} = J_\pm^{w_2} \equiv J_\pm$ and $|I^{w_1}| = |I^{w_2}| \equiv |I|$ (and so $L^{w_1} = L^{w_2} \equiv L$). In such a set, the states differ only by their I^{w_1} and I^{w_2} , and the set has dimension $\binom{|L|}{|I|}$. The scalar product of two states w_1 and w_2 belonging to this set is

$$\langle w_1 | w_2 \rangle = \begin{cases} |K^{w_1}| & \text{if } w_1 = w_2, \\ 1 & \text{if } |I^{w_1} \cap I^{w_2}| = |I| - 1, \\ 0 & \text{otherwise.} \end{cases} \quad (3.B.2)$$

The matrix $M(L, |I|)$ of this scalar product is simply $M(L, |I|) = |K| \text{id} + A(|L|, |I|) : |w\rangle$, with $I^w = \{i_1, i_2, \dots, i_{|I|}\}$, is represented by a subset of length $|I|$ of L and is identified to a vertex of the Johnson graph $J(|L|, |I|)$. The eigenvalues are given by

$$\underbrace{|L| - |I|}_{|K|} + |I|(|L| - |I|) - j(|L| + 1 - j), \quad j = 0, \dots, |I|.$$

Because $-j(|L| + 1 - j)$ is a strictly decreasing function of j on the interval $[0, |I|]$, the extrema are on the boundaries; they are $(1 + |I|)(|L| - |I|)$ and $|L| - 2|I|$, both positive. Also because $|L| - 2|I| > 1$, every degeneracy is positive. As all the eigenvalues are positive, there are no null states, and the independence is proved.

For N even, the proof requires a few subtleties. $(S^{+(2)})'$ has a $b_0 b_{-1}$ contribution which can be ignored. We therefore consider vectors like (3.B.1), but with $I^w \cup J_+^w \cup J_-^w \cup K^w = \{1, \dots, (N-2)/2\}$, and the possibility to have the a_{-1} excitation. L^w is then defined as $\{1, \dots, (N-2)/2\} \setminus (J_+^w \cup J_-^w)$. The sets of states with and without this excitation, say S_1 and S_2 , can be treated separately because, for any $w_1 \in S_1$ and $w_2 \in S_2$, $\langle w_1 | w_2 \rangle = 0$. For S_1 , $|L| - 2|I| \geq 1$, and for S_2 , $|L| - 2|I| \geq 2$. In both cases, all eigenvalues are positive.

The case $d = 0$ is particular. States of the second kind in S_2 are

$$|w\rangle = \prod_i a_i \sum_{k \in K^w} a_k a_{N-k} |0\rangle, \quad (3.B.3)$$

and the product on i has $N/2 - 2$ terms, all in $\{1, \dots, N - 1\} \setminus \{N/2\}$. Their number is $\binom{N-2}{N/2-2}$. These are removed from the states

$$|w\rangle = \prod_{i'} a_{i'} |0\rangle, \quad (3.B.4)$$

where the product on i' has $N/2$ terms, also in $\{1, \dots, N - 1\} \setminus \{N/2\}$. Their number is $\binom{N-2}{N/2}$. But these two numbers are equal and all states from (3.B.3) are independent from the previous argument. In other words, all the states (3.B.4) are removed, leaving no degeneracy in $\rho(\mathcal{H}_N)$. This is the result of proposition 3.2.5. \square

CHAPITRE 4: LA STRUCTURE DE JORDAN DES MODÈLES DE BOUCLES AVEC CONDITIONS PÉRIODIQUES

Objectifs et méthodologie

Le calcul de la fonction de partition du modèle de Fortuin-Kasteleyn sur le tore peut aussi être faite au moyen d'une matrice de transfert de boucles, $T_N(\lambda, \nu)$ (ν est l'anisotropie, notée u dans les chapitres précédents). Deux représentations ρ et ω_d de vecteurs de connectivités joueront un rôle ici ; elles sont différentes de celles sur le ruban puisqu'il faut considérer la possibilité des enroulements autour du cylindre. Comparativement au cas sur le ruban, les représentations ω_d dépendent de deux paramètres supplémentaires : le poids α pour les boucles non contractiles entourant le cylindre et le paramètre de torsion (*twist parameter*) ν qui tient compte de l'enroulement des défauts. La représentation ρ est introduite dans l'article de Pearce, Rasmussen et Villani [47], qui trouvent les valeurs propres de la matrice de transfert $T_N(\pi/2, \nu)$ du modèle de polymères denses critique ($\beta = 0$) sur le cylindre, émettent les conjectures à propos des règles de sélection et étudient les propriétés du spectre dans la limite thermodynamique. Ils observent que, pour de petits N , dans certaines représentations les matrices de transfert et les hamiltoniens sont non diagonalisables et ont des blocs de Jordan qui apparaissent entre les secteurs étiquetés par d , le nombre de défauts, mais aussi à l'intérieur même des secteurs. Dans cet article, nous procédons à l'étude de la structure des blocs de Jordan intrasectoriels et intersectoriels de $T_N(\lambda, \nu)$. Voici la méthode utilisée et les résultats :

- Nous rappelons les définitions de l'algèbre de Temperley-Lieb périodique et introduisons ses représentations ρ et celles avec torsion ω_d .
- Pour étudier les blocs de Jordan intersectoriels de ρ , nous nous inspirons de l'argument fait au chapitre 2 : nous étudions l'élément central F_N et les singularités dans les composantes de ses vecteurs propres. Cela nous permet de prouver, dans certains cas, l'existence de blocs de Jordan dont le rang est supérieur à 2 et grandit sans cesse avec la taille du réseau N . Nous identifions les circonstances nécessaires à leur présence.

- L'étude des blocs de Jordan intrasectoriels est beaucoup plus ardue, elle se fait à l'aide de l'hamiltonien de boucles. Nous introduisons une autre représentation de l'algèbre de Temperley-Lieb périodique, qui agit sur les spins des modèles XXZ et inclut le paramètre de torsion v , dans laquelle l'hamiltonien est hermitien. Nous montrons qu'il existe un homomorphisme $\tilde{\mathfrak{I}}_{\mathbb{N}}^d$ entre les représentations de boucles et celles des spins XXZ, et que les représentations de part et d'autre sont de grandeurs identiques.
- Nous répondons alors à la question suivante : quand cet homomorphisme est-il un isomorphisme ? C'est là une question cruciale puisque, lorsque deux représentations sont isomorphes, elles ont le même spectre et la même structure de Jordan. Nous introduisons alors une forme bilinéaire, le *produit de Gram*, sur l'espace des vecteurs de connectivités et montrons qu'il y a un isomorphisme lorsque le déterminant de la matrice de cette forme bilinéaire est non nul. Nous montrons que la matrice de Gram se factorise en un produit de deux copies de $\tilde{\mathfrak{I}}_{\mathbb{N}}^d$. Le calcul des déterminants de Gram et de $\tilde{\mathfrak{I}}_{\mathbb{N}}^d$ (exprimées dans des bases appropriées) est ardu, mais possible. Le résultat montre qu'il y a un isomorphisme sauf sur certaines courbes dans le plan (q, v) . Dans ces cas, les valeurs propres des deux représentations sont identiques, et un argument de continuité permet d'étendre ce résultat aux courbes où l'isomorphisme est brisé.
- Enfin, nous utilisons la transformation $\tilde{\mathfrak{I}}_{\mathbb{N}}^d$ aux points où elle est singulière (c'est-à-dire où elle n'est pas un isomorphisme) et l'invariance de l'hamiltonien XXZ sous l'algèbre $U_q(\mathfrak{sl}_2)$ pour certaines valeurs de q et v pour construire certains vecteurs de Jordan de rang 2 de l'hamiltonien de boucles associés à la valeur propre nulle.
- Nous terminons en discutant la présence de blocs de Jordan intrasectoriels décelés par nos explorations par ordinateur, qui peuvent être reliés à des valeurs propres autres que 0 et avoir des rangs plus grands que 2.

Au moment du dépôt de la thèse, cet article était prêt à être soumis dans une revue spécialisée à déterminer. La référence incomplète est :

→ A. Morin-Duchesne, Y. Saint-Aubin, *Jordan cells of periodic loop models*.

Ma contribution à cet article comprend la quasi-totalité des résultats qui sont présentés et énumérés ci-dessus, soit :

- Le développement des représentations de vecteurs de connectivités et des représentations XXZ avec torsion (sections 4.2.3 et 4.3.1) ;

- Le calcul des valeurs propres de F_N , des singularités des composantes de ses vecteurs propres et des blocs de Jordan de F_N et $T_N(\lambda, \nu)$ (section 4.4);
- L'identification de l'homomorphisme entre les représentations XXZ et des vecteurs de connectivité (section 4.3.2);
- La factorisation de la matrice de Gram, le calcul de son déterminant et de celui de la matrice I_N^d de l'homomorphisme (sections 4.3.3 et 4.5);
- Les propriétés d'invariance de l'hamiltonien H du modèle XXZ sous $U_q(\mathfrak{sl}_2)$ (section 4.6.2);
- L'utilisation de sous-espaces caractéristiques de \tilde{i}_N^d autour des valeurs critiques (q_c, ν_c) dans la construction explicite des vecteurs de Jordan intersecto-riels (sections 4.6.1, 4.6.3 et 4.6.4).

Jordan cells of periodic loop models

Alexi Morin-Duchesne

Département de physique

Université de Montréal, C.P. 6128, succ. centre-ville, Montréal

Québec, Canada, H3C 3J7

Yvan Saint-Aubin

Département de mathématiques et de statistique

Université de Montréal, C.P. 6128, succ. centre-ville, Montréal

Québec, Canada, H3C 3J7

Abstract

We study finite loop models on a lattice wrapped around a cylinder. A section of the cylinder has N sites. We use a family of link modules of the periodic Temperley-Lieb algebra $\mathcal{E}TLP_N(\beta, \alpha)$ introduced by Martin and Saleur, and Graham and Lehrer. These extend the link modules \tilde{V}_N^d (standard modules) that are labeled by the numbers of sites N and of defects d . Beside the defining parameters $\beta = u^2 + u^{-2}$ with $u = e^{i\lambda/2}$ (weight of contractible loops) and α (weight of non-contractible loops), this family also depends on a *twist parameter* ν that keeps track of how the defects wind around the cylinder. The transfer matrix $T_N(\lambda, \nu)$ depends on an anisotropy parameter ν and the number λ that fixes the model. (The thermodynamic limit of T_N is believed to describe a conformal field theory of central charge $c = 1 - 6\lambda^2/(\pi(\lambda - \pi))$.)

The family of periodic XXZ Hamiltonians is extended to depend on this new parameter ν and the relationship between this family and the loop models is established. The Gram determinant for the natural bilinear form on these link modules is shown to factorize in terms of a linear map \tilde{i}_N^d between these link modules and the eigenspaces of S^z of the XXZ models. This map is shown to be an isomorphism for generic values of u and ν and the critical curves in the plane of these parameters for which \tilde{i}_N^d fails to be an isomorphism are given. The singular behavior of \tilde{i}_N^d around critical points is shown to provide information about Jordan cells of loop models. An explicit example for an infinite family is constructed.

Keywords : periodic Temperley-Lieb algebra, cylinder Temperley-Lieb algebra, af-

fine Temperley-Lieb algebra, loop models, Gram determinant, Gram matrix, Hamiltonian XXZ, Jordan structure, indecomposable representations, standard modules, Ising model, percolation, Potts models.

4.1 Introduction

Starting from the seminal work of Belavin, Polyakov and Zamolodchikov [16], the description of conformal field theory has been rooted in the representation theory of the Virasoro algebra. The Schramm-Loewner description of critical phenomena, despite its enormous successes, has not provided an easy way to understand the emergence of these representations. (Some efforts were devoted to this problem. See for example [88].) How the Virasoro algebra appears through a limiting process starting from finite lattice models remains an outstanding question of the field.

A while ago, Koo and Saleur [89] proposed a program to build the Virasoro generators L_n starting from lattice models. This program is now being fleshed out in a series of papers by Gainutdinov, Read and Saleur [90, 91] for the $gl(1|1)$ spin chain. Its extension to other models is even more ambitious and will likely require new techniques in the representation theory of the periodic Temperley-Lieb algebra, whose study has been launched by Martin and Saleur [92], Graham and Lehrer [93], and Green and Erdmann [94, 95].

The XXZ Hamiltonians and loop models, with their natural link to Potts models, provide a natural setting to study the emergence of the Virasoro algebra. Both families of models can be formulated using an evolution operator, either a transfer matrix or a Hamiltonian. The linear operators act on natural vector spaces (link modules for the loop models and a tensor product of copies of \mathbb{C}^2 for the XXZs). These vector spaces carry representations of the Temperley-Lieb algebra and the evolution operator can be seen to be an element of this structure.

One of the key elements in identifying the Virasoro representations that may appear in the limiting conformal field theory (CFT) is the Jordan structure of the transfer matrix (or Hamiltonian) of the finite model. Since the generator L_0 of the Virasoro algebra usually arises from some scaling limit of these matrix or Hamiltonian, a non-trivial Jordan structure in them, if it survives the limiting process, would rule out, as building blocks of the underlying CFT, highest-weight representations where L_0 acts diagonally. Many before us have argued that such Jordan cells are a signature of logarithmic conformal field theories. If this is so, a better un-

derstanding of these cells might also reveal physical observables that are genuinely logarithmic, that is, observables that do not appear in usual CFT.

For specific boundary conditions, Pearce, Rasmussen and Zuber [45] showed that, at least in a few specific cases, the transfer matrix of the loop models has Jordan blocks. In [77] a general analysis of these transfer matrices for open boundary conditions led to a precise criterion on the closed loop weight $\beta = 2 \cos \lambda$ (the central charge is then $c = 1 - 6\lambda^2/(\pi(\lambda - \pi))$) and the size of the lattice N for such Jordan blocks to exist. In the case of the XXZ models, the algebra $U_q(\mathfrak{sl}_2)$ also acts on the vector space and the presence of indecomposable representations of the latter structure gave early in [35] a clear indication of non-diagonalizability of the Hamiltonians. It is clear that precise criteria for other models and boundary conditions need to be proved.

In this paper we start putting together tools to study the loop models on the cylinder. It is first useful to survey the tools that were previously successful for other boundary conditions. One of them is a central element of the Temperley-Lieb algebra (called the *braid transfer matrix* in [45, 47] and F_N in [77]) that appears as a Fourier coefficient of the transfer matrix. Since this central element is non-diagonal on certain representations, it allows one to identify some Jordan blocks of the transfer matrix. Unfortunately, the analogous element in the periodic case turns out to be diagonal on many of the representations of interest. One other tool is the homomorphism, hereafter denoted by \tilde{i}_N^d , of some submodules of the loop models into eigensubspaces of S^z used for the XXZ models. This will be particularly useful in the periodic case because, for generic values of the parameters, this map turns out to be an isomorphism of modules. This tool is intimately related to one other : the Gram matrix. There is a bilinear form on link modules that is invariant under the action of the Temperley-Lieb algebra. The Gram matrix represents this bilinear form in the link state basis. The radical of this bilinear form, that is the set of vectors that have a zero pairing with any other, is easily shown to be a submodule. It is non-trivial if and only if the determinant of the Gram matrix vanishes [96, 64, 97]. Non-trivial Jordan structure are often related to the radical being non-zero and it would be useful to know for which values of the parameters the Gram determinant vanishes. However the map \tilde{i}_N^d will soon appear to be a finer tool.

The Jordan structure of the transfer matrix is of course not the only relevant property of this object. The transfer matrix can also be used in partition functions to compute physical properties. For example periodic boundary conditions are of

course relevant for a cylindrical geometry. Then winding properties of clusters as they evolve along the cylinder should be somehow computable from this transfer matrix. If the two ends of a finite cylinder are joined, the homotopy properties of the clusters on the torus may also be considered [98, 99]. However the link modules used to describe loop models (also known as standard modules) do not keep track of the winding of loops. One way to circumvent this problem was proposed by Richard and Jacobsen [55]. We propose here another one. We choose to use modules [92, 93] that depend on one more parameter than the usual link modules. As will be seen, the new parameter, called the *twist parameter* v , is related to the winding of loops. Most results in this paper characterize this family of modules and the homomorphism $\tilde{\mathfrak{i}}_{\mathbb{N}}^d$.

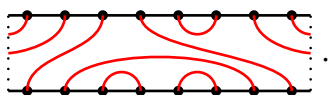
The paper is organized as follows. Section 4.2 defines the periodic Temperley-Lieb algebras, the transfer matrix for the loop models and the family of representations depending on a *twist parameter*. Section 4.3 extends the periodic XXZ Hamiltonians into a family that, like the representations, depends on one more parameter. It is then possible to introduce a linear map $\tilde{\mathfrak{i}}_{\mathbb{N}}^d$ between link modules and the vector spaces upon which the XXZ Hamiltonians act. The factorization of the Gram matrix in terms of the map $\tilde{\mathfrak{i}}_{\mathbb{N}}^d$ is proven there. Section 4.4 tackles the problem of Jordan blocks between sectors of link modules, that is sectors characterized by different numbers of defects (see subsection 4.2.3 for the definition of defects). The techniques used there were developed in [77] and do not require the homomorphism $\tilde{\mathfrak{i}}_{\mathbb{N}}^d$. (The sections that follow are independent of it.) The rest of the paper is aimed at probing Jordan cells within a given sector, one with a fixed number of defects. Section 4.5 gives a new computation of the Gram determinant, one that leads to the identification of the critical curves where the map $\tilde{\mathfrak{i}}_{\mathbb{N}}^d$ becomes singular. This is where the proof that $\tilde{\mathfrak{i}}_{\mathbb{N}}^d$ is actually an homomorphism ends. Finally section 4.6 analyzes the behavior of the map $\tilde{\mathfrak{i}}_{\mathbb{N}}^d$ as a function of its parameters, in a neighborhood of a point on a critical curve. The information around such a point is shown to provide explicit expressions for Jordan cells in an infinite family of loop models. Though limited this example gives a glimpse of the power of these new tools.

4.2 Periodic Temperley-Lieb algebras and loop models

4.2.1 Periodic Temperley-Lieb algebras

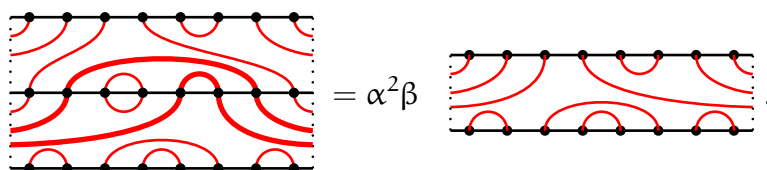
On a vertical cylinder, we draw N equidistant points (or entries) on each of two parallel sections and label them 1 to N . A connectivity is a set of N curves connecting points pairwise by non-intersecting curves. Two connectivities are equivalent (or equal) if the curves of the first can be continuously deformed into those of the second. Clearly a rotation of $2\pi/N$ of the cylinder maps a connectivity onto another; these two connectivities, the original and the rotated, are usually distinct as their patterns of connections are then different.

Throughout this article we will depict connectivities by planar diagrams on a periodic strip, as in the following



The leftmost point on the top and bottom slices bears the label 1, the rightmost the label N . The cut along a line parallel to the cylinder axis that allows this planar representation is depicted using dotted lines at $x = 1/2$ and $x = N + 1/2$. These lines will be called *imaginary boundaries*.

A product between two connectivities c_1 and c_2 with N entries is now defined. The product $c_1 c_2$ is obtained by drawing c_2 on top of c_1 and connecting the N points on the bottom of c_2 with those at the top of c_1 . The result is the connectivity obtained from this new diagram, with a multiplicative factor of $\beta^{n_\beta} \alpha^{n_\alpha}$ where n_β and n_α are respectively the numbers of contractible and non-contractible loops closed in the process. For instance,



The two non-contractible loops, responsible for the factor α^2 , are drawn thicker here. Because curves can wind around the cylinder indefinitely, the number of connectivities is infinite.

DEFINITION 4.2.1 *The algebra $\mathcal{TL}\mathcal{P}_N(\beta, \alpha)$ is the vector space generated by connectivities and endowed with the product just defined and extended linearly to linear combinations of connectivities. The unit in $\mathcal{TL}\mathcal{P}_N(\beta, \alpha)$ is the connectivity that connects the point i on the bottom to the point i on the top, for all i , with no winding.*

We now define an abstract algebra, the periodic Temperley-Lieb algebra. Note that we use capital letters to denote it, instead of calligraphic ones for the algebra of connectivities.

DEFINITION 4.2.2 *The periodic Temperley-Lieb algebra $\text{TLP}_N(\beta)$ is the algebra generated by a unit id and the generators e_i , $i = 1, \dots, N$, constrained by the following relations*

$$\begin{aligned} e_i^2 &= \beta e_i, \\ e_i e_j &= e_j e_i, \quad \text{for } |i - j| > 1 \\ e_i e_{i\pm 1} e_i &= e_i. \end{aligned} \tag{4.2.1}$$

The indices are understood to be taken, modulo N , in the range $1, \dots, N$, and therefore $e_0 \equiv e_N$ and $e_{N+1} \equiv e_1$.

DEFINITION 4.2.3 *The enlargement of $\text{TLP}_N(\beta)$, denoted $\mathcal{E}\text{TLP}_N(\beta)$, is generated by id , the e_i s and two more generators, Ω and Ω^{-1} , satisfying (4.2.1) together with*

$$\begin{aligned} \Omega e_i \Omega^{-1} &= e_{i-1}, \\ \Omega \Omega^{-1} &= \Omega^{-1} \Omega = \text{id}, \\ (\Omega^{\pm 1} e_N)^{N-1} &= \Omega^{\pm N} (\Omega^{\pm 1} e_N) \end{aligned} \tag{4.2.2}$$

with, again, the indices i of the e_i s taken modulo N . The last relation can also be written as $e_{N-1} \dots e_1 = \Omega^2 e_1$ and $e_1 \dots e_{N-1} = \Omega^{-2} e_{N-1}$.

The generator Ω will be referred to as the *translation operator*. The relations (4.2.1) can be translated in terms of three generators of $\mathcal{E}\text{TLP}_N(\beta)$,

$$\begin{aligned} e_N^2 &= \beta e_N, \\ e_N \Omega^j e_N \Omega^{-j} &= \Omega^j e_N \Omega^{-j} e_N, \quad \text{for } 2 \leq j \leq N-2, \\ e_N \Omega^{\mp 1} e_N \Omega^{\pm 1} e_N &= e_N. \end{aligned} \tag{4.2.3}$$

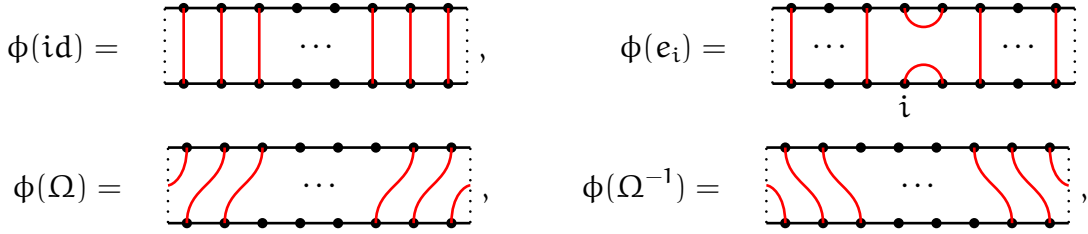
The identification of e_N and e_0 is simply $\Omega^N e_N \Omega^{-N} = e_N$. The algebra $\mathcal{E}\text{TLP}_N(\beta)$ is then just $\langle e_N, \Omega, \Omega^{-1} \rangle$ constrained by these relations. Finally a last algebra will be used.

DEFINITION 4.2.4 *For N even, we define $\mathcal{E}\text{TLP}_N(\beta, \alpha)$ to be the quotient of $\mathcal{E}\text{TLP}_N(\beta)$ by the relation*

$$E \Omega^{\pm 1} E = \alpha E, \quad \text{where } E = e_2 e_4 \dots e_{N-2} e_N. \tag{4.2.4}$$

From this quotient, it also follows that $F\Omega^{\pm 1}F = \alpha F$, where $F = e_1 e_3 e_5 \dots e_{N-1}$. Despite this quotient, the algebra $\mathcal{E}TLP_N(\beta, \alpha)$ is still infinite as it contains the infinite subalgebra $\langle \Omega \rangle$. For N odd, we take no further quotient, but, for simplicity, we will still write $\mathcal{E}TLP_N(\beta, \alpha)$ for the enlargement of the $TLP_N(\beta)$ algebra.

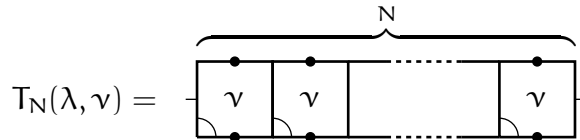
To each $g \in \mathcal{E}TLP_N(\beta, \alpha)$, we associate a connectivity $c = \phi(g) \in \mathcal{TLP}(\beta, \alpha)$ as follows : to each generator we associate



and for any $g = \prod_i f_i$ a product of the generators of $\mathcal{E}TLP_N(\beta, \alpha)$ (with $f_i \in \{e_1, \dots, e_N, \Omega, \Omega^{-1}\}$), we set $\phi(g) = \prod_i \phi(f_i)$, with the same product of diagrams defined for $\mathcal{TLP}_N(\beta, \alpha)$. One can verify that equations (4.2.1) and (4.2.2) are satisfied if we replace e_i, Ω and Ω^{-1} by $\phi(e_i), \phi(\Omega)$ and $\phi(\Omega^{-1})$. So $\phi : \mathcal{E}TLP_N(\beta, \alpha) \rightarrow \mathcal{TLP}_N(\beta, \alpha)$ is a homomorphism of algebras. It is clearly surjective as all generators of $\mathcal{TLP}_N(\beta, \alpha)$ have preimages. Moreover, Green and Fan [100] have shown that ϕ is injective. In this sense, $\mathcal{E}TLP_N(\beta, \alpha)$ and $\mathcal{TLP}_N(\beta, \alpha)$ are isomorphic, and throughout the rest of this paper we will use $\mathcal{E}TLP_N(\beta, \alpha)$ to denote both the algebra of connectivities and $\langle e_N, \Omega, \Omega^{-1} \rangle / (\text{relations (4.2.2), (4.2.3), (4.2.4)})$.

4.2.2 The loop transfer matrix $T_N(\lambda, \nu)$

DEFINITION 4.2.5 *The loop transfer matrix $T_N(\lambda, \nu)$ is an element of $\mathcal{E}TLP_N(\beta, \alpha)$ defined by*



where the boxes are given by

$$\boxed{\nu} = \sin(\lambda - \nu) \begin{array}{|c|} \hline \text{red loop} \\ \hline \end{array} + \sin \nu \begin{array}{|c|} \hline \text{red loop} \\ \hline \end{array} = \boxed{\lambda - \nu},$$

$\beta = 2 \cos \lambda, \nu$ is the anisotropy and the leftmost and rightmost boxes are connected.

The loop transfer matrix, or simply *transfer matrix*, is related to the Fortuin-Kasteleyn description of two-dimensional lattice models and has many crucial mathematical

properties. (Several of the following properties were proved in a general context in [63]. Proofs and discussion of these properties in a context similar to the present one can be found in [45, 47]. The tie with lattice models is found in [52] or, for a presentation similar to the one here, in [77] for example.)

- (i) It satisfies the Yang-Baxter equation : $[T_N(\lambda, \nu_1), T_N(\lambda, \nu_2)] = 0$ for all ν_1 and ν_2 .
- (ii) It satisfies a crossing-reflection symmetry : $T_N(\lambda, \lambda - \nu) = R^{-1}T_N(\lambda, \nu)R$ where R is the left-right reflection : $e_i = R^{-1}e_{N-i}R$.
- (iii) It is invariant under translation : $[T_N(\lambda, \nu), \Omega] = 0$.
- (iv) Its expansion around $\nu = 0$ is

$$T_N(\lambda, \nu) \simeq \Omega \sin^N \lambda [(1 - \nu N \cot \lambda) \text{id} + \nu \mathcal{H} / \sin \lambda] + \mathcal{O}(\nu^2)$$

where

$$\mathcal{H} = \sum_{i=1}^N e_i. \quad (4.2.5)$$

It is this transfer matrix whose properties we seek to elucidate. In many situations, we shall have to settle for the simpler task of studying the linear term \mathcal{H} which will be called the Hamiltonian for loop models.

4.2.3 Link states and representations of $\mathcal{E}TLP_N(\beta, \alpha)$

In the following, we will work with link representations of $\mathcal{E}TLP_N(\beta, \alpha)$ similar to those introduced in [47]. They extend to the periodic case the link representations of the (original) Temperley-Lieb algebra introduced for models on a strip [58, 64]. (See also [45, 77].)

Again N points (sometimes called *entries*) are aligned equidistant on a section of a vertical cylinder. A *link state* w (or *link pattern*) is a graph where the N points are either connected pairwise by non-intersecting curves or connected by a straight line to $+\infty$. The non-intersecting curves and half-lines are drawn above the section, that is, on one side of it. A point connected to infinity will be called a *defect* and the number of defects of a link state will usually be denoted by d . The set \tilde{B}_N of link states with N entries is naturally partitioned in the subsets \tilde{B}_N^d s of link states with N entries and d defects (with $N \equiv d \pmod{2}$), each containing $\binom{N}{(N-d)/2}$ elements. The vector spaces generated by \tilde{B}_N and \tilde{B}_N^d are noted \tilde{V}_N and \tilde{V}_N^d respectively.

By convention, the elements of \tilde{B}_N are ordered in ascending number of defects. When drawn in the plane, entries are placed on the horizontal axis at points of coordinates $(1, 0)$, $(2, 0)$, ..., $(N, 0)$, and the diagram for link states is taken to be periodic in the x direction with $x + N \equiv x$. The curves connecting the entries can connect through the imaginary boundary line at $x = 1/2$ and $x = N + 1/2$. We will call these curves *boundary curves* or *boundary bubbles*. Here are the three subsets \tilde{B}_N^d for $N = 4$:

$$\begin{aligned} \tilde{B}_4^0 &= \{ \text{diagram 1}, \text{diagram 2}, \text{diagram 3}, \text{diagram 4}, \text{diagram 5} \}, \\ \tilde{B}_4^2 &= \{ \text{diagram 6}, \text{diagram 7}, \text{diagram 8}, \text{diagram 9} \}, \quad \tilde{B}_4^4 = \{ \text{diagram 10} \}. \end{aligned} \quad (4.2.6)$$

The sets B_N^d and B_N , without “~”, will refer to the subsets of \tilde{B}_N^d and \tilde{B}_N containing link patterns with no boundary curves (and similarly for V_N and V_N^d , the vector spaces they span). These form the sets of link states used for representations of the (original) Temperley-Lieb algebra. We note that the set \tilde{B}_N^d corresponds to the set of *distinct link states* used by Pearce, Rasmussen and Villani [47]. (We shall not use their set of *identified link states*.)

DEFINITION 4.2.6 (THE MAP $\omega_d : \mathcal{E}TLP_N(\beta, \alpha) \rightarrow \text{END}(\tilde{V}_N^d)$) *Let c be a connectivity in $\mathcal{E}TLP_N(\beta, \alpha)$ and $w \in \tilde{B}_N^d$. An action of the diagram c on w is defined by joining the N entries of the link state w to the N top entries of c . The resulting link pattern is found by reading the new connections at the bottom N points of c . The result is then multiplied by the following factors: weights related to closed loops (a factor of β for each contractible loop and one of α for each non-contractible one) and weights due to the lateral twist of defects. These are computed as follows. First, if two defects are connected in the diagram cw , the result is set to 0. Second, for each defect in w , a multiplicative factor of v^Δ is added, where Δ is the distance the defect has traveled toward the left, that is, its position in the original state w minus its new one in the resulting cw . (Again, consecutive positions in w are at distance of 1.) The constant v is the twist parameter. The map ω_d is obtained by extending this action linearly to all elements in $\mathcal{E}TLP_N(\beta, \alpha)$ and depends on v : $\omega_d = \omega_d(v)$.*

DEFINITION 4.2.7 (THE MAP $\rho : \mathcal{E}TLP_N(\beta, \alpha) \rightarrow \text{END}(\tilde{V}_N)$) *The action of a connectivity c is defined as for ω_d except that defects may be connected. Consequently the number of defects may stay the same or decrease. The multiplicative factors of α and β are computed as for ω_d , but no powers of v is added (or v is set to 1).*

Examples are useful in understanding the product just defined. Here are computations for ω_d .

$$\begin{aligned}
 &= \beta^2 v^{-2} \downarrow \text{---} \downarrow \\
 &= 0 \\
 &= \alpha^2 \beta \downarrow \text{---} \downarrow
 \end{aligned}$$

In the first example, the first defect has $\Delta_1 = 2$ and the second $\Delta_2 = -4$, resulting in an overall factor of $v^{\Delta_1 + \Delta_2} = v^{-2}$. As a last example, note that Ω shifts the link pattern w one position to the left and therefore multiplies the resulting state by a factor v^d . Had we used the action of ρ instead, the results of the first and second examples would have been $\beta^2 \downarrow \text{---} \downarrow$ and $\beta \downarrow \text{---} \downarrow$ while that of the third example would have remained unchanged.

PROPOSITION 4.2.1 ω_d and ρ are representations of $\mathcal{ETLP}_N(\beta, \alpha)$.

We do not give the details of this proof as the verification is standard, though tedious. It suffices to show that the defining relations (4.2.1), (4.2.2) and (4.2.4) hold when acting on any link state $w \in \tilde{\mathcal{B}}_N^d$. The relations (4.2.1) and (4.2.2) involve at most four entries of the link state (except for the last one of (4.2.2)) so that, for these, one may concentrate on the two, three or four connections changed. The other two equations can also be seen to hold, and we leave the verifications to the reader. The result is nevertheless non-trivial. Indeed, imposing that connecting defects give 0 is essential, as the map ω_d would not be a representation of $\mathcal{ETLP}_N(\beta, \alpha)$ otherwise. For example,

$$\begin{aligned}
 e_3 e_1 \left(\downarrow \text{---} \downarrow \right) &= \text{---} = v^{-2} \text{---} = v^{-2} \text{---} \\
 e_1 e_3 \left(\downarrow \text{---} \downarrow \right) &= \text{---} = v^2 \text{---} = v^2 \text{---}
 \end{aligned}$$

Because $e_1 e_3 = e_3 e_1$ in $\mathcal{E}TLP_N$, $N \geq 4$, this would not have been a representation. This also means that, to define an action of the whole link space \tilde{V}_N like that of ρ , the twist v should solve some algebraic constraints, like the above $v^4 = 1$. The choice $v = 1$ works for all $\mathcal{E}TLP_N$.

The usefulness of the representation ω_d with its twist parameter v stems from the fact that $\omega_d(\Omega^N) = v^{Nd} \text{id}$ and not simply id . It therefore allows one to keep track of the winding number of Fortuin-Kasteleyn clusters along the cylinder, a physical property that plays an important role in the mathematical description of these models [98, 99, 38]. Another appropriate name for the parameter v would have been the *momentum parameter*. Indeed Ω acts as a translation operator around the cylinder, or a rotation operator. Clearly its eigenvalues are expressed in terms of v and should be interpreted as the possible values of the momentum.

4.3 The loop transfer matrix and the Hamiltonians H_{XXZ}

On the strip, the loop models are intimately related to another family of physically relevant ones. Both models are defined by an “evolution operator”: the transfer matrix for the loop models and a Hamiltonian for the XXZ models. Even though the vector spaces upon which the evolution operators act do not have the same dimensions, they both carry a representation of the (original) Temperley-Lieb algebra. Often properties of one of the models can teach us something about the properties of the other and we therefore introduce in this section a similar relation between loop models and the XXZ Hamiltonians on the cylinder.

4.3.1 An extended family of XXZ models

Instead of working with the full transfer matrix, we concentrate on the first non-trivial term in its expansion around $u = 0$, given in (4.2.5): $\mathcal{H} = \sum_{1 \leq i \leq N} e_i$. Since the usual XXZ Hamiltonians are maps of $(\mathbb{C}^2)^{\otimes N}$ onto itself, we need to define a representation of $\mathcal{E}TLP(\beta, \alpha)$ on this vector space, or at least of $TLP_N(\beta)$. Then the XXZ Hamiltonians will simply be $H = \sum_{1 \leq i \leq N} \bar{e}_i$ where \bar{e}_i are the matrices representing the generators e_i of $\mathcal{E}TLP_N(\beta, \alpha)$.

We use the usual notation

$$\sigma_j^a = \underbrace{\text{id}_2 \otimes \cdots \otimes \text{id}_2}_{j-1} \otimes \sigma^a \otimes \underbrace{\text{id}_2 \otimes \cdots \otimes \text{id}_2}_{N-j}$$

for $1 \leq j \leq N$ and $a \in \{x, y, z, +, -\}$, and we set $\sigma_{N+1}^a \equiv \sigma_1^a$. The tensor product contains N two-by-two matrices and σ^a is the j -th factor in this product. The matrices $\bar{e}_j \in \text{End}((\mathbb{C}^2)^{\otimes N})$ are

$$\begin{aligned} \bar{e}_j &= \frac{1}{2} \left(\frac{v^2 + v^{-2}}{2} (\sigma_j^x \sigma_{j+1}^x + \sigma_j^y \sigma_{j+1}^y) + \frac{v^2 - v^{-2}}{2i} (\sigma_j^x \sigma_{j+1}^y - \sigma_j^y \sigma_{j+1}^x) \right. \\ &\quad \left. - \frac{u^2 + u^{-2}}{2} (\sigma_j^z \sigma_{j+1}^z - \text{id}) + \frac{u^2 - u^{-2}}{2} (\sigma_j^z - \sigma_{j+1}^z) \right) \\ &= v^{-2} \sigma_j^- \sigma_{j+1}^+ + v^2 \sigma_j^+ \sigma_{j+1}^- - (u^2 + u^{-2}) \sigma_j^+ \sigma_j^- \sigma_{j+1}^+ \sigma_{j+1}^- + u^2 \sigma_j^+ \sigma_j^- + u^{-2} \sigma_{j+1}^+ \sigma_{j+1}^- \\ &= \underbrace{\text{id}_2 \otimes \text{id}_2 \otimes \cdots \otimes \text{id}_2}_{j-1} \otimes \bar{e} \otimes \underbrace{\text{id}_2 \otimes \text{id}_2 \otimes \cdots \otimes \text{id}_2}_{N-j-1} \end{aligned} \quad (4.3.1)$$

with

$$\bar{e} = \begin{pmatrix} 0 & 0 & 0 & 0 \\ 0 & u^2 & v^2 & 0 \\ 0 & v^{-2} & u^{-2} & 0 \\ 0 & 0 & 0 & 0 \end{pmatrix},$$

where the allowed values for j are from 1 to N for the first two forms and from 1 to $N - 1$ for the last. The periodic XXZ Hamiltonian found in [35] also depends upon a twist parameter (named $e^{i\varphi}$ therein) which only enters in the definition of first generator \bar{e}_N . We note however that a similarity transformation $\mathcal{O} \bar{e}_i \mathcal{O}^{-1}$, with $\mathcal{O} = v^{\sum_{j=1}^N j \sigma_j^z}$, maps our generators to theirs if $e^{i\varphi} = v^{2N}$.

If $S^z = \frac{1}{2} \sum_{1 \leq i \leq N} \sigma_i^z$, it is clear from the second form that each \bar{e}_j commutes with S^z . The matrices \bar{e}_j are not hermitian. But, when u and v are on the unit circle, the first three terms of the first form in (4.3.1) are clearly hermitian. Only the term $\frac{1}{2}(u^2 - u^{-2})(\sigma_j^z - \sigma_{j+1}^z)$ is not. Finally one can verify that these matrices satisfy the relations (4.2.1), with $\bar{e}_{N+1} \equiv \bar{e}_1$ and $\beta = u^2 + u^{-2}$. Therefore

PROPOSITION 4.3.1 *The matrices \bar{e}_i , $1 \leq i \leq N$, form a representation of $\text{TLP}_N(\beta = u^2 + u^{-2})$ for all $v \in \mathbb{C}^\times$.*

We shall often use the following parametrization for u and v : $u = e^{i\lambda/2}$, $v = e^{i\mu}$. When μ and λ are real, the Hamiltonian $H = H(u, v) = \sum_{i=1}^N \bar{e}_i$ is therefore hermitian, since the sum $\sum_j (\sigma_j^z - \sigma_{j+1}^z)$ then vanishes. The usual XXZ model corresponds

to the case $v^2 = 1$ (for the case with boundary see for example [35] and also [101] where the interplay between loop models and XXZ Hamiltonian has been exploited).

We finally introduce the matrices $t^{\pm 1}$ and $\bar{\Omega}^{\pm 1}$. The operators t and t^{-1} are left and right translations around the cylinder. In the basis $|x_1, x_2, \dots, x_N\rangle$ where every $x_i \in \{+1, -1\}$, they act as

$$\begin{aligned} t|x_1, x_2, \dots, x_N\rangle &= |x_2, x_3, \dots, x_N, x_1\rangle \\ t^{-1}|x_1, x_2, \dots, x_N\rangle &= |x_N, x_1, x_2, \dots, x_{N-1}\rangle \end{aligned}$$

and satisfy $t^{\pm 1}\sigma_j^a = \sigma_{j\mp 1}^a t^{\pm 1}$. Then we define $\bar{\Omega}^{\pm 1} = v^{\pm 2S^z} t^{\pm 1}$. Because $t\bar{e}_j = \bar{e}_{j-1}t$ and $[v^{2S^z}, \bar{e}_j] = 0$, the first and second equations of (4.2.2), $\bar{\Omega}\bar{e}_j\bar{\Omega}^{-1} = \bar{e}_{j-1}$ and $\bar{\Omega}\bar{\Omega}^{-1} = \bar{\Omega}^{-1}\bar{\Omega} = \text{id}$, are both satisfied. That

$$(\bar{\Omega}^{\pm 1}\bar{e}_N)^{N-1} = \bar{\Omega}^{\pm N}(\bar{\Omega}^{\pm 1}\bar{e}_N) \quad (4.3.2)$$

holds is far less trivial. Moreover, to check that the matrices \bar{e}_i and $\bar{\Omega}^{\pm 1}$ form a representation of $\mathcal{E}\text{TLP}(\beta, \alpha)$, we would have also to check that, when N is even,

$$\bar{E}\bar{\Omega}^{\pm 1}\bar{E} = \alpha\bar{E} \quad (4.3.3)$$

for $\bar{E} = \bar{e}_2\bar{e}_4\bar{e}_6\dots\bar{e}_N$ and some $\alpha = \alpha(u, v)$. There might be a way to prove (4.3.2) and (4.3.3) by direct computation. We prefer a more roundabout way. Let us denote by X the map defined on the generators by $e_i \mapsto \bar{e}_i$ and $\Omega^{\pm} \mapsto \bar{\Omega}^{\pm}$. This map is a representation of $\text{TLP}_N(\beta)$ and satisfies also the two first relations in (4.2.2). In section 4.5.5 we shall show that there exists an isomorphism \tilde{i}_N^d of vector spaces, for generic values of u and v , between the XXZ and the link state representations that intertwines the Ω and $\bar{\Omega}$: $\tilde{i}_N^d \circ \Omega^{\pm 1} = \bar{\Omega}^{\pm 1} \circ \tilde{i}_N^d$. It will then follow that equations (4.3.2) and (4.3.3) are satisfied for *all* values of u and v and that X is a representation of $\mathcal{E}\text{TLP}_N(\beta, \alpha)$ where the parameter α is equal to $v^N + v^{-N}$. Thus v comes into play both as a twist parameter and in the weight of non-contractible loops wrapping around the cylinder.

4.3.2 The map \tilde{i}_N^d between link and spin states

Let $w \in \tilde{\mathcal{B}}_N^d$ be a link state containing $n = (N - d)/2$ bubbles and let $\psi(w) = \{(p_1, q_1), (p_2, q_2), \dots, (p_n, q_n)\}$, where the p_i s are positions where bubbles start and the q_i s the positions where they end. The p_i s are chosen in the interval $1, \dots, N$ while

the q_i s satisfy $p_i + 1 \leq q_i \leq N + p_i - 1$. In $\psi(w)$, the pairs (p_i, q_i) are ordered such that the p_i s increase, even though this will play no role.

DEFINITION 4.3.1 Let $w \in \tilde{B}_N^d$. We define the linear transformation $\tilde{i}_N^d : \tilde{V}_N^d \rightarrow (\mathbb{C}^2)^{\otimes N}|_{S^z=d/2}$ whose action on the basis elements of \tilde{B}_N^d is :

$$\tilde{i}_N^d(w) = \prod_{(i,j) \in \psi(w)} \tilde{T}_{i,j}|0\rangle \quad \text{where} \quad \tilde{T}_{i,j} = v^{j-i}u\sigma_j^- + v^{-(j-i)}u^{-1}\sigma_i^-, \quad (4.3.4)$$

and $|0\rangle = |+, +, \dots, +\rangle$ is the unique state with all spins up.

Some states have boundary bubbles, that is bubbles that cross the imaginary boundaries at $x = 1/2$ and $x = N + 1/2$. This happens when a point i is connected to a point $j \geq N + 1$. As usual we then use the convention that $\sigma_j^\pm \equiv \sigma_{j \bmod N}^\pm$.

PROPOSITION 4.3.2 For all $c \in \mathcal{E}TLP_N(\beta, \alpha)$ and all $w \in \tilde{V}_N^d$, $\tilde{i}_N^d(cw) = X(c)\tilde{i}_N^d(w)$, where $\beta = u^2 + u^{-2}$, $\alpha = v^N + v^{-N}$, the twist parameter is v and the action on \tilde{V}_N^d is that of the representation ω_d .

Once equations (4.3.2) and (4.3.3) have been established, this proposition will simply state that \tilde{i}_N^d is an intertwiner between the representations ω_d and X when the parameters of $\mathcal{E}TLP_N(\beta, \alpha)$ are chosen to be $\beta = u^2 + u^{-2}$ and $\alpha = v^N + v^{-N}$.

PROOF It actually suffices to check that $\tilde{i}_N^d(cw) = X(c)\tilde{i}_N^d(w)$ holds when c is one of the generators e_i , Ω or Ω^{-1} , and $w \in \tilde{B}_N^d$. Let $Y(w) = \prod_{(m,n) \in \psi'(w)} \tilde{T}_{m,n}$ and $\psi'(w)$ be the part of $\psi(w)$ that does not touch points i , $i + 1$, j and k (see the diagrams below for the meaning of these indices). We give below a list of relations that are sufficient to establish the result. For each element of this list, we give the diagrammatic relation and its algebraic counterpart to be checked explicitly. For the diagrammatic relations, we draw in w only the positions that play a role in the verification. For example, in the first, the check is for all vectors w whose positions i and $i + 1$ are defects and, because e_i acts only on these positions, they are the only ones drawn.

$$\begin{aligned} 1) & X \left(\begin{array}{c} \text{blue arcs} \\ \text{red dots} \\ \text{position } i \end{array} \right) \tilde{i}_N^d \left(\begin{array}{c} \text{blue arcs} \\ \text{red dots} \\ \text{position } i \end{array} \right) = \tilde{i}_N^d \left(\begin{array}{c} \text{blue arcs} \\ \text{red dots} \\ \text{position } i \end{array} \right) = 0 \\ & \rightarrow \bar{e}_i Y(w)|0\rangle = 0, \\ 2) & X \left(\begin{array}{c} \text{blue arcs} \\ \text{red dots} \\ \text{position } i \end{array} \right) \tilde{i}_N^d \left(\begin{array}{c} \text{blue arcs} \\ \text{red dots} \\ \text{position } i \end{array} \right) = (u^2 + u^{-2}) \tilde{i}_N^d \left(\begin{array}{c} \text{blue arcs} \\ \text{red dots} \\ \text{position } i \end{array} \right) \\ & \rightarrow \bar{e}_i \tilde{T}_{i,i+1} Y(w)|0\rangle = (u^2 + u^{-2}) \tilde{T}_{i,i+1} Y(w)|0\rangle, \end{aligned}$$

$$\begin{aligned}
3) & X \left(\begin{array}{c} \text{---} \text{---} \text{---} \\ \text{---} \text{---} \text{---} \\ \text{---} \text{---} \text{---} \\ \text{---} \text{---} \text{---} \\ \text{---} \text{---} \text{---} \\ \text{---} \text{---} \text{---} \end{array} \right) \tilde{i}_N^d \left(\begin{array}{c} \text{---} \text{---} \text{---} \\ \text{---} \text{---} \text{---} \\ \text{---} \text{---} \text{---} \\ \text{---} \text{---} \text{---} \\ \text{---} \text{---} \text{---} \\ \text{---} \text{---} \text{---} \end{array} \right) = v^{i-j} \tilde{i}_N^d \left(\begin{array}{c} \text{---} \text{---} \text{---} \\ \text{---} \text{---} \text{---} \\ \text{---} \text{---} \text{---} \\ \text{---} \text{---} \text{---} \\ \text{---} \text{---} \text{---} \\ \text{---} \text{---} \text{---} \end{array} \right) \\
& \rightarrow \bar{e}_i \tilde{T}_{i+1,j} Y(w) |0\rangle = v^{i-j} \tilde{T}_{i,i+1} Y(w) |0\rangle, \\
4) & X \left(\begin{array}{c} \text{---} \text{---} \text{---} \\ \text{---} \text{---} \text{---} \\ \text{---} \text{---} \text{---} \\ \text{---} \text{---} \text{---} \\ \text{---} \text{---} \text{---} \\ \text{---} \text{---} \text{---} \end{array} \right) \tilde{i}_N^d \left(\begin{array}{c} \text{---} \text{---} \text{---} \\ \text{---} \text{---} \text{---} \\ \text{---} \text{---} \text{---} \\ \text{---} \text{---} \text{---} \\ \text{---} \text{---} \text{---} \\ \text{---} \text{---} \text{---} \end{array} \right) = v^{i+1-j} \tilde{i}_N^d \left(\begin{array}{c} \text{---} \text{---} \text{---} \\ \text{---} \text{---} \text{---} \\ \text{---} \text{---} \text{---} \\ \text{---} \text{---} \text{---} \\ \text{---} \text{---} \text{---} \\ \text{---} \text{---} \text{---} \end{array} \right) \\
& \rightarrow \bar{e}_i \tilde{T}_{j,i} Y(w) |0\rangle = v^{i+1-j} \tilde{T}_{i,i+1} Y(w) |0\rangle, \\
5) & X \left(\begin{array}{c} \text{---} \text{---} \text{---} \\ \text{---} \text{---} \text{---} \\ \text{---} \text{---} \text{---} \\ \text{---} \text{---} \text{---} \\ \text{---} \text{---} \text{---} \\ \text{---} \text{---} \text{---} \end{array} \right) \tilde{i}_N^d \left(\begin{array}{c} \text{---} \text{---} \text{---} \\ \text{---} \text{---} \text{---} \\ \text{---} \text{---} \text{---} \\ \text{---} \text{---} \text{---} \\ \text{---} \text{---} \text{---} \\ \text{---} \text{---} \text{---} \end{array} \right) = \tilde{i}_N^d \left(\begin{array}{c} \text{---} \text{---} \text{---} \\ \text{---} \text{---} \text{---} \\ \text{---} \text{---} \text{---} \\ \text{---} \text{---} \text{---} \\ \text{---} \text{---} \text{---} \\ \text{---} \text{---} \text{---} \end{array} \right) \\
& \rightarrow \bar{e}_i \tilde{T}_{i,k} \tilde{T}_{i+1,j} Y(w) |0\rangle = \tilde{T}_{i,i+1} \tilde{T}_{j,k} Y(w) |0\rangle, \\
6) & X \left(\begin{array}{c} \text{---} \text{---} \text{---} \\ \text{---} \text{---} \text{---} \\ \text{---} \text{---} \text{---} \\ \text{---} \text{---} \text{---} \\ \text{---} \text{---} \text{---} \\ \text{---} \text{---} \text{---} \end{array} \right) \tilde{i}_N^d \left(\begin{array}{c} \text{---} \text{---} \text{---} \\ \text{---} \text{---} \text{---} \\ \text{---} \text{---} \text{---} \\ \text{---} \text{---} \text{---} \\ \text{---} \text{---} \text{---} \\ \text{---} \text{---} \text{---} \end{array} \right) = \tilde{i}_N^d \left(\begin{array}{c} \text{---} \text{---} \text{---} \\ \text{---} \text{---} \text{---} \\ \text{---} \text{---} \text{---} \\ \text{---} \text{---} \text{---} \\ \text{---} \text{---} \text{---} \\ \text{---} \text{---} \text{---} \end{array} \right) \\
& \rightarrow \bar{e}_i \tilde{T}_{j,i} \tilde{T}_{i+1,k} Y(w) |0\rangle = \tilde{T}_{i,i+1} \tilde{T}_{j,k} Y(w) |0\rangle, \\
7) & X \left(\begin{array}{c} \text{---} \text{---} \text{---} \\ \text{---} \text{---} \text{---} \\ \text{---} \text{---} \text{---} \\ \text{---} \text{---} \text{---} \\ \text{---} \text{---} \text{---} \\ \text{---} \text{---} \text{---} \end{array} \right) \tilde{i}_N^d \left(\begin{array}{c} \text{---} \text{---} \text{---} \\ \text{---} \text{---} \text{---} \\ \text{---} \text{---} \text{---} \\ \text{---} \text{---} \text{---} \\ \text{---} \text{---} \text{---} \\ \text{---} \text{---} \text{---} \end{array} \right) = \tilde{i}_N^d \left(\begin{array}{c} \text{---} \text{---} \text{---} \\ \text{---} \text{---} \text{---} \\ \text{---} \text{---} \text{---} \\ \text{---} \text{---} \text{---} \\ \text{---} \text{---} \text{---} \\ \text{---} \text{---} \text{---} \end{array} \right) \\
& \rightarrow \bar{e}_i \tilde{T}_{j,i+1} \tilde{T}_{k,i} Y(w) |0\rangle = \tilde{T}_{i,i+1} \tilde{T}_{j,k} Y(w) |0\rangle, \\
8) & X \left(\begin{array}{c} \text{---} \text{---} \text{---} \\ \text{---} \text{---} \text{---} \\ \text{---} \text{---} \text{---} \\ \text{---} \text{---} \text{---} \\ \text{---} \text{---} \text{---} \\ \text{---} \text{---} \text{---} \end{array} \right) \tilde{i}_N^d \left(\begin{array}{c} \text{---} \text{---} \text{---} \\ \text{---} \text{---} \text{---} \\ \text{---} \text{---} \text{---} \\ \text{---} \text{---} \text{---} \\ \text{---} \text{---} \text{---} \\ \text{---} \text{---} \text{---} \end{array} \right) = (v^N + v^{-N}) \tilde{i}_N^d \left(\begin{array}{c} \text{---} \text{---} \text{---} \\ \text{---} \text{---} \text{---} \\ \text{---} \text{---} \text{---} \\ \text{---} \text{---} \text{---} \\ \text{---} \text{---} \text{---} \\ \text{---} \text{---} \text{---} \end{array} \right) \\
& \rightarrow \bar{e}_i \tilde{T}_{i+1,N+i} Y(w) |0\rangle = (v^N + v^{-N}) \tilde{T}_{i,i+1} Y(w) |0\rangle, \\
9) & X \left(\begin{array}{c} \text{---} \text{---} \text{---} \\ \text{---} \text{---} \text{---} \\ \text{---} \text{---} \text{---} \\ \text{---} \text{---} \text{---} \\ \text{---} \text{---} \text{---} \\ \text{---} \text{---} \text{---} \end{array} \right) \tilde{i}_N^d(w) = \tilde{i}_N^d \left(\begin{array}{c} \text{---} \text{---} \text{---} \\ \text{---} \text{---} \text{---} \\ \text{---} \text{---} \text{---} \\ \text{---} \text{---} \text{---} \\ \text{---} \text{---} \text{---} \\ \text{---} \text{---} \text{---} \end{array} w \right) \\
& \rightarrow \bar{\Omega}^{\pm 1} \tilde{i}_N^d(w) = \tilde{i}_N^d(\Omega^{\pm 1} w).
\end{aligned}$$

A few observations are useful. First, if the four indices of $\tilde{T}_{i,j}$ and $\tilde{T}_{k,l}$ are distinct, then these two linear maps commute. Second, because $Y(w)$ commutes with \bar{e}_i and with those \tilde{T} s with indices in $\{i, i+1, j, k\}$, we can ignore it in our calculation. And third, the usual $\sigma_j^+ \sigma_j^- |0\rangle = |0\rangle$ and $\sigma_j^+ |0\rangle = 0$ are keys in the computations to follow. Because of the latter identities, the relation 1) is trivially satisfied. Under the action of X , the number of defects is conserved, as it is in the representation ω_d . The computations for the elements 2), 3) and 5) are

$$\begin{aligned}
\bar{e}_i \tilde{T}_{i,i+1} |0\rangle &= (uv^{-1} \sigma_i^- + u^3 v \sigma_{i+1}^- + u^{-1} v \sigma_{i+1}^- + u^{-3} v^{-1} \sigma_i^-) |0\rangle \\
&= (u^2 + u^{-2}) (uv \sigma_{i+1}^- + (uv)^{-1} \sigma_i^-) |0\rangle = (u^2 + u^{-2}) \tilde{T}_{i,i+1} |0\rangle, \\
\bar{e}_i \tilde{T}_{i+1,j} |0\rangle &= u^{-1} v^{-j+i+1} (v^{-2} \sigma_i^- + u^2 \sigma_{i+1}^-) |0\rangle = v^{i-j} \tilde{T}_{i,i+1} |0\rangle, \\
\bar{e}_i \tilde{T}_{i,k} \tilde{T}_{i+1,j} |0\rangle &= ((v^{k-i} u) (v^{-(j-i-1)} u^{-1}) (v^{-2} \sigma_i^- \sigma_k^- + u^2 \sigma_k^- \sigma_{i+1}^-) \\
&\quad + (v^{-(k-i)} u^{-1}) (v^{j-i-1} u) (v^2 \sigma_{i+1}^- \sigma_j^- + u^{-2} \sigma_i^- \sigma_j^-)) |0\rangle,
\end{aligned}$$

$$\begin{aligned}
&= (uv\sigma_{i+1}^-(uv^{k-j}\sigma_k^- + u^{-1}v^{-(k-j)}\sigma_j^-) + (uv)^{-1}\sigma_i^-(uv^{k-j}\sigma_k^- + u^{-1}v^{-(k-j)}\sigma_j^-))|0\rangle \\
&= \tilde{T}_{i,i+1}\tilde{T}_{j,k}|0\rangle,
\end{aligned}$$

and for 8), the link state w has a boundary bubble connecting positions $i + 1$ and $i + N$ and

$$\begin{aligned}
\bar{e}_i\tilde{T}_{i+1,N+i}|0\rangle &= (uv^{N-1}(v^2\sigma_{i+1}^- + u^{-2}\sigma_i^-) + u^{-1}v^{1-N}(v^{-2}\sigma_i^- + u^2\sigma_{i+1}^-))|0\rangle \\
&= (v^N + v^{-N})\tilde{T}_{i,i+1}|0\rangle.
\end{aligned}$$

The proofs of 4), 6) and 7) are similar. For 9), from the definition of $\bar{\Omega}^{\pm 1}$, we have $\bar{\Omega}^{\pm 1}\tilde{T}_{i,j} = v^{\mp 2}\tilde{T}_{i\mp 1,j\mp 1}\bar{\Omega}^{\pm 1}$ and $v^{\pm 2S^z}|0\rangle = v^{\pm N}|0\rangle$. In the subspace with d defects, the number $|\psi(w)|$ of pairs (p_i, q_i) in ψ is $(N - d)/2$ and

$$\begin{aligned}
\bar{\Omega}^{\pm 1}\tilde{i}_N^d(w) &= \bar{\Omega}^{\pm 1}\left(\prod_{(i,j)\in\psi(w)}\tilde{T}_{i,j}\right)|0\rangle = v^{\mp 2|\psi(w)|}\left(\prod_{(i,j)\in\psi(w)}\tilde{T}_{i\mp 1,j\mp 1}\right)\bar{\Omega}^{\pm 1}|0\rangle \\
&= v^{\mp(N-d)}v^{\pm N}\left(\prod_{(i,j)\in\psi(w)}\tilde{T}_{i\mp 1,j\mp 1}\right)|0\rangle = \tilde{i}_N^d(\bar{\Omega}^{\pm 1}w),
\end{aligned}$$

as required. \square

The proofs of equations (4.3.2) and (4.3.3) have been left out. To complete these, we will show that \tilde{i}_N^d is an isomorphism between \tilde{V}_N^d and the eigenspace where $S^z = d/2$, except for some critical values of u and v . Because the analogs of equations (4.3.2) and (4.3.3) hold in the link state representation, then they will also hold in the spin eigenspace since the previous proposition showed that $\tilde{i}_n^d \circ \Omega^{\pm 1} = \bar{\Omega}^{\pm 1} \circ \tilde{i}_n^d$.

4.3.3 The factorization of the Gram matrix in terms of the map \tilde{i}_N^d

Let I_N^d be the matrix of the transformation \tilde{i}_N^d expressed in the bases of link states for the domain and of spin states for $(\mathbb{C}^2)^{\otimes N}|_{S^z=d/2} : \{\vec{x} = |x_1, \dots, x_N\rangle, x_i \in \{+1, -1\}$ and $\sum_i x_i = d\}$, so that $\tilde{i}_N^d(w) = \sum_{\vec{x}} |\vec{x}\rangle (I_N^d)_{\vec{x},w}$ for the basis vector $w \in \tilde{B}_N^d$. The matrix I_N^d is square of size $\binom{N}{(N-d)/2}$, and the linear map \tilde{i}_N^d is an isomorphism if and only if $\det I_N^d \neq 0$.

Let w_1 and w_2 be link states $\in \tilde{B}_N$. The Gram diagram $D_G(w_1, w_2)$ is obtained by taking the mirror image of w_2 by a horizontal axis and by connecting the entries of this state to those of w_1 .

DEFINITION 4.3.2 *The Gram product $\langle \cdot | \cdot \rangle_G : \tilde{V}_N \times \tilde{V}_N \rightarrow \mathbb{C}$ is a bilinear form defined on w_1 and $w_2 \in \tilde{B}_N$ by*

$$\langle w_1 | w_2 \rangle_G = \begin{cases} 0 & \text{if in } D_G(w_1, w_2), \text{ two defects of } w_1 \text{ (or } w_2) \text{ are connected,} \\ \alpha^{n_\alpha} \beta^{n_\beta} v^{n_v} & \text{otherwise,} \end{cases}$$

where n_β and n_α are respectively the numbers of contractible and non-contractible closed loops in $D_G(w_1, w_2)$, and $n_v = \sum_l \Delta_l$ where Δ_l is the displacement (to the left) of defect l of w_1 connecting to another defect of w_2 . Of course, only one of n_α or n_v can be non-zero.

Thus, when $w_1 \in \tilde{B}_N^{d_1}$ and $w_2 \in \tilde{B}_N^{d_2}$, $\langle w_1 | w_2 \rangle_G = 0$ if $d_1 \neq d_2$. The matrix of the Gram product restricted to \tilde{B}_N^d is noted \tilde{G}_N^d . Here are a few examples.

- 1) $w_1 = \text{---} \curvearrowright \text{---} \curvearrowright \text{---} \curvearrowright \text{---} \curvearrowright \text{---}$, $w_2 = \text{---} \curvearrowright \text{---} \curvearrowright \text{---} \curvearrowright \text{---} \curvearrowright \text{---}$, $D_G(w_1, w_2) = \text{---} \curvearrowright \text{---} \curvearrowright \text{---} \curvearrowright \text{---} \curvearrowright \text{---}$, $\langle w_1 | w_2 \rangle = \beta v^8$,
- 2) $w_1 = \text{---} \curvearrowright \text{---} \curvearrowright \text{---} \curvearrowright \text{---} \curvearrowright \text{---}$, $w_2 = \text{---} \curvearrowright \text{---} \curvearrowright \text{---} \curvearrowright \text{---} \curvearrowright \text{---}$, $D_G(w_1, w_2) = \text{---} \curvearrowright \text{---} \curvearrowright \text{---} \curvearrowright \text{---} \curvearrowright \text{---}$, $\langle w_1 | w_2 \rangle = 0$,
- 3) $w_1 = \text{---} \curvearrowright \text{---} \curvearrowright \text{---} \curvearrowright \text{---} \curvearrowright \text{---}$, $w_2 = \text{---} \curvearrowright \text{---} \curvearrowright \text{---} \curvearrowright \text{---} \curvearrowright \text{---}$, $D_G(w_1, w_2) = \text{---} \curvearrowright \text{---} \curvearrowright \text{---} \curvearrowright \text{---} \curvearrowright \text{---}$, $\langle w_1 | w_2 \rangle = \alpha^2 \beta^3$.

For simplicity, we will sometimes denote $\langle w_1 | w_2 \rangle_G$ by the corresponding Gram diagram. With this convention, example 3) becomes

$$\text{---} \curvearrowright \text{---} \curvearrowright \text{---} \curvearrowright \text{---} \curvearrowright \text{---} = \alpha^2 \beta^3.$$

Here are some remarks on this bilinear form. First the Gram product verifies $\langle w_1 | e_i w_2 \rangle_G = \langle e_i w_1 | w_2 \rangle_G$ for $1 \leq i \leq N$ and $w_1, w_2 \in \tilde{B}_N$, where the e_i s act as $\omega_d(v)$ on the first entry of the bilinear form and as $\omega_d(v^{-1})$ on the second. It is then natural to define the adjoint u^\dagger of a word $u = e_{i_1} \dots e_{i_{k-1}} e_{i_k}$ in the generators as $e_{i_k} e_{i_{k-1}} \dots e_{i_1}$. With that definition, $\langle w_1 | u w_2 \rangle_G = \langle u^\dagger w_1 | w_2 \rangle_G$ for all words u and w_1, w_2 . The second remark follows from the first : the radical of Gram bilinear form $\text{Rad}_N^d = \{w \in \tilde{V}_N^d | \langle v | w \rangle_G = 0, \text{ for all } v \in \tilde{V}_N^d\}$ is a subspace of \tilde{V}_N^d stable under the action of $\mathcal{E}TLP_N$. Third the matrix \tilde{G}_N^d is symmetric for $d = 0$. For $d > 0$, the Gram product is not symmetric but still satisfies $\langle w_1 | w_2 \rangle_G = \langle w_2 | w_1 \rangle_G|_{v \rightarrow v^{-1}}$ for $w_1, w_2 \in \tilde{B}_N$. Finally it will be useful to consider the Gram matrix restricted to link states in B_N^d . This matrix will be noted G_N^d without the “~”.

The relation between I_N^d and the Gram product is given by the following proposition.

THEOREM 4.3.3 *Let $Q_N^d = (I_N^d(u, v^{-1}))^T I_N^d(u, v)$. Then $Q_N^d = \tilde{G}_N^d$ with $\beta = u^2 + u^{-2}$, $\alpha = v^N + v^{-N}$ and twist parameter v .*

Note that the v^{-1} in $(I_N^d(u, v^{-1}))^T$ is consistent with the previous remark that $\tilde{\mathcal{G}}_N^d = (\tilde{\mathcal{G}}_N^d)^T|_{v \rightarrow v^{-1}}$. Here is a simple example of this remarkable factorization for $N = 4$ and $d = 0$. The bases are ordered as

$$\{|+-+ -\rangle, |++--\rangle, |-++-\rangle, |-+-+\rangle, |+- -+\rangle, |--++\rangle\}$$

for the spin basis and as (4.2.6) for the link state basis. The matrices are

$$I_4^0(u, v) = \begin{pmatrix} u^2 v^2 & v^2 & v^{-2} & u^{-2} v^{-2} & v^{-2} & v^2 \\ 0 & u^2 v^4 & 0 & 1 & 0 & u^{-2} v^{-4} \\ 1 & 0 & u^2 v^4 & 0 & u^{-2} v^{-4} & 0 \\ u^{-2} v^{-2} & v^{-2} & v^2 & u^2 v^2 & v^2 & v^{-2} \\ 1 & 0 & u^{-2} v^{-4} & 0 & u^2 v^4 & 0 \\ 0 & u^{-2} v^{-4} & 0 & 1 & 0 & u^2 v^4 \end{pmatrix}, \quad \tilde{\mathcal{G}}_4^2 = \begin{pmatrix} \beta^2 & \beta & \alpha\beta & \alpha & \alpha\beta & \beta \\ \beta & \beta^2 & \alpha & \alpha\beta & \alpha & \alpha^2 \\ \alpha\beta & \alpha & \beta^2 & \beta & \alpha^2 & \alpha \\ \alpha & \alpha\beta & \beta & \beta^2 & \beta & \alpha\beta \\ \alpha\beta & \alpha & \alpha^2 & \beta & \beta^2 & \alpha \\ \beta & \alpha^2 & \alpha & \alpha\beta & \alpha & \beta^2 \end{pmatrix}. \quad (4.3.5)$$

The equality can be checked by doing the product $(I_4^0(u, v^{-1}))^T I_4^0(u, v)$ and replacing in $\tilde{\mathcal{G}}_4^2$ the two variables α and β by $v^4 + v^{-4}$ and $u^2 + u^{-2}$ respectively. Clearly this factorization is non-trivial.

PROOF We see Q_N^d as an endomorphism of \tilde{V}_N^d whose matrix elements in the link state basis are

$$(Q_N^d)_{w_1, w_2} = \sum_{\vec{x}} (I_N^d(u, v^{-1}))_{w_1, \vec{x}}^T (I_N^d(u, v))_{\vec{x}, w_2}.$$

With the usual scalar product on spin states $\langle s_1 s_2 \dots s_N | t_1 t_2 \dots t_N \rangle = \prod_i \delta_{s_i, t_i}$ for $s_i, t_i \in \{+1, -1\}$, matrix elements can be rewritten as

$$\begin{aligned} (I_N^d(u, v^{-1}))_{w_1, \vec{x}}^T &= (I_N^d(u, v^{-1}))_{\vec{x}, w_1} = \langle \vec{x} | \prod_{(i,j) \in \psi(w_1)} \tilde{T}_{i,j}(u, v^{-1}) | 0 \rangle \\ &= \langle 0 | \prod_{(i,j) \in \psi(w_1)} \tilde{T}_{i,j}^T(u, v^{-1}) | \vec{x} \rangle, \end{aligned}$$

and then

$$\begin{aligned} (Q_N^d)_{w_1, w_2} &= \sum_{\vec{x}} \langle 0 | \prod_{(i,j) \in \psi(w_1)} \tilde{T}_{i,j}^T(u, v^{-1}) | \vec{x} \rangle \langle \vec{x} | \prod_{(k,l) \in \psi(w_2)} \tilde{T}_{k,l}(u, v) | 0 \rangle \\ &= \langle 0 | \prod_{(i,j) \in \psi(w_1)} \tilde{T}_{i,j}^T(u, v^{-1}) \prod_{(i,j) \in \psi(w_2)} \tilde{T}_{i,j}(u, v) | 0 \rangle. \end{aligned}$$

Notice that all the elements of the second product commute among each other, and the same goes for those of the first. However, elements of the first product do not commute with some elements of the second. More precisely, an element $\tilde{T}_{i,j}$ of the first product does not commute with a $\tilde{T}_{k,l}$ of the second if $\{i, j\} \cap \{k, l\} \neq \emptyset$. This suggests to break down the above products into clusters, namely subsets of indices

corresponding to connected components of the Gram diagram $D_G(w_1, w_2)$. Such a cluster is the set of labels visited by one loop or one defect in the diagram. Then $(Q_N^d)_{w_1, w_2}$ factors as a product over clusters :

$$(Q_N^d)_{w_1, w_2} = \langle 0 | \prod_{m=1}^{n_c} \left(\prod_{(i,j) \in \psi(w_1) \cap c_m} \tilde{T}_{i,j}^T(u, v^{-1}) \prod_{(k,l) \in \psi(w_2) \cap c_m} \tilde{T}_{k,l}(u, v) \right) | 0 \rangle,$$

where the c_m s are the clusters and n_c is their number in $D_G(w_1, w_2)$. We want to show that

$$(Q_N^d)_{w_1, w_2} = \begin{cases} 0 & \text{if defects of } w_1 \text{ or } w_2 \text{ are connected,} \\ (v^N + v^{-N})^{n_\alpha} (u^2 + u^{-2})^{n_\beta} v^{n_\nu} & \text{otherwise,} \end{cases} \quad (4.3.6)$$

where n_α , n_β and n_ν have been defined in definition 4.3.2. To show this, we can concentrate on a single cluster, say the one containing the point i , and simplify it by removing pairs of indices recursively. More precisely, we proceed as in proposition 4.3.2 : we identify local relations between the \tilde{T} s and \tilde{T}^T s that, if true, would show that each cluster gives rise to its proper contribution in the final result of (4.3.6). Here are these local relations where the u and v dependence of $\tilde{T}_{i,j}(u, v)$ and $\tilde{T}_{i,j}^T(u, v^{-1})$ has been removed and therefore $T_{i,j}$ and $T_{i,j}^T$ stand for $\tilde{T}_{i,j}(u, v)$ and $\tilde{T}_{i,j}^T(u, v^{-1})$ respectively.

1)

$$\begin{array}{c} \bullet \\ \circlearrowleft \\ \bullet \\ i \quad j \end{array} = u^2 + u^{-2} \quad \rightarrow \quad T_{i,j}^T T_{i,j} | 0 \rangle = (u^2 + u^{-2}) | 0 \rangle,$$

2)

$$\begin{array}{c} \bullet \\ \cup \\ \bullet \\ i \quad j \end{array} = v^N + v^{-N} \quad \rightarrow \quad T_{i,j}^T T_{j, i+N} | 0 \rangle = (v^N + v^{-N}) | 0 \rangle,$$

3)

$$\begin{array}{c} \bullet \\ | \\ \bullet \\ i \quad j \end{array} = 0 = \begin{array}{c} \bullet \\ | \\ \bullet \\ i \quad j \end{array} \quad \rightarrow \quad T_{i,j}^T | 0 \rangle = 0 = \langle 0 | T_{i,j},$$

4)

$$\begin{array}{c} \bullet \quad \bullet \\ \cup \quad \cup \\ \bullet \quad \bullet \\ i \quad j \quad k \quad l \end{array} = \begin{array}{c} \bullet \quad \bullet \\ | \quad | \\ \bullet \quad \bullet \\ i \quad j \quad k \quad l \end{array} \quad \rightarrow \quad T_{j,k}^T T_{i,j} T_{k,l} | 0 \rangle \simeq T_{i,l} | 0 \rangle,$$

5)

$$\begin{array}{c} \bullet \quad \bullet \\ \cup \quad \cup \\ \bullet \quad \bullet \\ i \quad j \quad k \quad l \end{array} = \begin{array}{c} \bullet \quad \bullet \\ | \quad | \\ \bullet \quad \bullet \\ i \quad j \quad k \quad l \end{array} \quad \rightarrow \quad T_{i,j}^T T_{i,l} T_{j,k} | 0 \rangle \simeq T_{k,l} | 0 \rangle,$$

6)

$$\begin{array}{c} \bullet \quad \bullet \\ \cup \quad \cup \\ \bullet \quad \bullet \\ i \quad j \quad k \quad l \end{array} = \begin{array}{c} \bullet \quad \bullet \\ | \quad | \\ \bullet \quad \bullet \\ i \quad j \quad k \quad l \end{array} \quad \rightarrow \quad T_{k,l}^T T_{i,l} T_{j,k} | 0 \rangle \simeq T_{i,j} | 0 \rangle,$$

7)

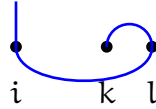
$$\begin{array}{c} \bullet \\ \cup \\ \bullet \\ i \quad j \quad k \end{array} = v^{i-k} \begin{array}{c} \bullet \\ | \\ \bullet \\ i \quad j \quad k \end{array} \quad \rightarrow \quad T_{i,j}^T T_{j,k} | 0 \rangle = v^{i-k} | 0 \rangle,$$

$$\begin{aligned}
8) \quad & \begin{array}{c} \bullet \quad \bullet \quad \bullet \\ i \quad j \quad k \end{array} \begin{array}{c} \text{---} \\ \text{---} \\ \text{---} \end{array} = v^{k-i} \begin{array}{c} \bullet \quad \bullet \quad \bullet \\ i \quad j \quad k \end{array} \quad \rightarrow \quad T_{j,k}^T T_{i,j} |0\rangle = v^{k-i} |0\rangle, \\
9) \quad & \begin{array}{c} | \\ | \\ \dots \\ | \end{array} = 1 \quad \rightarrow \quad \langle 0|0\rangle = 1,
\end{aligned}$$

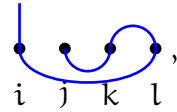
where \simeq means the equality holds modulo terms that will be 0 when the product with $\langle 0|$ is computed. For instance, relation 4) is checked as follows

$$\begin{aligned}
T_{j,k}^T T_{i,j} T_{k,l} |0\rangle &= (uv^{j-k} \sigma_k^+ + u^{-1} v^{k-j} \sigma_j^+) (uv^{j-i} \sigma_j^- + u^{-1} v^{i-j} \sigma_i^-) (uv^{l-k} \sigma_l^- + u^{-1} v^{k-l} \sigma_k^-) |0\rangle \\
&= (uv^{2j-i-l} \sigma_j^- + u^{-1} v^{i-l} \sigma_i^- + uv^{l-i} \sigma_l^- + u^{-1} v^{2k-i-l} \sigma_k^-) |0\rangle \\
&= (T_{i,l} + uv^{2j-i-l} \sigma_j^- + u^{-1} v^{2k-i-l} \sigma_k^-) |0\rangle \simeq T_{i,l} |0\rangle
\end{aligned}$$

where, in the last step, we used the fact that in what remains of $\prod T^T \prod T$, everything commutes with σ_k^- and σ_j^- and $\langle 0|\sigma_j^- = \langle 0|\sigma_k^- = 0$. Relation 9) is trivial and the seven others are proved in a similar fashion. Finally, we note that the case



does not need to be studied because there has to be a j (with $i < j < k$) for which the diagram reads



and then relation 6) (or rather its transpose) may be used first. In conclusion, in calculating $(Q_N^d)_{w_1, w_2}$, each cluster gives rise to a factor through relations 1), 2), 7) and 8) that is equal to the factor obtained from the corresponding closed loop in the Gram diagram and the proof is complete. \square

From the previous proposition, $\det I_N^d(u, v) \det I_N^d(u, v^{-1}) = \det \tilde{\mathcal{G}}_N^d$. The computation of these determinants will be done in section 4.5, that of $\tilde{\mathcal{G}}_N^d$ leading naturally to that of I_N^d . The latter will reveal when the map \tilde{i}_N^d is actually an isomorphism.

4.4 Jordan blocks between sectors of loop models

In this section, the action of the periodic Temperley-Lieb algebra on the space \tilde{V}_N spanned by all link states is that of representation ρ . The following sections are independent of the

present one. The following notation will be used extensively :

$$C_n = \cos n\Lambda, \quad S_n = \sin n\Lambda, \quad \text{with} \quad \Lambda = \pi - \lambda.$$

The double-row transfer matrix D_N on the strip with open boundary conditions was studied in [77] where Jordan blocks were shown to exist between V_N^d and $V_N^{d'}$ for specific values of β , N and pairs d, d' . Although a proof is still missing, it is believed that this double-row transfer matrix does not have Jordan blocks when restricted to a given V_N^d . As opposed to the case with open boundaries, the transfer matrix $T_N(\lambda, u)$ introduced in Definition 4.2.5 can have two types of Jordan blocks : within a sector with a given number of defects d and between sectors with distinct d and d' . Jordan blocks of the transfer matrix between sectors may be seen only if the action allows for an increase in the number of bubbles or, equivalently, for a change in the number of defects. This is why the representation ρ , introduced in Definition 4.2.7, will be used throughout this section.

In this section, we use the top Fourier coefficient f_N of $T_N(\lambda, u)$ to study the Jordan structure between sectors of $T_N(\lambda, u)$. We follow ideas developed in [77] and use the following conventions. Let $c \in \mathcal{E}TLP_N(\beta, \alpha)$ and $v, w \in \tilde{B}_N$. In a link pattern v , a *1-bubble* is a bubble that does not surround any other bubble and an *n-bubble* one that contains at least one $(n - 1)$ -bubble. The link state with N defects is noted v^N . A state with m bubbles is labeled by integers k_1, \dots, k_m with $1 \leq k_i \leq N$, that stand for midpoints of the bubbles that have to be closed (starting with k_1 , then k_2, \dots) to create the link state v . (Note that the k_i s actually label the edges between the tiles of T_N .) Such a state is denoted v_{k_1, \dots, k_m}^N . The matrix element $\rho(c)_{w,v}$ will often be denoted by $\langle w|c v \rangle$. (There should be no confusion with Gram products, denoted by $\langle \cdot | \cdot \rangle_G$.) Graphically, the exiting state w in $\rho(c)_{w,v}$ is depicted by dashed curves. Restrictions of the matrix $\rho(c)$ to \tilde{V}_N^d is noted by $\rho(c)|_d$; similarly $\rho(c)|_{[d,d']}$ is the restriction to $\oplus_{e=d}^{d'} \tilde{V}_N^e$. Finally we shall be using the subspace $\text{UpTo}_d = \oplus_{e \leq d} \tilde{V}_N^e$ (direct sum of vector spaces). Under the action of the representation ρ , the subspaces \tilde{V}_N^d are not stable, but the subspaces UpTo_d are.

DEFINITION 4.4.1 *The element $F_N(\Lambda) \in \mathcal{E}TLP_N(\beta, \alpha)$ is*

$$F_N(\Lambda) = \begin{array}{c} \overbrace{\hspace{10em}}^N \\ \begin{array}{|c|c|c|c|} \hline \bullet & \bullet & \dots & \bullet \\ \hline \bullet & \bullet & \dots & \bullet \\ \hline \bullet & \bullet & \dots & \bullet \\ \hline \bullet & \bullet & \dots & \bullet \\ \hline \end{array} \end{array}$$

where

$$\begin{array}{|c|} \hline | \\ \hline | \\ \hline \end{array} = -ie^{i\lambda/2} \lim_{u \rightarrow +i\infty} \frac{1}{\sin(\lambda - u)} \begin{array}{|c|} \hline u \\ \hline \end{array} = e^{-i\Lambda/2} \begin{array}{|c|} \hline \curvearrowright \\ \hline \end{array} + e^{i\Lambda/2} \begin{array}{|c|} \hline \curvearrowleft \\ \hline \end{array}$$

and $\Lambda = \pi - \lambda$.

$F_N(\Lambda)$ possesses two crucial properties [77]. First $e_i F_N(\Lambda) = F_N(\Lambda) e_i$ for all $1 \leq i \leq N$. Since $[F_N(\Lambda), \Omega] = [F_N(\Lambda), \Omega^{-1}] = 0$, F_N is in the center of $\mathcal{E}TLP_N(\beta, \alpha)$. Second the transfer matrix $T_N(\lambda, u)$ can be expanded into a Fourier series : $T_N(\lambda, z + \lambda/2) = \sum_{k=-N}^N f_k e^{ikz}$ with the Fourier coefficients $f_k \in \mathcal{E}TLP_N(\beta, \alpha)$. Then $F_N(\Lambda) = 2^N f_N$.

The rest of the section is devoted to the study of Jordan cells in $F_N(\Lambda)$. In fact lemma 4.1 and proposition 4.10 of [77] shows that, because of the commuting property (i) of the transfer matrix T_N (see paragraph 4.2.2), any Jordan cells in one of its Fourier modes will be present in $T_N(\lambda, \nu)$ for all but a finite set of values of ν .

PROPOSITION 4.4.1 *In the representation ρ , the central element $F_N(\Lambda)$ acts as an upper block-triangular matrix (in a basis ordered with increasing defect number) and its spectrum can be read from its restrictions to the subspaces \tilde{V}_N^d :*

$$\rho(F_N(\Lambda))|_d = 2C_{d/2} \text{id}, \quad \text{for } d > 0, \quad \text{and} \quad \rho(F_N(\Lambda))|_{d=0} = \alpha \text{id}.$$

PROOF The proof rests upon the deceptively simple identity

$$\begin{array}{|c|} \hline \curvearrowright \\ \hline \end{array} = \begin{array}{|c|} \hline \curvearrowleft \\ \hline \end{array}, \tag{4.4.1}$$

that can be shown by expanding the two tiles. Thus the $(n-d)/2$ bubbles of any $w \in \tilde{B}_N^d$ pass through F_N unchanged and the component of $\rho(F_N(\Lambda))w$ in \tilde{V}_N^d is along w itself. Its coefficient $\langle w | F_N(\Lambda) w \rangle$ is then $\langle v^d | F_d(\Lambda) v^d \rangle$. This constant is computed diagrammatically

$$\begin{aligned} \langle v^d | F_d(\Lambda) v^d \rangle &= \overbrace{\begin{array}{|c|} \hline \bullet \bullet \bullet \bullet \\ \hline \bullet \bullet \bullet \bullet \\ \hline \end{array}}^d \\ &= e^{id\Lambda/2} \begin{array}{|c|} \hline \curvearrowright \curvearrowright \curvearrowright \curvearrowright \\ \hline \bullet \bullet \bullet \bullet \\ \hline \bullet \bullet \bullet \bullet \\ \hline \end{array} + e^{-id\Lambda/2} \begin{array}{|c|} \hline \curvearrowleft \curvearrowleft \curvearrowleft \curvearrowleft \\ \hline \bullet \bullet \bullet \bullet \\ \hline \bullet \bullet \bullet \bullet \\ \hline \end{array} \\ &= 2 \cos \frac{d\Lambda}{2}. \end{aligned}$$

The case $d = 0$ is particular : all $N/2$ bubbles go through F_N and a non-contractible loop is created, giving rise to a factor of α . \square

Because of the identity (4.4.1), all matrix elements of $\rho(F_N(\Lambda))$ can be computed. Indeed, once the bubbles of a link state $v \in \tilde{B}_N^d$ have been pushed through F_N , it remains only to compute $F_d v^d$. It is thus sufficient to calculate the column of $\rho(F_s(\Lambda))$ corresponding to the components of the vector $F_s v^s$, for $0 \leq s \leq N$ and $N \equiv s \pmod 2$, that is, the elements $\langle w | F_s(\Lambda) v^s \rangle$. Because $F_s(\Lambda)$ has only one row of boxes, any w with n -bubbles with $n \geq 2$ has $\langle w | F_s(\Lambda) v^s \rangle = 0$.

LEMMA 4.4.2 *Let $v_{k_1, \dots, k_m}^s \in \tilde{B}_s^d$ be a link state with only 1-bubbles centered at k_1, \dots, k_m , $k_{i+1} > k_i + 1$ and $k_i \in [1, s]$ for all i . Then,*

$$\langle v_{k_1, \dots, k_m}^s | F_s(\Lambda) v^s \rangle = \prod_{i=1}^m S_{(k_{i+1} - k_i - 1)/2} / S_{1/2}$$

where $k_{m+1} = k_1 + N$.

PROOF As noted before, dashed segments (curves) under $F_s(\Lambda)$ indicate that the outgoing state must contain a defect (a bubble) at this position. Because $F_s(\Lambda)$ has only one row of tiles, the only way to close a bubble is to force both tiles adjacent to the edge k_i to draw a 1-bubble. With these remarks, the direct calculation of $\langle v_{k_1, \dots, k_m}^s | F_s(\Lambda) v^s \rangle$ is straightforward and yields

$$\begin{aligned} \langle v_{k_1, \dots, k_m}^s | F_s(\Lambda) v^s \rangle &= \text{Diagram 1} \\ &= \text{Diagram 2} \\ &= A(N + k_1 - k_m) \prod_{i=1}^{m-1} A(k_{i+1} - k_i) \end{aligned}$$

where

$$\begin{aligned}
A(n) &= \text{Diagram with } n \text{ sites, blue vertical lines, red arcs, and purple dashed lines} \\
&= e^{i(n-2)\Lambda/2} \text{Diagram} + e^{i(n-4)\Lambda/2} \text{Diagram} \\
&+ e^{i(n-6)\Lambda/2} \text{Diagram} + \dots + e^{-i(n-2)\Lambda/2} \text{Diagram} \\
&= e^{-i(n-2)\Lambda/2} \sum_{j=0}^{n-2} e^{ij\Lambda} = \frac{S_{(n-1)/2}}{S_{1/2}}.
\end{aligned}$$

□

We now construct a basis of eigenstates of $\rho(F_N(\Lambda))$. By the same argument as before, it is sufficient to find the unique eigenstate ψ^s of $\rho(F_s(\Lambda))$ that has a non-zero component in \tilde{V}_s^s . This vector has eigenvalue $2C_{s/2}$. By convention, we choose $\langle v^s | \psi^s \rangle = 1$. In the next proposition, we calculate other components of ψ^s .

Jordan blocks between sectors occur only when $\Lambda = \pi a/b$ with $a \in \mathbb{Z}$, $b \in \mathbb{Z}^\times$. For the purpose of the next propositions, a generic Λ is π times any complex number that is not a (real) rational number of the form a/b with $\gcd(a, b) = 1$ and $b \leq N$. We shall note soon that this definition is too restrictive.

LEMMA 4.4.3 *Let $v_{m^m}^s$ be the state $\in \tilde{B}_s^{s-2m}$ with m concentric bubbles against the left imaginary boundary and let $X_m^s = \langle v_{m^m}^s | \psi^s \rangle$. Then, for generic Λ , the components X_m^s are*

$$X_m^s = (-1)^m \prod_{k=1}^m \frac{S_{(s+1-2k)/2}}{4S_{1/2}S_{k/2}S_{(s-k)/2}}, \quad \text{for } m = 0 \text{ up to } \begin{cases} (s-1)/2 & \text{for } s \text{ odd,} \\ (s-2)/2 & \text{for } s \text{ even,} \end{cases} \quad (4.4.2)$$

$$X_{s/2}^s = \frac{(-1)^{s/2}}{\alpha - 2C_{s/2}} \prod_{k=1}^{s/2-1} \frac{S_{(s+1-2k)/2}}{4S_{1/2}S_{k/2}S_{(s-k)/2}}. \quad (4.4.3)$$

PROOF Because $F_s(\Lambda)$ commutes with the translation operator Ω , the eigenstate ψ^s is invariant under translation. The component along $v_{m^m}^s$ of the equation $F_s(\Lambda)\psi^s =$

$2C_{s/2}\psi^s$ for the eigenvector ψ^s is then

$$\begin{aligned}
2C_{s/2}X_m^s &= \langle v_{m^m}^s | F_s(\Lambda) \psi^s \rangle \\
&= \langle v_{m^m}^s | F_s(\Lambda) v_{m^m}^s \rangle \langle v_{m^m}^s | \psi^s \rangle + \langle v_{m^m}^s | F_s(\Lambda) v_{m^{m-1}}^s \rangle \langle v_{m^{m-1}}^s | \psi^s \rangle \\
&= \langle v^{s-2m} | F_{s-2m}(\Lambda) v^{s-2m} \rangle \langle v_{m^m}^s | \psi^s \rangle + \langle v_1^{s-2m+2} | F_{s-2m+2}(\Lambda) v^{s-2m+2} \rangle \langle v_{m^{m-1}}^s | \psi^s \rangle \\
&= 2C_{s/2-m} \langle v_{m^m}^s | \psi^s \rangle + A(s-2m+2) \langle v_{(m-1)^{m-1}}^s | \psi^s \rangle \\
&= 2C_{s/2-m} X_m^s + \frac{S_{(s-2m+1)/2}}{S_{1/2}} X_{m-1}^s.
\end{aligned}$$

To obtain the second equality, we have used the fact that the only two link states w with non-zero contribution to $\langle v_{m^m}^s | F_s(\Lambda) w \rangle$ are $v_{m^m}^s$ and $v_{m^{m-1}}^s$. And for the third equality, the identity (4.4.1) allows for the removal of all bubbles entering F_s . Finally, for the fourth, we used the invariance under translation of ψ^s to write $\langle v_{m^{m-1}}^s | \psi^s \rangle = \langle v_{(m-1)^{m-1}}^s | \psi^s \rangle$. The result is a recurrence relation for X_m^s :

$$X_m^s = -\frac{X_{m-1}^s S_{(s-2m+1)/2}}{4S_{1/2} S_{m/2} S_{(s-m)/2}}$$

which can be used, along with the initial condition $X_0^s = 1$, to complete the proof of the first part. When s is even, $\langle v_{(s/2)^{s/2}}^s | F_s(\Lambda) v_{(s/2)^{s/2}}^s \rangle = \alpha$ and the recurrence relation reads instead

$$2C_{s/2}X_{s/2}^s = \alpha X_{s/2}^s + X_{s/2-1}^s$$

and the rest of the argument is identical. \square

It is clear that the coefficients X_m^s in (4.4.2) and (4.4.3) are valid as long as they are finite for the value of Λ of interest. The definition of genericity for Λ should therefore be partially relaxed to allow rational numbers a/b for which no zeroes appear in the denominators of these expressions or, even better, to allow for rational numbers such that the zeroes in the denominators are cancelled by those in the numerators.

Calculating other components is also possible. However, the X_m^s s will be sufficient to probe the Jordan structure of $F_N(\Lambda)$ and of T_N .

LEMMA 4.4.4 *For generic Λ , the eigenvector ψ^s satisfies $e_i \psi^s = 0$ for all $i = 1, \dots, s$.*

PROOF Because $F_s(\Lambda)(e_i \psi^s) = e_i F_s(\Lambda) \psi^s = 2C_{s/2} e_i \psi^s$, the vector $e_i \psi^s$ is an eigensate of $F_s(\Lambda)$ with eigenvalue $2C_{s/2}$. But $e_i \psi^s \in \text{UpTo}_{s-2}$ and, on this subspace, the eigenvalues of F_s are $2C_{k/2}$, $0 \leq k \leq s-2$, which are all different from $2C_{s/2}$ for a generic Λ . \square

DEFINITION 4.4.2 We define the linear transformation $\Psi^d : \tilde{V}_N^d \rightarrow \text{UpTo}_d$ whose action on link states $v \in \tilde{B}_N^d$ is given by the following rule. We first remove all bubbles of v and then replace the d defects of v by the linear combination ψ^d . We finally reinsert the bubbles in their original locations. The result is a linear combination of link states in UpTo_d . The set of link states obtained by acting with Ψ^d on the states of \tilde{B}_N^d will be noted $\Psi\tilde{B}_N^d$.

From the previous construction, $\Psi\tilde{B}_N^d$ is a basis of eigenvectors of $F_N(\Lambda)$ for generic Λ .

PROPOSITION 4.4.5 For Λ generic, the set $\Psi\tilde{B}_N^d$ is stable under $\mathcal{E}\text{TLP}_N(\beta, \alpha)$.

PROOF When e_i acts on any state in $\Psi\tilde{B}_N^d$, the result is always in $\Psi\tilde{B}_N^d$. Indeed, let $w \in \tilde{B}_N^d$ and let consider the action of e_i on $\Psi^d w$. Only three cases need to be considered :

- If e_i acts on two positions where w had defects, the result is zero by the previous lemma.
- If e_i acts on one position where w had a defect and a bubble, the resulting link state is simply $\Psi^d(e_i w)$ and one of the position where w had a defect has moved.
- If e_i does not act on any positions where w had defects, the result is still in $\Psi\tilde{B}_N^d$. Indeed the positions where w had defects are unchanged, but the pattern of bubbles might be different, with a possible overall factor of β . Again, $e_i \Psi^d(w) = \Psi^d(e_i w)$.

□

From the first case of the last proposition, any $c \in \mathcal{E}\text{TLP}_N(\beta, \alpha)$ has $\rho'(c)_{d,d'} = 0$ for $d \neq d'$, where $\rho'(c)$ is the matrix representing c in the basis $\Psi\tilde{B}_N^d$. For Λ generic, there are no Jordan blocks between sectors.

The next proposition proves the existence of Jordan blocks for some non-generic values Λ . For this proof, we will denote γ_d the (unique) eigenvalue of $\rho(F_N(\Lambda))|_d$ (computed in proposition 4.4.1).

PROPOSITION 4.4.6 Let Λ (non-generic) and d_1, \dots, d_n be integers such that $0 \leq d_1 < \dots < d_n \leq N$, $N - d_i \equiv 0 \pmod{2}$ for $i = 1, \dots, n$, $\gamma \equiv \gamma_{d_1} = \gamma_{d_2} = \dots = \gamma_{d_n}$ and $A(d_1+2), A(d_1+4), \dots, A(d_n) \neq 0$. Then there is at least one Jordan cell of size n in $F_N(\Lambda)$ connecting sectors d_1, \dots, d_n .

PROOF We are interested in the Jordan structure between sectors d_1, d_2, \dots, d_n , so we restrict our study to $\rho(F_N)|_{[d_1, d_n]}$. In this matrix, some eigenvalues are (usually) different from γ . We call them $\gamma_i, i = 1, \dots, m$, and each appears in n_i different sectors. Because Jordan blocks can only occur between sectors, $\rho(F_N)|_{[d_1, d_n]}$ satisfies the polynomial equation

$$(\rho(F_N - \gamma \cdot \text{id})|_{[d_1, d_n]})^n \times \prod_{i=1}^m (\rho(F_N - \gamma_i \cdot \text{id})|_{[d_1, d_n]})^{n_i} = 0.$$

To prove that a Jordan block of size n exists, we show that

$$\rho(G)|_{[d_1, d_n]} \neq 0 \quad \text{for} \quad G \equiv (F_N - \gamma \cdot \text{id})^{n-1} \times \prod_{i=1}^m (F_N - \gamma_i \cdot \text{id})^{n_i},$$

by computing one non-zero matrix element. Taking for simplicity $N/2 < x < N$, we will show indeed that $\langle v_{x^{(N-d_1)/2}}^N | G v_{x^{(N-d_n)/2}}^N \rangle$ is non-zero. From its definition, G is a polynomial in F_N with degree $(d_n - d_1)/2$ and leading coefficient 1. Both the initial and final states have been chosen to have only concentric bubbles, so each application of F_N adds one concentric bubbles and the only term contributing is $F_N^{(d_n-d_1)/2}$:

$$\begin{aligned} \langle v_{x^{(N-d_1)/2}}^N | G v_{x^{(N-d_n)/2}}^N \rangle &= \langle v_{x^{(N-d_1)/2}}^N | F_N^{(d_n-d_1)/2} v_{x^{(N-d_n)/2}}^N \rangle \\ &= \langle v_{y^{(d_n-d_1)/2}}^{d_n} | F_{d_n}^{(d_n-d_1)/2} v_{y^{d_n}}^{d_n} \rangle \quad \text{with} \quad y = x - (N - d_n)/2 \\ &= \prod_{i=0}^{(d_n-d_1-2)/2} \langle v_{y^{i+1}}^{d_n} | F_{d_n} v_{y^i}^{d_n} \rangle = \prod_{i=0}^{(d_n-d_1-2)/2} \langle v_{y^{-i}}^{d_n-2i} | F_{d_n-2i} v_{y^{-i}}^{d_n-2i} \rangle \\ &= \prod_{i=0}^{(d_n-d_1-2)/2} A(d_n - 2i) = \prod_{i=0}^{(d_n-d_1-2)/2} \frac{S_{(d_n-2i-1)/2}}{S_{1/2}} \neq 0. \end{aligned}$$

□

In this proof, we used a starting state with only concentric bubbles, but in fact for any initial state w_1 in $V_N^{d_n}$, one can find a state in w_2 in $V_N^{d_1}$ such that $\langle w_2 | G w_1 \rangle \neq 0$. In general our numerical exploration shows that, whenever $d_n \neq N$, there is more than one Jordan blocks connecting the sectors d_n and d_1 .

In the derivation of (4.4.2), we found that

$$X_{(d_n-d_1)/2}^{d_n} = \frac{\prod_{i=0}^{(d_n-d_1-2)/2} A(d_n - 2i)}{\prod_{d=d_1, d_1+2, \dots, d_n-2} (\gamma_{d_n} - \gamma_d)}.$$

The condition that $A(d_1 + 2), A(d_1 + 4), \dots, A(d_n)$ be non-zero is therefore equivalent to requiring that $X_{(d_n - d_1)/2}^{d_n}$ has a pole $(\gamma_{d_n} - \gamma_{d_i})^{-1}$ for each $d_i = d_1, d_2, \dots, d_{n-1}$.

The constraint $\prod_{i=0}^{(d_n - d_1 - 2)/2} A(d_n - 2i) \neq 0$ appears to be the simplest formulation of the condition for Jordan blocks to appear, but it can be translated in terms of constraints for N, d and Λ . The following corollary is obtained by first identifying, for a given parity of N , the numbers n for which $A(n)$ vanishes (for $n \equiv N \pmod{2}$) and then selecting a maximal consecutive range of n s such that the $A(n)$ s do not vanish. The second step consists in choosing sectors d, d', d'', \dots in this range that share the same eigenvalue γ_d . Note that $\gamma_d = \gamma_{d'}$ if and only if $(d' + d)\Lambda/4$ or $(d' - d)\Lambda/4$ is π times an integer.

COROLLARY 4.4.7 *Let $\Lambda = \pi a/b$ with a and b coprime integers. Then*

(a) *if N is even :*

(i) *α odd : $A(n)$ with n an even integer is never zero. A given sector d , with $0 \leq d \leq 2b$ and d even, is coupled to all sectors $4bj - d, 4bj + d$, for $j \geq 1$, with at least one high-rank Jordan block. The sector $d = 0$ also couples to these sectors if $\alpha = 2C_{a/2}$.*

(ii) *α even (and b odd) : $A(n)$ with n even is zero if and only if $n = (2s + 1)b + 1$ for some integer $s \geq 0$. Sectors can be tied in a Jordan cell if they are labeled by even numbers in the range $[(2s + 1)b + 1, (2s + 3)b + 1[$ for some fixed $s \geq 0$. In the above range, this occurs only for pairs (d, d') with $d' = 4(s + 1)b - d$ and the Jordan cell is of rank 2. The sector $d = 0$ couples to the sector d' with a rank 2 Jordan cell if $\alpha = 2C_{a'/2}$ and $d' < b$.*

(b) *if N is odd : $A(n)$ with n odd is zero if and only if $n = 2sb + 1$ for some integer $s \geq 0$. Sectors can be tied in a Jordan cell if they are labeled by odd integers in the range $[2sb + 1, 2(s + 1)b + 1[$ for some fixed $s \geq 0$.*

(i) *α odd : all eigenvalues for the sectors in this range are distinct and there are no Jordan blocks.*

(ii) *α even (and b odd) : In the above range, this occurs only for pairs (d, d') with $d' = 2(2s + 1)b - d$ and the Jordan cell is of rank 2.*

Of course a given sector can never couple to itself even when $d = d'$.

4.5 The intertwiner \tilde{i}_N^d and its critical curves

All equalities involving $\det \tilde{G}_N^d$ or $\det I_N^d$ are valid up to a sign.

The goal of this section is (partially) to finish the proof that the map \tilde{i}_N^d is a $\mathcal{E}TLP_N$ -homomorphism, therefore proving that it intertwines loop and spin representations (theorem 4.5.6). But the crucial result of the section is theorem 4.5.5 which gives the *critical curves* in the complex plane (u, v) where \tilde{i}_N^d stops being an isomorphism. As section 4.6 shall prove, only on these curves may the loop Hamiltonian \mathcal{H} have non-trivial Jordan cells. The identification of these critical curves amounts to computing the determinant of \tilde{i}_N^d in some appropriate bases. We shall recover, along the way, the determinant of the Gram matrix.

The computation of $\det \tilde{\mathcal{G}}_N^d$ and $\det I_N^d$ is technical. Fortunately it is significantly simplified by a change of bases. In this new basis, the determinant for the periodic Gram matrix $\tilde{\mathcal{G}}_N^d$ can be seen to be related to that of the Gram matrix \mathcal{G}_N^d for the open boundary case, that is the restriction of $\tilde{\mathcal{G}}_N^d$ to B_N^d . For $v = 1$, the latter determinant is already known (see for example [102] and [64]) :

$$\det \mathcal{G}_N^d = \prod_{k=1}^{(N-d)/2} (S_{d+k+1}/S_k)^{\dim V_N^{d+2k}} \quad (4.5.1)$$

where the following notation is used :

$$S_k = \sin(k\Lambda), \quad C_k = \cos(k\Lambda), \quad \Lambda = \pi - \lambda, \quad \beta = -2C_1$$

and, as usual, $\dim V_N^d = \binom{N}{(N-d)/2} - \binom{N}{(N-d-2)/2}$. Section 4.5.1 is devoted to generalizing this result for arbitrary values of v . In section 4.5.2, we show that an appropriate change of bases allows for the factorization of the Gram determinant in the periodic case in terms of Gram determinants on the strip and factors $K_{d,r}$. The computation of these new factors $K_{d,r}$ will be the following step. It will require treating the subspaces with $d = 0$ and $d > 0$ separately, as non-contractible loops yield factors of α in the former, while in the latter defects are twisted, yielding powers of the twist parameter v . We shall then be able to prove the following theorem (theorem 4.5.3) and characterize when \tilde{i}_N^d is singular (theorem 4.5.5).

THEOREM *The determinant of the Gram matrices $\tilde{\mathcal{G}}_N^d$ are*

$$\det \tilde{\mathcal{G}}_N^0 = \prod_{k=1}^{N/2} (\alpha^2 - 4C_k^2)^{\binom{N}{N/2-k}}, \quad (4.5.2)$$

$$\text{and} \quad \det \tilde{\mathcal{G}}_N^d = \prod_{k=1}^{(N-d)/2} (4 \cos^2(\mu N) - 4C_{k+d/2}^2)^{\binom{N}{(N-d)/2-k}}, \quad \text{when } d > 0, \quad (4.5.3)$$

where $v = e^{i\mu}$. Trivially, when $d = N$, $\det \tilde{\mathcal{G}}_N^N = 1$.

Formulas (4.5.2) and (4.5.3) have been proved in various contexts before. To our knowledge, they first appeared in Martin and Saleur's work [92] on the representation theory of the full Temperley-Lieb algebra on a graph G . (The periodic Temperley-Lieb corresponds to choosing the graph G to be the affine \hat{A}_N .) Graham and Lehrer [93] gave a full description of the representation theory of the periodic Temperley-Lieb algebra (affine Temperley-Lieb algebra) within the context of category theory. Their work provides detailed proofs and includes the formulas above. Their affine cell representation $W_{t,z}$ is introduced as a functor between two categories. For a given n (our N), their modules $W_{t,z}(n)$ are related to our ω_d , with their t fixing our d . Their parameter z is tied to our parameter v , though the exact relationship depends on d . Their proof is (very) different from ours. Chen and Przytycki [103] recovered recently the case $d = 0$ in still another way. Clearly this result is crucial and different proofs will bring into light different properties of the problem. Ours rests upon the Wenzl-Jones projectors and underlines a remarkable property of the Gram determinant for the (original) Temperley-Lieb to be proved next.

4.5.1 The Gram determinant on the strip

The goal of this section is to show that equation (4.5.1), which gives $\det(\mathcal{G}_N^d)$ for $v = 1$, actually holds for any value of the twist parameter. In fact, we will pursue an even more ambitious goal. Let $\langle \cdot | \cdot \rangle_G^v : V_N^d \times V_N^d \rightarrow \mathbb{C}$, with $\mathbf{v} = (v_1, v_2, \dots, v_d)$, be the bilinear form defined for $w_1, w_2 \in B_N^d$ as

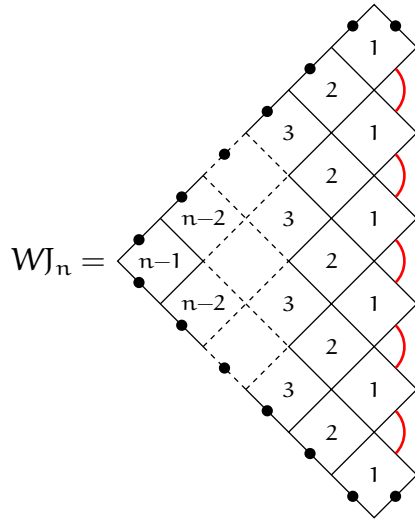
$$\langle w_1 | w_2 \rangle_G^v = \begin{cases} 0 & \text{if, in } D_G(w_1, w_2), \text{ defects of } w_1 \text{ (or } w_2) \text{ are connected,} \\ \alpha^{n_\alpha} \beta^{n_\beta} \prod_i v_i^{\Delta_i} & \text{otherwise,} \end{cases}$$

where now Δ_i denotes the displacement, towards the left, of defect i with the index i labelling defects from left to right. Note that this new bilinear form coincides with the usual one on V_N^d when $d = 0$. Because w_1 and w_2 are in B_N^d , $\langle w_1 | w_2 \rangle_G^v$ is non zero only when defect i from w_1 is connected to defect i of w_2 . In this section we show that the determinant of the matrix $\mathcal{G}_N^{d,v}$ of this bilinear form is independent of the v_i s and therefore

$$\det \mathcal{G}_N^{d,v} = \det \mathcal{G}_N^d. \quad (4.5.4)$$

The main tool will be the Wenzl-Jones projector (see [57, 67]).

DEFINITION 4.5.1 For each $1 \leq n \leq N$, the Wenzl-Jones projector $WJ_n \in \mathcal{ETLP}_N(\beta, \alpha)$ is defined as $WJ_1 = \text{id}$ and for $n > 1$ as



where each box is

$$\diamond_k = \begin{array}{c} \text{---} \\ \diagup \quad \diagdown \\ \text{---} \end{array} = \begin{array}{c} \text{---} \\ \diagup \quad \diagdown \\ \text{---} \end{array} + \frac{S_k}{S_{k+1}} \begin{array}{c} \text{---} \\ \diagdown \quad \diagup \\ \text{---} \end{array} = \frac{(-1)^k}{S_{k+1}} \begin{array}{c} \text{---} \\ \diagdown \quad \diagup \\ \text{---} \end{array} \quad (4.5.5)$$

The projector WJ_n acts on n of the N positions of \mathcal{ETLP}_N . If these positions are chosen to be 1 to n , then WJ_n satisfies the three properties [57, 67, 60] :

- (i) $WJ_n e_i = e_i WJ_n = 0$ for $n \geq 2$ and $i = 1, 2, \dots, n - 1$.
- (ii) $(WJ_n)^2 = WJ_n$.
- (iii) the reflection through a horizontal mirror of the diagram defining WJ_n is equal to WJ_n . Equivalently $WJ_n = (WJ_n)^\dagger$. (See the definition of “ \dagger ” before theorem 4.3.3.)
- (iv) WJ_n is also unchanged if the diagram defining the projector is reflected through a vertical mirror. This follows from the unicity of the projector defined by (i) and (ii), as proved for example in [60].

If WJ_n is chosen to act on positions k to $k + n - 1$ or, even, on a subset of $\{1, 2, \dots, N\}$ of n elements, then (ii), (iii) and (iv) still stand, but (i) then needs to be replaced by the statement that any bubble joining neighboring positions on WJ_n gives zero [45, 77]. The property (iii) implies that $\langle v | WJ_n w \rangle_G = \langle WJ_n v | w \rangle_G$ for $v, w \in \tilde{V}_N$. Note that the projector WJ is defined only when none of the sine functions in the denominators (equation (4.5.5)) vanish ; this requirement is clearly a condition on Λ .

To show equation (4.5.4), we partition B_N^d as $\mathcal{W}_1 \cup \mathcal{W}_2$: \mathcal{W}_1 contains all link states in B_N^d with a defect in first position, while \mathcal{W}_2 contains link states with a bubble starting in first position. For $N = 5, d = 1$,

$$B_5^1 = \left\{ \underbrace{\downarrow \curvearrowright \downarrow \curvearrowright \downarrow}_{\mathcal{W}_1}, \underbrace{\downarrow \curvearrowright \downarrow \curvearrowright \downarrow \curvearrowright \downarrow}_{\mathcal{W}_2} \right\}.$$

The next step is to replace the elements of \mathcal{W}_2 . To each $w \in \mathcal{W}_2$, we do the following manipulations: remove all arcs except the one in first position, apply a projector WJ_{d+1} on the d defects and on the right part of the arc in first position and, finally, restore the $(N - d - 2)/2$ arcs into their original positions. We note by $\mathcal{V}(w) \in V_N^d$ the resulting vector and by $\mathcal{V}\mathcal{W}_2$ the new set.

Note that the action of the projector WJ on the link states with d defects is that of definition 4.2.6, but with d different twist parameters, one for each defect. Such an action is a representation of the (usual) Temperley-Lieb algebra (generated by e_i s, with $i = 1, \dots, N - 1$, satisfying equation (4.2.1)). The proof of this claim is identical to that of proposition 4.2.1. Again one can check that the relations (4.2.1) are always satisfied (each involves at most four entries of the link state) and that a given defect i is always associated with the same twist parameter v_i , a property that is lost for the periodic case.

For the above example, we get

$$\mathcal{V}\mathcal{W}_2 = \left\{ \downarrow \curvearrowright \downarrow \curvearrowright \downarrow \curvearrowright \downarrow, \downarrow \curvearrowright \downarrow \curvearrowright \downarrow \curvearrowright \downarrow, \downarrow \curvearrowright \downarrow \curvearrowright \downarrow \curvearrowright \downarrow \right\}.$$

To compute the twist factor $\prod_i v_i^{\Delta_i}$ in a Gram diagram, one has to be cautious to identify correctly the position of the defects. For example, the second element of $\mathcal{V}\mathcal{W}_2$ above will be a sum of two link states. The (only) defect is at position 1 in one of the two link states (with an added factor v_1^4) and at position 5 in the other (with no factor added).

By construction, when Λ is chosen such that WJ_{d+1} exists, the vector $\mathcal{V}(w)$ for $w \in \mathcal{W}_2$ has the form $w + w'$ for some w' in \mathcal{W}_1 . Therefore $\mathcal{W}_1 \cup \mathcal{V}\mathcal{W}_2$ is a basis of V_N^d and the determinant of the change of bases is 1.

Our interest in this new basis is that for $w_1 \in \mathcal{W}_1$ and $w_2 \in \mathcal{W}_2$, $\langle w_1 | \mathcal{V}(w_2) \rangle_G = 0$. Indeed, the entries at positions 2 to $N - 1$ in $\mathcal{V}(w_2)$ are connected to $d + 1$ entries of a WJ_{d+1} and $(N - d - 2)/2$ bubbles, while those of w_1 are connected to $d - 1$ defects and $(N - d)/2$ bubbles. In $D_G(w_1, \mathcal{V}(w_2))$, two entries of the projector are tied by

bubbles and the result is 0. The new Gram product $\langle u_1 | w_1 \rangle_G^{\mathbf{v}}$ between two states u_1 and w_1 in \mathcal{W}_1 is just the Gram product between states in V_{N-1}^{d-1} obtained from u_1 and w_1 by removing the defect at the first position, and with $\mathbf{v}' = (v_2, \dots, v_d)$.

The product $\langle \mathcal{Y}(u_2) | \mathcal{Y}(w_2) \rangle_G^{\mathbf{v}}$ for $u_2, w_2 \in \mathcal{W}_2$ can be seen to factor into a constant L_d independent of \mathbf{v} times $\langle \mathcal{Y}(u_2) | \mathcal{Y}(w_2) \rangle_G^{\mathbf{v}''}$ where $\mathcal{Y}(w)$ stands for the link states in B_{N-1}^{d+1} obtained by removing the bubble connecting positions 1 and x , putting a defect at x and removing position 1 altogether. The added defect is considered to have $i = 0$, and we must impose $v_0 = 1$ for the twist factor to be evaluated correctly, so $\mathbf{v}'' = (1, v_1, \dots, v_d)$. The v_i dependence in the original $\langle \mathcal{Y}(u_2) | \mathcal{Y}(w_2) \rangle_G^{\mathbf{v}}$ is contained in $\langle \mathcal{Y}(u_2) | \mathcal{Y}(w_2) \rangle_G^{\mathbf{v}''}$. Finally, the constant L_d is given by

$$L_d = \text{[Diagram 1]} = \text{[Diagram 2]} = -\frac{S_{d+2}}{S_{d+1}} \text{[Diagram 3]} = -\frac{S_{d+2}}{S_{d+1}} \text{[Diagram 4]}$$

where, at the last step, the only configuration contributing has all tiles set to \diamond . From the previous remarks, up to a sign, the Gram determinants obey the recursion relation

$$\det(\mathcal{G}_N^{d,\mathbf{v}}) = \det(\mathcal{G}_{N-1}^{d-1,\mathbf{v}'}) \times \left(\frac{S_{d+2}}{S_{d+1}} \right)^{\dim V_{N-1}^{d+1}} \det(\mathcal{G}_{N-1}^{d+1,\mathbf{v}''}). \quad (4.5.6)$$

Two limiting cases are known :

$$\det \mathcal{G}_N^{0,\mathbf{v}} = \det \mathcal{G}_N^0 \quad \text{and} \quad \det \mathcal{G}_N^{N,\mathbf{v}} = 1. \quad (4.5.7)$$

The use of (4.5.6) lowers the bottom index N . Its repeated use will lead either to an upper index $d = 0$ through the first term of the right side or to equal upper and lower indices through its second term. Thus equations (4.5.6) and (4.5.7) determine $\det(\mathcal{G}_N^{d,\mathbf{v}})$ completely. The expression given in equation (4.5.1) satisfies all these and must thus be the solution. Even though the matrices \mathcal{G}_N^d explicitly depend upon the

twist parameters v_i , their determinants do not! Again, for the previous example, the Gram matrix is

$$G_5^{1,v} = \begin{pmatrix} \beta^2 & \beta & \beta v^{-2} & v^{-4} & \beta v^{-4} \\ \beta & \beta^2 & v^{-2} & \beta v^{-4} & v^{-4} \\ \beta v^2 & v^2 & \beta^2 & \beta v^{-2} & v^{-2} \\ v^4 & \beta v^4 & \beta v^2 & \beta^2 & \beta \\ \beta v^4 & v^4 & v^2 & \beta & \beta^2 \end{pmatrix}$$

and a direct computation gives

$$\det(G_5^{1,v}) = (\beta^2 - 1)^4(\beta^2 - 2) = (S_3/S_1)^{\dim V_5^3} (S_4/S_2)^{\dim V_5^2}.$$

4.5.2 The relation between the open and the periodic cases

DEFINITION 4.5.2 *The subset $\tilde{B}_N^{d,r} \subset \tilde{B}_N^d$ contains the link patterns that have precisely r bubbles crossing the imaginary boundaries at $x = \frac{1}{2}$ and $x = N + \frac{1}{2}$. Then $\tilde{B}_N^d = \cup_{0 \leq r \leq (N-d)/2} \tilde{B}_N^{d,r}$ is a partition of \tilde{B}_N^d and $\tilde{V}_N^{d,r} \subset \tilde{V}_N^d$ is the subspace spanned by $\tilde{B}_N^{d,r}$.*

A bijection C between $\tilde{B}_N^{d,r}$ and B_N^{d+2r} is defined by identifying $w \in \tilde{B}_N^{d,r}$ to $C(w) \in B_N^{d+2r}$ obtained by replacing the r boundary bubbles of w by defects, and leaving the rest of w unchanged. When $r = 0$, $C(w) = w$.

From now on, the basis \tilde{B}_N^d will be (partially) ordered in ascending order of r . Here are examples of pairs $w \leftrightarrow C(w)$:

$$C(\text{diagram with 3 bubbles}) = \text{diagram with 3 defects}, \quad C(\text{diagram with 1 bubble and 1 defect}) = \text{diagram with 1 defect}.$$

We now introduce a linear transformation \mathcal{U} such that, in the new basis $\{\mathcal{U}(w), w \in \tilde{B}_N^d\}$, the Gram matrix is block-diagonal.

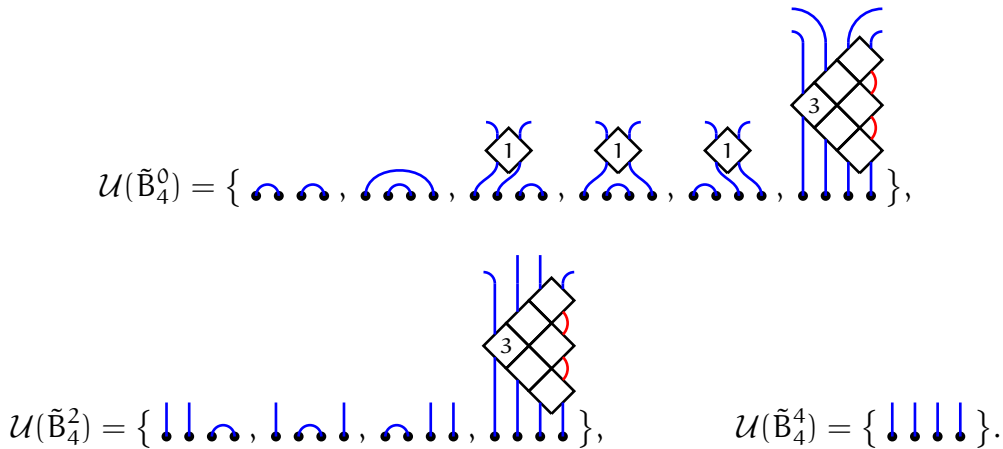
DEFINITION 4.5.3 *The linear transformation $\mathcal{U} : \tilde{V}_N^d \rightarrow \tilde{V}_N^d$ is defined by its action on elements w of each $\tilde{B}_N^{d,r}$. If $r > 0$, $\mathcal{U}(w)$ is obtained by first removing all arcs of w that do not cross the boundary, acting with WJ_{d+2r} on the r remaining bubbles and the d defects, and then inserting back the bubbles that were first removed at their original positions. If $r = 0$, $\mathcal{U}(w) = w$.*

Here is an example for $w \in \tilde{B}_8^{4,1}$:

$$\mathcal{U}(\text{diagram with 1 bubble and 4 defects}) = \text{diagram with a grid and 4 defects}.$$

The Wenzl-Jones projector WJ_n is a product of terms of the form $(\text{id} + e_i S_k / S_{k+1})$ and therefore its expansion contains words $e_{i_1} e_{i_2} \dots e_{i_\ell}$ in the $(n - 1)$ first generators of \mathcal{ETLP}_N . The identity id , that is the empty word, occurs with a factor one. The removal of the bubbles that do not cross the boundary in $w \in \tilde{B}_N^{d,r}$ gives a state in $\tilde{B}_{d+2r}^{d,r}$. But the non-empty words $e_{i_1} e_{i_2} \dots e_{i_\ell}$ cannot create new bubbles, they can only move them around. So these words either act as zero or give, up to a constant, a vector in $\tilde{B}_{d+2r}^{d,r'}$ with $r' < r$. Thus $\mathcal{U}(w) = w + w'$ where w' is a linear combination of vectors in the $\tilde{B}_N^{d,r'}$'s with $r' < r$. The matrix U_N^d representing the linear transformation \mathcal{U} in the basis \tilde{B}_N^d , ordered with increasing r 's, is therefore upper block triangular with identity matrices along the diagonal. For Λ s where the projectors WJ exist, the matrix \mathcal{U} exists, is invertible and $\mathcal{U}(\tilde{B}_N^d) = \{\mathcal{U}(w) | w \in \tilde{B}_N^d\}$ is a basis of \tilde{V}_N^d . The matrix elements of U_N^d depend on β , through Λ , and on v . When N is even and $d = 0$, some words of WJ may close non-contractible loops and α may also appear.

Here are the new bases of the three \tilde{V}_N^d for $N = 4$:



The Gram matrix is much simpler in these new bases for the V_N^d 's.

PROPOSITION 4.5.1 For $w_1 \in \tilde{B}_N^{d,r_1}, w_2 \in \tilde{B}_N^{d,r_2}$

$$\langle \mathcal{U}(w_2) | \mathcal{U}(w_1) \rangle_G = \delta_{r_1, r_2} K_{d,r_1} \langle \mathcal{C}(w_2) | \mathcal{C}(w_1) \rangle_G^{\mathbf{v}}, \quad \text{with} \quad K_{d,r} = \langle w^{d,r} | WJ_{d+2r} w^{d,r} \rangle_G \tag{4.5.8}$$

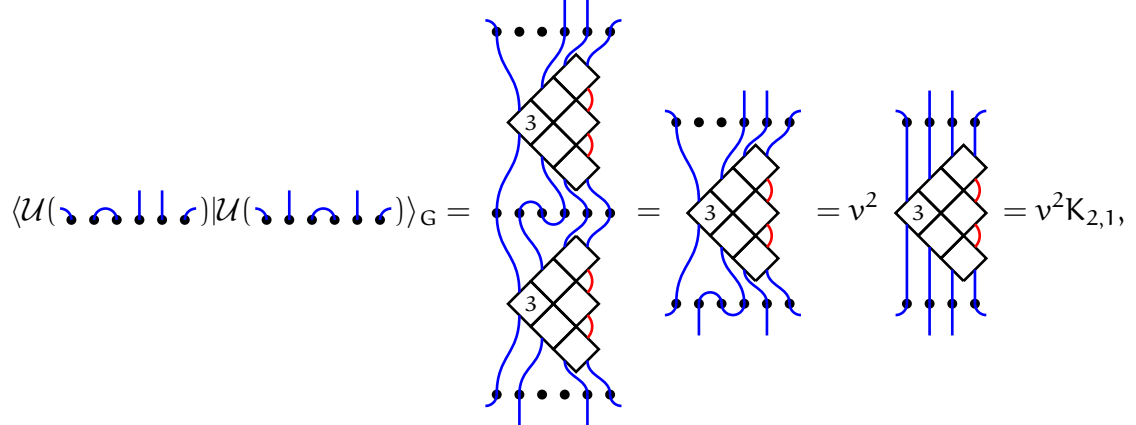
where $w^{d,r}$ is the (unique) link state $\in \tilde{B}_{d+2r}^{d,r}$ and $\mathbf{v} = (\underbrace{1, \dots, 1}_r, \underbrace{v, \dots, v}_d, \underbrace{1, \dots, 1}_r)$.

PROOF The only states w_3 that can potentially satisfy $\langle w_3 | \mathcal{U}(w_1) \rangle_G \neq 0$ are those in V_N^d . This is why w_1 and w_2 have been taken with the same number of defects.

What happens when we calculate explicitly $\langle \mathcal{U}(w_2) | \mathcal{U}(w_1) \rangle_G$? If $r_1 > r_2$, in the Gram diagram, WJ_{d+2r_1} has more entries than WJ_{d+2r_2} and some entries of WJ_{d+2r_1} are necessarily connected pairwise by some (non-boundary) bubbles of the original w_2 . From the property (i) of the WJ projector, the result is zero when $r_1 > r_2$, so we restrict our study to $r_1 = r_2 \equiv r$. Two scenarios may occur for the diagram $D_G(\mathcal{U}(w_2), \mathcal{U}(w_1))$.

In the first, the bottom $d + 2r$ points of the top projector are not all connected to entries of the bottom projector. When this happens, the top WJ has some of its N points connected to non-boundary bubbles and the result is 0, by the same argument used above for $r_1 \neq r_2$. Under these conditions, $\langle \mathcal{C}(w_2) | \mathcal{C}(w_1) \rangle_G$ vanishes. Indeed, the bubbles connecting entry points of the Wenzl-Jones projector, say in $\mathcal{U}(w_1)$, now connect two defects of $\mathcal{C}(w_1)$ in $D_G(\mathcal{C}(w_2), \mathcal{C}(w_1))$ and the result is zero.

In the second scenario, the $d + 2r$ entries of the top Wenzl-Jones projector coincide with those of the bottom one. Then the pattern of contractible bubbles is the same in $D_G(\mathcal{U}(w_2), \mathcal{U}(w_1))$ and $D_G(\mathcal{C}(w_2), \mathcal{C}(w_1))$ and the corresponding factors of β are equal. Let us then concentrate on the d defects and r boundary bubbles of each diagram. The $d + 2r$ corresponding entries of the diagram $D_G(\mathcal{U}(w_2), \mathcal{U}(w_1))$ start, from the top, as a state with d defects and r boundary bubbles, that is $w^{d,r}$, go through two copies of the Wenzl-Jones projector WJ_{d+2r} and then connect with a second $w^{d,r}$, as in the following example,



where properties (ii) and (iii) of the WJ projector were used at the second equality. The product $\langle \mathcal{U}(w_2) | \mathcal{U}(w_1) \rangle_G$ is thus $\beta^{n_\beta} v^{\tilde{\Delta}} K_{d,r}$ for some $\tilde{\Delta}$, and with $K_{d,r}$ given by

$$K_{d,r} = \langle w^{d,r} | WJ_{d+2r} w^{d,r} \rangle_G.$$

For a given configuration of the WJ projector, each defect i will contribute a factor $v^{\tilde{\Delta}_i + \Delta'_i}$ to the total weight, where $\tilde{\Delta}_i$ is the displacement of the defect $i + r$ in the diagram $D_{\mathcal{G}}(\mathcal{C}(w_2), \mathcal{C}(w_1))$ and Δ'_i depends upon the configuration chosen for the WJ projector. Defects 1 to r and $d + r + 1$ to $d + 2r$ in $D_{\mathcal{G}}(\mathcal{C}(w_2), \mathcal{C}(w_1))$ correspond to boundary bubbles of the original diagram $D_{\mathcal{G}}(\mathcal{U}(w_2), \mathcal{U}(w_1))$ and must contribute v^0 , which justifies our choice of \mathbf{v} in $\langle \mathcal{C}(w_2) | \mathcal{C}(w_1) \rangle_{\mathcal{G}}^{\mathbf{v}}$. For example, the diagram above has a twist factor of v^2 which is exactly the twist one finds in computing

$$\langle \mathcal{C}(\text{diagram}) | \mathcal{C}(\text{diagram}) \rangle_{\mathcal{G}}^{\mathbf{v}} = \langle \text{diagram} \rangle_{\mathcal{G}}^{\mathbf{v}} = v^2$$

with $\mathbf{v} = (1, v, v, 1)$ and where $\tilde{\Delta}_1 = 2$ and $\tilde{\Delta}_2 = 0$. The factor $v^{\tilde{\Delta}_i + \Delta'_i}$ will depend on the choice of configuration of the projector WJ and will be accounted for in the computation of $K_{d,r}$. This will be apparent in section 4.5.3. The product $\langle \mathcal{U}(w_2) | \mathcal{U}(w_1) \rangle_{\mathcal{G}}$ is thus given by $K_{d,r} \langle \mathcal{C}(w_2) | \mathcal{C}(w_1) \rangle_{\mathcal{G}}^{\mathbf{v}}$, as given in the proposition. \square

For $d = 0$, the dependence on α is hidden in the constant $K_{d,r}$, while for $d > 0$ both $K_{d,r}$ and $\langle \mathcal{C}(w_2) | \mathcal{C}(w_1) \rangle_{\mathcal{G}}^{\mathbf{v}}$ have a v dependence. The calculation of $K_{d,r}$ will be done in section 4.5.3. But we can already sum up the simplification afforded by the new basis.

COROLLARY 4.5.2

$$\det \tilde{\mathcal{G}}_N^d = \prod_{r=0}^{(N-d)/2} \det(\mathcal{G}_N^{d+2r}) K_{d,r}^{\dim V_N^{d+2r}} \tag{4.5.9}$$

PROOF For the proof, we calculate the matrix $\Gamma_N^d = (U_N^d)^T \tilde{\mathcal{G}}_N^d U_N^d$, whose matrix elements are given by

$$(\Gamma_N^d)_{w_1, w_2} = \langle \mathcal{U}(w_2) | \mathcal{U}(w_1) \rangle_{\mathcal{G}}.$$

Because U_N^d is upper triangular and has only 1s on the diagonal, $\det \tilde{\mathcal{G}}_N^d = \det \Gamma_N^d$. In the previous proposition, we have found $\Gamma_N^d|_{\tilde{V}_N^{d,r}} = K_{d,r} \mathcal{G}_N^{d+2r, \mathbf{v}}$. But $\det \mathcal{G}_N^{d+2r, \mathbf{v}}$ is independent of v and given by (4.5.1), and this completes the proof. \square

Again examples are useful :

$$\Gamma_4^0 = \left(\begin{array}{cccccc} \text{diagram} & 0 & 0 & 0 & 0 & 0 \\ \text{diagram} & 0 & 0 & 0 & 0 & 0 \\ 0 & 0 & \text{diagram} & \text{diagram} & \text{diagram} & 0 \\ \text{diagram} & \text{diagram} & \text{diagram} & \text{diagram} & \text{diagram} & 0 \\ 0 & 0 & \text{diagram} & \text{diagram} & \text{diagram} & 0 \\ \text{diagram} & \text{diagram} & \text{diagram} & \text{diagram} & \text{diagram} & 0 \\ 0 & 0 & \text{diagram} & \text{diagram} & \text{diagram} & 0 \\ \text{diagram} & \text{diagram} & \text{diagram} & \text{diagram} & \text{diagram} & 0 \\ 0 & 0 & 0 & 0 & 0 & \text{diagram} \\ 0 & 0 & 0 & 0 & 0 & \text{diagram} \end{array} \right) = \begin{pmatrix} \beta^2 & \beta & 0 & 0 & 0 & 0 \\ \beta & \beta^2 & 0 & 0 & 0 & 0 \\ 0 & 0 & \beta K_{0,1} & K_{0,1} & 0 & 0 \\ 0 & 0 & K_{0,1} & \beta K_{0,1} & K_{0,1} & 0 \\ 0 & 0 & 0 & K_{0,1} & \beta K_{0,1} & 0 \\ 0 & 0 & 0 & 0 & 0 & K_{0,2} \end{pmatrix}$$

$$\Gamma_4^2 = \left(\begin{array}{cccc} \text{diagram} & 0 & 0 & 0 \\ \text{diagram} & 0 & 0 & 0 \\ \text{diagram} & 0 & 0 & 0 \\ 0 & 0 & 0 & \text{diagram} \\ 0 & 0 & 0 & \text{diagram} \end{array} \right) = \begin{pmatrix} \beta & v^{-2} & 0 & 0 \\ v^2 & \beta & v^{-2} & 0 \\ 0 & v^2 & \beta & 0 \\ 0 & 0 & 0 & K_{2,1} \end{pmatrix}, \quad \Gamma_4^4 = (1)$$

with $K_{0,1} = \text{diag}(1)$, $K_{0,2} = \text{diag}(3)$, $K_{2,1} = \text{diag}(3)$.

The next section is devoted to the computation of $K_{d,r}$.

4.5.3 The factor $K_{d,r}$

We construct recursion relations for $K_{d,r}$ and use them to find their values. For $d = 0$, $K_{0,r}$ satisfies the relation

$$K_{0,r} = K_{0,r-1}(\alpha^2 - 4C_r^2) \frac{S_r^2}{S_{2r}S_{2r-1}} \tag{4.5.10}$$

To show this, we sum over all configurations of the top diagonal row. Many of these have weight 0. All configurations with $\text{diag}(1)$ give 0 from property (i) of the WJ projector. Also, the top entries of the WJ_{2r} are of two types : those connected to the boundary at $x = N + 1/2$ and those connected to the boundary at $x = 1/2$. Configurations with $\text{diag}(1)$ connecting two entries of the same type also give 0. In the end, only two configurations have non-zero contribution :

$$K_{0,r} = \frac{S_r}{S_{2r}} \text{diag}(1) + 1 \text{diag}(1)$$

In the first term, a non-contractible loop is closed and a factor of α is added. Summing over the lower diagonal row and using the same arguments as before gives a unique contribution, and the result is

$$\alpha \frac{S_r^2}{S_{2r}S_{2r-1}} \text{diag}(1) = \alpha^2 \frac{S_r^2}{S_{2r}S_{2r-1}} K_{0,r-1}$$

In the second term, we use property (iv) of the WJ projector and find

$$= -\frac{S_{2r}}{S_{2r-1}} = -\frac{S_{2r}}{S_{2r-1}} K_{0,r-1}$$

where we used

$$= -\frac{S_{k+2}}{S_{k+1}}$$

to obtain the second equality. This concludes the proof of equation (4.5.10). One can compute the initial condition $K_{0,1} = (\alpha^2 - 4C_1^2) \frac{S_1}{S_2}$ and find, finally,

$$K_{0,r} = \prod_{k=1}^r \frac{S_k^2}{S_{2k}S_{2k-1}} (\alpha^2 - 4C_k^2) = \prod_{k=1}^r \frac{S_k}{S_{r+k}} (\alpha^2 - 4C_k^2). \quad (4.5.11)$$

The case $d > 0$ depends on the twist parameter $v = e^{i\mu}$ of which we must keep track when writing the recurrence relation

$$K_{d,r} = K_{d,r-1} (4 \cos^2 \mu N - 4C_{r+d/2}^2) \frac{S_r S_{r+d}}{S_{2r+d} S_{2r+d-1}}. \quad (4.5.12)$$

The steps are otherwise similar to those of the case $d = 0$:

$$= \frac{S_r}{S_{2r+d}} + \frac{S_{r+d}}{S_{2r+d}} + 1. \quad (4.5.13)$$

Top entries of the projector are of three types : besides the left and right boundary bubbles encountered before, they can also be connected to defects. Whenever connects two entries of the same type, the result is 0 as before. The connections of the first and second term of (4.5.13) are identical, but the weight due to the twist in the defects is not and remains to be computed. When computing twist factors, we must not forget that the original diagram has N positions and that contractible loops can be present between the entries of the projector WJ . The first diagram provides

a good example. Entries of the projector WJ are labeled by integers $i = 1, \dots, 2r + d$ (defects occupy positions $r + 1$ to $r + d$) and correspond to some positions p_i in the original diagram. In (4.5.13), the $(d - 1)$ leftmost defects entering the projector WJ all connect two positions to the right of their entry point, so their contribution to the twist factor is $v^{p_i - p_{i+2}}$, for $i = r + 1, \dots, r + d - 1$. The rightmost defect enters from the top at position $r + d$, moves right across the imaginary boundary, and then connects at position $r + 2$. Because the original diagram has N positions, this last defect contributes $v^{p_{r+d} - (N + p_{r+2})}$. The total twist weight of the d defects of this first diagram sums to $v^{-(N + \delta)}$, with $\delta = p_{r+d+1} - p_{r+1}$. Each defect of the second diagram has the same entry and exit points, except for the leftmost defect that wraps around in the left direction. This defect gives the only contribution to the second diagram, namely $v^{(N - \delta)}$. With these twist weights, contributions of the first and second diagrams combine and give

$$\begin{aligned}
 & \underbrace{v^{-\delta} \left(v^N \frac{S_{r+d}}{S_{2r+d}} + v^{-N} \frac{S_r}{S_{2r+d}} \right)}_A \text{Diagram} = A \left(\text{Diagram} + \text{Diagram} \right) \\
 & = v^{-\delta} \left(v^N \frac{S_{r+d}}{S_{2r+d}} + v^{-N} \frac{S_r}{S_{2r+d}} \right) v^{\delta} \left(v^{-N} \frac{S_{r+d}}{S_{2r+d-1}} + v^N \frac{S_r}{S_{2r+d-1}} \right) K_{d,r-1} \\
 & = \frac{4 \cos^2(\mu N) S_r S_{r+d} + (2C_{r+d/2} S_{d/2})^2}{S_{2r+d} S_{2r+d-1}} K_{d,r-1},
 \end{aligned}$$

where we have summed over configurations of the lower diagonal row and computed twist weights as explained earlier. The last term in (4.5.13) can be seen to give $-(S_{2r+d}/S_{2r+d-1})K_{d,r-1}$ by the same argument as the one given for $d = 0$. A simple exercise using trigonometric functions shows that the two contributions sum up to equation (4.5.12). Because the v^δ s have cancelled out, $K_{d,r}$ is independent of the positions of the contractible loops of the original diagram. With the initial condition $K_{d,0} = 1$, we find

$$K_{d,r} = \prod_{k=1}^r \frac{S_k S_{k+d}}{S_{2k+d} S_{2k+d-1}} (4 \cos^2(\mu N) - 4C_{k+d/2}^2) = \prod_{k=1}^r \frac{S_k}{S_{r+d+k}} (4 \cos^2(\mu N) - 4C_{k+d/2}^2). \quad (4.5.14)$$

4.5.4 The determinant of the Gram matrix

The purpose of the previous paragraph was to compute the constants $K_{d,r}$. Note that the result (4.5.14) for $K_{d,r}$ gives the expression (4.5.11) for $K_{0,r}$ when d is set to zero and $2 \cos \mu N$ is replaced by α .

PROPOSITION 4.5.3 *The determinant of the Gram matrix is*

$$\det \tilde{\mathcal{G}}_N^d = \prod_{k=1}^{(N-d)/2} (\alpha^2 - 4C_{k+d/2}^2)^{\binom{N-d}{2-k}} = \prod_{k=1}^{(N-d)/2} (\langle k-d/2 \rangle \langle k+d/2 \rangle)^{\binom{N-d}{2-k}} \quad (4.5.15)$$

where $\alpha = 2 \cos(\mu N)$ for $d > 0$ and, in the second form, $\langle x \rangle = q^x v^N - q^{-x} v^{-N}$ with $v = e^{i\mu}$ and $q = e^{-i\Lambda}$.

PROOF The results of the previous section are

$$K_{d,r} = \frac{\prod_{i=1}^r S_i}{\prod_{j=r+d+1}^{2r+d} S_j} \prod_{k=1}^r (\alpha^2 - 4C_{k+d/2}^2)$$

where, for $d > 0$, α stands for $2 \cos \mu N$. Using (4.5.1) and (4.5.9), we get

$$\begin{aligned} \det \tilde{\mathcal{G}}_N^d &= \prod_{r=0}^{(N-d)/2-1} \prod_{k=1}^{(N-d)/2-r} (S_{d+2r+k+1}/S_k)^{\dim V_N^{d+2r+2k}} \\ &\quad \times \prod_{r=1}^{(N-d)/2} \left(\prod_{i=1}^r (S_i/S_{r+d+i}) \prod_{k=1}^r (\alpha^2 - 4C_{k+d/2}^2) \right)^{\dim V_N^{d+2r}}. \end{aligned}$$

The factors of the form $(\alpha^2 - 4C_{k+d/2}^2)$ yield

$$\begin{aligned} \prod_{r=1}^{(N-d)/2} \prod_{k=1}^r (\alpha^2 - 4C_{k+d/2}^2)^{\dim V_N^{d+2r}} &= \prod_{k=1}^{(N-d)/2} \prod_{r=k}^{(N-d)/2} (\alpha^2 - 4C_{k+d/2}^2)^{\dim V_N^{d+2r}} \\ &= \prod_{k=1}^{(N-d)/2} (\alpha^2 - 4C_{k+d/2}^2)^{\sum_{r=k}^{(N-d)/2} \dim V_N^{d+2r}} \\ &= \prod_{k=1}^{(N-d)/2} (\alpha^2 - 4C_{k+d/2}^2)^{\dim \tilde{V}_N^{d+2k}} \\ &= \prod_{k=1}^{(N-d)/2} (\alpha^2 - 4C_{k+d/2}^2)^{\binom{N-d}{2-k}}. \end{aligned}$$

Thus one must show that the rest is 1. For this, the order of products is inverted in each of the subfactors :

$$\begin{aligned}
\prod_{r=1}^{(N-d)/2} \prod_{i=1}^r S_i^{\dim V_N^{d+2r}} &= \prod_{i=1}^{(N-d)/2} S_i^{\sum_{r=i}^{(N-d)/2} \dim V_N^{d+2r}}, \\
\prod_{r=1}^{(N-d)/2} \prod_{j=r+d+1}^{2r+d} S_j^{\dim V_N^{d+2r}} &= \left(\prod_{j=d+2}^{(N+d)/2} \prod_{r=\lceil (j-d)/2 \rceil}^{j-d-1} S_j^{\dim V_N^{d+2r}} \right) \\
&\quad \times \left(\prod_{j=(N+d)/2+1}^N \prod_{r=\lceil (j-d)/2 \rceil}^{(N-d)/2} S_j^{\dim V_N^{d+2r}} \right) \\
&= \left(\prod_{j=d+2}^{(N+d)/2} S_j^{\sum_{r=\lceil (j-d)/2 \rceil}^{j-d-1} \dim V_N^{d+2r}} \right) \left(\prod_{j=(N+d)/2+1}^N S_j^{\sum_{r=\lceil (j-d)/2 \rceil}^{(N-d)/2} \dim V_N^{d+2r}} \right),
\end{aligned}$$

$$\begin{aligned}
\prod_{r=0}^{(N-d)/2-1} \prod_{k=1}^{(N-d-2r)/2} S_{d+2r+k+1}^{\dim V_N^{d+2r+2k}} &= \prod_{r=0}^{(N-d)/2-1} \prod_{k'=2r+d+2}^{(N+d)/2+r+1} S_{k'}^{\dim V_N^{2k'-2r-d-2}} \\
&= \left(\prod_{k=d+2}^{(N+d)/2} \prod_{r=0}^{\lfloor (k-d-2)/2 \rfloor} S_k^{\dim V_N^{2k-2r-d-2}} \right) \left(\prod_{k=(N+d)/2+1}^N \prod_{r=k-1-(N+d)/2}^{\lfloor (k-d-2)/2 \rfloor} S_k^{\dim V_N^{2k-2r-d-2}} \right) \\
&= \left(\prod_{k=d+2}^{(N+d)/2} S_k^{\sum_{r=0}^{\lfloor (k-d-2)/2 \rfloor} \dim V_N^{2k-2r-d-2}} \right) \left(\prod_{k=(N+d)/2+1}^N S_k^{\sum_{r=k-1-(N+d)/2}^{\lfloor (k-d-2)/2 \rfloor} \dim V_N^{2k-2r-d-2}} \right) \\
&= \left(\prod_{k=d+2}^{(N+d)/2} S_k^{\sum_{s=\lceil (k-d)/2 \rceil}^{k-d-1} \dim V_N^{d+2s}} \right) \left(\prod_{k=(N+d)/2+1}^N S_k^{\sum_{s=\lceil (k-d)/2 \rceil}^{(N-d)/2} \dim V_N^{d+2s}} \right),
\end{aligned}$$

$$\begin{aligned}
\prod_{r=0}^{(N-d)/2-1} \prod_{k=1}^{(N-d-2r)/2} S_k^{\dim V_N^{d+2r+2k}} &= \prod_{k=1}^{(N-d)/2} \prod_{r=0}^{(N-d)/2-k} S_k^{\dim V_N^{d+2r+2k}} \\
&= \prod_{k=1}^{(N-d)/2} S_k^{\sum_{r=0}^{(N-d)/2-k} \dim V_N^{d+2r+2k}} = \prod_{k=1}^{(N-d)/2} S_k^{\sum_{s=k}^{(N-d)/2} \dim V_N^{d+2s}}.
\end{aligned}$$

It is then clear that everything cancels out. \square

The second form of the determinant (4.5.15) shows that its zeroes all lie on curves $q^{2x}v^{2N} = 1$ and that the structure of the action ω_d depends only on the twist parameter through its $2N$ -th power. This is related to the observation made at the end of section 4.3.1 that the two actions on the XXZ models defined in [35] and here are

ted by their parameters as $e^{i\varphi} = v^{2N}$. The theorem 4.5.6 to be proven in the next section will go further in showing that these two actions are generically isomorphic to that of ω_d on \tilde{V}_N^d .

4.5.5 The determinant of $I_N^d(u, v)$

In theorem 4.3.3, we found that $\det I_N^d(u, v) \det I_N^d(u, v^{-1}) = \det \tilde{\mathcal{G}}_N^d$ with $\beta = u^2 + u^{-2}$, $\alpha = v^N + v^{-N}$ and with v as the twist parameter. In this section, we show how to calculate $\det I_N^d(u, v)$.

We first introduce paths and the height function. The set P_y^N of paths with endpoint y is the set of $\vec{x} = \{x_1, x_2, \dots, x_N\}$, where each step x_i is either $+1$ or -1 and such that $\sum_{i=1}^N x_i = y$. The height $H(\vec{x})$ of a path \vec{x} is $H(\vec{x}) = \sum_{j=1}^N h_j$ with $h_j = \sum_{i=1}^j x_i$. Clearly $H(\vec{x}) = (N + 1)y - \sum_{j=1}^N jx_j$. There are two natural bijections between \tilde{B}_N^d on the one hand and P_d^N or P_{-d}^N on the other hand. (See figure 4.1 for an example.) If $w \in \tilde{B}_N^d$, then $\mathcal{B}^+(w)$ is the path $\vec{x} = \{x_i, 1 \leq i \leq N\}$ where x_i is $+1$ if a bubble starts at i in w , and -1 if a bubble ends at i . Finally, if position i is a defect, then $x_i = +1$ in $\mathcal{B}^+(w)$ and -1 in $\mathcal{B}^-(w)$. When $d = 0$, $\mathcal{B}^+(w) = \mathcal{B}^-(w) \equiv \mathcal{B}(w)$. The fact that both \mathcal{B}^\pm are bijections is straightforward.

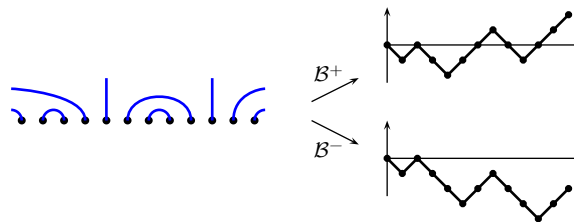


FIGURE 4.1 – A depiction of the two bijections for a link state with $N = 12$, $d = 2$ and $r = 2$. The link state w has $\psi(w) = \{(2, 3), (6, 9), (7, 8), (11, 16), (12, 13)\}$, $\sum_{(i,j) \in \psi(w)} j - i = 11$, $H(\mathcal{B}^+(w)) = -2$ and $H(\mathcal{B}^-(w)) = -24$.

LEMMA 4.5.4 *Let $w \in \tilde{B}_N^{d,r}$. Then $\sum_{(i,j) \in \psi(w)} (j - i) = \frac{1}{2}(H(\mathcal{B}^+(w)) + H(\mathcal{B}^-(w))) + Nr$.*

PROOF We start by considering the case $d = 0$. When $r = 0$, every i and j forming a pair $(i, j) \in \psi(w)$ are in the range $1, \dots, N$. A bubble that closes at position $+j$ (i.e. $x_j = -1$) contributes j to the sum $-\sum ix_i$, and one that opens at j ($x_j = +1$) contributes $-j$. Therefore $H(\vec{x}) = \sum_{(i,j) \in \psi(w)} (j - i)$. Whenever $r > 0$, some bubbles close at positions $j \geq N$ and contribute j to $\sum_{(i,j) \in \psi(w)} (j - i)$ but only $j - N$ to $H(w)$.

For every one of these r bubbles, we must add to $-\sum_{j=1}^N jx_j$ a factor of N , which yields the correct result.

For $d > 0$ and $r = 0$, the $\sum_{(i,j) \in \psi(w)} (j-i)$ has contribution j when a bubble closes at j , $-j$ when a bubble opens at j , and 0 when there is a defect at position j . This sum is therefore $-\sum_j jy_j$ where $\vec{y} = (y_1, y_2, \dots, y_N)$ is not a path of P_d^N or P_{-d}^N , but rather the y_j s are in $\{1, 0, -1\}$ and obtained from w by setting $y_j = +1$ or -1 when a bubble starts or ends at j , and 0 when a defect is at position j . In fact, $\vec{y} = \frac{1}{2}(\mathcal{B}^+(w) + \mathcal{B}^-(w))$ does this exactly. Finally, generalizing to $r > 0$ is no harder than in the case $d = 0$. \square

THEOREM 4.5.5 *The determinant of the linear map \tilde{i}_N^d , expressed between the vectors of \tilde{B}_N^d and the spin basis, is, up to a sign,*

$$\det I_N^d(u, v) = \prod_{k=1}^{(N-d)/2} \left(2i \sin \left(\Lambda(k + d/2) - \mu N \right) \right)^{\binom{\frac{N-d}{2}-k}{k}} = \prod_{k=1}^{(N-d)/2} \langle k + d/2 \rangle^{\binom{\frac{N-d}{2}-k}{k}} \quad (4.5.16)$$

where $v = e^{i\mu}$, $u = e^{i\lambda/2}$ and $\Lambda = \pi - \lambda$ and, in the second form, $q = e^{-i\Lambda}$ and $\langle x \rangle = q^x v^N - q^{-x} v^{-N}$.

PROOF The Gram determinant allows for the following factorization :

$$\det \tilde{\mathcal{G}}_N^d = \prod_{k=1}^{(N-d)/2} \left(2i \sin \left(\Lambda(k + d/2) - \mu N \right) \right)^{\binom{\frac{N-d}{2}-k}{k}} \times \prod_{k=1}^{(N-d)/2} \left(2i \sin \left(\Lambda(k + d/2) + \mu N \right) \right)^{\binom{\frac{N-d}{2}-k}{k}}$$

and the proposition is that $\det I_N^d(u, v)$ is the first product and $\det I_N^d(u, v^{-1})$ the second. This is compatible with the symmetry $v \leftrightarrow v^{-1}$ that corresponds to $\mu \leftrightarrow -\mu$. In fact, $\det I_N^d(u, v)$ is a polynomial in u and v (and their negative powers), and for each $\sin(\Lambda(k + d/2) + \mu N) \sin(\Lambda(k + d/2) - \mu N)$, one factor must contribute to $\det I_N^d(u, v)$ and the other to $\det I_N^d(u, v^{-1})$. To understand how they are distributed, we look at the $u, v \rightarrow \infty$ limit. From (4.3.4), we find, in this limit,

$$\tilde{i}_N^d(w) \rightarrow \left(\prod_{(i,j) \in \psi(w)} v^{j-i} u \sigma_j^- \right) |0\rangle = u^{|\psi(w)|} v^{\sum_{(i,j) \in \psi(w)} (j-i)} \left(\prod_{(i,j) \in \psi(w)} \sigma_j^- \right) |0\rangle.$$

It is easy to show that there is a one-to-one correspondence between states of the form $(\prod_{(i,j) \in \psi(w)} \sigma_j^-) |0\rangle$ and the link states $|w\rangle \in \tilde{B}_N^d$. Therefore, up to sign,

$$\det I_N^d \xrightarrow{u, v \rightarrow \infty} \prod_{w \in \tilde{B}_N^d} u^{|\psi(w)|} v^{\sum_{(i,j) \in \psi(w)} (j-i)} = u^{X_1} v^{X_2},$$

$$\text{with } X_1 = \sum_{w \in \tilde{\mathcal{B}}_N^d} |\psi(w)| = |\tilde{\mathcal{B}}_N^d| \frac{N-d}{2} = \binom{N}{\frac{N-d}{2}} \frac{N-d}{2} = N \binom{N-1}{\frac{N-d}{2}-1} \quad (4.5.17)$$

$$\begin{aligned} \text{and } X_2 &= \sum_{w \in \tilde{\mathcal{B}}_N^d} \sum_{(i,j) \in \psi(w)} (j-i) = \sum_{r=0}^{(N-d)/2} \sum_{w \in \tilde{\mathcal{B}}_N^{d,r}} \left(\frac{1}{2} (H(\mathcal{B}^+(w)) + H(\mathcal{B}^-(w))) + Nr \right) \\ &= \sum_{r=0}^{(N-d)/2} Nr |\tilde{\mathcal{B}}_N^{d,r}| = \sum_{r=0}^{(N-d)/2} Nr |\mathcal{B}_N^{d+2r}| \\ &= \sum_{r=0}^{(N-d)/2} Nr \left(\binom{N}{\frac{N-d}{2}-r} - \binom{N}{\frac{N-d}{2}-r-1} \right) = \sum_{s=0}^{(N-d)/2-1} N \binom{N}{s} \end{aligned} \quad (4.5.18)$$

where, for X_2 , the second equality follows from lemma 4.5.4. For the third, we used the fact that

$$\sum_{w \in \tilde{\mathcal{B}}_N^d} (H(\mathcal{B}^+(w)) + H(\mathcal{B}^-(w))) = 0. \quad (4.5.19)$$

Indeed, in terms of paths, this sum can be rewritten as $\sum_{\vec{x} \in P_d^N \cup P_{-d}^N} H(\vec{x})$. The sum is thus over all paths using edges drawn in Figure 4.2, a step in the north-east (south-east) direction corresponding to a positive x_i (negative x_i). Paths in P_d^N reach the upper dot, those in P_{-d}^N the lower one. Because the shaded domain is symmetric under a horizontal mirror, each path $\vec{x} \in P_d^N$ has a partner $-\vec{x} \in P_{-d}^N$ such that $H(\vec{x}) + H(-\vec{x}) = 0$ and the sum is 0. We now compare this result with the limiting behavior of the proposed $\det I_N^d(u, v)$. For $u, v \rightarrow \infty$,

$$\det I_N^d(u, v) = \prod_{k=1}^{(N-d)/2} (u^{2k+d} v^N - (-1)^d u^{-2k-d} v^{-N})^{\binom{N}{\frac{N-d}{2}-k}} \xrightarrow{u, v \rightarrow \infty} u^{X'_1} v^{X'_2},$$

up to a sign. The constants X'_1 and X'_2 are

$$X'_1 = \sum_{k=1}^{(N-d)/2} (2k+d) \binom{N}{\frac{N-d}{2}-k}, \quad X'_2 = \sum_{k=1}^{(N-d)/2} N \binom{N}{\frac{N-d}{2}-k} = \sum_{s=0}^{(N-d)/2-1} N \binom{N}{s}.$$

X'_2 already coincides with X_2 and a simple exercise with combinatorial coefficients shows that X_1 and X'_1 are also identical. Any other choice of distribution of the factors $\sin(\Lambda(k+d/2) \pm \mu N)$ between $I_N^d(u, v)$ and $I_N^d(u, v^{-1})$ would have changed either X'_1 , X'_2 or both, and the choice in (4.5.16) is the only possible one. \square

Let $u = e^{i\lambda/2}$ and $v = e^{i\mu}$ be fixed. A pair (N, d) is *critical* if it belongs to

$$\{(N, d) \mid \sin(\Lambda(k+d/2) - \mu N) = 0 \text{ for some } k, 1 \leq k \leq (N-d)/2\}.$$

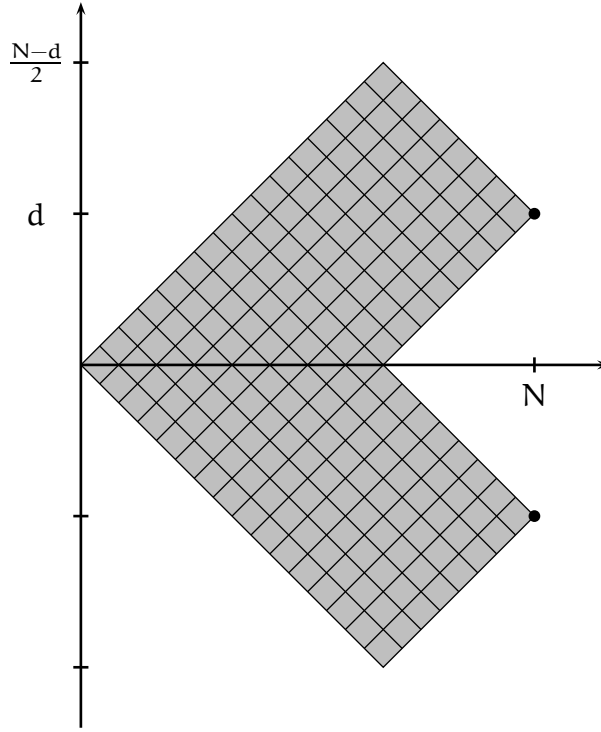


FIGURE 4.2 – The domain containing all paths in the sum (4.5.19).

Clearly the criticality of (N, d) depends on μ and $\lambda = \pi - \Lambda$ and the matrix I_N^d (or the map \tilde{i}_N^d) is singular if and only if (N, d) is critical. Equivalently the map $\tilde{i}_N^d(q, v)$ is singular if and only if the point (q, v) lies on one of the *critical curves* defined by $\langle k + d/2 \rangle = q^{k+d/2}v^N - q^{-(k+d/2)}v^{-N} = 0, 1 \leq k \leq (N - d)/2$.

THEOREM 4.5.6 *Let $u = e^{i\lambda/2}$ and $v = e^{i\mu}$ be fixed. The map $X : \mathcal{E}TLP_N(\beta, \alpha) \rightarrow \text{End}((\mathbb{C}^2)^{\otimes N})$ defined by $e_i \mapsto \bar{e}_i$ and $\Omega^{\pm 1} \mapsto \bar{\Omega}^{\pm 1}$ is a representation of $\mathcal{E}TLP_N(\beta, \alpha)$ with $\beta = u^2 + u^{-2}$ and $\alpha = v^N + v^{-N}$. Moreover, if (N, d) is not critical, then $\tilde{i}_N^d : \tilde{V}_N^d \rightarrow (\mathbb{C}^2)^{\otimes N}|_{S^z=d/2}$ is an isomorphism between modules of $\mathcal{E}TLP_N(\beta, \alpha)$. (The action on \tilde{V}_N^d is that of ω_d .)*

PROOF We left out in section 4.3 the question of whether the matrices \bar{e}_i s and $\bar{\Omega}^{\pm 1}$ verified equations (4.3.2) and (4.3.3). Clearly the matrix elements of $((\bar{\Omega}^{\pm 1}\bar{e}_N)^{N-1} - \bar{\Omega}^{\pm N}(\bar{\Omega}^{\pm 1}\bar{e}_N))$ and $(\bar{E}\bar{\Omega}^{\pm 1}\bar{E} - (v^N + v^{-N})\bar{E})$ are polynomials in u, u^{-1}, v and v^{-1} . For all non-critical values of (N, d) , these matrices are zero since then $\det I_N^d \neq 0$ and $\bar{\Omega}^{\pm 1} = (\tilde{i}_N^d)^{-1} \circ \Omega \circ \tilde{i}_N^d$ on $(\mathbb{C}^2)^{\otimes N}|_{S^z=d/2}$. (See the end of section 4.3.2.) Since the critical conditions $\Lambda(k + d/2) - \mu N \in \pi\mathbb{Z}$ represent a finite number of surfaces in

the parameter space $(\mathbb{C}^\times)^2$ of (u, v) , then these matrices with polynomial elements vanish everywhere. So equations (4.3.2) and (4.3.3) and all other defining relations are verified by the \bar{e}_i s and $\bar{\Omega}^{\pm 1}$. The fact that \tilde{i}_N^d is an isomorphism of modules follows from the previous discussion and theorem 4.5.5. \square

4.6 Jordan blocks within sectors of loop models

The goal of this section is to show how the intertwiner \tilde{i}_N^d can be used to identify Jordan cells in the restriction of the loop Hamiltonian \mathcal{H} to a given sector \tilde{V}_N^d . The whole section uses the action of ω_d on \tilde{V}_N^d . The parameter $q = -u^2 = e^{-i\Lambda}$ is preferred here to the parameter u used in sections 4.2, 4.3 and 4.5.

Finding Jordan cells in $\mathcal{H}|_{\tilde{V}_N^d}$ requires new techniques. The method used in section 4.4 and based on our previous work [77] fails here, simply because the central element F_N acts diagonally in the representation ω_d . The new method relies on the singularity of \tilde{i}_N^d at critical pairs (q_c, v_c) . The next subsection will show that, if \mathcal{H} has a Jordan cell, the eigenvector of this cell and all the first Jordan partners, except maybe the very “last” one, must belong to the kernel of $\tilde{i}_N^d(q_c, v_c)$. The following subsection will show how the algebra $U_q(\mathfrak{sl}_2)$ provides, at some critical (q_c, v_c) , some maps commuting with the spin Hamiltonian H . These will eventually be used to explore the (image by I_N^d of the) generalized eigensubspace of \mathcal{H} . The last two subsections describe the left nullspace of \tilde{i}_N^d and construct explicitly an infinite family of Jordan cells of \mathcal{H} for some specific values of the pair (q, v) .

4.6.1 Basic observations and identities

Both \mathcal{H} and the XXZ Hamiltonian H are representatives of the abstract element $\sum_{1 \leq i \leq N} e_i \in \mathcal{E}TLP_N$. The spin Hamiltonian H is hermitian when $q (= -u^2)$ and v are both on the unit circle and is therefore diagonalizable. When $\tilde{i}_N^d : \tilde{V}_N^d \rightarrow (\mathbb{C}^2)^{\otimes N}|_{S^z=d/2}$ is an isomorphism and therefore invertible, any eigenvector $|\nu\rangle$ of H is mapped by $(\tilde{i}_N^d)^{-1}$ onto an eigenvector of \mathcal{H} with the same eigenvalue. In this case \mathcal{H} is thus also diagonalizable.

Suppose now that \mathcal{H} has a non-trivial $n \times n$ Jordan cell ($n > 1$) associated with the eigenvalue λ and that vectors $v_i \in \tilde{V}_N^d$, $1 \leq i \leq n$, have been chosen so they satisfy the canonical relations :

$$\mathcal{H}v_1 = \lambda v_1 \quad \text{and} \quad \mathcal{H}v_i = \lambda v_i + v_{i-1}, \quad 2 \leq i \leq n.$$

Let $|\nu_i\rangle = \tilde{i}_N^d(\nu_i)$ be their images in $(\mathbb{C}^2)^{\otimes N}$. The subspaces $W_i = \text{sp}\{|\nu_1\rangle, |\nu_2\rangle, \dots, |\nu_i\rangle\}$, $1 \leq i \leq n$, are all stable under the action of H . Since H is diagonalizable on any subspace stable under its action, the restrictions of H to the W_i s must be diagonalizable. For example, it must be diagonalizable on W_2 where its action is

$$(H - \lambda \cdot \text{id})|\nu_1\rangle = 0, \quad (H - \lambda \cdot \text{id})|\nu_2\rangle = |\nu_1\rangle.$$

Since all Jordan cells in H are 1×1 , $|\nu_1\rangle$ must vanish. This argument may be repeated for the following pairs $|\nu_{i-1}\rangle$ and $|\nu_i\rangle$. Only $|\nu_n\rangle = \tilde{i}_N^d(\nu_n)$ might thus be distinct from zero. Our computer explorations show that this image $\tilde{i}_N^d(\nu_i)$ is indeed non-zero in all cases we considered.

The map \tilde{i}_N^d is singular along curves in the complex plane (q, ν) or, more precisely, in $(\mathbb{C}^\times)^2$. Suppose the structure of \mathcal{H} at a given singular point (q_c, ν_c) is to be studied. Fix ν_c once for all and consider the matrix I_N^d representing \tilde{i}_N^d in the link and spin bases. It is now a polynomial in q and q^{-1} when $(N - d)/2$ is even, and in $q^{\frac{1}{2}}$ and $q^{-\frac{1}{2}}$ when it is odd. (See equation (4.3.4) and recall that $q = -u^2$.) For simplicity we discuss the case when it is a polynomial in q and q^{-1} . An expansion is therefore possible :

$$I_N^d(q) = I_N^d(q, \nu_c) = I_0 + (q - q_c)I_1 + \dots$$

in a neighborhood of q_c . (Note that multiplication by a power of q transforms I_N^d into a polynomial in q and this factor does not change the singular behavior of I_N^d at (q_c, ν_c) . Some expressions might be simpler with this additional factor.) The zeroes of the determinant of $I_N^d(q)$ were obtained in section 4.5.5. They occur when $\langle k + d/2 \rangle = 0$ in (4.5.16), that is when $q^{2k+d} \nu_c^{2N} = 1$ for some k , $1 \leq k \leq (N - d)/2$. Suppose ι is the degree of the zero at (q_c, ν_c) . For some $q \neq q_c$ in a neighborhood of q_c , the inverse $I_N^d(q)$ can be written as $A / \det I_N^d$ where A is the matrix of cofactors which are polynomials in q . Because the polynomial $\det I_N^d$ has a zero at q_c of a certain (positive) degree, there must be an integer ι such that the function $(I_N^d)^{-1}(q)$ can be cast into the following Laurent series

$$(I_N^d)^{-1}(q) = \frac{1}{(q - q_c)^\iota} M_0 + \frac{1}{(q - q_c)^{\iota-1}} M_1 + \dots$$

where M_0 and M_1 are constant matrices and M_0 is non-zero. It is important to remember between which spaces these act :

$$I_0, I_1 : \tilde{V}_N^d \rightarrow (\mathbb{C}^2)^{\otimes N} \Big|_{S^z=d/2} \quad \text{and} \quad M_0, M_1 : (\mathbb{C}^2)^{\otimes N} \Big|_{S^z=d/2} \rightarrow \tilde{V}_N^d.$$

Here is an example, building on the expression for I_4^0 given in (4.3.5). When ν is set to $\nu_c = 1$, all non-zero elements of $I_4^0(q, \nu = 1)$ are either 1, $-q$ or $-q^{-1}$. Its determinant has a zero at $q_c = i$ of degree 1 and its expansion is the following polynomial where I_0, I_1 and I_2 can be easily read off :

$$\begin{aligned} q \cdot I_4^0(q, \nu = 1) = & \begin{pmatrix} 1 & i & i & -1 & i & i \\ 0 & 1 & 0 & i & 0 & -1 \\ i & 0 & 1 & 0 & -1 & 0 \\ -1 & i & i & 1 & i & i \\ i & 0 & -1 & 0 & 1 & 0 \\ 0 & -1 & 0 & i & 0 & 1 \end{pmatrix} + (q - i) \begin{pmatrix} -2i & 1 & 1 & 0 & 1 & 1 \\ 0 & -2i & 0 & 1 & 0 & 0 \\ 1 & 0 & -2i & 0 & 0 & 0 \\ 0 & 1 & 1 & -2i & 1 & 1 \\ 1 & 0 & 0 & 0 & -2i & 0 \\ 0 & 0 & 0 & 0 & 1 & -2i \end{pmatrix} \\ & + (q - i)^2 \begin{pmatrix} -1 & 0 & 0 & 0 & 0 & 0 \\ 0 & -1 & 0 & 0 & 0 & 0 \\ 0 & 0 & -1 & 0 & 0 & 0 \\ 0 & 0 & 0 & -1 & 0 & 0 \\ 0 & 0 & 0 & 0 & -1 & 0 \\ 0 & 0 & 0 & 0 & 0 & -1 \end{pmatrix}. \end{aligned}$$

The inverse can be similarly expanded to get the first M_0 and M_1 :

$$(q \cdot I_4^0(q, \nu = 1))^{-1} = \frac{1}{q - i} \cdot \frac{1}{8} \begin{pmatrix} 0 & 0 & 0 & 0 & 0 & 0 \\ -1 & i & -i & 1 & -i & i \\ 1 & -i & i & -1 & i & -i \\ 0 & 0 & 0 & 0 & 0 & 0 \\ 1 & -i & i & -1 & i & -i \\ -1 & i & -i & 1 & -i & i \end{pmatrix} + \frac{1}{16} \begin{pmatrix} 4 & -4i & -4i & -4 & -4i & -4i \\ -3i & 3 & 1 & -i & 1 & -5 \\ -i & 1 & 3 & -3i & -5 & 1 \\ -4 & -4i & -4i & 4 & -4i & -4i \\ -i & 1 & -5 & -3i & 3 & 1 \\ -3i & -5 & 1 & -i & 1 & 3 \end{pmatrix} + \dots$$

Since, in the neighborhood of q_c , they satisfy

$$I_N^d(q)(I_N^d)^{-1}(q) = \text{id} = (I_N^d)^{-1}(q)I_N^d(q)$$

for $q \neq q_c$, these matrices must satisfy

$$I_0 M_0 = 0 = M_0 I_0 \quad \text{and} \quad I_1 M_0 + I_0 M_1 = \text{id} = M_0 I_1 + M_1 I_0. \quad (4.6.1)$$

We conclude from the first that $\text{im } I_0 \subset \ker M_0$ and that $\text{im } M_0 \subset \ker I_0$. In the family of examples presented in section 4.6.4, these inclusions will actually be equalities. This family includes the above case of I_4^0 around $(q_c, \nu_c) = (i, 1)$.

Finally, since both the loop and the XXZ Hamiltonians are polynomials in q , they enjoy similar expansions around q_c :

$$\mathcal{H}(q) = \mathcal{H}_0 + (q - q_c)\mathcal{H}_1 + \dots \quad \text{and} \quad H(q) = H_0 + (q - q_c)H_1 + \dots$$

The intertwining property of \tilde{i}_N^d gives, for the leading orders in $q - q_c$, the relations :

$$\mathcal{H}_0 M_0 = M_0 H_0 \quad \text{and} \quad \mathcal{H}_0 M_1 + \mathcal{H}_1 M_0 = M_1 H_0 + M_0 H_1. \quad (4.6.2)$$

4.6.2 An extended family of representations of $\mathcal{U}_q(\mathfrak{sl}_2)$

Non-trivial Jordan cells may occur only if some generalized eigenspaces are of dimension larger than one. Therefore some eigenvalues must be degenerate. A natural way to find degenerate eigenvalues of the Hamiltonian H and the corresponding eigenvectors is to construct maps that commute with H . It is well-known that,

for the open spin chain [35], the algebra $U_q(\mathfrak{sl}_2)$ provides a wealth of such commuting operators. The role of this quantum group is much more limited for the periodic XXZ Hamiltonian. Still, for particular values of the pair (q, v) , some maps commuting with H can be constructed out of the elements of $U_q(\mathfrak{sl}_2)$. This section introduces an $U_q(\mathfrak{sl}_2)$ -action on $(\mathbb{C}^2)^{\otimes N}$ that depends on the twist parameter v . It then gives some maps that, for specific (q, v) , commute with the Hamiltonian H .

Definitions and generalities A lot of the results presented here are generalizations of results found in [82]. The algebra $U_q(\mathfrak{sl}_2)$ is generated by generators q^{S^z} , S^+ and S^- that satisfy the relations

$$q^{S^z} S^\pm q^{-S^z} = q^{\pm 1} S^\pm, \quad [S^+, S^-] = \frac{q^{2S^z} - q^{-2S^z}}{q - q^{-1}}. \quad (4.6.3)$$

A v -dependent representation of this algebra is given by

$$\begin{aligned} q^{S^z} &= q^{\sigma^z/2} \otimes q^{\sigma^z/2} \otimes \dots \otimes q^{\sigma^z/2} = \prod_{j=1}^N q^{\sigma_j^z/2}, \\ S^\pm &= \sum_{k=1}^N \underbrace{v^{\mp 1} q^{-\sigma^z/2} \otimes \dots \otimes v^{\mp 1} q^{-\sigma^z/2}}_{k-1} \otimes \sigma^\pm \otimes \underbrace{v^{\pm 1} q^{\sigma^z/2} \otimes \dots \otimes v^{\pm 1} q^{\sigma^z/2}}_{N-k} \\ &= v^{\pm(N+1)} \sum_{k=1}^N v^{\mp 2k} \left(\prod_{i=1}^{k-1} q^{-\sigma_i^z/2} \right) \sigma_k^\pm \left(\prod_{j=k+1}^N q^{\sigma_j^z/2} \right) \equiv \sum_{k=1}^N S_k^\pm, \end{aligned}$$

whose validity one can verify by checking equation (4.6.3) for $N = 1$ and by using the coproduct

$$\Delta(q^{S^z}) = q^{S^z} \otimes q^{S^z}, \quad \Delta(S^\pm) = v^{\mp 1} q^{-S^z} \otimes S^\pm + v^{\pm 1} S^\pm \otimes q^{S^z}$$

to build representations for $N > 1$. These v -dependent representations are useful because they satisfy $[S^\pm, \bar{e}_i] = 0$ for $i = 1, \dots, N-1$. However, $[S^\pm, \bar{e}_N] \neq 0$ in general and the commutation of $U_q(\mathfrak{sl}_2)$ with the XXZ Hamiltonian H that holds for the *open* spin chain is lost for the *periodic* one. Another representation of the algebra $U_q(\mathfrak{sl}_2)$ is obtained by replacing q by q^{-1} in the definition of the S^\pm generators :

$$\begin{aligned} T^\pm &= \sum_{k=1}^N \underbrace{v^{\mp 1} q^{\sigma^z/2} \otimes \dots \otimes v^{\mp 1} q^{\sigma^z/2}}_{k-1} \otimes \sigma^\pm \otimes \underbrace{v^{\pm 1} q^{-\sigma^z/2} \otimes \dots \otimes v^{\pm 1} q^{-\sigma^z/2}}_{N-k} \\ &= v^{\pm(N+1)} \sum_{k=1}^N v^{\mp 2k} \left(\prod_{i=1}^{k-1} q^{\sigma_i^z/2} \right) \sigma_k^\pm \left(\prod_{j=k+1}^N q^{-\sigma_j^z/2} \right) \equiv \sum_{k=1}^N T_k^\pm. \end{aligned}$$

In this last representation, T^\pm no longer commutes with \bar{e}_i , $i = 1, \dots, N-1$, but instead, $[T^\pm, \bar{e}_i^*] = 0$, where $\bar{e}_i^* = \bar{e}_i|_{q \rightarrow q^{-1}}$. Taking powers of the generators S^\pm and T^\pm gives

$$(S^\pm)^x = [x]! v^{\pm x(N+1)} \sum_{1 \leq j_1 < j_2 < \dots < j_x \leq N} v^{\mp 2 \sum_{k=1}^x j_k} \left\{ \prod_{i=1}^{x+1} \left(\prod_{l=j_{i-1}+1}^{j_i-1} q^{-(x/2+1-i)\sigma_l^\mp} \right) \right\} \sigma_{j_1}^\pm \sigma_{j_2}^\pm \dots \sigma_{j_x}^\pm, \quad (4.6.4)$$

$$(T^\pm)^x = [x]! v^{\pm x(N+1)} \sum_{1 \leq j_1 < j_2 < \dots < j_x \leq N} v^{\mp 2 \sum_{k=1}^x j_k} \left\{ \prod_{i=1}^{x+1} \left(\prod_{l=j_{i-1}+1}^{j_i-1} q^{(x/2+1-i)\sigma_l^\mp} \right) \right\} \sigma_{j_1}^\pm \sigma_{j_2}^\pm \dots \sigma_{j_x}^\pm,$$

where $j_0 \equiv 0$ and $j_{x+1} \equiv N+1$ and, as usual, $[n] = (q^n - q^{-n})/(q - q^{-1})$ and $[n]! = \prod_{k=1}^n [k]$. Because $[x]!$ can be zero when q is a root of unity, it is usual to introduce the renormalized generators

$$S^{\pm(x)} = (S^\pm)^x / [x]! \quad \text{and} \quad T^{\pm(x)} = (T^\pm)^x / [x]!$$

which are non-zero for every value of q . Note that the values of q for which $(S^\pm)^x$ and $(T^\pm)^x$ vanish are independent of v . We finally quote the following commutation relations without proofs (see [82] and references therein) :

$$[S^+, T^+] = [S^-, T^-] = 0. \quad (4.6.5)$$

Some maps commuting with H The goal of this section is to construct objects that commute with the (periodic) XXZ Hamiltonian H , for specific values of the parameters q and v . We use the shorthand notation $S^z \equiv n \pmod{P}$ to say that the identities hold when the action is restricted to the subspace where S^z acts as the identity times an integer congruent to n modulo P . For the special value $v = 1$, the following result, as well as the next one, were proved in [82].

PROPOSITION 4.6.1 *When $q^{2P} = 1$, $S^z \equiv n \pmod{P}$ and $q^{2n} v^{\pm 2N} = 1$,*

$$\bar{\Omega} S^{\pm(P)} \bar{\Omega}^{-1} = q^P S^{\pm(P)}, \quad \bar{\Omega} T^{\mp(P)} \bar{\Omega}^{-1} = q^P T^{\mp(P)}, \quad [S^{\pm(P)}, H] = [T^{\mp(P)}, H] = 0. \quad (4.6.6)$$

PROOF The proof of the commutations with H will be a direct consequence of the commutation or anticommutation relation with $\bar{\Omega}$ (as $q^P \in \{+1, -1\}$). Indeed,

$$[S^{\pm(P)}, H] = [S^{\pm(P)}, \bar{e}_N] = S^{\pm(P)} (\bar{\Omega}^{-1} \bar{e}_1 \bar{\Omega}) - (\bar{\Omega}^{-1} \bar{e}_1 \bar{\Omega}) S^{\pm(P)} = 0$$

because $S^{\pm(P)}$ commutes with \bar{e}_1 . To extend the argument to $T^{\pm(P)}$, we note that

$$\bar{e}_j^* = \bar{e}_j + \frac{(q - q^{-1})}{2} (\sigma_j^z - \sigma_{j+1}^z) \quad (4.6.7)$$

so that $H = \sum_{j=1}^N \bar{e}_j = \sum_{j=1}^N \bar{e}_j^*$, and because $[T^{\pm(P)}, \bar{e}_1^*] = 0$, the same argument carries through. It only remains to prove the commutation relations with $\bar{\Omega}$. From the definitions,

$$\begin{aligned} \bar{\Omega} S^{\pm} \bar{\Omega}^{-1} &= q^{-\sigma_N^z} ((S^{\pm} - S_N^{\pm}) + q^{2S^z} v^{\pm 2N} S_N^{\pm}) \\ \bar{\Omega} T^{\pm} \bar{\Omega}^{-1} &= q^{\sigma_N^z} ((T^{\pm} - T_N^{\pm}) + q^{-2S^z} v^{\pm 2N} T_N^{\pm}) \end{aligned}$$

where the second is obtained from the first by changing q for q^{-1} . A slightly tedious computation yields

$$(\bar{\Omega} S^{\pm} \bar{\Omega}^{-1})^x = q^{-x\sigma_N^z} ((S^{\pm})^x + q^{\mp(x-1)} [x] (S^{\pm})^{x-1} S_N^{\pm} (q^{2(S^z \pm x)} v^{\pm 2N} - 1)) \quad (4.6.8)$$

$$(\bar{\Omega} T^{\pm} \bar{\Omega}^{-1})^x = q^{x\sigma_N^z} ((T^{\pm})^x + q^{\pm(x-1)} [x] (T^{\pm})^{x-1} T_N^{\pm} (q^{-2(S^z \pm x)} v^{\pm 2N} - 1)) \quad (4.6.9)$$

Note that these two identities hold for all q, v and for all S^z -eigenspaces. Dividing on both sides by $[x]!$, setting $x = P$ and choosing v such that $q^{2S^z} v^{\pm 2N} = 1$ in the first equation but $q^{2S^z} v^{\mp 2N} = 1$ in the second, we obtain the correct result, as $q^{\pm x\sigma_N^z} \rightarrow q^P$ and the dependence on the last spin disappears. \square

We immediately extend the previous statement.

PROPOSITION 4.6.2 *When $q^{2P} = 1$, $S^z \equiv n \pmod{P}$, $k \in \mathbb{N}$*

– and $q^{2(n \pm k)} v^{\pm 2N} = 1$,

$$\bar{\Omega} (T^{\mp(k)} S^{\pm(k+P)}) \bar{\Omega}^{-1} = q^P (T^{\mp(k)} S^{\pm(k+P)}), \quad [T^{\mp(k)} S^{\pm(k+P)}, H] = 0; \quad (4.6.10)$$

– and $q^{-2(n \pm k)} v^{\pm 2N} = 1$,

$$\bar{\Omega} (S^{\mp(k)} T^{\pm(k+P)}) \bar{\Omega}^{-1} = q^P (S^{\mp(k)} T^{\pm(k+P)}), \quad [S^{\mp(k)} T^{\pm(k+P)}, H] = 0. \quad (4.6.11)$$

PROOF To prove the first, we start with equations (4.6.8) and (4.6.9) and compute

$$\begin{aligned} \bar{\Omega} (T^{\mp(k)} S^{\pm(k+x)}) \bar{\Omega}^{-1} &= (T^{\mp(k)} + q^{\mp(k-1)} T^{\mp(k-1)} T_N^{\mp} (q^{-2S^z} v^{\mp 2N} - 1)) q^{-x\sigma_N^z} \\ &\quad \times (S^{\pm(k+x)} + q^{\mp(x+k-1)} S^{\pm(k+x-1)} S_N^{\pm} (q^{2(S^z \pm (k+x))} v^{\pm 2N} - 1)). \end{aligned}$$

When $x = P$, $q^{2P} = 1$, $S^z \equiv n \pmod{P}$, the second term of the second parenthesis vanishes. Because

$$(q^{-2S^z} v^{\mp 2N} - 1) S^{\pm(k+x)} = S^{\pm(k+x)} (q^{-2(S^z \pm (k+x))} v^{\mp 2N} - 1) \rightarrow 0,$$

the second term of the first parenthesis is also 0 and equation (4.6.10) follows. Proving the commutation with H is not as straightforward as before. For $j = 1, \dots, N-1$,

$$[T^{\mp(k)}S^{\pm(k+P)}, \bar{e}_j] = [T^{\mp(k)}, \bar{e}_j]S^{\pm(k+P)} = \frac{(q - q^{-1})}{2} [T^{\mp(k)}, \sigma_{j+1}^z - \sigma_j^z] S^{\pm(k+P)},$$

where we have used (4.6.7) and $[T^{\pm(P)}, \bar{e}_1^*] = 0$ at the second equality. Then,

$$[T^{\mp(k)}S^{\pm(k+P)}, \sum_{j=1}^{N-1} \bar{e}_j] = \frac{(q - q^{-1})}{2} [T^{\mp(k)}, \sigma_N^z - \sigma_1^z] S^{\pm(k+P)}. \quad (4.6.12)$$

The term $j = N$ is problematic and has to be treated differently,

$$\begin{aligned} [T^{\mp(k)}S^{\pm(k+P)}, \bar{e}_N] &= q^P \bar{\Omega} [T^{\mp(k)}S^{\pm(k+P)}, \bar{e}_1] \bar{\Omega}^{-1} \\ &= q^P \frac{(q - q^{-1})}{2} \bar{\Omega} [T^{\mp(k)}, \sigma_2^z - \sigma_1^z] S^{\pm(k+P)} \bar{\Omega}^{-1} \\ &= q^P \frac{(q - q^{-1})}{2} [\bar{\Omega} T^{\mp(k)} \bar{\Omega}^{-1}, \sigma_1^z - \sigma_N^z] \bar{\Omega} S^{\pm(k+P)} \bar{\Omega}^{-1}. \end{aligned}$$

With the conditions given in the propositions, equations (4.6.8) and (4.6.9) lead to the following substitutions :

$$\bar{\Omega} S^{\pm(k+P)} \bar{\Omega}^{-1} \rightarrow q^P q^{-k\sigma_N^z} S^{\pm(k+P)}, \quad \bar{\Omega} T^{\mp(k)} \bar{\Omega}^{-1} \rightarrow q^{k\sigma_N^z} T^{\mp(k)}.$$

Then the $q^{k\sigma_N^z}$ s cancel out and

$$[T^{\mp(k)}S^{\pm(k+P)}, \bar{e}_N] = \frac{(q - q^{-1})}{2} [T^{\mp(k)}, \sigma_1^z - \sigma_N^z] S^{\pm(k+P)}$$

and, from (4.6.12), $[T^{\mp(k)}S^{\pm(k+P)}, H] = 0$. The equations with $S^{\mp(k)}T^{\pm(k+P)}$ are obtained by replacing q by q^{-1} everywhere, as H and $\bar{\Omega}$ are invariant under this transformation. \square

4.6.3 The left nullspace of \tilde{i}_N^d

This technical section describes partially the left nullspace of \tilde{i}_N^d . Its necessity stems from the role played in the following by the map M_0 , the first singular term in the expansion of $(I_N^d)^{-1}$ around a critical q_c . Because of the relation (4.6.1), a vector $M_0 x$ with $x \in (\mathbb{C}^2)^{\otimes N} \Big|_{S^z=d/2}$ will be non-zero only if x has a component in that left kernel.

For critical values of q and v , the linear map \tilde{i}_n^d is singular by theorem 4.5.5. Let $v_{N_y}^N$ be the link state with $y = (N - d)/2$ concentric boundary bubbles, all centered

at position N . Note that \tilde{V}_N^d , under the action of ω_d , is cyclic with generator $v_{N_y}^N$. This means that any link state w in \tilde{V}_N^d can be written as $(\prod_i e_{k_i}) v_{N_y}^N$ for some k_i s. The set allowed for the indices k_i can even be restricted to $\{1, \dots, N-1\}$. Because S^+ commutes with all e_i s with $1 \leq i \leq N-1$, any link state w satisfies $S^{+(x)} \tilde{i}_N^d(w) = (\prod_i \bar{e}_{k_i}) S^{+(x)} \tilde{i}_N^d(v_{N_y}^N)$.

Suppose now that q and v are such that $S^{+(x)} \tilde{i}_N^d(v_{N_y}^N)$ is zero for some integer x . By the previous observations, $S^{+(x)} \tilde{i}_N^d(w) = 0$ for any link state w and therefore $S^{+(x)} \tilde{i}_N^d$ acts as zero on \tilde{V}_N^d . In other words, $\text{im } \tilde{i}_N^d \subset \ker S^{+(P)}$ and the vectors $\langle 0 | \sigma_{j_1}^+ \sigma_{j_2}^+ \dots \sigma_{j_{y-x}}^+ S^{+(x)}$, for all choices of j_1, j_2, \dots, j_{y-x} , are in the left nullspace of the matrix I_N^{N-2y} . This section is devoted to the computation of $S^{+(x)} \tilde{i}_N^d(v_{N_y}^N)$.

PROPOSITION 4.6.3 For $1 \leq x \leq y \leq N/2$

$$S^{+(x)} \tilde{i}_N^d(v_{N_y}^N) = i^y q^{(y-x)/2} \frac{\langle d/2+x \rangle!}{\langle d/2 \rangle!} \sum_{\substack{1 \leq j_1 < j_2 < \dots < j_x \leq y \\ J = \{j_1, j_2, \dots, j_x\}}} \left(\prod_{\substack{1 \leq r \leq y \\ r \notin J}} G_{r, s(r, J)} \right) |0\rangle \quad (4.6.13)$$

where

- $\langle x \rangle = v^N q^x - v^{-N} q^{-x}$ and $\langle x \rangle! = \prod_{k=1}^x \langle k \rangle$ if $x > 0$ and $\langle 0 \rangle! = 1$;
- $G_{j,k} = q^{-k} v^{2j-1} \sigma_j^- - q^{k-1} v^{-(2j-1)} \sigma_{N+1-j}^-$;
- $s(r, J) = -|\{j \in J | j > r\}|$.

PROOF The proof is by induction. We start by noting that $\tilde{i}_N^d(v_{N_y}^N) = (\prod_{j=1}^y T_{N+1-j, N+j}) |0\rangle = (i q^{1/2})^y \times (\prod_{j=1}^y G_{j,0}) |0\rangle$. When $x = 0$, J is the empty set and the sum in equation (4.6.13) is zero which is the correct answer. We now assume the result for x . If $F_{i,j} = q^{-j} S_i^+ + q^j S_{N+1-i}^+$ we can then write

$$S^{+(x+1)} \tilde{i}_N^d(v_{N_y}^N) = \frac{1}{[x+1]} \left(\sum_{j=1}^y F_{j,0} \right) S^{+(x)} \tilde{i}_N^d(v_{N_y}^N).$$

One can compute the following multiplication rules :

$$F_{i,j} G_{k,l} = \begin{cases} G_{k,l} F_{i,j+1}, & i < k, \\ G_{k,l-1} F_{i,j}, & i > k, \end{cases} \quad (4.6.14)$$

$$F_{i,j} G_{i,k} |0\rangle = |0\rangle q^{-1/2} \langle N/2 + 1 - j - k - i \rangle. \quad (4.6.15)$$

Then,

$$\begin{aligned} S^{+(x+1)} \tilde{i}_N^d(v_{N^y}^N) &= \frac{i^y q^{(y-x)/2} \langle d/2 + x \rangle!}{[x+1] \langle d/2 \rangle!} \sum_{j=1}^y \sum_{\substack{1 \leq j_1 < j_2 < \dots < j_x \leq y \\ J = \{j_1, j_2, \dots, j_x\}}} \left(F_{j,0} \prod_{\substack{1 \leq r \leq y \\ r \notin J}} G_{r,s(r,J)} \right) |0\rangle \\ &= \frac{i^y q^{(y-x)/2} \langle d/2 + x \rangle!}{[x+1] \langle d/2 \rangle!} \sum_{t=1}^{x+1} \sum_{\substack{1 \leq j_1 < \dots < j_{t-1} < j_t < j_{t+1} < \dots < j_x \leq y \\ J = \{j_1, j_2, \dots, j_x\}}} \left(F_{j,0} \prod_{\substack{1 \leq r \leq y \\ r \notin J}} G_{r,s(r,J)} \right) |0\rangle, \end{aligned}$$

where in the last line it is implicit that $j_0 = 0$ and $j_{x+1} = y + 1$. On the first line, whenever j equals j_i for some $i = 1, \dots, x$, $F_{j,0}$ acts directly on $|0\rangle$ and the result is zero. We now rename the variables

$$k_i = \begin{cases} j_i, & i < t, \\ j, & i = t, \\ j_{i-1}, & i > t. \end{cases}$$

and get

$$S^{+(x+1)} \tilde{i}_N^d(v_{N^y}^N) = \frac{i^y q^{(y-x)/2} \langle d/2 + x \rangle!}{[x+1] \langle d/2 \rangle!} \sum_{\substack{1 \leq k_1 < k_2 < \dots < k_{x+1} \leq y \\ K = \{k_1, \dots, k_{x+1}\}}} \sum_{t=1}^{x+1} \left(F_{k_t,0} \prod_{\substack{1 \leq r \leq y \\ r \notin K \setminus \{k_t\}}} G_{r,s(r,J)} \right) |0\rangle.$$

Using the multiplication rules (4.6.14), we simplify the summand :

$$\begin{aligned} \left(F_{k_t,0} \prod_{\substack{1 \leq r \leq y \\ r \notin K \setminus \{k_t\}}} G_{r,s(r,J)} \right) |0\rangle &= \left(\prod_{\substack{1 \leq r \leq k_t-1 \\ r \notin K}} G_{r,s(r,J)-1} \right) \left(\prod_{\substack{k_t+1 \leq r \leq y \\ r \notin K}} G_{r,s(r,J)} \right) \\ &\quad \times F_{k_t, y-k_t-(x+1-t)} G_{k_t, s(k_t, J)} |0\rangle \\ &= q^{-1/2} \langle N/2 + 1 - y + 2(x+1-t) \rangle \left(\prod_{\substack{1 \leq r \leq y \\ r \notin K}} G_{r,s(r,K)} \right) |0\rangle \end{aligned}$$

because $s(k_t, J) = -(x+1-t)$. Finally,

$$\begin{aligned} S^{+(x+1)} \tilde{i}_N^d(v_{N^y}^N) &= \frac{i^y q^{(y-x-1)/2} \langle d/2 + x \rangle!}{[x+1] \langle d/2 \rangle!} \sum_{\substack{1 \leq k_1 < k_2 < \dots < k_{x+1} \leq y \\ K = \{k_1, \dots, k_{x+1}\}}} \left(\prod_{\substack{1 \leq r \leq y \\ r \notin K}} G_{r,s(r,K)} \right) |0\rangle \\ &\quad \times \sum_{t=1}^{x+1} \langle N/2 + 1 - y + 2(x+1-t) \rangle \end{aligned}$$

which yields the correct result when we use the identity $\sum_{t=1}^{x+1} \langle A + (x+2-2t) \rangle = [x+1] \langle A \rangle$ with $A = N/2 + x - y + 1 = d/2 + x + 1$. This completes the induction. \square

Note that the sum over subsets $J \subset \{1, 2, \dots, y\}$ in (4.6.13) gives a non-zero vector. Indeed $S^{+(x)}\tilde{i}_N^d(v_{N_y}^N)$ is in the subspace with $S^z = N/2 - (y - x)$. Because $G_{j,k}$ changes the spin states at positions $j \leq y$ or $j \geq N + 1 - y$ only, the coefficient of the state $|\dots - + \dots +\rangle$ starting with precisely $(y - x)$ minus signs comes only from the subset $J = \{y - x + 1, y - x + 2, \dots, y\}$ and is non-zero.

COROLLARY 4.6.4 *Let $1 \leq x \leq y \leq N/2$. The vector $S^{+(x)}\tilde{i}_N^d(v_{N_y}^N)$ is zero if and only if there is an integer x_c in the range $1 \leq x_c \leq x \leq y$ such that $\langle d/2 + x_c \rangle = 0$. Moreover, if q, v and the integer x_c , $1 \leq x_c \leq y$, are such that $\langle d/2 + x_c \rangle = 0$, then the states $\langle 0 | \sigma_{j_1}^+, \dots, \sigma_{j_{y-x}}^+ S^{+(x)}$ are in the left nullspace of \tilde{i}_N^{N-2y} , for all $x \in \{x_c, x_c + 1, \dots, y\}$ and all choices $1 \leq j_1 < j_2 < \dots < j_{y-x} \leq N$.*

Note that propositions 4.6.1 and 4.6.2 both require that q be a root of unity. Neither proposition 4.6.3 nor corollary 4.6.4 do.

4.6.4 A construction of Jordan generalized eigenvectors : a simple example

We shall now construct a family of examples in a simple case. The family is limited by the following hypotheses :

- q is a root of unity with $P \in [2, N/2]$ the smallest integer such that $q^{2P} = 1$;
- the twist parameter v satisfies $(qv^2)^N = 1$;
- the number of defects d is $N - 2P$.

The Jordan cell to be constructed will belong to the generalized eigenspace of \mathcal{H} of eigenvalue $\lambda = 0$ and will lie in the subspace $(\mathbb{C}^2)^{\otimes N}|_{S^z=N/2-P}$. The four following vectors, all in this subspace or its dual, will play the central role here :

$$\begin{aligned} \langle \mu_1 | &= \langle 0 | T^{+(P)}, & | \nu_1 \rangle &= T^{-(P)} | 0 \rangle, \\ \langle \mu_2 | &= \langle 0 | S^{+(P)}, & | \nu_2 \rangle &= S^{+(P)} T^{-(2P)} | 0 \rangle. \end{aligned}$$

We argued in section 4.6.1 that a non-trivial Jordan cell may occur only when \tilde{i}_N^d is singular. Theorem 4.5.5 gave the determinant of the matrix I_N^d representing the intertwiner \tilde{i}_N^d between the link and the spin bases. Up to a sign, it is

$$\det I_N^d = \prod_{j=1}^{(N-d)/2} \langle j + d/2 \rangle \binom{N}{(N-d)/2-j} = \prod_{j=1}^P \langle j + N/2 - P \rangle \binom{N}{P-j}$$

if the number of defects is $N - 2P$. The factors $\langle j + N/2 - P \rangle = q^{j+N/2-P} v^N - q^{-(j+N/2-P)} v^{-N}$ are zero if and only if $q^{2j+N-2P} v^{2N} = 1$. With the above hypotheses,

this happens only for the last term in the product ($j = P$) and the zero at $q = q_c$ is of degree 1. All other terms are non-zero. The images and kernels of $I_0 = I_N^d(q_c)$ and M_0 will now be explored. For the rest of the section, the twist parameter ν is fixed to one of the values ν_c satisfying the above hypotheses.

We know that the map $S^{+(P)}$ is non-zero, being a sum of $\sigma_{j_1}^+ \sigma_{j_2}^+ \dots \sigma_{j_p}^+$ with weights that are polynomials in q and do not vanish when q_c is a primitive $2P$ -root of unity. Therefore $\langle \mu_2 | = \langle 0 | S^{+(P)}$ is non-zero for all q in a neighborhood of q_c . By proposition 4.6.3, with $x = y = P$, we note that

$$\langle \mu_2 | \tilde{i}_N^d(\nu_{N^P}^N) = i^P \frac{\langle N/2 \rangle!}{\langle N/2 - P \rangle!} \langle 0 | \nu \rangle$$

where $|\nu\rangle$ is the complicated sum and products of (4.6.13) and is non-zero. (Note that, in the present case, $S^{+(P)} \tilde{i}_N^d(\nu_{N^P}^N) \in (\mathbb{C}^2)^{\otimes N} \Big|_{S^z = N/2}$ and must therefore be a non-zero multiple of $|0\rangle$.) Suppose that one of the vectors in the spin basis of $(\mathbb{C}^2)^{\otimes N} \Big|_{S^z = N/2 - P}$ is replaced by $\langle \mu_2 |$ in such a way that the new set \mathcal{B} is still a basis in a neighborhood of q_c . The determinant of \tilde{i}_N^d in this basis \mathcal{B} is likely to be different, but only by a polynomial that does not vanish at q_c . Since the line in I_N^d corresponding to $\langle \mu_2 |$ has now an overall factor $i^P \langle N/2 \rangle! / \langle N/2 - P \rangle!$, the zero at q_c of degree one is accounted for by $\langle N/2 \rangle$, the only factor that vanishes in the two factorials. Could there be another vector $\langle \mu |$, linearly independent from $\langle \mu_2 |$, in the left nullspace of \tilde{i}_N^d ? If such a vector existed, it could still take the place of another spin vector of the original basis. Again, in this new basis, the matrix would still have polynomial entries and its determinant would have a further zero at q_c . But the zero at q_c is of degree one, as seen above, and the existence of such a $\langle \mu |$ must be ruled out. The left nullspace of $\tilde{i}_N^d(q_c)$ is therefore one-dimensional and spanned by $\langle \mu_2 | = \langle 0 | S^{+(P)}$.

The matrix M_0 is non-zero because, if it were zero, the determinant of $(I_N^d(q))^{-1}$ would not have a pole at q_c . Its rank is at least one. However, since $\text{im } M_0 \subset \ker I_0$ by (4.6.1), this rank is bounded by $\dim \ker I_0$ which has just been shown to be one. Therefore $\text{im } M_0 = \ker I_0$ and, by dimension counting, $\ker M_0 = \text{im } I_0$.

The image of M_0 is therefore one-dimensional. Let $\nu_0 \in \tilde{V}_N^d$ be a non-zero vector in this image. Then M_0 can be written as

$$M_0 = k \cdot \nu_0 \langle 0 | S^{+(P)} \tag{4.6.16}$$

where k is a non zero constant. We now show that $\mathcal{H}_0 \nu_0 = 0$. Because of (4.6.2), the operator M_0 maps each eigenspace of H_0 with eigenvalue γ on the generalized

eigenspace of \mathcal{H}_0 with the same eigenvalue. Because the image of v_0 spans a one-dimensional subspace, all but one of these eigenspaces are sent to 0. We will show in the next lemma that the state $|\nu_1\rangle$ is such that $\langle 0|S^{+(P)}|\nu_1\rangle = \binom{N}{P} \neq 0$ (see equation (4.6.4)), so that M_0 maps it to a non-zero multiple of v_0 . Because $H_0|\nu_1\rangle = 0$, then $\mathcal{H}_0 v_0$ must be zero. This closes the description of M_0 .

We turn now to the study of the four vectors $\langle \mu_1|, \langle \mu_2|$ and $|\nu_1\rangle, |\nu_2\rangle$. First we know, by proposition 4.6.1 and the fact that the \bar{e}_i s annihilate $|0\rangle$, that the vectors $T^{-(P)}|0\rangle$ and $S^{+(P)}T^{-(2P)}|0\rangle$ are eigenstates of $H_0 = H(q_c)$, both with eigenvalue 0. The second key property is the following.

LEMMA 4.6.5 *Under the hypotheses stated at the beginning of the section, the states $|\nu_1\rangle$ and $|\nu_2\rangle \in (\mathbb{C}^2)^{\otimes N}|_{S^z=N/2-P}$ are linearly independent.*

PROOF We prove that the determinant of the matrix

$$\mathcal{S} = \begin{pmatrix} \langle \mu_1|\nu_1\rangle & \langle \mu_1|\nu_2\rangle \\ \langle \mu_2|\nu_1\rangle & \langle \mu_2|\nu_2\rangle \end{pmatrix}$$

is non-zero. This computation is done for a general q before the limit $q \rightarrow q_c$ is taken. To calculate these matrix elements, we will need the formula (see [82] or [104]):

$$[(S^+)^m, (S^-)^n] = \sum_{j=1}^{\min(m,n)} \begin{bmatrix} m \\ j \end{bmatrix} \begin{bmatrix} n \\ j \end{bmatrix} [j]!(S^-)^{n-j}(S^+)^{m-j} \prod_{k=0}^{j-1} [2S^z + m - n - k] \quad (4.6.17)$$

or, in terms of the renormalized $S^{\pm(m)}$,

$$[S^{+(m)}, S^{-(n)}] = \sum_{j=1}^{\min(m,n)} \frac{S^{-(n-j)}S^{+(m-j)}}{[j]!} \prod_{k=0}^{j-1} [2S^z + m - n - k], \quad (4.6.18)$$

where $\begin{bmatrix} m \\ j \end{bmatrix} = \frac{[m]!}{[j]![m-j]!}$ is the q -binomial. This equation can be derived directly from the defining relations of $U_q(\mathfrak{sl}_2)$ and is therefore independent of the twist parameter v . Because q -numbers and q -binomials are invariant under $q \rightarrow q^{-1}$, equation (4.6.17) also gives $[(T^+)^m, (T^-)^n]$ if we replace every S by a T . This allows one to calculate

$$\langle \mu_1|\nu_1\rangle = \langle 0|[T^{+(P)}, T^{-(P)}]|0\rangle = \langle 0|\begin{bmatrix} 2S^z \\ P \end{bmatrix}|0\rangle = \begin{bmatrix} N \\ P \end{bmatrix}. \quad (4.6.19)$$

To calculate $\langle \mu_2|\nu_1\rangle$, we note that

$$T^{-(P)}|0\rangle = (qv^2)^{-(N+1)P/2} \sum_{1 \leq j_1 < j_2 < \dots < j_P \leq N} (qv^2)^{\sum_{k=1}^P j_k} \sigma_{j_1}^- \dots \sigma_{j_P}^- |0\rangle$$

and

$$S^{+(P)} \sigma_{j_1}^- \dots \sigma_{j_p}^- |0\rangle = (qv^2)^{(N+1)P/2} (qv^2)^{-\sum_{k=1}^p j_k} |0\rangle. \quad (4.6.20)$$

Combining these results, we find

$$\langle \mu_2 | \nu_1 \rangle = \sum_{1 \leq j_1 < j_2 < \dots < j_p \leq N} \langle 0 | 0 \rangle = \binom{N}{P}$$

where $\binom{x}{y}$ is the usual binomial coefficient. The last two elements of \mathcal{S} are

$$\langle \mu_1 | \nu_2 \rangle = \binom{N}{P} \begin{bmatrix} N-P \\ P \end{bmatrix}, \quad \langle \mu_2 | \nu_2 \rangle = \binom{N}{2P} \begin{bmatrix} 2P \\ P \end{bmatrix}.$$

The computation of the second does not require any new argument while that of the first starts by the exchange of $T^{+(P)}$ and $S^{+(P)}$ (see (4.6.5)). The determinant of \mathcal{S} is

$$\det \mathcal{S} = \binom{N}{2P} \begin{bmatrix} 2P \\ P \end{bmatrix} \begin{bmatrix} N \\ P \end{bmatrix} - \binom{N}{P}^2 \begin{bmatrix} N-P \\ P \end{bmatrix}. \quad (4.6.21)$$

This determinant is zero when $q = \pm 1$, as $\langle \mu_1 | \nu_i \rangle = \langle \mu_2 | \nu_i \rangle$ for both $i = 1$ and 2 . This was to be expected : for example, the operators T^\pm and S^\pm are equal when $q = 1$. For $P \geq 2$ and $q^{2P} = 1$, we need to simplify the q -binomials by using the limiting relation

$$\lim_{q \rightarrow q_c} \begin{bmatrix} Ps + a \\ P \end{bmatrix} = sq_c^{Pa} \times \begin{cases} 1 & \text{for } s \text{ odd,} \\ q_c^{P^2} & \text{for } s \text{ even,} \end{cases} \quad (4.6.22)$$

that holds for integers a and s , $0 \leq a < P$ and $s > 0$, when q_c stands for a solution of $q^{2P} = 1$. Equation (4.6.21) is then

$$\lim_{q \rightarrow q_c} \det \mathcal{S} = q_c^{2nP} \times \begin{cases} 4r \binom{N}{2P} - (2r-1) \binom{N}{P}^2 & 0 \leq 2n < P, \\ 2(2r+1) \binom{N}{2P} - 2r \binom{N}{P}^2 & P \leq 2n < 2P. \end{cases}$$

The inequalities

$$(2P)! > 5(P!)^2, \quad \text{and} \quad \frac{N!}{(N-2P)!} < \left(\frac{N!}{(N-P)!} \right)^2,$$

valid for $P \geq 2$ and $N \geq 2P$, allows one to prove that $\binom{N}{2P} < \frac{1}{5} \binom{N}{P}^2$ and that $q_c^{2nP} \det \mathcal{S}$ is strictly negative. This ends the proof. \square

The explicit construction of the Jordan pair is our final result.

PROPOSITION 4.6.6 *Under the hypotheses stated at the beginning of the section, the state*

$$v_J = M_1|\chi\rangle \in \tilde{V}_N^d, \quad \text{where} \quad |\chi\rangle = x_1|v_1\rangle - x_2|v_2\rangle \in (\mathbb{C}^2)^{\otimes N} \Big|_{S^z = N/2 - P},$$

with

$$x_1 = \langle 0|S^{+(P)}|v_2\rangle \quad \text{and} \quad x_2 = \langle 0|S^{+(P)}|v_1\rangle,$$

is a (non-zero) generalized eigenvector of $\mathcal{H}_0 = \mathcal{H}(q_c)$ with eigenvalue 0.

PROOF The constants $x_1 = \langle \mu_2|v_2\rangle$ and $x_2 = \langle \mu_2|v_1\rangle$ have been chosen such that the state $|\chi\rangle$ is in $\ker M_0$. These constants have already been calculated in the preceding proposition, and are non-zero when evaluated at $q = q_c$:

$$x_1 = \langle \mu_2|v_2\rangle = 2q_c^{P^2} \binom{N}{2P}, \quad x_2 = \langle \mu_2|v_1\rangle = \binom{N}{P}.$$

We now proceed to prove that at q_c

$$\mathcal{H}_0 v_J \neq 0, \quad \text{but} \quad \mathcal{H}_0^2 v_J = 0.$$

The argument studies the behavior of these vectors in the neighborhood of $q = q_c$. We therefore highlight the dependence on q whenever suitable. (Again the twist parameter ν is set to one of the values ν_c satisfying the hypotheses.) We write $\mathcal{H}_0 v_J$ as

$$\mathcal{H}_0 v_J = \lim_{q \rightarrow q_c} \mathcal{H}(q) M_1 |\chi\rangle = \lim_{q \rightarrow q_c} \mathcal{H}(q) (\tilde{i}_N^d(q))^{-1} |\chi\rangle = \lim_{q \rightarrow q_c} (\tilde{i}_N^d(q))^{-1} H(q) |\chi\rangle$$

where we have used the intertwining property of the inverse of \tilde{i}_N^d in a neighborhood of q_c and the fact that $M_0 |\chi\rangle = 0$ for the second equality. Note that $H(q)$ is a polynomial in q and q^{-1} and $\lim_{q \rightarrow q_c} H(q) |\chi\rangle$ is simply its value at $q = q_c$. As noted before lemma 4.6.5, the vectors $|v_1\rangle$ and $|v_2\rangle$ are both eigenvectors of H_0 with eigenvalue 0. The vector $H(q) |\chi\rangle$ has polynomial components in the spin basis and vanishes at q_c . Therefore $\lim_{q \rightarrow q_c} (q - q_c)^{-1} H(q) |\chi\rangle$ exists and

$$\mathcal{H}_0 v_J = \lim_{q \rightarrow q_c} \frac{1}{q - q_c} M_0 H(q) |\chi\rangle = k \cdot v_0 \lim_{q \rightarrow q_c} \frac{1}{q - q_c} \langle 0|S^{+(P)}(q_c) H(q) |\chi\rangle$$

where the form (4.6.16) of M_0 was used. The fact that $\mathcal{H}_0^2 v_J = 0$ is then a direct consequence of $\mathcal{H}_0 v_0 = 0$.

It remains to show that $\mathcal{H}_0 v_J \neq 0$. (This will also prove that v_J is non-zero.) For this we compute

$$\begin{aligned} A \equiv \lim_{q \rightarrow q_c} \frac{1}{q - q_c} \langle 0|S^{+(P)}(q_c) H(q) |\chi\rangle &= \lim_{q \rightarrow q_c} \frac{1}{q - q_c} \langle 0|S^{+(P)}(q) \bar{e}_{N(q)} |\chi\rangle \\ &= \lim_{q \rightarrow q_c} \frac{1}{q - q_c} \langle 0|S^{+(P)}(q) \bar{\Omega}^{-1} \bar{e}_{N-1(q)} \bar{\Omega} |\chi\rangle. \end{aligned}$$

where we have used the fact that $[S^\pm, \bar{e}_i] = 0$ for all $1 \leq i \leq N-1$. We can use proposition 4.6.1 to replace $\bar{\Omega}|\chi\rangle$ by $v^N q_c^P |\chi\rangle$, and equation (4.6.8) to write

$$\langle 0|S^{+(P)}\bar{\Omega}^{-1} = v^{-N}\langle 0|q^{-P\sigma_N^z} (S^{+(P)} + q^{-(P-1)}S^{+(P-1)}S_N^+(q^{2(S^z+P)}v_c^{2N} - 1)). \quad (4.6.23)$$

The first term is annihilated by $\bar{e}_{N-1}(q)$, so that

$$A = q_c^P \lim_{q \rightarrow q_c} \frac{1}{q - q_c} q^{-(P-1)} \langle 0|S^{+(P-1)}(q)S_N^+(q)\bar{e}_{N-1}(q)(q^{2(S^z+P)}v_c^{2N} - 1)|\chi\rangle.$$

Because $S^z|\chi\rangle = (N/2 - P)|\chi\rangle$, the last parenthesis gives rise to a factor

$$\lim_{q \rightarrow q_c} (q^N v_c^{2N} - 1)/(q - q_c) = Nq_c^{-1}.$$

The remaining terms in the limit are now polynomials in q and q^{-1} . We therefore omit the limit sign and any reference to q . All expressions are at q_c and, when some q -numbers are zero, appropriate limits are understood.

We can move $S^{+(P-1)}$ across $S_N^+ \bar{e}_{N-1}$ by using the identity $S^+ S_N^+ = q^2 S_N^+ S^+$. The expression A is then, up to a global non-zero factor, the difference $(x_1 A_1 - x_2 A_2)$, where

$$A_1 = \langle 0|S_N^+ \bar{e}_{N-1} S^{+(P-1)} T^{-(P)} |0\rangle \quad \text{and} \quad A_2 = \langle 0|S_N^+ \bar{e}_{N-1} S^{+(P-1)} S^{+(P)} T^{-(2P)} |0\rangle.$$

Both terms can be cast in a similar form if we define $\mathcal{A}(x) = \langle 0|S_N^+ \bar{e}_{N-1} (S^+)^{x-1} (T^-)^x |0\rangle$. Then $A_1 = \mathcal{A}(P)/([P]![P-1]!)$ and $A_2 = \mathcal{A}(2P)/([2P]![P]![P-1]!)$. We group the terms in S^\pm and T^\pm as

$$S^\pm = \underbrace{\sum_{j=1}^{N-2} S_j^\pm}_{S_A^\pm} + \underbrace{S_{N-1}^\pm + S_N^\pm}_{S_B^\pm} \quad T^\pm = \underbrace{\sum_{j=1}^{N-2} T_j^\pm}_{T_A^\pm} + \underbrace{T_{N-1}^\pm + T_N^\pm}_{T_B^\pm} \quad (4.6.24)$$

in order to expand the powers of S^\pm and T^\pm :

$$(S^\pm)^{x-1} = (S_A^\pm)^{x-1} + [x-1]q^{\pm(x-2)}S_B^\pm(S_A^\pm)^{x-2} + q^{\pm 2(x-3)}\begin{bmatrix} x-1 \\ 2 \end{bmatrix}(S_B^\pm)^2(S_A^\pm)^{x-3},$$

$$(T^\pm)^x = (T_A^\pm)^x + [x]q^{\mp(x-1)}T_B^\pm(T_A^\pm)^{x-1} + q^{\mp 2(x-2)}\begin{bmatrix} x \\ 2 \end{bmatrix}(T_B^\pm)^2(T_A^\pm)^{x-2}. \quad (4.6.25)$$

Because $\bar{e}_{N-1}S_B^+ = 0$, $[\bar{e}_{N-1}, S_A^+] = [\bar{e}_{N-1}, T_A^-] = 0$ and $S_A^+ T_B^- = q^{-2}T_B^- S_A^+$, only one term survives :

$$\begin{aligned} \mathcal{A}(x) &= q^{-(x-1)}[x] \underbrace{\langle 0|S_N^+ \bar{e}_{N-1} T_B^- |0\rangle}_{=-(q-q^{-1})} \langle 0|(S_A^+)^{x-1} (T_A^-)^{x-1} |0\rangle \\ &= -q^{-(x-1)}[x]![x-1]!(q - q^{-1}) \binom{N-2}{x-1}. \end{aligned}$$

With the use of equation (4.6.22), A_1 and A_2 are found to be

$$A_1 = -q_c^{P+1}(q_c - q_c^{-1}) \binom{N-2}{P-1} \quad \text{and} \quad A_2 = -q_c^{P^2+P+1}(q_c - q_c^{-1}) \binom{N-2}{2P-1}.$$

Showing that $(x_1 A_1 - x_2 A_2)$ does not vanish is now straightforward and, therefore, $\mathcal{H}_{0vJ} \neq 0$. \square

It is useful to stress that no restrictions have been put on the parity of N . The simplest Jordan blocks obtained in proposition 4.6.6 appear when $P = 2$. These (generalized) eigenspaces of \mathcal{H} lie in the sector with $S^z = 0$ when $N = 4$ and with $S^z = \frac{1}{2}$ when $N = 5$. We close this section by giving explicitly the case of $N = 4$ and $d = 0$ at $(q_c, v_c) = (i, 1)$ which corresponds to $\beta = 0$ and $\alpha = 2$. These values satisfy the hypotheses of this section when $N = 4$ and $d = 0$. They are those used in sections 4.3.3 and 4.6.1 to provide examples of the relation between $\tilde{\mathcal{G}}_N^d$ and I_N^d and of the expansions of the latter. The Hamiltonian \mathcal{H} and its Jordan decomposition are

$$\mathcal{H} = \begin{pmatrix} 2\beta & 2 & \alpha & 0 & \alpha & 2 \\ 1 & \beta & 0 & 0 & 0 & 0 \\ 0 & 0 & \beta & 1 & 0 & 0 \\ 0 & \alpha & 2 & 2\beta & 2 & \alpha \\ 0 & 0 & 0 & 1 & \beta & 0 \\ 1 & 0 & 0 & 0 & 0 & \beta \end{pmatrix}$$

$$\text{and Jordan form of } \mathcal{H}|_{(\beta=0, \alpha=2)} = \begin{pmatrix} 0 & 0 & 0 & 0 & 0 & 0 \\ 0 & 0 & 0 & 0 & 0 & 0 \\ 0 & 0 & 0 & 1 & 0 & 0 \\ 0 & 0 & 0 & 0 & 0 & 0 \\ 0 & 0 & 0 & 0 & -2\sqrt{2} & 0 \\ 0 & 0 & 0 & 0 & 0 & 2\sqrt{2} \end{pmatrix}.$$

4.7 Concluding remarks

The example closing the previous section shows how the tools developed in the present paper can be put together to construct explicitly Jordan cells in loop models. It shows the interplay between (i) the freedom introduced by the twist parameter in the representation $\omega_d = \omega_d(q, v)$ and the condition $(qv^2)^N = 1$ (hypotheses of section 4.6.4), (ii) the necessity of the extended representations of $U_q(\mathfrak{sl}_2)$ depending on the twist (section 4.6.2), and (iii) the crucial role played by the intertwiner \tilde{i}_N^d and its characterization (section 4.3.2, and theorems 4.3.3 and 4.5.5), not only at the critical point (q_c, v_c) , but in a neighborhood of it (section 4.6.1). The new technique is

clearly promising. Still the example covers a family of models that, though infinite, is limited. Many extensions need to be considered.

First the construction has been for a generalized eigenspace of the loop Hamiltonian \mathcal{H} associated to the eigenvalue zero. The choice of the two vectors $|v_1\rangle$ and $|v_2\rangle$ in section 4.6.4 forces this eigenvalue. How can one probe generalized eigenspaces whose eigenvalue is non-zero? Second other critical pairs (q_c, v_c) need to be considered. Note that proposition 4.6.2 was not used by the example. This proposition was left in the text because it gives maps commuting with H that could explain Jordan blocks seen through our computer explorations and that appear at pairs (q_c, v_c) not allowed by the hypotheses of proposition 4.6.1, but included in those of proposition 4.6.2. Finally a third possible extension could aim at describing larger Jordan cells within a fixed sector \tilde{V}_N^d . Our computer explorations show that Jordan cells larger than 2×2 do exist.

Figure 4.3 shows, for the value $P = 2$ ($q = e^{i\pi/2}$, $\beta = 0$, $a = -1$ and $b = 2$, that is $\Lambda = -\pi/2$), the sectors \tilde{V}_N^d denoted by (N, d) (with action $\omega_d(q, v)$) where our explorations found non-trivial cells. The construction of Jordan partners of section 4.6.4 works on the diagonal $N - d = 4$ (the (N, d) s appear in solid boxes). On this diagonal, our explorations suggest the appearance of Jordan blocks associated with the eigenvalue 0 when $q^{N-2}v^{2N} = 1$ if $N \geq 6$. Jordan blocks associated with other eigenvalues are found on lower diagonals $N - d > 6$ (appearing within dashed boxes) when $q^{N-2k}v^{2N} = 1$, $k = 0, 1$. On the diagonals $N - d \geq 8$, we find Jordan cells of rank larger than 2 and, for $(N, d) = (12, 0)$, a Jordan cell with rank 4 appears for the first time. The figure also shows how Jordan cells tie different sectors in the representation ρ .

Additional techniques complementing those of section 4.6.4 will be needed in order to explore this figure deeper. A first reason is that the kernel of I_0 is larger than one-dimensional in general. The useful form (4.6.16) of M_0 will not be available in these cases. A second reason is that, for $k \neq 0$, explicit computations show that the vector $M_1|\chi\rangle$ is not in the generalized eigenspace of \mathcal{H} with eigenvalue 0. A new component must be added to it before it can play its role as Jordan partner. Clearly more work needs to be done before a global picture emerges.

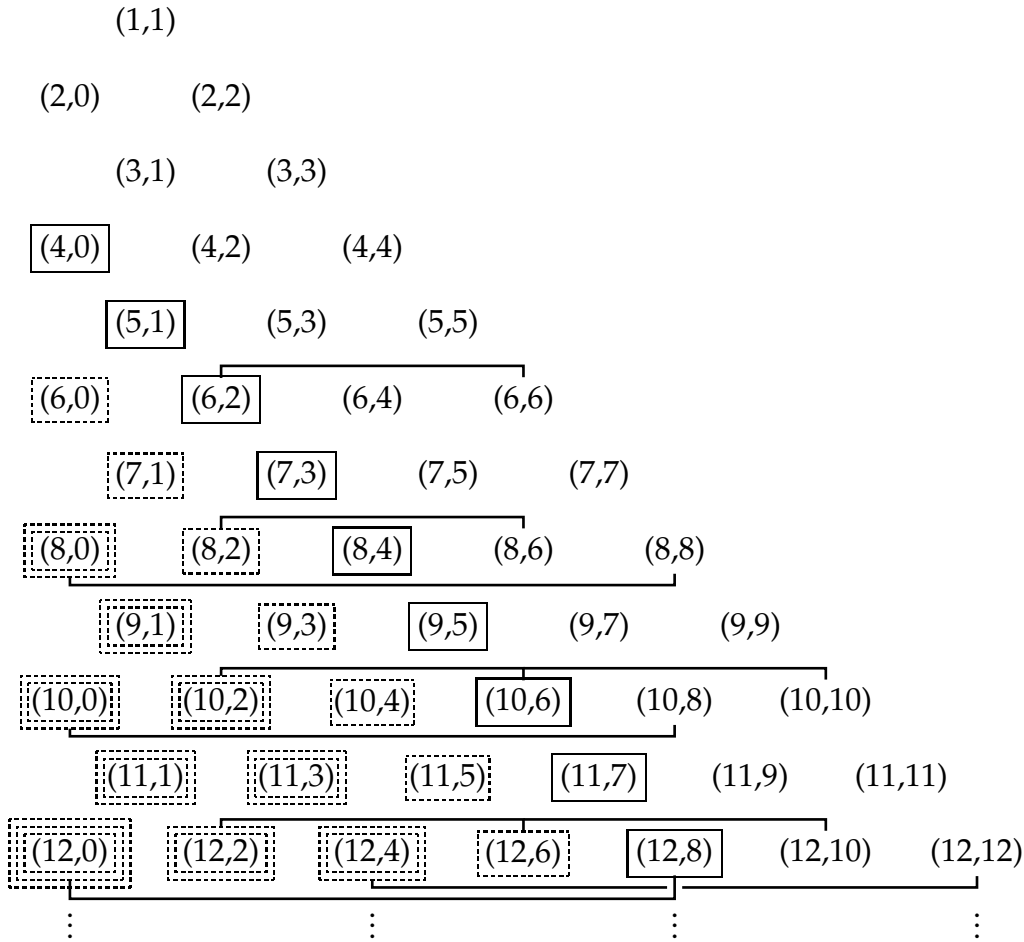


FIGURE 4.3 – The Bratelli diagram for $q = e^{i\pi/2}$. Jordan cells in ω_d occur when pairs (N, d) are contained in a box. The construction of section 4.6.4 is for boxes with solid segments, while boxes with dashed lines are for Jordan blocks found by our exploration on a computer. The number of multiple dashed boxes indicates the number of Jordan partners in the largest Jordan cell of the given \tilde{V}_N^d . The first occurrence of rank 4 Jordan blocks within a sector appears for $(N, d) = (12, 0)$. Jordan cells between sectors d and d' in the representation ρ are indicated by solid segments connecting pairs (N, d) . For these, $\alpha = 2$ is assumed when N is even.

Acknowledgements

We would like to thank David Ridout and Jørgen Rasmussen for helpful discussions and encouragement, and Hubert Saleur for bringing to our attention his work [92] with Paul Martin. AMD holds a scholarship and YSA a grant of the Canadian Natural Sciences and Engineering Research Council. This support is gratefully acknowledged.

CHAPITRE 5: CONCLUSION

Les résultats de nos travaux confirment que les modèles de boucles sont des laboratoires miniatures, sur réseau, pour les théories des champs logarithmiques. L'existence des blocs de Jordan n'est pas une coïncidence n'apparaissant qu'aux petites tailles du système, mais bien une caractéristique propre aux modèles de boucles qui persiste pour toutes les tailles du réseau N . Sur le ruban, nous avons étudié les représentations de vecteurs de connectivité ρ et avons montré que des blocs de Jordan apparaissent pour $D_N(\lambda, u)$ et pour son plus haut coefficient de Fourier F_N . Les cellules de Jordan couplent des secteurs d et d' lorsque λ prend des valeurs rationnelles (voir la proposition 2.4.10). Parmi les valeurs critiques se trouvent les valeurs de λ pour lesquelles la matrice de transfert $D_N(\lambda, u)$ sert au calcul des fonctions de partition des modèles de percolation, d'Ising et de Q-Potts pour $Q \leq 4$.

Le cas $\beta = 0$ est particulier puisqu'une relation d'inversion permet le calcul des valeurs propres de $D_N(\lambda, u)$ pour tout N . En utilisant une correspondance entre l'hamiltonien \mathcal{H} de boucles et l'hamiltonien XXZ avec conditions aux frontières ouvertes, nos travaux ont permis de démontrer la conjecture des règles de sélection de Pearce et Rasmussen [45] qui donne les dégénérescences de ces valeurs propres dans le spectre de $\rho(D_N(\lambda, u))$ dans le secteur à d défauts. Le calcul montre aussi que l'hamiltonien du modèle XXZ a une structure avec des blocs de Jordan de rang 2 lorsque N est pair uniquement, et que \mathcal{H} est diagonalisable pour les deux parités de N .

Sur le cylindre, à cause de la possibilité d'enroulement des connectivités, les représentations des vecteurs de connectivité sont de plus grandes dimensions que celles sur le ruban. Notre étude démontre la présence de blocs de Jordan à l'intérieur des représentations ω_d , de même que dans la représentation ρ , entre des secteurs étiquetés par des nombres de défauts d et d' différents. L'approche utilisant les hamiltoniens XXZ, développée pour la preuve des règles de sélection sur le ruban, a été le point de départ pour étudier les cellules de Jordan à l'intérieur des secteurs, menant à la construction d'un isomorphisme entre les modules de spins et de boucles. Nous montrons que les blocs de Jordan apparaissent précisément

lorsque la transformation linéaire cesse d'être un isomorphisme et l'hamiltonien XXZ a une invariance sous certains éléments de l'algèbre $U_q(\mathfrak{sl}_2)$. Ceci se produit pour des valeurs particulières de q et v et nécessite entre autre que q soit une racine de l'unité. Des cellules de Jordan d'ordre 2 associées à la valeur propre nulle de \mathcal{H} ont été construites explicitement. Ce sont les cas les plus simples. Nous discutons également de l'existence de blocs de Jordan intrasectoriels de plus haut rang et associées à d'autres valeurs propres de \mathcal{H} . Pour les blocs de Jordan entre les secteurs, la technique développée pour sonder les blocs de Jordan entre secteurs sur le ruban admet une généralisation qui permet de diagnostiquer des cellules de Jordan, dont le rang devient de plus en plus grand lorsque N augmente.

Même si les avancées faites dans cette thèse sont importantes, plusieurs questions restent en suspens. Les conditions aux frontières paramétrées par deux entiers r, s introduites dans [45], parmi lesquelles figure celle du chapitre 2, ont aussi des structures de Jordan non triviales qui restent à être comprises, et nous avons espoir que les techniques développées ici aient une généralisation simple. Tel que prédit par les théories des champs conformes, la non diagonalisabilité survient toujours pour des valeurs rationnelles de la charge centrale. Dans la limite $N \rightarrow \infty$, nous aimerions comprendre quelles représentations de l'algèbre de Virasoro reproduisent les formes de Jordan des modèles de boucles que nous avons démontrées. Les représentations de Virasoro émergeant à la limite $N \rightarrow \infty$ sont-elles des types proposées par Rohsiepe (voir section 1.5.3)? Ces représentations permettent peut-être de démontrer la conjecture de Pearce et de Rasmussen des plus hauts poids des représentations de Virasoro correspondant aux conditions aux frontières r, s de la matrice de transfert. Existe-t-il des éléments de l'algèbre de Temperley-Lieb qui, dans la limite $N \rightarrow \infty$, reproduisent les autres générateurs de l'algèbre de Virasoro? Une réponse (positive) à cette dernière question a été donnée récemment pour les polymères denses critique ($\beta = 0$) [90, 91], mais pour les autres valeurs de β , la question demeure ouverte. Finalement, nous aimerions pouvoir construire des observables pour les modèles sur réseau qui possèdent, dans la limite thermodynamique, la dépendance logarithmique prédite dans les LCFTs. Une première construction a été faite récemment pour le modèle de percolation [44], mais pour les autres valeurs de β , le chemin qui y mène n'est pas clair.

BIBLIOGRAPHIE

- [1] J.J. Binney, N.J. Dowrick, A.J. Fisher, M.E.J. Newman, *The theory of critical phenomena : an introduction to the renormalization group*, Clarendon Press (1992).
- [2] R. Langlands, P. Pouliot, Y. Saint-Aubin, *Conformal invariance in two-dimensional percolation*, Bull. Amer. Math. Soc. (N.S.) **30** (1994) 1–61.
- [3] H. Kesten, *Percolation theory for mathematicians*, Birkhäuser (1982) 423 p.
- [4] M.J. Lee, *Pseudo-random-number generators and the square site percolation threshold*, Phys. Rev. E **78** (3) (2008) 031131-1 – 031131-11.
- [5] J. Asikainen, A. Aharony, B.B. Mandelbrot, E.M. Rauch, J.P. Hovi, *Fractal geometry of critical Potts clusters*, Eur. Phys. J. **B34** (2003) 479–487.
- [6] A.G. Dunn, J.W. Essam, D.S. Ritchie, *Series expansion study of the pair connectedness in bond percolation models*, J. Phys. C : Solid State Phys. **8** (1975) 4219–4235.
- [7] S. Smirnov, *Critical percolation in the plane : conformal invariance, Cardy's formula, scaling limits*, C. R. Acad. Sci. Paris Sr. I Math. **333** (2001) 239–244.
- [8] R.J. Baxter, *Exactly solved models in statistical mechanics*, Academic Press (1982).
- [9] D.J. Griffiths, *Introduction to electrodynamics*, Prentice-Hall (1999) 576 p.
- [10] C. Cohen-Tannoudji, B. Diu, F. Laloë, *Mécanique quantique II*, Hermann, éditeurs des sciences et des arts (1973).
- [11] C.J. Thompson, *Mathematical statistical mechanics*, The Macmillan Company (1972).
- [12] L. Onsager, *A 2d model with an order-disorder transition*, Phys. Rev. **65** (1944) 117–149.
- [13] E. Ising, *Beitrag zur Theorie des Ferromagnetismus*, Z. Physik **31** (1925) 253–258.
- [14] B. Kaufman, *Crystal statistics II. Partition function evaluated by spinor analysis*, Phys. Rev. **76** (1949) 1232–1243.
- [15] H.A. Kramers, G.H. Wannier, *Statistics of the two-dimensional ferromagnet*, Phys. Rev. **60** (1941) 252–262.

- [16] A.A. Belavin, A.M. Polyakov, A.B. Zamolodchikov, *Infinite conformal symmetry in two-dimensional quantum field theory*, Nucl. Phys. B **241** (1984) 333–380.
- [17] D.L. O'Brien, P.A. Pearce, S. Ole Warnaar, *Finitized conformal spectrum of the Ising model on the cylinder and torus*, Physica A, **228** (1996) 63–77.
- [18] C.N. Yang, *The Spontaneous Magnetization of a Two-Dimensional Ising Model*, Phys. Rev. **85** (1952) 808–816.
- [19] F. Camia, C. Garban, C.M. Newman, *The Ising magnetization exponent is $\frac{1}{15}$* , (2012) 10 p.; arXiv : 1205.6612v2 [math.PR].
- [20] T. T. Wu, B.M. McCoy, C.A. Tracy, E. Barouch, *Spin-spin correlation functions for the two-dimensional Ising model : Exact theory in the scaling region*, Phys. Rev. B **13** (1976) 316–374.
- [21] R.B. Potts, *Some Generalized Order-Disorder Transformations*, Proc. Camb. Phil. Soc. **48** (1952) 106–109.
- [22] A. Hintermann, H. Kunz, F.Y. Wu, *Exact Results for the Potts Model in Two Dimensions*, J. Stat. Phys. **19** (1978) 623–632.
- [23] C.M. Fortuin, P.W. Kasteleyn, *On the random cluster model I : Introduction and relation to other models*, Physica **57** (1972) 536–564.
- [24] P. Di Francesco, P. Mathieu, D. Sénéchal, *Conformal field theory*, Springer (1996).
- [25] Y. Saint-Aubin, *The Virasoro Algebra and its Representation Theory*, Notes de cours (1990) 64 p.; *Chapitre 2 : Théorie des champs conforme*, Notes de cours (2008) 42 p.
- [26] J.L. Cardy, *Critical Percolation in Finite Geometries*, J. Phys. A **25** (1992) L201–L206.
- [27] S. Smirnov, *Conformal invariance in random cluster models. I. Holomorphic fermions in the Ising model*, Ann. of Math. (2) **172** (2010) 1435–1467.
- [28] D. Friedan, Z. Qin, S. Shenker, *Conformal invariance, unitarity and critical exponents in two dimensions*, Phys. Rev. Lett. **52** (1984) 1575–1578; *Conformal invariance, unitarity and two-dimensional critical exponents*, in J. Lepowsky, S. Mandelstam, I.M. Singer, eds., *Vertex operators in mathematics and physics*, Springer (1985) 482 p.; *Details of non-unitarity proof for the highest weight representations of the Virasoro Algebra*, Commun. Math. Phys. **107** (1986) 535–542.
- [29] A. Rocha-Caridi, *Vacuum vector representations of the Virasoro algebra*, in J. Lepowsky, S. Mandelstam, I.M. Singer, eds., *Vertex operators in Mathematics and Physics 3*, Springer (1985).

- [30] H. Saleur, B. Duplantier, *Exact Determination of the Percolation Hull Exponent in Two Dimensions* Phys. Rev. Lett. **58** (1987) 2325–2328.
- [31] C.M. Bender, *Making sense of non-hermitian Hamiltonians*, Rep. Prog. Phys. **70** (2007) 947–1018.
- [32] K. Hoffman, R. Kunze, *Linear algebra*, Prentice Hall (1961).
- [33] K. Kytölä, *Introduction to Hopf algebras and representations*, Notes de cours (2011) 91 p.
- [34] F.C. Alcaraz, M.N. Barber, M.T. Batchelor, R.J. Baxter, G.R.W. Quispel, *Surface exponents of the quantum XXZ, Ashkin-Teller and Potts models*, J. Phys. A **20** (1987) 6397–6409.
- [35] V. Pasquier, H. Saleur, *Common structures between finite systems and conformal field theories through quantum groups*, Nucl. Phys. B **330** (1990) 523–556.
- [36] N. Read, H. Saleur, *Exact spectra of conformal supersymmetric nonlinear sigma models in two dimensions*, Nucl. Phys. B **613** (2001) 409–444, arXiv : hep-th/0106124.
- [37] L.-P. Arguin, Y. Saint-Aubin, *Non-unitary observables in the 2d critical Ising model*, Phys. Lett. **B541** (2002) 384–389, arXiv : hep-th/0109138.
- [38] A. Morin-Duchesne, Y. Saint-Aubin, *Critical exponents for the homology of Fortuin-Kasteleyn clusters on a torus*, Phys. Rev. **E80**, 021130 (2009) 13 p. ; arXiv : 0812.2925v2 [cond-mat.stat-mech].
- [39] F. Rohsiepe, *On Reducible but Indecomposable Representations of the Virasoro Algebra*, 37 p. ; arXiv : hep-th/9611160v1.
- [40] K. Kytölä, D. Ridout, *On staggered indecomposable Virasoro modules*, J. Math. Phys. **50** (2009) 123503 ; arXiv : math-ph/0905.0108v2.
- [41] M. Flohr, *Singular Vectors in Logarithmic Conformal Field Theories*, Nucl. Phys. B **514** (1998), 523–552 ; *Bits and Pieces in Logarithmic Conformal Field Theory*, Int. J. Mod. Phys. A **18** (2003) 4497–4592.
- [42] M. Flohr, *Operator Product Expansion in Logarithmic Conformal Field Theory*, Nucl. Phys. B **634** (2002) 511–545.
- [43] J.L. Cardy, R.M. Ziff, *Exact results for the universal area distribution of clusters in percolation, Ising and Potts models*, J. Stat. Phys. **110** (2003) 1–33.
- [44] R. Vasseur, J.L. Jacobsen, H. Saleur, *Logarithmic observables in critical percolation* (2012) 11 p. ; arXiv : 1206.2312.

- [45] P.A. Pearce, J. Rasmussen, J.-B. Zuber, *Logarithmic minimal models*, J. Stat. Mech. **P11017** (2006) 36 p. ; arXiv : hep-th/0607232.
- [46] P.A. Pearce, J. Rasmussen, *Solvable Critical Dense Polymers*, J. Stat. Mech. **P02015** (2007) 32 p. ; arXiv : hep-th/0610273.
- [47] P.A. Pearce, J. Rasmussen, S.P. Villani, *Solvable Critical Dense Polymers on the Cylinder*, J. Stat. Mech. **P02010** (2010) 43 p. ; arXiv : hep-th/0910.4444v3.
- [48] G.M.T. Watts, *A crossing probability for critical percolation in two dimensions*, J. Phys. A : Math. Gen. **29** (1996) L363–L368.
- [49] B. Nienhuis, *Exact Critical Point and Critical Exponents of $O(n)$ Models in Two Dimensions*, Phys. Rev. Lett. **49** (1982) 1062–1065.
- [50] H. Duminil-Copin, S. Smirnov, *The connective constant of the honeycomb lattice equals $\sqrt{2 + \sqrt{2}}$* , Ann. Math. **175** (2012) 1653–1665 ; arXiv : math-ph/1007.0575.
- [51] J.W. Essam, *Graph theory and statistical physics*, Disc. Math **1** (1971) 83–112.
- [52] R.J. Baxter, S.B. Kelland, F.Y. Wu, *Equivalence of the Potts model or Whitney polynomial with an ice-type model*, J. Phys. A : Math. Gen. **9** (1976) 397–406.
- [53] Y.K. Zhou, P. A. Pearce, *Fusion of A-D-E Lattice Models*, Int. J. Mod. Phys. B **8** (1994) 3531–3577 ; arXiv : hep-th/9405019.
- [54] P. Di Francesco, *Inhomogeneous loop models with open boundaries*, J. Phys. A : Math. Gen. **38** (2005) 6091–6120.
- [55] J.-F. Richard, J.L. Jacobsen, *Character decomposition of Potts model partition functions. I. Cyclic geometry*, Nucl. Phys. B **750** (2006) 250–264, arXiv : math-ph/0605016v1 ; *Eigenvalue amplitudes of the Potts model on a torus*, Nucl. Phys. B **769** (2007) 256–274, arXiv : math-ph/0608055v1.
- [56] V. Gurarie, *Logarithmic operators in conformal field theory*, Nucl. Phys. B. **410** (1993) 535–549. V. Gurarie, A.W.W. Ludwig, *Conformal field theory at central charge $c = 0$ and two-dimensional critical systems with quenched disorder* (2005) arXiv : hep-th/0409105.
- [57] F.M. Goodman, H. Wenzl, *The Temperley-Lieb algebra at roots of unity*, Pacific Journal of Mathematics **161** (1993) 307–334.
- [58] P. Martin, *Potts Models and Related Problems in Statistical Mechanics*, World Scientific (1991) 360 p.
- [59] D. Ridout, *On the percolation BCFT and the crossing probability of Watts*, Nucl. Phys. B **810** (2009) 503–526 ; arXiv : hep-th/0808.3530.

- [60] L.H. Kauffman, S. Lins, *Temperley-Lieb recoupling theory and invariant of 3-manifolds*, Princeton Univ. Press (1994) 312 p.
- [61] J.L. Jacobsen, H. Saleur, *Combinatorial aspects of boundary loop models*, J. Stat. Mech. **P01021** (2008) 37 p. ; arXiv : math-th/07090912.
- [62] J. Dubail, J.L. Jacobsen, H. Saleur, *Conformal two-boundary loop model on the annulus*, Nucl. Phys. B **813** (2008) 430–459 ; arXiv : math-th/0812.2746 .
- [63] R.E. Behrend, P.A. Pearce, D.L. O'Brien, *Interaction-Round-a-Face Models with Fixed Boundary Conditions : The ABF Fusion Hierarchy*, J. Stat. Phys. **84** (1996) 1–48 ; arXiv : cond-mat/9511081.
- [64] B.W. Westbury, *The representation theory of the Temperley-Lieb algebras*, Math. Z. **219** (1995) 539–565.
- [65] R.L. Graham, D.E. Knuth, O. Patashnik, *Concrete Mathematics*, Addison-Wesley (1989).
- [66] V.F.R. Jones, *Index of subfactors*, Inv. Math. **72** (1983) 1–25.
- [67] H. Wenzl, *Hecke algebras of type A_n and subfactors*, Inv. Math. **92** (1988) 349–383.
- [68] T. Kato, *Perturbation theory for linear operators*, Springer (1966).
- [69] C. Korff, R. Weston, *PT Symmetry on the Lattice : The Quantum Group Invariant XXZ Spin-Chain*, J. Phys. A. : Math. Theor. **40** (2007) 8845. C. Korff, *PT symmetry of the non-Hermitian XX spin-chain : non-local bulk interaction from complex boundary fields*, J. Phys. A. : Math. Theor. **41** (2008) 295206.
- [70] J. Dubail, J.L. Jacobsen, H. Saleur, *Conformal field theory at central charge $c = 0$: a measure of the indecomposability (b) parameters*, Nucl. Phys. B **834** (2010) 399–422 ; iv :math-ph/1001.1151.
- [71] J.L. Jacobsen, H. Saleur, *Conformal boundary loop models*, Nucl. Phys. B **788** (2008) 137–166 ; arXiv : math-th/0611078.
- [72] P.A. Pearce, J. Rasmussen, P. Ruelle, *Integrable Boundary Conditions and \mathcal{W} -Extended Fusion in the Logarithmic Minimal Models $\mathcal{LM}(1, p)$* , J. Phys. A : Math. Theor. **43** (2008) 295201 ; arXiv : hep-th/0907.0134.
- [73] H. Bethe, *Zur theorie der Metalle. I. Eigenwerte und eigenfunktionen der linearen Atomkette*, Z. Phys. **71** (1931) 205–226.
- [74] M. Gaudin, *La fonction d'onde de Bethe*, Serie scientifique du CEA [Masson] (1983) 330 p.

- [75] V.E. Korepin, A.G. Izergin, N.M. Bogoliubov, *Quantum Inverse Scattering Method and Correlation Functions*, Cambridge monographs on mathematical physics [Cambridge University Press] (1993) 555 p.
- [76] P. Jordan, E. Wigner, *fiber das Paulische Aquivalenzverbot*, Z. Phys. **47** (1928) 631–651.
- [77] A. Morin-Duchesne, Y. Saint-Aubin, *The Jordan Structure of Two Dimensional Loop Models*, J. Stat. Mech. **P04007** (2011) 65 p. ; arXiv : 1101.2885v4 [math-ph].
- [78] R. Vasseur, J.L. Jacobsen, H. Saleur, *Indecomposability parameters in chiral Logarithmic Conformal Field Theory*, Nucl. Phys. B **851** (2011) 314–345.
- [79] J. de Gier, P. Pyatov, *Bethe Ansatz for the Temperley-Lieb loop model with open boundaries*, J. Stat. Mech. **P03002** (2004) ; arXiv : hep-th/0312235.
- [80] A. Nichols, *The Temperley-Lieb algebra and its generalizations in the Potts and XXZ models*, J. Stat. Mech. **P01003** (2006) 51 p. ; arXiv : hep-th/0509069.
- [81] E. Lieb, T. Schultz, D. Mattis, *Two Soluble Models of an Antiferromagnetic Chain*, Ann. Phys. **16** (1961) 407–466.
- [82] T. Deguchi, K. Fabricius, B.M. McCoy, *The sl_2 Loop Algebra Symmetry of the Six-Vertex Model at Roots of Unity*, J. Stat. Phys. **102** (2001) 701–736 ; arXiv : cond-mat/9912141.
- [83] U. Bilstein, B. Wehefritz, *The XX-model with boundaries : Part I. Diagonalization of the finite chain*, J. Phys. A : Math. Gen. **32** (1999) 191–233 ; arXiv : cond-mat/9807166.
- [84] G. Lusztig, *Modular representations and quantum groups*, Contemp. Math. **82** (1989) 59–77 ; *Quantum deformations of certain simple modules over enveloping algebras*, Adv. in Math. **70** (1988) 237–249.
- [85] A.E. Brouwer, A.M. Cohen, A. Neumaier, *Distance-Regular Graphs* [Springer-Verlag] (1980) 495 p.
- [86] C. Godsil, *Algebraic Graph Theory*, Graduate Texts in Mathematics [Springer] (2001) 439 p.
- [87] C. Godsil, *Association Schemes*, Lectures notes (2005) 146 p.
- [88] K. Kytölä, *Virasoro module structure of local martingales of SLE variants*, Rev. Math. Phys. **19** (2007) 455–509 ; arXiv : math-ph/0604047v4.
- [89] W.M. Koo, H. Saleur, *Representations of the Virasoro algebra from lattice models*, Nucl. Phys. B **246** (1994) 459–504 ; arXiv : hep-th/9312156v1.

- [90] A.M. Gainutdinov, N. Read, H. Saleur, *Continuum limit and symmetries of the periodic $gl(1|1)$ spin chain* (2012) 42 p. ; arXiv : 1112.3403 [hep-th].
- [91] A.M. Gainutdinov, N. Read, H. Saleur, *Bimodule structure in the periodic $gl(1|1)$ spin chain* (2012) 39 p. ; arXiv : 1112.3407v2 [hep-th].
- [92] P. Martin, H. Saleur, *On an algebraic approach to higher dimensional statistical mechanics*, Commun. Math. Phys. **158** (1993) 155–190 ; arXiv : hep-th/9208061v1.
- [93] J.J. Graham, G.I. Lehrer, *The representation theory of affine Temperley-Lieb algebras*, Enseign. Math. **44** (1998) 173–218.
- [94] R.M. Green, *On representations of affine Temperley-Lieb algebras*, Algebras and Modules II, CMS Conference Proceedings **24**, Amer. Math. Soc. (1998) 365–386.
- [95] K. Erdmann, R.M. Green, *On representations of affine Temperley-Lieb algebras, II*, Pac. Jour. Math **191** (1999) 243–274 ; arXiv : math/9811017v1 [math.RT].
- [96] J.J. Graham, G.I. Lehrer, *Cellular algebras*, Inv. Math. **123** (1996) 1–34.
- [97] D. Ridout, Y. Saint-Aubin, *The structure of the Temperley-Lieb algebra through its standard modules* ; arXiv : 1204.4505v2 [math-ph].
- [98] T. H. Pinson, *Critical Percolation on the Torus*, J. Stat. Phys. **75** (1994) 1167–1177.
- [99] L.-P. Arguin, *Homology of Fortuin-Kasteleyn clusters of Potts models on the torus*, J. Stat. Phys. **109** (2002) 301–310 ; arXiv : hep-th/0111193.
- [100] R.M. Green, C.K. Fan, *On the affine Temperley-Lieb algebras*, J. London Math. Soc. **2 60** (1999) 366–380 ; arXiv : q-alg/9706003v1.
- [101] A. Morin-Duchesne, *A proof of selection rules for critical dense polymers*, J. Phys. A : Math. Theor. **44 495003** (2011) 32 p. ; arXiv : math-ph/1109.6397.
- [102] P. Di Francesco, *Meander Determinants*, Commun. Math. Phys. **191** (1998) 543–583 ; arXiv : hep-th/9612026v1.
- [103] Qi Chen, J.H. Przytycki, *The Gram determinant of the type B Temperley-Lieb algebra*, Adv. in Appl. Math. **43** (2008) 156–161 ; arXiv : 0802.1083v2 [math.GT].
- [104] C. De Concini, V.G. Kac, *Representations of Quantum Groups at Roots of 1*, in Operator algebras, unitary representations, enveloping algebras, and invariant theory, eds. A. Connes, M. Duflo, A. Joseph, R. Rentschle, 471–506, Progr. Math., **92** (1990).